

QC 852  
. C6  
no. 419  
ATSL

LIBRARIES  
JAN 47 1966  
COLORADO STATE UNIVERSITY

# ANALYSIS OF BOUNDARY LAYER SOUNDING DATA FROM THE FIRE MARINE STRATOCUMULUS PROJECT

by

Wayne H. Schubert, Paul E. Ciesielski, Thomas B. McKee,  
John D. Kleist, Stephen K. Cox, Christopher M. Johnson-Pasqua,  
and William L. Smith Jr.

FIRE VOLUME 2



Atmospheric Science  
PAPER NO.  
419

DEPARTMENT OF ATMOSPHERIC SCIENCE  
COLORADO STATE UNIVERSITY  
FORT COLLINS, COLORADO

QC852  
1C6  
no. 419  
ATSL

## ANALYSIS OF BOUNDARY LAYER SOUNDING DATA FROM THE FIRE MARINE STRATOCUMULUS PROJECT

WAYNE H. SCHUBERT, PAUL E. CIESIELSKI, THOMAS B. MCKEE, JOHN D. KLEIST,  
STEPHEN K. COX, CHRISTOPHER M. JOHNSON-PASQUA, AND WILLIAM L. SMITH JR.

*Department of Atmospheric Science, Colorado State University, Fort Collins, CO 80523*

(October 1987)

### ABSTRACT

We present an analysis of the boundary layer thermodynamic data obtained by the CLASS radiosonde system during the marine boundary layer experiment on San Nicolas Island in the summer of 1987. The analysis procedure retains the highest possible vertical resolution in the data. Plots of temperature, dew point temperature, potential temperature, equivalent potential temperature and saturation equivalent potential temperature are presented for each of the sixty-nine soundings taken during FIRE. Conditions were mostly cloudy with fifty-five of the sixty-nine soundings being released with stratocumulus overhead. For the fifty-five cloudy soundings, cloud top jumps of equivalent potential temperature  $\theta_e$  and total water mixing ratio  $r$  were also determined. Each of these soundings is then represented by a point in the  $(\Delta\theta_e, \Delta r)$  plane. Fifteen of these soundings are on the unstable side of the evaporative instability line, and there appears to be some tendency for break-up under these conditions.

### 1. Introduction

The cross-chain Loran atmospheric sounding system (CLASS) is a portable upper air sounding system developed by NCAR for atmospheric science research. Nine such systems have been built under NSF and ONR sponsorship. A photograph of the system operated by CSU on San Nicolas Island during FIRE is shown in Fig. 1. The system is contained in a (3.6 m) · (2.4 m) · (2.1 m) single axle trailer weighing approximately 1500 kg. Helium filled balloons 1.3 m in diameter and weighing 200 g carry a Vaisala RS 80 sonde to an altitude of about 20 km. The balloons are inflated in a ripstop nylon bag inside the CLASS trailer and are launched through a retractable roof hatch. The PTU (pressure, temperature, humidity) sensors on the RS 80 sonde are capacitive and alternately control the frequency of an AF oscillator. The oscillator frequency and Loran time-of-arrival information is telemetered from the sonde to a 400 MHz receiver in the CLASS trailer. The Loran information is used by an ANI-7000 (Advanced Navigation, Inc.) Loran navigator to determine balloon position and hence winds. The frequency information from the capacitive sensors is sent to the PTU processor, which uses a fourth degree equation for each sensor to convert frequen-

cies to meteorological parameters. The coefficients of the fourth degree equations are provided by factory calibration of each sonde. The whole system is under the control of an HP-9816 computer. Real time displays are provided on the computer monitor and a variety of plots can be obtained from the HP Thinkjet printer. Further technical information on the CLASS system can be found in Lauritsen et al. (1986), which is reproduced as Appendix A. Further technical information on the RS 80 radiosonde can be found in Vaisala publication R 0422, some of which is reproduced as Appendix B.

During the FIRE project the CLASS system was set up at an elevation of 38 m on the northwest tip of San Nicolas Island, which provided good exposure to the prevailing northwesterly flow. During the period from 30 June to 19 July 1987, sixty-nine soundings were obtained. Observation times and maximum altitudes for these soundings are summarized in Table 1. In the following sections we discuss only high vertical resolution meteorological data in the lowest two kilometers.

### 2. Time lag effects

Whenever radiosondes ascend through inver-

sions there arise questions about errors due to sensor time lag. Before proceeding to the analysis of the CLASS data, let us briefly discuss these effects.

Let  $T$  denote the sensor temperature and  $T_e$  the environmental temperature. According to the Newtonian cooling law,  $T$  and  $T_e$  are related by the first order differential equation

$$\frac{dT}{dt} = -\frac{1}{\tau}(T - T_e),$$

where  $\tau$  is the sensor response time. Let us assume that the environmental temperature changes linearly in time as the balloon ascends so that  $dT_e/dt = \lambda$ . The above equation can then be written

$$\frac{d(T - T_e)}{dt} + \frac{1}{\tau}(T - T_e) = -\lambda,$$

which has the solution

$$T - T_e = [(T - T_e)_0 + \lambda\tau] \exp(-t/\tau) - \lambda\tau.$$

If we wait long enough for the initial condition  $(T - T_e)_0$  to be forgotten, the sensor temperature  $T$  and the environmental temperature  $T_e$  will differ by  $-\lambda\tau$ . If the sensor rises at  $5 \text{ ms}^{-1}$  in an atmosphere with a dry adiabatic lapse rate, then  $\lambda = -0.05 \text{ K s}^{-1}$ . Since the temperature sensor in the Vaisala RS 80 sonde has a 2.3 s lag constant,  $-\lambda\tau = 0.12 \text{ K}$ , i.e. the sensor reads 0.12 K too warm. On the other hand, if the sensor rises at  $5 \text{ ms}^{-1}$  through a 100 m thick temperature inversion of 10 K, then  $\lambda = 0.5 \text{ K s}^{-1}$  and  $\lambda\tau = 1.0 \text{ K}$ , which means the sensor reads 1.0 K too cold.

If a similar argument is applied to the humidity sensor, the slow rate of increase of relative humidity in the subcloud layer, coupled with the 1 s lag of the humicap element, causes the sensor to read too dry by only a few tenths of a per cent. However, an 80 % decrease in humidity in a 100 m layer above cloud top leads to a sensor reading about 4 % too high.

Although these lag effects are not entirely negligible in strong inversions, we have not corrected for them in any way.

### 3. Analysis of the data

The raw data from the CLASS system consists of pressure, temperature and relative humidity as a function of time. An example from 8 July 1987 12:11 GMT is shown in Table 2. Each row consists of time (in seconds from the start of data acquisition), pressure (mb), temperature (degrees Celsius) and relative humidity

(per cent). Several points are worth noting.

First of all, although 3.3 s time intervals are common, the data are not equally spaced in time. To obtain data equally spaced in time or equally spaced in height (to be determined hydrostatically), interpolation is necessary.

Secondly, although the average rate of pressure change is about  $-0.5 \text{ mb/s}$  (i.e. about  $5 \text{ m/s}$  rise rate), the pressure is not monotonic with time (e.g. note the changes around 826 mb and the bad data at 13.51 sec). Since downdrafts in stratocumulus are unlikely to be strong enough to force the balloon downward, the slight nonmonotonic nature of the pressure profile is probably a deficiency in the aneroid sensor. Thus, editing of obviously bad data and slight smoothing of the resulting pressure profile are apparently justified.

Finally, although the humidity sensor often reports humidities several percent below saturation (i.e., 100 %) when in cloud, the 2.3 s lag constant of the temperature sensor and the 1 s lag constant of the humidity sensor allow resolution of the sharp temperature and humidity gradients just above cloud top. To preserve these sharp gradients, smoothing of the temperature and humidity data should be avoided.

With these points in mind we have proceeded as follows. After editing obviously bad data we have fit cubic spline interpolation functions to the raw data pairs  $(t_i, p_i)$ ,  $(t_i, T_i)$  and  $(t_i, U_i)$ ,  $i = 1, 2, \dots$ , to obtain the continuous functions  $p(t)$ ,  $T(t)$ ,  $U(t)$ . Since noise in the aneroid sensor causes  $p(t)$  to be nonmonotonic, we have sampled  $p(t)$  at 3 sec intervals and then applied an eleven point filter with the weights  $(-1, -5, -5, 20, 70, 98, 70, 20, -5, -5, -1)/256$ . This filter has the monotone spectral response shown in Fig. 2. More detail on this filter can be found in Hamming (1983, pages 143-144). We next perform a cubic spline fit to the filtered pressure data, thus obtaining the monotonic continuous function  $\bar{p}(t)$ . We then convert filtered pressure data into height data using the discrete hydrostatic relation

$$z_j = z_{j-1} + \frac{R}{2g} (T(t_j) + T(t_{j-1})) \ln \left( \frac{\bar{p}(t_{j-1})}{\bar{p}(t_j)} \right) \quad (1)$$

where the  $t_j$  ( $j = 1, 2, \dots$ ) are discrete times at 3 sec intervals. This upward integration commences at the 38 m launch elevation. A cubic spline is then fit to the  $(z_j, t_j)$  data to obtain the monotonic function  $t(z)$ . From the continuous functions  $t(z)$ ,  $\bar{p}(t)$ ,  $U(t)$  and  $T(t)$  we then obtain the first five columns of Table 3 by evaluation of  $t(z)$  at 5 m increments of  $z$ .

From the pressure  $\bar{p}$ , temperature  $T$  and relative humidity  $U$  we now wish to compute the water vapor mixing ratio  $q$ , saturation water vapor mixing ratio  $q_s$ , potential temperature  $\theta$ , equivalent potential temperature  $\theta_e$  and saturation equivalent potential temperature  $\theta_{es}$ . By first computing the saturation vapor pressure  $e_s(T)$  from

$$e_s(T) = 6.112 \exp\left(\frac{17.67(T - 273.15)}{T - 29.65}\right) \quad (2)$$

(where  $e_s(T)$  is in millibars and  $T$  in Kelvin) and the actual vapor pressure  $e$  from

$$e = U e_s(T), \quad (3)$$

we can compute the water vapor mixing ratio  $q$  and the saturation water vapor mixing ratio  $q_s$  from

$$q = \frac{\epsilon e}{p - e} \quad (4)$$

and

$$q_s = \frac{\epsilon e_s(T)}{p - e_s(T)}, \quad (5)$$

where  $\epsilon = 0.622$  is the ratio of the molecular weight of water vapor to the molecular weight of dry air. Equation (2) is Bolton's (1980) fit to the highly accurate (0.005%) formula of Wexler (1976). The accuracy of (2) is 0.1%. Since the dew point temperature  $T_d$  is defined by  $e_s(T_d) = e$ , we can rearrange (2) to obtain

$$T_d = 273.15 + \frac{243.5 \ln(e/6.112)}{17.67 - \ln(e/6.112)}, \quad (6)$$

which allows explicit determination of  $T_d$  from the vapor pressure  $e$ .

We can next compute the potential temperature, equivalent potential temperature and the saturation equivalent potential temperature from

$$\theta = T(p_0/p)^\kappa, \quad (7)$$

$$\theta_e = \theta \exp(2.67q/T_s), \quad (8)$$

and

$$\theta_{es} = \theta \exp(2.67q_s/T), \quad (9)$$

where the saturation level temperature  $T_s$  is given by

$$T_s = \frac{1}{\frac{1}{T-55} - \frac{\ln(U/100)}{2840}} + 55. \quad (10)$$

The constants in (8) and (9) were suggested by Betts (1982) and those in (10) by Bolton

(1980). The use of (2)–(10) results in the remaining columns in Table 3.

#### 4. Sounding data

Each of the sixty-nine soundings was processed by the techniques described in section 3. Thus, a table similar to Table 3 is available for each sounding. Here we have chosen to present the data in graphical rather than tabular form. The vertical profiles of  $T$ ,  $T_d$ ,  $\theta$ ,  $\theta_e$  and  $\theta_{es}$  for each sounding are shown in Fig. 3. The CLASS sounding data presented here can be obtained from the FIRE Central Archive or through NCAR's computer network. Additional information for obtaining this data is contained in Appendix C.

In addition to the CLASS soundings we also obtained a continuous record of stratocumulus cloud base height using a laser ceilometer located nearby. More information on this system and the data acquired can be found in the report by Schubert et al. (1987). The ceilometer record shows that the 30 June – 19 July time period can be characterized as quite cloudy; fifty-five of the sixty-nine CLASS soundings were released with stratocumulus overhead. For each of these fifty-five soundings we have determined the cloud top total water jump  $\Delta r$  as follows. We first compute the vertically averaged water vapor mixing ratio in the layer which extends from 60 m to 240 m above cloud top. We then subtract from this the average water vapor mixing ratio in the layer which extends from 65 m to 165 m above sea level (the island sounding site being 38 m above sea level). This water vapor mixing ratio difference should be equivalent to the cloud top jump in total water if the boundary layer is well-mixed. The procedure for determining  $\Delta\theta_e$  is identical. In this way each of the fifty-five soundings was characterized by a point in the  $(\Delta r, \Delta\theta_e)$  plane as shown in Fig. 4. As can be seen, 40 of the 55 points lie on the stable side of the Randall (1980) stability line (the line labeled  $\Delta\theta_e = \kappa L \Delta r / c_p$ ), and 15 lie on the unstable side. According to the ceilometer record, 7 of the unstable cases show cloud break-up within 12 hours while 4 of the stable cases show break-up within 12 hours. The cases exhibiting break-up are indicated in Fig. 4 by the partially blackened symbols, with the fraction of blackening indicating the fraction of 12 hours before cloud disappearance. The occurrence of partially blackened symbols on the stable side of the critical stability line indicates that cloud top evaporative instability is not the only mechanism for break-up. For further discussion the reader is referred to Kuo and Schubert (1988), who report on model experiments

designed to understand the existence of persistent cloud decks with soundings which are unstable according to theory.

*Acknowledgments.* Our participation in the FIRE project has been supported by the Marine Meteorology Program of the Office of Naval Research under contract N00014-87-K-0228 and by the National Aeronautics and Space Administration under contract NAG1-554.

#### REFERENCES

- Betts, A. K., 1982: Saturation point analysis of moist convective overturning. *J. Atmos. Sci.*, **39**, 1484-1505.
- Bolton, D., 1980: The computation of equivalent potential temperature. *Mon. Wea. Rev.*, **108**, 1046-1053.
- Kuo, H.-C., and W. H. Schubert, 1988: Stability of cloud-topped boundary layers. *Quart. J. Roy. Meteor. Soc.*, **114**, in press.
- Lauritsen, D., Z. Malekmadani, C. Morel and R. McBeth, 1986: The cross-chain Loran atmospheric sounding system (CLASS). NCAR CLASS System User's Manual.
- Hamming, R. W., 1983: *Digital Filters*, Second Edition. Prentice-Hall, Englewood Cliffs, New Jersey, 257 pp.
- Randall, D. A., 1980: Conditional instability of the first kind upside-down. *J. Atmos. Sci.*, **37**, 125-130.
- Schubert, W. H., S. K. Cox, P. E. Ciesielski and C. M. Johnson-Pasqua, 1987: Operation of a ceilometer during the FIRE marine stratocumulus experiment. Colorado State University Atmospheric Science Paper No. 420.
- Wexler, A., 1976: Vapor pressure formulation for water in range 0 to 100°C. A revision. *J. Res. Nat. Bur. Stand.*, **80A**, 775-785.

Table 1. Summary of CLASS soundings taken during the FIRE experiment.

Sounding Number	Date	Start Time (GMT)	End Time (GMT)	Maximum Altitude (km)
1	June 30	11:55:00	13:37:39	21.5
2	June 30	23:51:28	01:41:48	24.1
3	July 1	12:16:51	13:28:37	18.7
4	July 1	20:05:16	20:58:01	13.0
5	July 1	23:11:39	00:15:45	16.6
6	July 2	17:50:00	18:57:32	20.7
7	July 2	22:53:39	23:52:14	16.8
8	July 3	12:08:46	13:24:00	39.4
9	July 3	18:08:34	19:24:02	21.1
10	July 4	00:36:55	02:00:34	7.1
11	July 4	12:15:10	13:38:41	21.6
12	July 5	00:34:11	01:48:03	19.7
13	July 5	11:58:40	13:07:09	18.9
14	July 6	01:45:48	03:01:10	19.5
15	July 6	12:14:14	13:32:45	18.8
16	July 6	16:07:18	17:35:41	21.0
17	July 6	23:50:14	00:15:17	--
18	July 7	11:19:34	12:33:38	19.9
19	July 8	00:11:58	01:21:07	20.0
20	July 8	12:11:57	13:14:15	18.8
21	July 9	11:54:19	12:53:09	17.9
22	July 9	18:14:58	19:27:51	20.0
23	July 10	01:15:14	02:39:12	20.8
24	July 10	12:22:51	13:11:10	9.6
25	July 10	15:50:39	17:00:19	19.6
26	July 10	18:00:56	19:37:41	22.0
27	July 10	20:06:53	21:14:59	20.4
28	July 10	21:59:53	23:05:08	20.0
29	July 11	00:05:46	01:27:35	20.8
30	July 11	02:00:25	03:12:40	20.1
31	July 11	03:53:52	05:16:38	21.1
32	July 11	06:16:41	07:26:30	19.5
33	July 11	09:51:50	11:06:57	20.2
34	July 11	12:12:45	13:27:27	19.2
35	July 11	14:10:50	15:21:15	20.6
36	July 11	18:08:30	19:40:40	22.1
37	July 11	22:08:06	23:33:40	21.5
38	July 11	23:49:42	01:21:01	22.1
39	July 12	01:54:12	03:12:19	20.8
40	July 12	06:10:54	07:32:45	19.5
41	July 12	12:34:09	14:34:14	21.5
42	July 12	15:10:57	16:34:09	21.3
43	July 12	10:05:10	11:32:05	19.7
44	July 12	17:55:31	19:12:51	22.0
45	July 13	00:05:41	01:27:34	20.4
46	July 13	11:54:13	12:58:54	18.2
47	July 13	21:20:07	22:50:25	22.8
48	July 14	00:14:06	01:30:02	19.3
49	July 14	11:58:11	13:02:58	20.0
50	July 15	00:15:59	01:09:54	14.9
51	July 15	12:00:54	13:12:57	16.2
52	July 15	17:03:55	18:21:47	20.2
53	July 15	19:35:49	20:43:39	18.6
54	July 16	00:11:18	01:37:34	21.5
55	July 16	11:39:09	13:31:11	24.2
56	July 16	16:00:08	17:17:54	21.6
57	July 16	20:04:08	21:29:00	23.6
58	July 16	23:42:05	00:59:44	21.3
59	July 17	12:06:30	13:31:06	21.0
60	July 17	15:58:23	17:09:44	20.7
61	July 17	20:02:15	21:24:24	22.0
62	July 18	00:20:31	01:32:37	20.6
63	July 18	12:06:33	13:43:42	21.7
64	July 18	15:57:44	17:07:40	20.3
65	July 18	19:51:33	21:27:11	22.0
66	July 19	00:19:47	02:08:49	24.0
67	July 19	12:01:01	13:25:58	21.6
68	July 19	16:08:32	17:48:35	23.1
69	July 19	20:15:35	21:28:17	21.1

Table 2. An example of the raw sounding data from the CLASS system. Each set of four numbers consists of time, pressure, temperature and relative humidity. This example shows the first six minutes of the 12:11 GMT 8 July 1987.

2.89, 1005.836, 17.9, 67	168.49, 899.647, 23.4, 32
4.61, 1004.854, 17.9, 67	173.53, 896.796, 23.1, 32
7.99, 1005.345, 18.1, 68	178.63, 893.081, 22.9, 33
9.65, 1004.609, 18.1, 66	182.01, 891.121, 22.7, 33
13.51, 564.912, 31.8, 41	190.43, 885.915, 22.4, 34
16.41, 1001.181, 15.4, 77	195.53, 880.954, 22.3, 33
19.79, 1000.204, 14.9, 81	198.87, 882.677, 22.5, 33
21.51, 997.765, 14.7, 82	202.25, 876.877, 21.8, 34
23.17, 996.791, 14.5, 83	207.35, 876.021, 21.9, 33
26.57, 994.603, 14.2, 85	210.73, 873.246, 21.7, 33
28.23, 993.147, 14.1, 86	219.15, 867.72, 21.5, 32
29.95, 990.967, 14, 87	222.53, 862.44, 21.2, 33
33.33, 989.275, 13.8, 88	225.91, 861.178, 21, 33
34.99, 988.068, 13.8, 89	229.29, 859.287, 21.1, 33
38.37, 986.14, 13.7, 90	232.67, 856.565, 21.1, 34
40.09, 983.496, 13.6, 90	237.76, 856.355, 21.1, 34
41.75, 983.496, 13.5, 90	241.14, 855.102, 20.7, 34
45.13, 981.337, 13.4, 92	249.56, 849.899, 20.8, 34
48.53, 979.183, 13.3, 92	252.94, 847.619, 20.5, 34
51.91, 977.511, 13.1, 92	258.04, 844.315, 20.3, 34
55.29, 974.414, 12.9, 93	263.08, 838.972, 20, 35
70.49, 965.416, 12.7, 94	268.18, 834.071, 20, 35
75.53, 963.061, 12.5, 94	271.56, 832.85, 19.4, 34
78.91, 962.826, 12.3, 94	279.98, 832.037, 19.4, 32
82.29, 957.669, 12.2, 94	283.36, 830.616, 19.4, 32
87.39, 954.867, 12.4, 94	288.42, 827.782, 19.3, 33
90.73, 952.771, 12.7, 88	293.52, 825.361, 19.2, 30
99.21, 946.281, 13, 70	298.56, 826.369, 19.5, 28
102.59, 944.434, 13.5, 64	301.94, 818.138, 18.7, 30
107.63, 940.752, 14.4, 61	310.42, 814.949, 18.5, 33
112.73, 935.256, 15.5, 61	315.46, 813.756, 18.3, 34
117.77, 932.975, 17.2, 56	318.84, 812.565, 18.1, 36
121.15, 931.382, 18.3, 52	322.22, 806.438, 17.4, 37
129.59, 926.393, 20.2, 45	327.32, 806.044, 17.7, 36
132.97, 924.36, 20.3, 44	330.7, 804.079, 17.7, 34
138.07, 919.857, 21.8, 39	339.12, 798.601, 17.5, 34
143.11, 916.943, 22.8, 36	342.5, 798.016, 17.4, 35
148.21, 906.481, 23.2, 34	347.6, 793.354, 17, 34
151.59, 911.586, 23.6, 32	352.64, 792.386, 17.3, 31
160.01, 902.286, 23.2, 32	357.7, 788.334, 17.5, 30
165.11, 907.145, 23.4, 39	361.08, 788.142, 17.1, 29

Table 3. Cubic spline interpolated data at 5 m intervals for 12:11 GMT 8 July 1987. A table with identical format has been produced for each of the sixty-nine FIRE soundings.

Z(M)	TIMES(S)	P(MB)	U(%)	T(C)	TD(C)	Q(G/KG)	QS(G/KG)	THETA(K)	THETAE(K)	THETAES(K)	
1	40.	17.1	1000.89	78.23	15.27	11.51	8.55	10.92	288.35	312.54	319.10
2	45.	18.7	1000.28	80.10	15.04	11.64	8.63	10.77	288.17	312.57	318.47
3	50.	19.9	999.61	81.06	14.89	11.67	8.65	10.67	288.07	312.52	318.09
4	55.	20.9	998.98	81.63	14.78	11.67	8.66	10.60	288.01	312.47	317.83
5	60.	21.6	998.41	82.08	14.68	11.66	8.66	10.55	287.96	312.42	317.62
6	65.	22.4	997.86	82.50	14.60	11.65	8.66	10.49	287.92	312.37	317.42
7	70.	23.1	997.29	82.94	14.51	11.65	8.66	10.44	287.88	312.34	317.24
8	75.	23.8	996.70	83.36	14.43	11.65	8.67	10.40	287.86	312.32	317.08
9	80.	24.5	996.10	83.79	14.36	11.66	8.68	10.36	287.84	312.33	316.95
10	85.	25.2	995.50	84.20	14.30	11.67	8.69	10.32	287.82	312.35	316.84
11	90.	25.9	994.89	84.61	14.25	11.69	8.71	10.29	287.82	312.39	316.75
12	95.	26.6	994.30	85.01	14.20	11.72	8.73	10.26	287.82	312.44	316.67
13	100.	27.3	993.71	85.43	14.15	11.75	8.75	10.24	287.82	312.51	316.62
14	105.	28.0	993.12	85.86	14.11	11.78	8.77	10.22	287.83	312.59	316.56
15	110.	28.7	992.54	86.32	14.07	11.82	8.80	10.20	287.84	312.68	316.52
16	115.	29.5	991.95	86.77	14.03	11.86	8.83	10.18	287.84	312.76	316.46
17	120.	30.3	991.36	87.12	13.98	11.87	8.84	10.15	287.84	312.79	316.39
18	125.	31.1	990.77	87.35	13.92	11.85	8.84	10.12	287.83	312.77	316.29
19	130.	31.9	990.17	87.53	13.86	11.83	8.83	10.09	287.82	312.74	316.20
20	135.	32.7	989.58	87.75	13.82	11.82	8.83	10.06	287.83	312.74	316.13
21	140.	33.6	989.00	88.13	13.80	11.87	8.86	10.06	287.85	312.86	316.14
22	145.	34.4	988.41	88.66	13.80	11.96	8.92	10.06	287.90	313.08	316.22
23	150.	35.3	987.82	89.17	13.80	12.05	8.98	10.07	287.95	313.30	316.30
24	155.	36.2	987.23	89.54	13.79	12.10	9.02	10.07	287.99	313.43	316.33
25	160.	37.0	986.64	89.79	13.76	12.12	9.03	10.06	288.01	313.50	316.33
26	165.	37.9	986.06	89.95	13.73	12.11	9.03	10.04	288.03	313.52	316.30
27	170.	38.7	985.47	90.02	13.68	12.08	9.02	10.02	288.03	313.49	316.25
28	175.	39.5	984.88	90.03	13.63	12.03	9.00	9.99	288.03	313.43	316.17
29	180.	40.4	984.29	89.97	13.58	11.97	8.96	9.96	288.03	313.34	316.09
30	185.	41.3	983.71	89.93	13.53	11.91	8.93	9.93	288.02	313.25	316.00
31	190.	42.2	983.12	90.15	13.48	11.90	8.93	9.91	288.03	313.25	315.94
32	195.	43.1	982.54	90.69	13.45	11.96	8.97	9.90	288.04	313.38	315.91
33	200.	44.1	981.95	91.38	13.42	12.05	9.03	9.89	288.07	313.57	315.91
34	205.	45.1	981.36	91.97	13.40	12.12	9.09	9.88	288.09	313.74	315.93
35	210.	46.1	980.78	92.24	13.38	12.15	9.11	9.87	288.12	313.83	315.94
36	215.	47.1	980.20	92.22	13.35	12.12	9.09	9.86	288.14	313.82	315.93
37	220.	48.1	979.61	92.07	13.32	12.06	9.06	9.84	288.16	313.75	315.90
38	225.	49.0	979.03	91.93	13.28	11.99	9.03	9.82	288.16	313.66	315.85
39	230.	50.0	978.44	91.87	13.22	11.93	9.00	9.79	288.16	313.57	315.77
40	235.	50.8	977.86	91.87	13.17	11.88	8.97	9.77	288.16	313.50	315.68
41	240.	51.7	977.27	91.96	13.12	11.84	8.95	9.74	288.15	313.44	315.60
42	245.	52.5	976.69	92.12	13.06	11.81	8.94	9.71	288.15	313.41	315.52
43	250.	53.2	976.11	92.33	13.01	11.80	8.94	9.68	288.15	313.40	315.44
44	255.	54.0	975.52	92.58	12.97	11.79	8.94	9.66	288.15	313.41	315.38
45	260.	54.7	974.94	92.82	12.93	11.79	8.95	9.64	288.16	313.43	315.34
46	265.	55.5	974.36	93.06	12.89	11.80	8.95	9.62	288.17	313.46	315.30
47	270.	56.2	973.78	93.26	12.86	11.80	8.96	9.61	288.19	313.50	315.29
48	275.	57.0	973.20	93.45	12.83	11.80	8.97	9.60	288.21	313.55	315.28
49	280.	57.8	972.62	93.61	12.81	11.81	8.98	9.59	288.24	313.60	315.29
50	285.	58.6	972.03	93.75	12.79	11.81	8.99	9.58	288.27	313.66	315.31
51	290.	59.4	971.45	93.87	12.78	11.82	8.99	9.58	288.30	313.72	315.34
52	295.	60.3	970.87	93.97	12.77	11.82	9.00	9.58	288.34	313.78	315.38
53	300.	61.3	970.29	94.05	12.76	11.83	9.01	9.58	288.38	313.85	315.42
54	305.	62.3	969.71	94.11	12.75	11.83	9.02	9.58	288.42	313.92	315.48
55	310.	63.3	969.13	94.14	12.75	11.83	9.03	9.59	288.47	313.99	315.54
56	315.	64.4	968.55	94.15	12.75	11.83	9.03	9.59	288.52	314.06	315.61
57	320.	65.5	967.97	94.14	12.75	11.83	9.03	9.60	288.57	314.12	315.68
58	325.	66.6	967.39	94.11	12.75	11.82	9.04	9.60	288.61	314.18	315.74
59	330.	67.8	966.82	94.08	12.74	11.81	9.03	9.60	288.66	314.22	315.79
60	335.	68.9	966.25	94.04	12.73	11.79	9.03	9.60	288.69	314.25	315.83
61	340.	70.1	965.67	94.01	12.71	11.77	9.02	9.59	288.72	314.26	315.85
62	345.	71.3	965.08	93.98	12.68	11.74	9.00	9.58	288.74	314.24	315.83
63	350.	72.7	964.50	93.97	12.63	11.69	8.98	9.56	288.75	314.18	315.77
64	355.	74.1	963.94	93.98	12.57	11.63	8.95	9.53	288.73	314.08	315.67
65	360.	75.5	963.37	94.00	12.50	11.56	8.92	9.49	288.71	313.96	315.53
66	365.	76.7	962.77	94.03	12.43	11.49	8.88	9.45	288.69	313.83	315.39
67	370.	77.8	962.18	94.04	12.36	11.43	8.85	9.41	288.67	313.74	315.29
68	375.	78.6	961.61	94.02	12.32	11.38	8.83	9.39	288.67	313.67	315.22
69	380.	79.4	961.05	93.97	12.28	11.34	8.80	9.37	288.68	313.62	315.18
70	385.	80.1	960.48	93.91	12.25	11.30	8.79	9.36	288.70	313.59	315.16
71	390.	80.7	959.91	93.88	12.23	11.27	8.78	9.35	288.73	313.59	315.17
72	395.	81.4	959.33	93.88	12.21	11.26	8.77	9.34	288.76	313.62	315.20
73	400.	82.1	958.75	93.95	12.20	11.26	8.78	9.34	288.80	313.68	315.24
74	405.	82.7	958.18	94.11	12.20	11.28	8.80	9.35	288.85	313.78	315.31
75	410.	83.4	957.61	94.32	12.20	11.32	8.83	9.36	288.90	313.92	315.39



78	425.	85.5	955.88	94.85	12.27	11.47	8.93	9.42	289.12	314.46	315.80
79	430.	86.3	955.31	94.71	12.32	11.50	8.95	9.45	289.22	314.62	316.01
80	435.	87.2	954.73	94.19	12.38	11.48	8.95	9.50	289.33	314.73	316.26
81	440.	88.1	954.17	93.15	12.46	11.39	8.90	9.55	289.46	314.74	316.55
82	445.	89.0	953.60	91.65	12.55	11.23	8.81	9.61	289.60	314.65	316.87
83	450.	89.9	953.04	89.85	12.63	11.01	8.69	9.67	289.73	314.46	317.18
84	455.	90.8	952.46	87.94	12.70	10.76	8.54	9.72	289.85	314.19	317.44
85	460.	91.6	951.89	86.08	12.75	10.48	8.39	9.75	289.95	313.88	317.64
86	465.	92.4	951.32	84.31	12.78	10.20	8.24	9.77	290.03	313.53	317.79
87	470.	93.2	950.75	82.61	12.79	9.91	8.08	9.78	290.09	313.17	317.90
88	475.	94.0	950.18	80.95	12.80	9.62	7.93	9.79	290.15	312.81	317.99
89	480.	94.7	949.62	79.31	12.81	9.32	7.77	9.80	290.21	312.45	318.08
90	485.	95.5	949.05	77.68	12.82	9.02	7.62	9.81	290.27	312.09	318.17
91	490.	96.3	948.49	76.03	12.83	8.72	7.47	9.82	290.33	311.73	318.28
92	495.	97.1	947.92	74.36	12.86	8.41	7.32	9.84	290.41	311.40	318.41
93	500.	97.9	947.35	72.64	12.90	8.10	7.17	9.87	290.50	311.08	318.59
94	505.	98.8	946.78	70.88	12.96	7.80	7.03	9.92	290.61	310.81	318.84
95	510.	99.7	946.22	69.10	13.05	7.52	6.90	9.98	290.75	310.59	319.17
96	515.	100.5	945.66	67.37	13.17	7.26	6.78	10.06	290.92	310.44	319.59
97	520.	101.4	945.09	65.76	13.31	7.04	6.68	10.16	291.11	310.37	320.07
98	525.	102.3	944.53	64.37	13.45	6.87	6.60	10.26	291.31	310.38	320.59
99	530.	103.2	943.97	63.27	13.60	6.76	6.56	10.36	291.51	310.47	321.10
100	535.	104.0	943.40	62.46	13.74	6.70	6.54	10.47	291.70	310.62	321.61
101	540.	104.7	942.84	61.88	13.88	6.69	6.54	10.56	291.89	310.82	322.09
102	545.	105.4	942.28	61.48	14.01	6.72	6.55	10.66	292.07	311.06	322.56
103	550.	106.1	941.72	61.22	14.13	6.77	6.58	10.75	292.24	311.32	323.01
104	555.	106.8	941.16	61.07	14.24	6.85	6.62	10.84	292.41	311.61	323.45
105	560.	107.4	940.60	61.01	14.36	6.94	6.67	10.93	292.58	311.92	323.88
106	565.	108.0	940.04	61.01	14.47	7.04	6.72	11.01	292.74	312.24	324.30
107	570.	108.6	939.48	61.06	14.58	7.16	6.78	11.10	292.90	312.58	324.73
108	575.	109.2	938.92	61.14	14.69	7.28	6.84	11.18	293.06	312.93	325.16
109	580.	109.8	938.37	61.23	14.80	7.41	6.90	11.27	293.23	313.30	325.60
110	585.	110.4	937.81	61.30	14.92	7.54	6.97	11.37	293.40	313.67	326.08
111	590.	111.0	937.26	61.33	15.06	7.68	7.04	11.48	293.59	314.07	326.59
112	595.	111.6	936.70	61.30	15.21	7.81	7.11	11.60	293.79	314.48	327.16
113	600.	112.3	936.14	61.16	15.38	7.94	7.18	11.73	294.01	314.92	327.80
114	605.	113.0	935.59	60.88	15.57	8.06	7.24	11.89	294.26	315.36	328.53
115	610.	113.7	935.05	60.39	15.81	8.16	7.29	12.08	294.55	315.83	329.39
116	615.	114.6	934.49	59.68	16.08	8.24	7.34	12.30	294.88	316.33	330.40
117	620.	115.5	933.93	58.71	16.41	8.30	7.38	12.57	295.26	316.85	331.60
118	625.	116.6	933.37	57.48	16.78	8.34	7.40	12.87	295.69	317.38	332.98
119	630.	117.7	932.83	56.09	17.17	8.35	7.41	13.21	296.14	317.90	334.47
120	635.	118.9	932.29	54.67	17.57	8.34	7.41	13.55	296.59	318.39	335.98
121	640.	120.0	931.74	53.28	17.95	8.31	7.40	13.89	297.03	318.84	337.46
122	645.	121.2	931.19	51.95	18.31	8.28	7.39	14.22	297.45	319.26	338.91
123	650.	122.3	930.64	50.73	18.66	8.25	7.37	14.54	297.86	319.67	340.31
124	655.	123.3	930.10	49.62	18.97	8.21	7.36	14.83	298.23	320.04	341.62
125	660.	124.3	929.56	48.62	19.26	8.18	7.35	15.11	298.57	320.37	342.83
126	665.	125.3	929.01	47.72	19.52	8.14	7.33	15.36	298.88	320.66	343.94
127	670.	126.2	928.47	46.93	19.74	8.09	7.31	15.58	299.16	320.91	344.92
128	675.	127.1	927.93	46.26	19.92	8.05	7.29	15.77	299.39	321.11	345.74
129	680.	128.0	927.39	45.70	20.06	8.00	7.27	15.91	299.59	321.26	346.40
130	685.	128.8	926.85	45.28	20.15	7.95	7.25	16.02	299.73	321.36	346.88
131	690.	129.7	926.31	44.97	20.20	7.89	7.23	16.07	299.83	321.40	347.17
132	695.	130.5	925.77	44.78	20.21	7.83	7.21	16.09	299.89	321.40	347.29
133	700.	131.3	925.23	44.61	20.21	7.78	7.18	16.10	299.94	321.38	347.37
134	705.	132.1	924.69	44.39	20.23	7.72	7.16	16.13	300.01	321.39	347.52
135	710.	132.9	924.15	44.05	20.29	7.66	7.13	16.20	300.12	321.44	347.87
136	715.	133.7	923.61	43.52	20.42	7.61	7.11	16.34	300.30	321.57	348.50
137	720.	134.5	923.08	42.82	20.61	7.54	7.08	16.54	300.55	321.76	349.41
138	725.	135.3	922.54	42.01	20.85	7.48	7.06	16.80	300.85	322.00	350.52
139	730.	136.0	922.00	41.15	21.11	7.41	7.03	17.08	301.16	322.26	351.74
140	735.	136.8	921.47	40.31	21.38	7.35	7.00	17.36	301.48	322.53	352.98
141	740.	137.5	920.94	39.54	21.62	7.29	6.97	17.64	301.78	322.78	354.17
142	745.	138.2	920.41	38.87	21.84	7.23	6.95	17.88	302.06	323.01	355.24
143	750.	138.8	919.87	38.33	22.02	7.19	6.94	18.10	302.30	323.22	356.17
144	755.	139.4	919.34	37.88	22.17	7.15	6.92	18.27	302.50	323.41	356.95
145	760.	139.9	918.81	37.53	22.30	7.12	6.91	18.42	302.67	323.56	357.60
146	765.	140.4	918.31	37.24	22.40	7.10	6.90	18.54	302.82	323.71	358.16
147	770.	140.9	917.81	36.99	22.48	7.08	6.90	18.65	302.96	323.83	358.65
148	775.	141.3	917.30	36.76	22.56	7.06	6.89	18.75	303.08	323.95	359.09
149	780.	141.7	916.77	36.56	22.63	7.03	6.89	18.83	303.21	324.06	359.51
150	785.	142.2	916.19	36.36	22.69	7.01	6.88	18.92	303.33	324.18	359.92
151	790.	142.7	915.56	36.16	22.75	6.99	6.87	19.00	303.45	324.29	360.32
152	795.	143.2	914.87	35.97	22.81	6.96	6.86	19.08	303.57	324.39	360.71
153	800.	143.7	914.18	35.79	22.86	6.93	6.85	19.15	303.68	324.49	361.06
154	805.	144.2	913.54	35.62	22.90	6.89	6.84	19.21	303.79	324.56	361.37
155	810.	144.7	912.97	35.46	22.93	6.86	6.83	19.26	303.87	324.62	361.62
156	815.	145.0	912.53	35.34	22.95	6.83	6.82	19.30	303.94	324.66	361.82
157	820.	145.3	912.22	35.24	22.97	6.80	6.81	19.32	303.99	324.69	361.96
158	825.	145.4	912.06	35.19	22.98	6.79	6.81	19.34	304.01	324.70	362.04
159	830.	145.5	911.95	35.16	22.99	6.78	6.80	19.35	304.03	324.71	362.09
160	835.	145.9	911.62	35.04	23.01	6.75	6.79	19.38	304.08	324.73	362.25
161	840.	146.7	910.87	34.72	23.06	6.67	6.76	19.46	304.21	324.77	362.65
162	845.	148.3	909.85	33.96	23.21	6.47	6.57	19.65	304.46	324.80	363.55
163	850.	150.7	909.26	32.49	23.52	6.10	6.51	20.03	304.83	324.71	363.16
164	855.	152.7	908.82	31.55	23.64	5.70	6.37	20.18	305.00	324.68	363.85

167	870.	156.1	907.01	31.18	23.46	5.46	6.24	20.00	304.99	324.07	365.28
168	875.	156.9	906.49	31.26	23.39	5.44	6.23	19.93	304.97	324.04	365.04
169	880.	157.4	906.16	31.34	23.35	5.43	6.23	19.88	304.95	324.02	364.87
170	885.	157.9	905.90	31.43	23.31	5.44	6.24	19.85	304.94	324.03	364.74
171	890.	159.3	905.23	31.79	23.22	5.53	6.28	19.75	304.91	324.12	364.42
172	895.	162.8	904.62	32.84	23.28	6.05	6.52	19.84	305.03	324.95	364.85
173	900.	165.4	903.72	32.95	23.41	6.21	6.60	20.03	305.25	325.43	365.69
174	905.	166.3	903.16	32.72	23.43	6.13	6.56	20.06	305.33	325.41	365.88
175	910.	166.4	903.06	32.68	23.43	6.11	6.56	20.06	305.34	325.40	365.90
176	915.	166.7	902.87	32.60	23.43	6.08	6.54	20.07	305.36	325.38	365.94
177	920.	167.1	902.48	32.45	23.43	6.01	6.51	20.07	305.39	325.33	366.01
178	925.	167.7	901.92	32.24	23.42	5.91	6.47	20.08	305.44	325.26	366.07
179	930.	168.4	901.25	32.03	23.40	5.80	6.43	20.07	305.49	325.18	366.10
180	935.	169.1	900.53	31.87	23.38	5.70	6.39	20.05	305.53	325.11	366.09
181	940.	169.7	899.86	31.77	23.34	5.63	6.36	20.02	305.56	325.06	366.05
182	945.	170.2	899.29	31.72	23.31	5.58	6.34	19.99	305.58	325.03	365.99
183	950.	170.8	898.77	31.71	23.28	5.54	6.33	19.97	305.59	325.01	365.92
184	955.	171.3	898.29	31.72	23.24	5.52	6.32	19.94	305.61	325.00	365.85
185	960.	171.8	897.81	31.75	23.21	5.50	6.32	19.90	305.62	325.00	365.77
186	965.	172.3	897.33	31.80	23.17	5.49	6.32	19.87	305.63	325.01	365.68
187	970.	172.9	896.82	31.89	23.13	5.50	6.33	19.84	305.64	325.04	365.58
188	975.	173.6	896.30	32.02	23.09	5.52	6.34	19.80	305.65	325.09	365.49
189	980.	174.4	895.78	32.18	23.06	5.57	6.36	19.77	305.66	325.18	365.41
190	985.	175.2	895.26	32.37	23.03	5.62	6.39	19.75	305.68	325.29	365.36
191	990.	176.0	894.74	32.57	23.00	5.69	6.43	19.72	305.70	325.40	365.32
192	995.	176.9	894.23	32.76	22.97	5.75	6.45	19.70	305.72	325.51	365.27
193	1000.	177.8	893.71	32.92	22.94	5.78	6.48	19.67	305.74	325.59	365.20
194	1005.	178.8	893.20	33.01	22.89	5.79	6.48	19.63	305.74	325.61	365.09
195	1010.	179.7	892.68	33.03	22.84	5.75	6.47	19.58	305.74	325.57	364.93
196	1015.	180.6	892.17	33.00	22.78	5.69	6.44	19.52	305.73	325.49	364.73
197	1020.	181.6	891.65	32.99	22.72	5.63	6.42	19.46	305.72	325.41	364.54
198	1025.	182.6	891.14	33.03	22.67	5.60	6.41	19.41	305.72	325.38	364.39
199	1030.	183.5	890.62	33.14	22.63	5.61	6.42	19.38	305.72	325.42	364.29
200	1035.	184.4	890.11	33.28	22.60	5.65	6.44	19.35	305.74	325.50	364.23
201	1040.	185.3	889.59	33.43	22.58	5.69	6.47	19.34	305.77	325.59	364.21
202	1045.	186.1	889.08	33.58	22.56	5.74	6.49	19.32	305.80	325.70	364.21
203	1050.	186.8	888.57	33.72	22.54	5.78	6.51	19.31	305.83	325.79	364.21
204	1055.	187.5	888.05	33.83	22.52	5.81	6.53	19.30	305.86	325.88	364.21
205	1060.	188.1	887.53	33.92	22.50	5.83	6.54	19.29	305.89	325.95	364.22
206	1065.	188.8	887.01	33.98	22.47	5.84	6.55	19.28	305.92	326.01	364.21
207	1070.	189.4	886.50	34.02	22.45	5.83	6.55	19.26	305.94	326.04	364.19
208	1075.	189.9	885.99	34.02	22.42	5.81	6.55	19.24	305.96	326.04	364.16
209	1080.	190.5	885.49	33.99	22.39	5.77	6.53	19.21	305.98	326.02	364.10
210	1085.	191.1	884.99	33.93	22.36	5.71	6.51	19.18	306.00	325.97	364.03
211	1090.	191.8	884.49	33.83	22.32	5.64	6.48	19.15	306.01	325.89	363.94
212	1095.	192.4	883.98	33.69	22.29	5.55	6.44	19.12	306.02	325.79	363.86
213	1100.	193.2	883.45	33.52	22.26	5.45	6.40	19.09	306.04	325.69	363.81
214	1105.	194.1	882.92	33.31	22.24	5.35	6.36	19.09	306.08	325.62	363.84
215	1110.	195.0	882.40	33.11	22.26	5.28	6.33	19.12	306.15	325.61	364.04
216	1115.	196.0	881.90	32.93	22.34	5.27	6.33	19.22	306.28	325.75	364.50
217	1120.	197.0	881.41	32.83	22.45	5.32	6.36	19.36	306.44	326.00	365.13
218	1125.	197.9	880.90	32.85	22.52	5.39	6.39	19.46	306.57	326.25	365.59
219	1130.	198.9	880.39	33.01	22.50	5.44	6.42	19.44	306.59	326.35	365.57
220	1135.	199.8	879.87	33.28	22.36	5.43	6.42	19.29	306.50	326.25	364.98
221	1140.	200.6	879.35	33.57	22.17	5.39	6.40	19.08	306.36	326.05	364.15
222	1145.	201.3	878.84	33.81	21.98	5.33	6.38	18.87	306.21	325.83	363.34
223	1150.	202.1	878.34	33.98	21.83	5.27	6.36	18.71	306.10	325.64	362.70
224	1155.	202.8	877.84	34.02	21.74	5.21	6.33	18.61	306.06	325.51	362.36
225	1160.	203.6	877.34	33.94	21.71	5.15	6.31	18.59	306.08	325.47	362.30
226	1165.	204.4	876.83	33.77	21.72	5.09	6.29	18.62	306.15	325.48	362.48
227	1170.	205.2	876.31	33.53	21.78	5.03	6.27	18.69	306.25	325.53	362.83
228	1175.	206.1	875.80	33.26	21.85	4.98	6.25	18.78	306.38	325.60	363.26
229	1180.	207.1	875.29	33.03	21.90	4.92	6.23	18.85	306.48	325.65	363.59
230	1185.	208.2	874.79	32.95	21.88	4.88	6.21	18.85	306.52	325.64	363.63
231	1190.	209.2	874.29	32.97	21.82	4.83	6.19	18.78	306.50	325.57	363.40
232	1195.	210.3	873.78	33.00	21.73	4.77	6.17	18.69	306.46	325.46	363.09
233	1200.	211.3	873.27	32.96	21.67	4.69	6.14	18.63	306.44	325.35	362.87
234	1205.	212.2	872.76	32.84	21.63	4.61	6.11	18.59	306.45	325.27	362.78
235	1210.	213.1	872.26	32.68	21.61	4.52	6.07	18.58	306.48	325.19	362.77
236	1215.	213.8	871.75	32.51	21.60	4.43	6.04	18.58	306.52	325.14	362.82
237	1220.	214.6	871.25	32.34	21.60	4.36	6.01	18.58	306.57	325.10	362.89
238	1225.	215.2	870.74	32.19	21.59	4.29	5.98	18.59	306.62	325.08	362.97
239	1230.	215.8	870.23	32.07	21.59	4.23	5.96	18.60	306.67	325.07	363.06
240	1235.	216.4	869.73	31.98	21.59	4.19	5.95	18.60	306.71	325.07	363.13
241	1240.	217.0	869.23	31.91	21.58	4.15	5.94	18.61	306.76	325.09	363.19
242	1245.	217.5	868.73	31.88	21.57	4.13	5.93	18.60	306.80	325.11	363.23
243	1250.	218.0	868.22	31.87	21.55	4.11	5.93	18.60	306.83	325.14	363.26
244	1255.	218.5	867.71	31.91	21.53	4.11	5.93	18.59	306.86	325.18	363.26
245	1260.	219.0	867.21	31.97	21.51	4.12	5.94	18.57	306.89	325.23	363.24
246	1265.	219.5	866.71	32.08	21.48	4.14	5.95	18.54	306.91	325.28	363.18
247	1270.	220.0	866.21	32.21	21.44	4.17	5.96	18.51	306.92	325.34	363.11
248	1275.	220.4	865.71	32.37	21.40	4.20	5.98	18.48	306.93	325.40	363.01
249	1280.	220.9	865.21	32.53	21.36	4.23	6.00	18.44	306.93	325.46	362.89
250	1285.	221.4	864.71	32.70	21.31	4.26	6.02	18.40	306.93	325.51	362.77
251	1290.	221.9	864.21	32.85	21.26	4.29	6.03	18.35	306.93	325.55	362.63
252	1295.	222.4	863.71	32.98	21.21	4.30	6.04	18.31	306.93	325.57	362.49
253	1300.	223.0	863.20	33.07	21.16	4.30	6.04	18.26	306.93	325.59	362.31

256	1315.	224.8	861.69	33.10	21.03	4.19	6.01	18.15	306.95	325.50	362.02
257	1320.	225.5	861.20	33.04	21.01	4.15	5.99	18.13	306.97	325.48	362.00
258	1325.	226.2	860.70	32.97	21.00	4.11	5.98	18.14	307.02	325.50	362.07
259	1330.	227.0	860.19	32.91	21.02	4.10	5.98	18.16	307.09	325.56	362.24
260	1335.	227.8	859.69	32.88	21.05	4.11	5.99	18.21	307.17	325.68	362.48
261	1340.	228.6	859.19	32.91	21.08	4.16	6.01	18.26	307.26	325.84	362.74
262	1345.	229.5	858.70	33.05	21.10	4.24	6.05	18.30	307.33	326.03	362.95
263	1350.	230.5	858.21	33.33	21.11	4.36	6.10	18.31	307.38	326.26	363.06
264	1355.	231.6	857.70	33.69	21.10	4.51	6.17	18.32	307.43	326.50	363.13
265	1360.	232.8	857.20	34.03	21.10	4.65	6.24	18.33	307.48	326.76	363.24
266	1365.	234.4	856.71	34.18	21.14	4.75	6.28	18.39	307.57	327.00	363.52
267	1370.	236.5	856.21	34.09	21.16	4.73	6.28	18.42	307.65	327.07	363.72
268	1375.	238.7	855.71	33.97	21.00	4.54	6.20	18.24	307.52	326.69	363.02
269	1380.	240.4	855.21	33.99	20.78	4.35	6.12	18.01	307.35	326.27	362.08
270	1385.	241.6	854.72	34.01	20.66	4.26	6.08	17.89	307.28	326.09	361.64
271	1390.	242.7	854.22	34.02	20.63	4.23	6.08	17.87	307.30	326.09	361.59
272	1395.	243.6	853.72	34.02	20.64	4.24	6.09	17.89	307.36	326.18	361.73
273	1400.	244.5	853.23	34.01	20.67	4.27	6.10	17.93	307.44	326.31	361.96
274	1405.	245.3	852.73	34.01	20.71	4.30	6.12	17.99	307.53	326.46	362.24
275	1410.	246.1	852.23	34.01	20.75	4.33	6.14	18.04	307.63	326.61	362.53
276	1415.	246.9	851.74	34.03	20.79	4.36	6.15	18.10	307.71	326.76	362.80
277	1420.	247.6	851.24	34.00	20.82	4.39	6.17	18.14	307.79	326.88	363.02
278	1425.	248.4	850.75	34.00	20.83	4.40	6.17	18.16	307.86	326.97	363.17
279	1430.	249.1	850.25	34.00	20.82	4.39	6.17	18.16	307.90	327.02	363.21
280	1435.	249.9	849.76	34.00	20.78	4.36	6.16	18.13	307.91	327.00	363.14
281	1440.	250.7	849.27	34.01	20.72	4.31	6.15	18.07	307.90	326.93	362.94
282	1445.	251.4	848.77	34.01	20.64	4.24	6.12	18.00	307.87	326.83	362.68
283	1450.	252.2	848.28	34.01	20.57	4.17	6.10	17.92	307.84	326.72	362.41
284	1455.	252.9	847.78	34.00	20.50	4.11	6.07	17.86	307.82	326.63	362.19
285	1460.	253.7	847.29	33.98	20.45	4.06	6.05	17.81	307.82	326.57	362.06
286	1465.	254.4	846.80	33.95	20.42	4.02	6.04	17.79	307.84	326.55	362.00
287	1470.	255.1	846.31	33.92	20.40	3.99	6.03	17.77	307.86	326.55	361.98
288	1475.	255.8	845.81	33.91	20.38	3.96	6.02	17.76	307.90	326.57	361.99
289	1480.	256.4	845.32	33.91	20.36	3.95	6.02	17.75	307.93	326.59	362.01
290	1485.	257.1	844.83	33.92	20.34	3.94	6.02	17.74	307.96	326.63	362.02
291	1490.	257.6	844.33	33.96	20.32	3.93	6.02	17.73	307.99	326.66	362.01
292	1495.	258.2	843.84	34.02	20.29	3.93	6.02	17.71	308.01	326.69	361.97
293	1500.	258.7	843.35	34.10	20.26	3.94	6.03	17.68	308.02	326.72	361.90
294	1505.	259.3	842.86	34.19	20.22	3.94	6.03	17.65	308.04	326.75	361.82
295	1510.	259.8	842.37	34.29	20.18	3.95	6.04	17.62	308.05	326.78	361.73
296	1515.	260.3	841.88	34.40	20.14	3.96	6.05	17.58	308.06	326.82	361.65
297	1520.	260.8	841.38	34.51	20.10	3.97	6.06	17.56	308.07	326.86	361.57
298	1525.	261.2	840.89	34.62	20.07	3.99	6.07	17.53	308.09	326.91	361.52
299	1530.	261.7	840.40	34.72	20.04	4.01	6.08	17.51	308.11	326.97	361.48
300	1535.	262.2	839.92	34.82	20.02	4.03	6.09	17.50	308.14	327.04	361.48
301	1540.	262.6	839.43	34.92	20.01	4.05	6.11	17.49	308.17	327.12	361.50
302	1545.	263.1	838.96	35.00	20.00	4.08	6.12	17.50	308.22	327.21	361.57
303	1550.	263.5	838.48	35.07	20.00	4.11	6.14	17.51	308.27	327.32	361.68
304	1555.	264.0	837.99	35.13	20.01	4.15	6.16	17.53	308.33	327.44	361.82
305	1560.	264.5	837.50	35.18	20.03	4.18	6.18	17.56	308.40	327.57	361.99
306	1565.	265.0	837.00	35.22	20.05	4.21	6.20	17.59	308.47	327.70	362.18
307	1570.	265.5	836.50	35.24	20.07	4.24	6.21	17.62	308.55	327.83	362.36
308	1575.	266.1	835.99	35.23	20.08	4.25	6.22	17.65	308.61	327.92	362.53
309	1580.	266.7	835.48	35.20	20.08	4.24	6.22	17.66	308.67	327.98	362.63
310	1585.	267.4	834.99	35.14	20.07	4.20	6.20	17.65	308.70	327.97	362.64
311	1590.	268.0	834.53	35.03	20.02	4.11	6.17	17.61	308.70	327.86	362.50
312	1595.	268.8	834.09	34.87	19.92	3.96	6.11	17.51	308.64	327.62	362.14
313	1600.	269.7	833.63	34.61	19.75	3.70	6.00	17.33	308.51	327.16	361.44
314	1605.	271.2	833.10	34.12	19.46	3.25	5.81	17.03	308.26	326.33	360.20
315	1610.	274.1	832.60	33.21	19.20	2.63	5.56	16.75	308.04	325.34	359.07
316	1615.	279.0	832.07	32.14	19.36	2.32	5.44	16.94	308.27	325.23	359.92
317	1620.	280.6	831.65	31.93	19.41	2.27	5.43	17.00	308.37	325.28	360.21
318	1625.	281.8	831.22	31.87	19.41	2.24	5.42	17.01	308.41	325.31	360.31
319	1630.	283.0	830.69	31.95	19.40	2.27	5.43	17.01	308.46	325.40	360.36
320	1635.	284.1	830.13	32.18	19.39	2.36	5.47	17.01	308.51	325.57	360.42
321	1640.	285.0	829.62	32.45	19.38	2.47	5.52	17.01	308.55	325.76	360.48
322	1645.	285.8	829.16	32.70	19.37	2.57	5.56	17.01	308.59	325.92	360.53
323	1650.	286.6	828.74	32.89	19.36	2.64	5.59	17.01	308.62	326.05	360.55
324	1655.	287.3	828.32	33.01	19.34	2.67	5.61	17.00	308.64	326.13	360.55
325	1660.	288.3	827.83	33.02	19.31	2.65	5.60	16.97	308.66	326.13	360.49
326	1665.	289.6	827.26	32.65	19.24	2.43	5.52	16.91	308.65	325.87	360.29
327	1670.	291.5	826.75	31.52	19.16	1.86	5.30	16.83	308.62	325.18	360.00
328	1675.	294.1	826.39	29.54	19.26	1.04	5.00	16.93	308.76	324.42	360.48
329	1680.	296.5	825.58	28.19	19.52	0.62	4.85	17.22	309.12	324.35	361.80
330	1685.	297.8	824.65	27.92	19.56	0.52	4.82	17.28	309.27	324.42	362.18
331	1690.	298.3	824.14	27.95	19.53	0.51	4.82	17.26	309.29	324.44	362.14
332	1695.	298.4	824.03	27.97	19.52	0.51	4.82	17.25	309.29	324.44	362.11
333	1700.	298.4	824.03	27.97	19.52	0.51	4.82	17.25	309.29	324.44	362.11
334	1705.	298.5	823.92	27.99	19.50	0.51	4.83	17.24	309.29	324.45	362.08
335	1710.	298.7	823.69	28.05	19.48	0.52	4.83	17.21	309.28	324.45	361.99
336	1715.	299.0	823.34	28.15	19.43	0.52	4.83	17.17	309.27	324.45	361.82
337	1720.	299.4	822.86	28.33	19.35	0.54	4.84	17.09	309.23	324.44	361.55
338	1725.	299.9	822.27	28.58	19.24	0.57	4.86	16.99	309.18	324.42	361.17
339	1730.	300.4	821.58	28.91	19.10	0.61	4.87	16.86	309.11	324.41	360.69
340	1735.	301.0	820.80	29.30	18.95	0.66	4.90	16.72	309.03	324.39	360.16
341	1740.	301.5	819.97	29.72	18.79	0.73	4.93	16.57	308.96	324.40	359.63
342	1745.	302.1	819.13	30.14	18.66	0.80	4.96	16.45	308.91	324.44	359.19

345	1760.	303.8	817.08	31.09	18.43	1.04	5.06	16.26	308.89	324.72	358.59
346	1765.	304.1	816.67	31.27	18.40	1.10	5.08	16.24	308.90	324.81	358.55
347	1770.	304.4	816.42	31.39	18.39	1.14	5.10	16.23	308.91	324.87	358.54
348	1775.	304.5	816.33	31.43	18.39	1.15	5.10	16.23	308.92	324.89	358.53
349	1780.	304.4	816.43	31.38	18.39	1.13	5.10	16.24	308.91	324.86	358.54
350	1785.	304.3	816.53	31.34	18.40	1.12	5.09	16.24	308.91	324.84	358.54
351	1790.	304.7	816.12	31.53	18.38	1.19	5.12	16.23	308.93	324.95	358.54
352	1795.	306.2	815.05	32.10	18.37	1.43	5.21	16.24	309.04	325.36	358.71
353	1800.	313.7	814.27	33.40	18.38	1.99	5.44	16.28	309.14	326.13	358.93
354	1805.	323.9	806.59	36.98	17.35	2.51	5.70	15.40	308.88	326.64	355.95
355	1810.	319.7	810.37	36.38	17.94	2.81	5.79	15.92	309.09	327.15	357.78
356	1815.	313.6	814.27	33.39	18.38	1.99	5.44	16.28	309.14	326.13	358.94
357	1820.	311.3	814.41	33.09	18.49	1.96	5.42	16.38	309.23	326.19	359.37
358	1825.	311.9	814.42	33.14	18.47	1.96	5.42	16.36	309.21	326.17	359.29
359	1830.	314.2	814.13	33.54	18.35	2.03	5.45	16.25	309.12	326.16	358.83
360	1835.	317.3	812.50	35.07	18.25	2.56	5.68	16.19	309.19	326.91	358.72
361	1840.	320.0	810.05	36.51	17.86	2.79	5.79	15.85	309.05	327.09	357.51
362	1845.	321.6	808.42	36.93	17.49	2.62	5.73	15.51	308.83	326.68	356.21
363	1850.	322.4	807.69	37.01	17.38	2.55	5.70	15.41	308.79	326.56	355.86
364	1855.	322.6	807.51	37.02	17.36	2.54	5.70	15.40	308.79	326.55	355.82
365	1860.	322.5	807.61	37.02	17.37	2.54	5.70	15.40	308.79	326.56	355.84
366	1865.	322.4	807.74	37.01	17.38	2.55	5.71	15.42	308.79	326.57	355.88
367	1870.	322.4	807.68	37.02	17.38	2.55	5.70	15.41	308.79	326.56	355.86
368	1875.	322.9	807.29	37.03	17.34	2.53	5.70	15.39	308.80	326.55	355.80
369	1880.	323.7	806.72	37.00	17.34	2.51	5.70	15.39	308.85	326.61	355.89
370	1885.	324.6	806.15	36.88	17.39	2.51	5.70	15.46	308.97	326.75	356.23
371	1890.	325.5	805.76	36.66	17.49	2.52	5.70	15.56	309.12	326.92	356.72
372	1895.	326.4	805.61	36.39	17.59	2.50	5.70	15.66	309.25	327.04	357.19
373	1900.	327.0	805.64	36.16	17.66	2.47	5.69	15.73	309.32	327.08	357.48
374	1905.	327.2	805.67	36.06	17.69	2.46	5.68	15.75	309.34	327.08	357.57
375	1910.	326.9	805.63	36.18	17.66	2.48	5.69	15.73	309.31	327.08	357.45
376	1915.	326.0	805.66	36.52	17.55	2.51	5.70	15.62	309.19	326.99	356.97
377	1920.	324.3	806.33	36.93	17.37	2.51	5.70	15.43	308.93	326.70	356.09

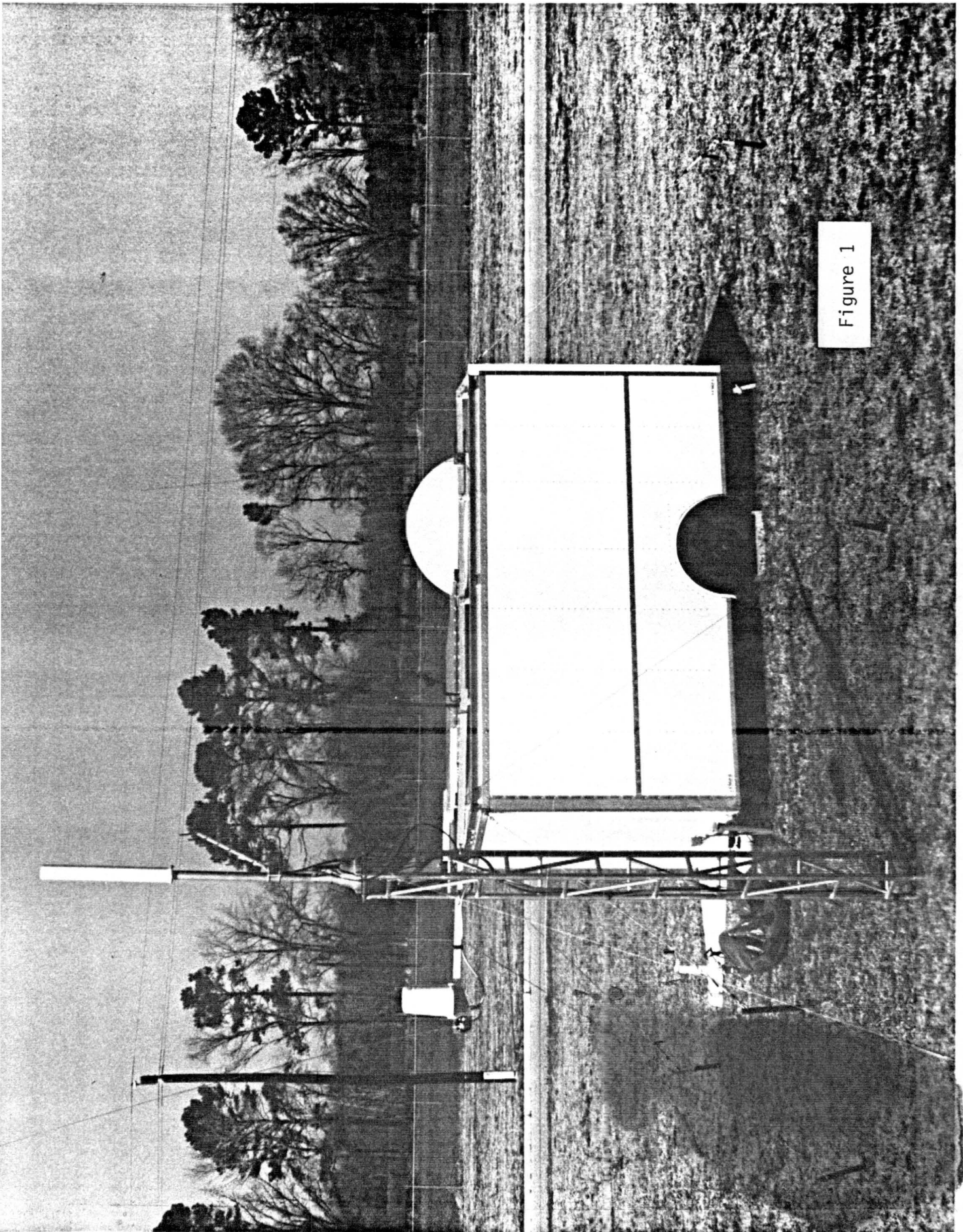


Figure 1

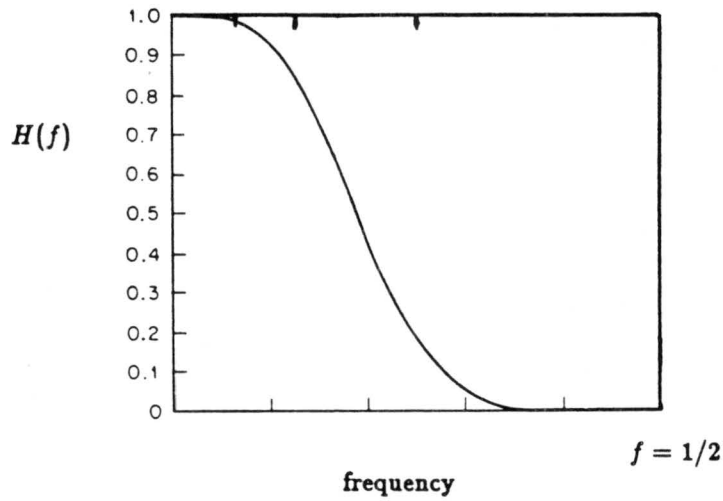
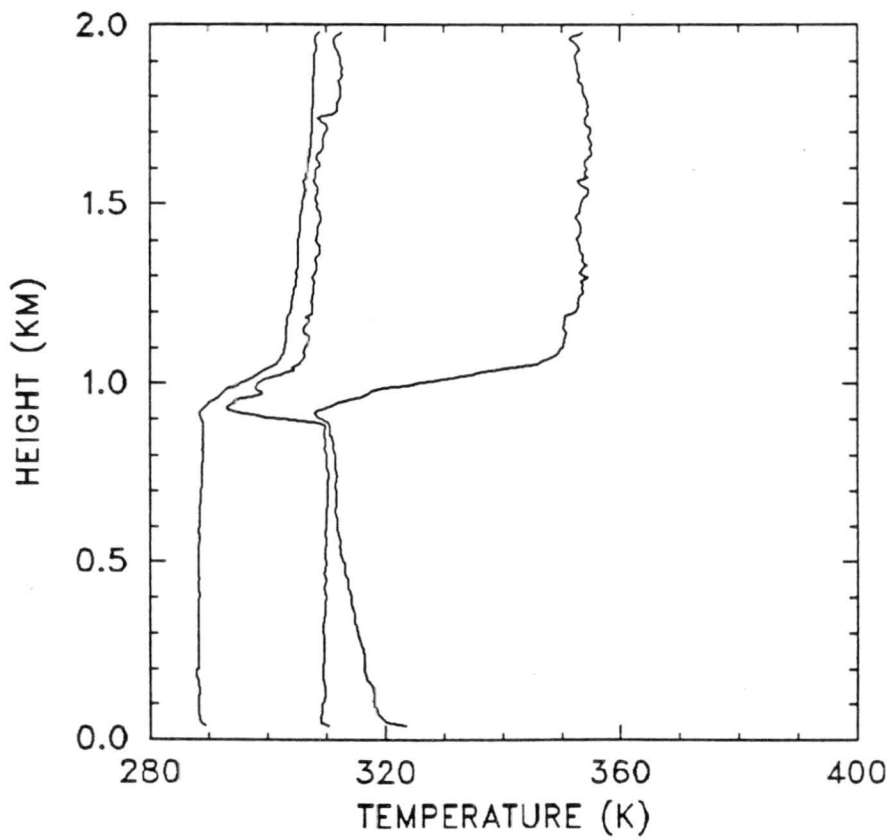
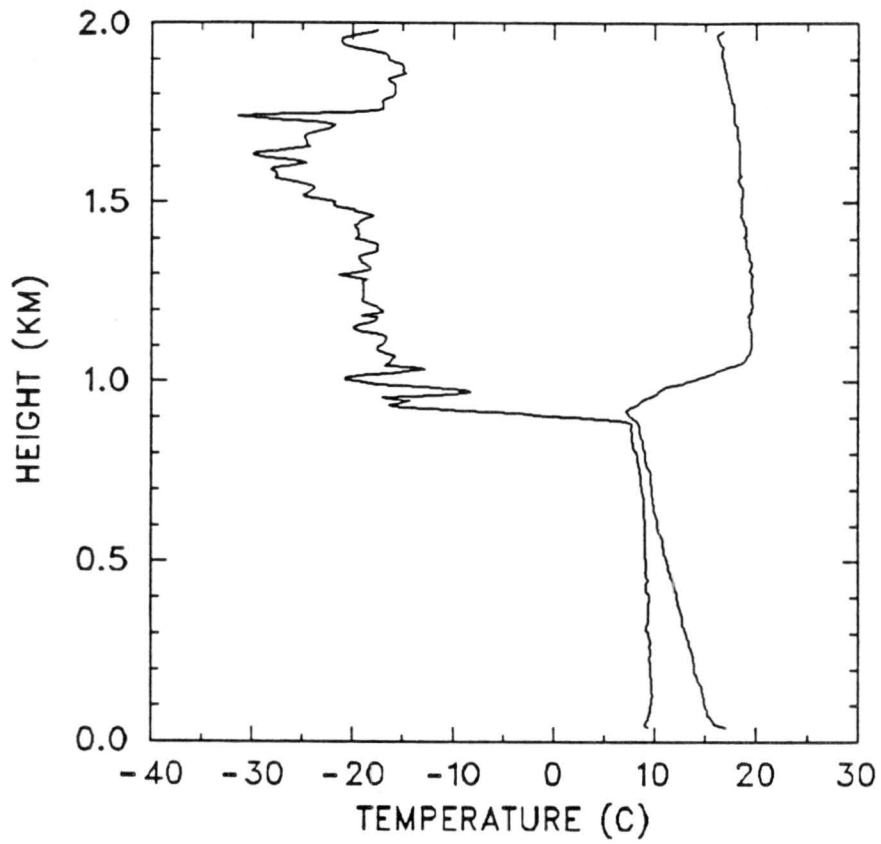


Figure 2. Response curve for the monotone filter described in text. The frequency  $f = 1/2$  corresponds to one-half of a cycle per observation interval; i.e.,  $f = 1/2$  is the Nyquist frequency.

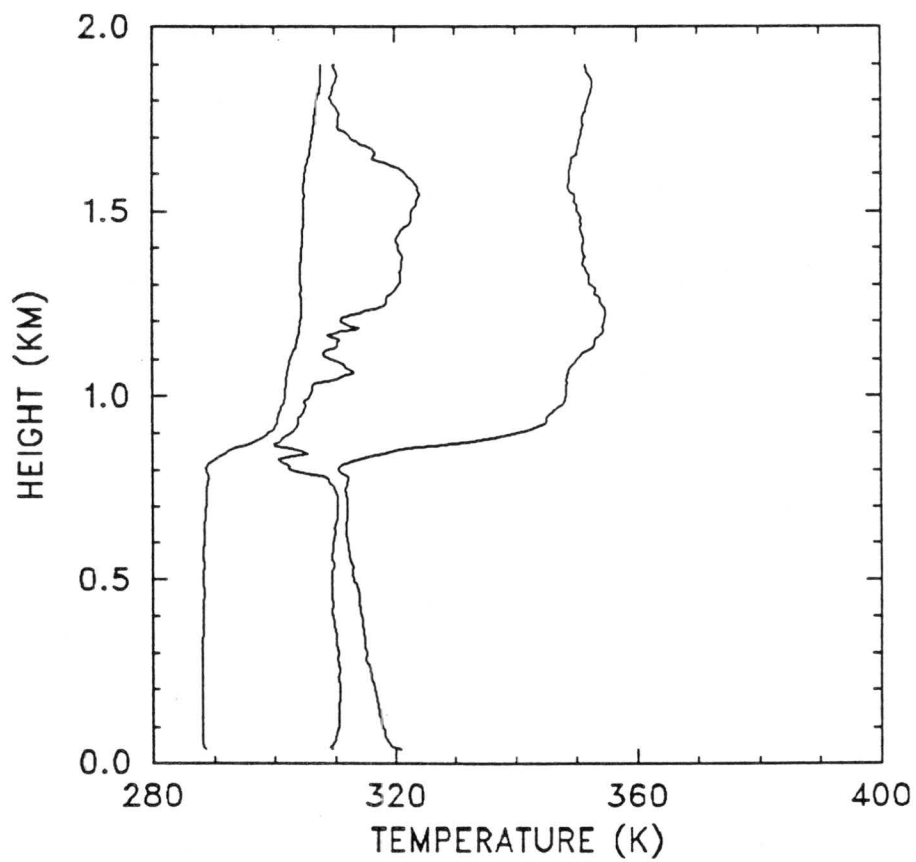
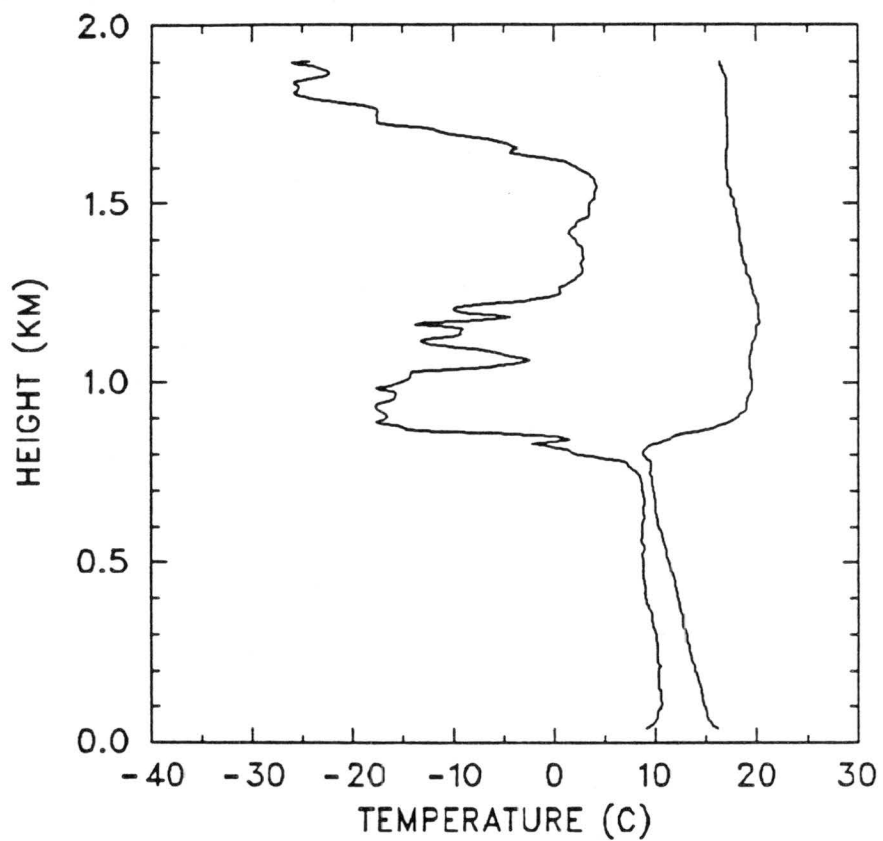
Figure 3. Top panel: vertical profile of  $T$  and  $T_d$ .  
Bottom panel: vertical profile of  $\theta$ ,  $\theta_e$  and  $\theta_{e,s}$ .

1155 GMT 30 JUNE 1987

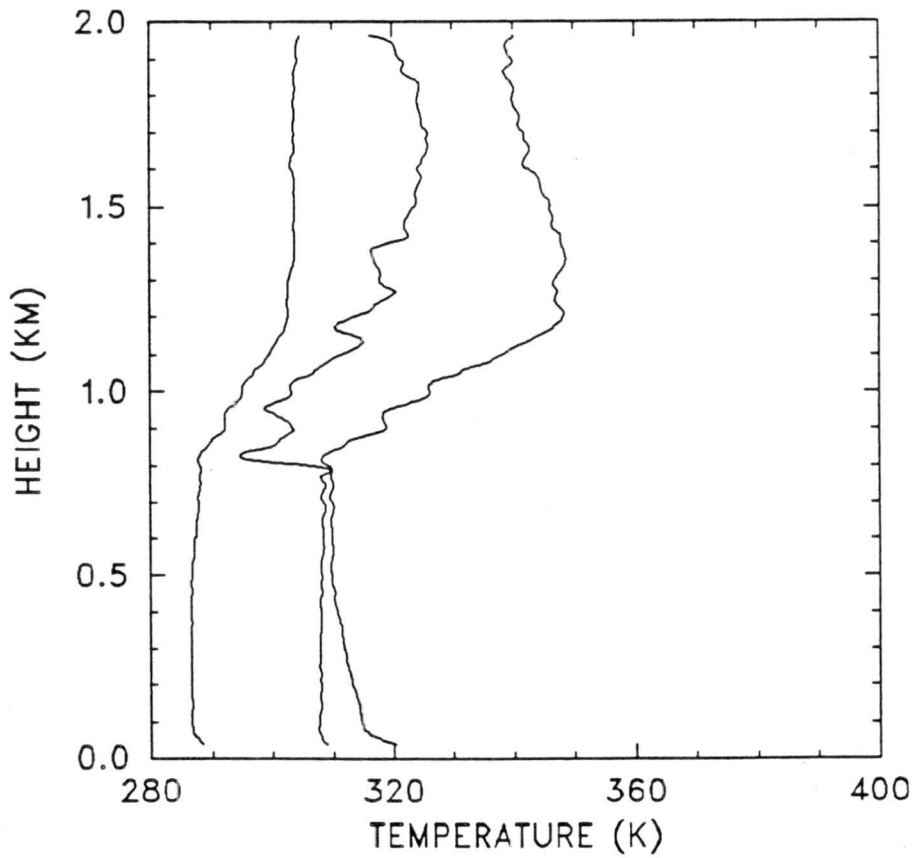
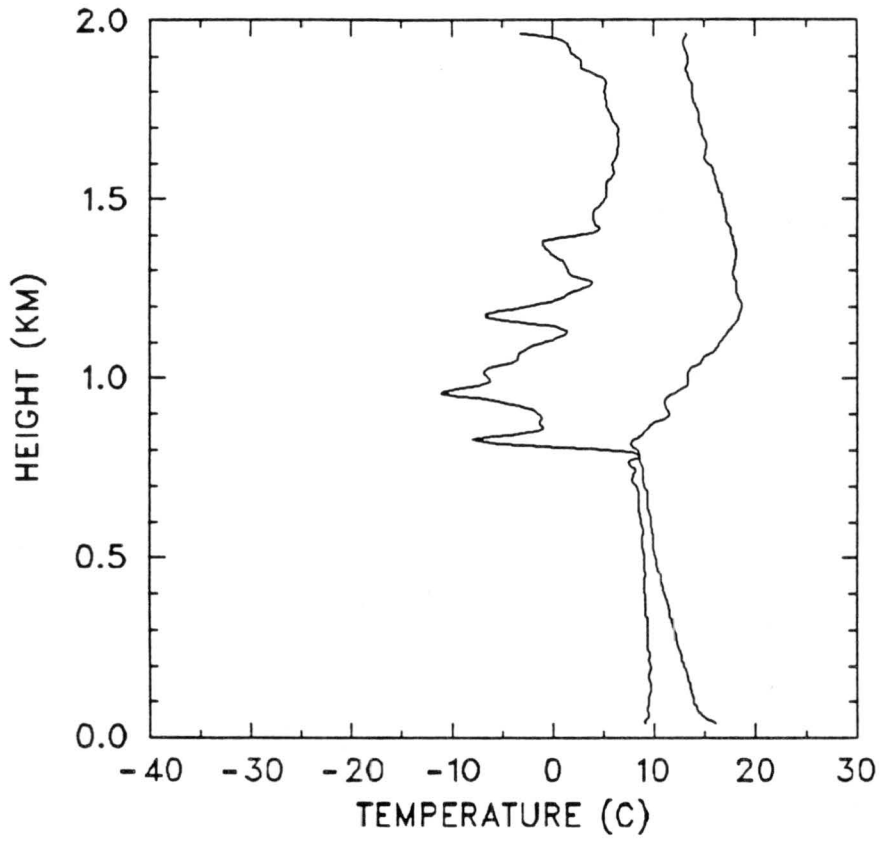




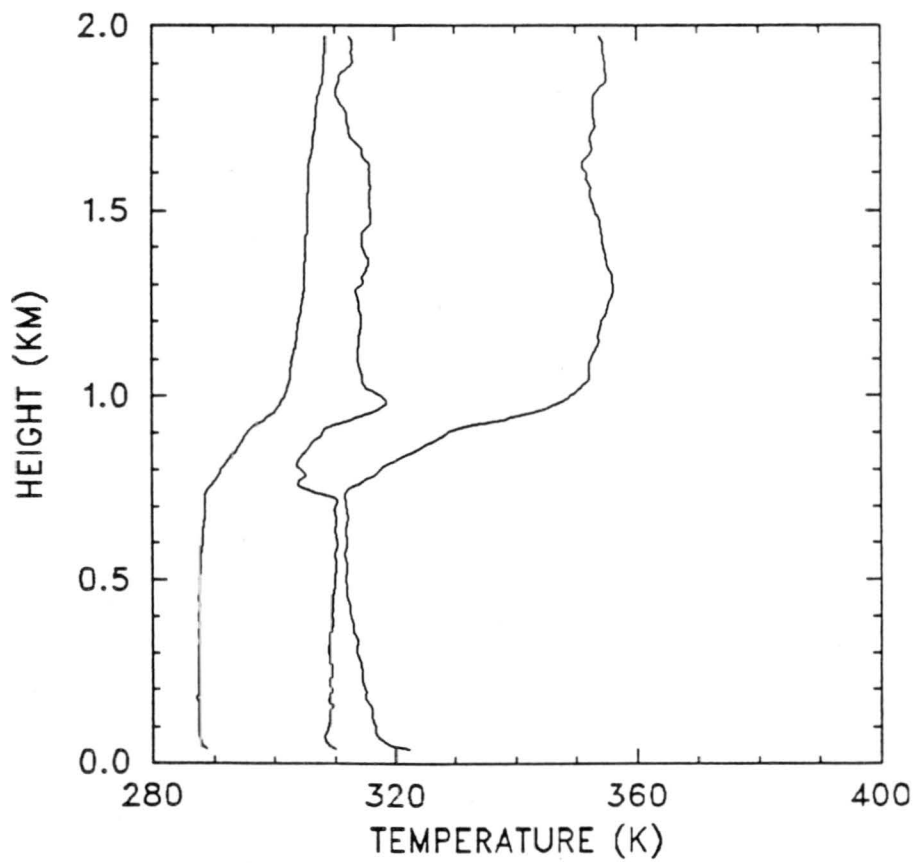
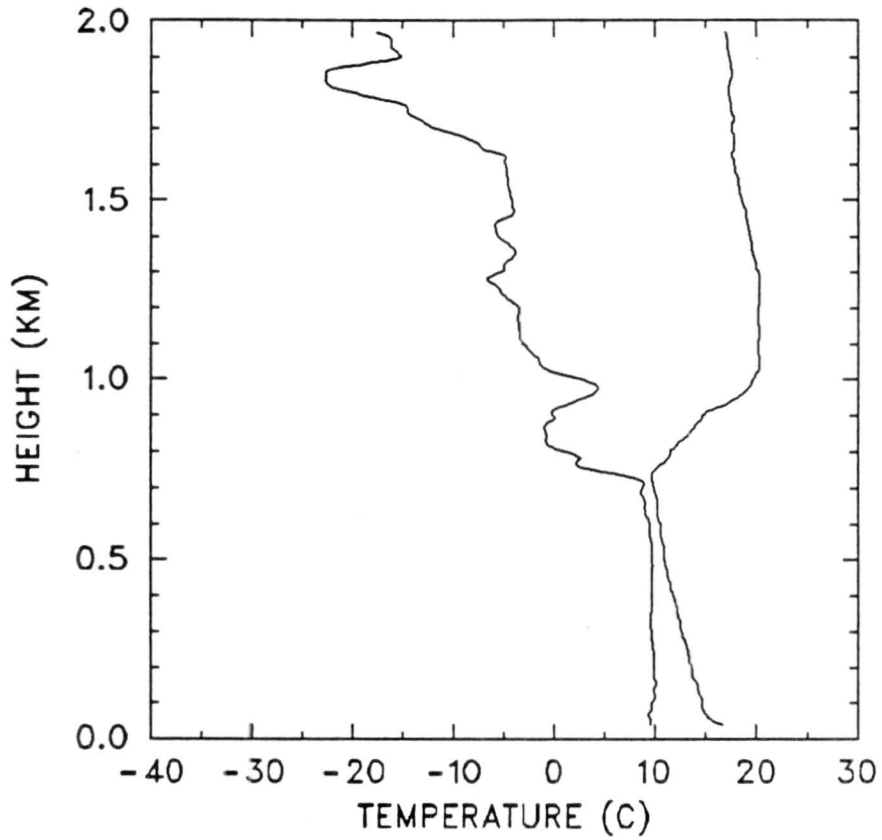
2351 GMT 30 JUNE 1987



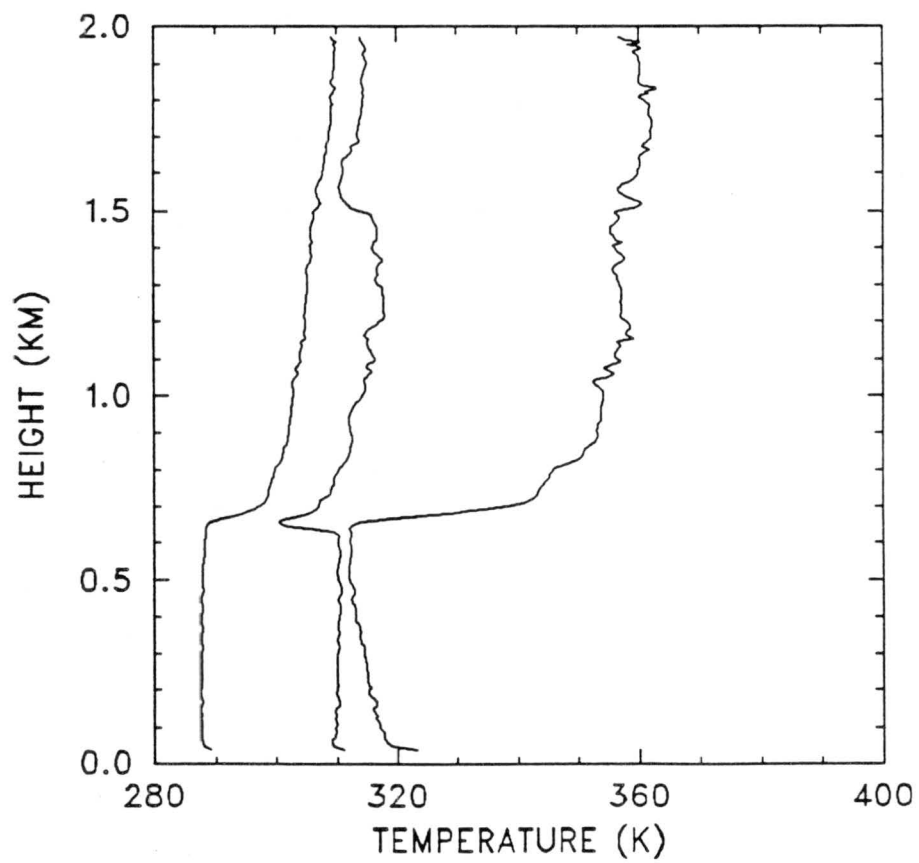
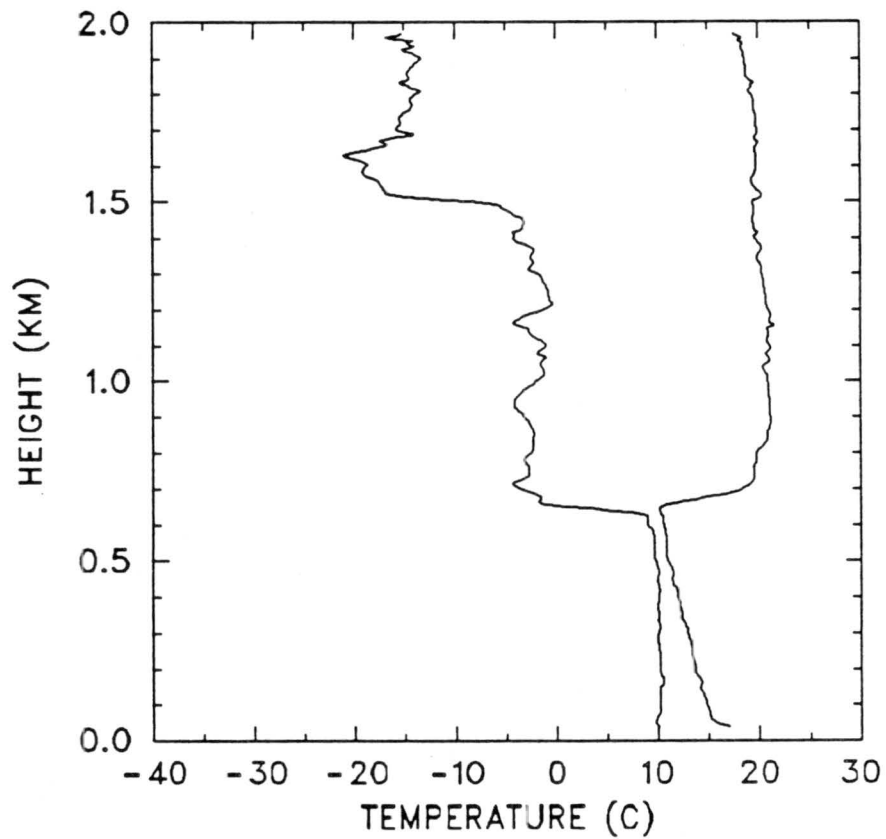
1216 GMT 01 JULY 1987



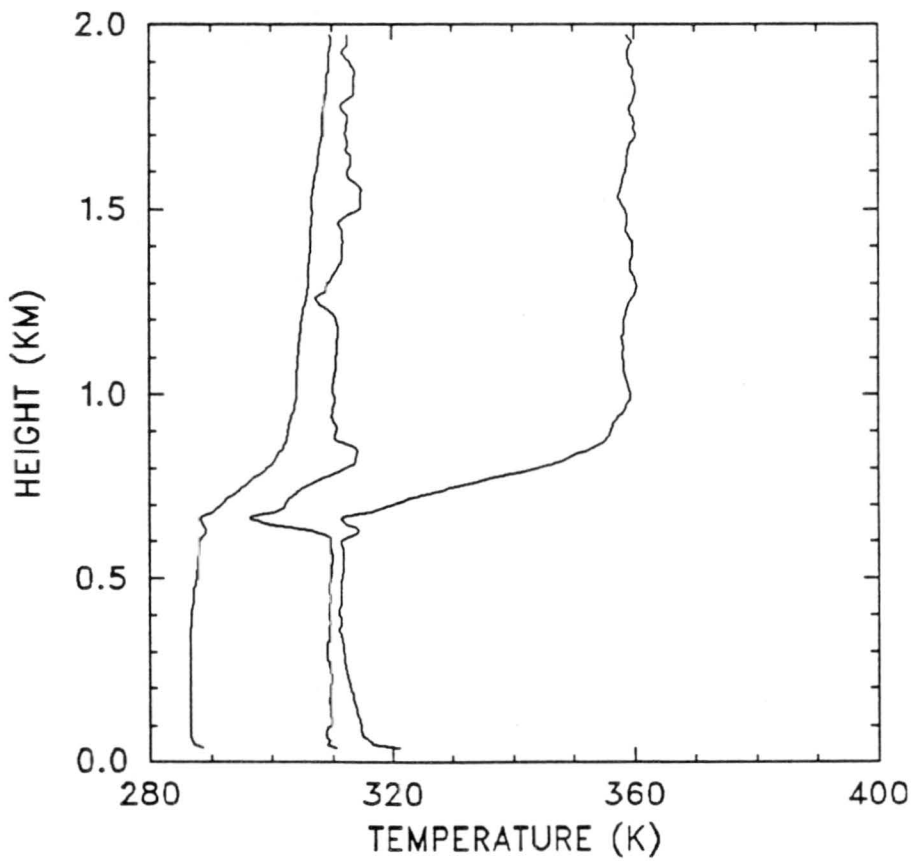
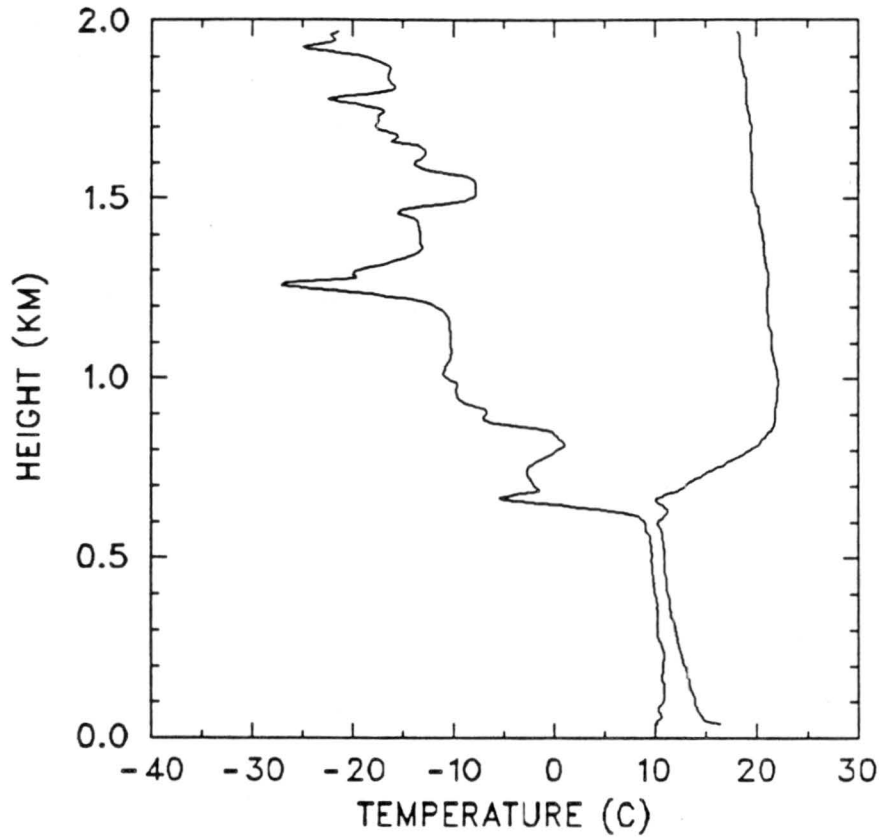
2009 GMT 01 JULY 1987



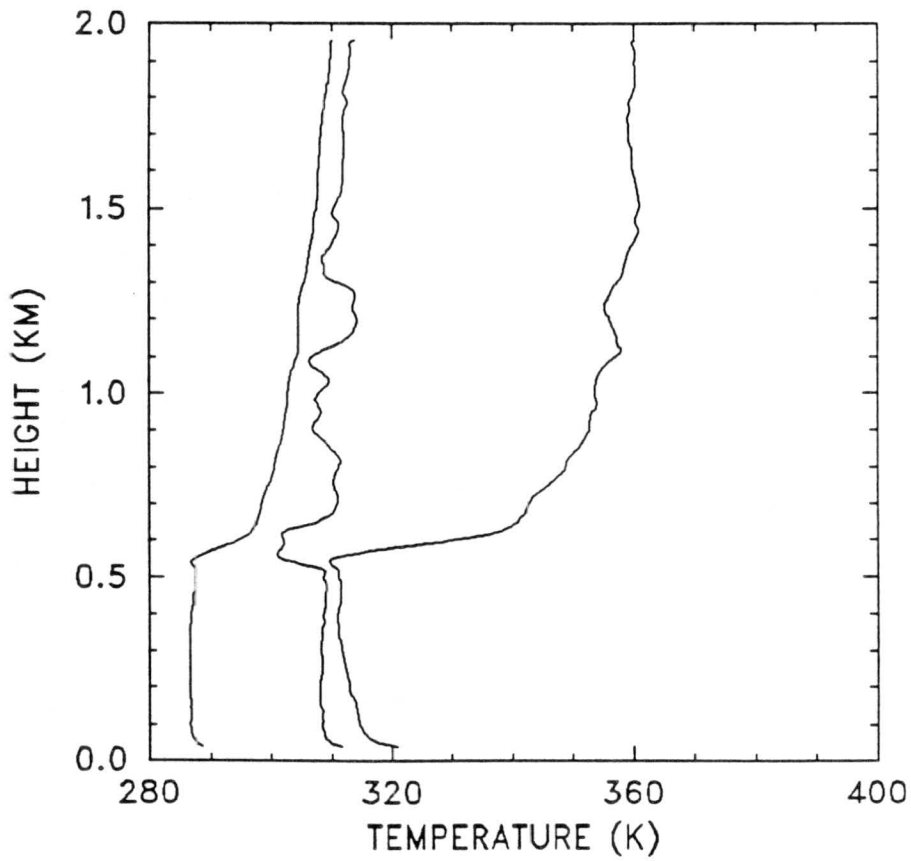
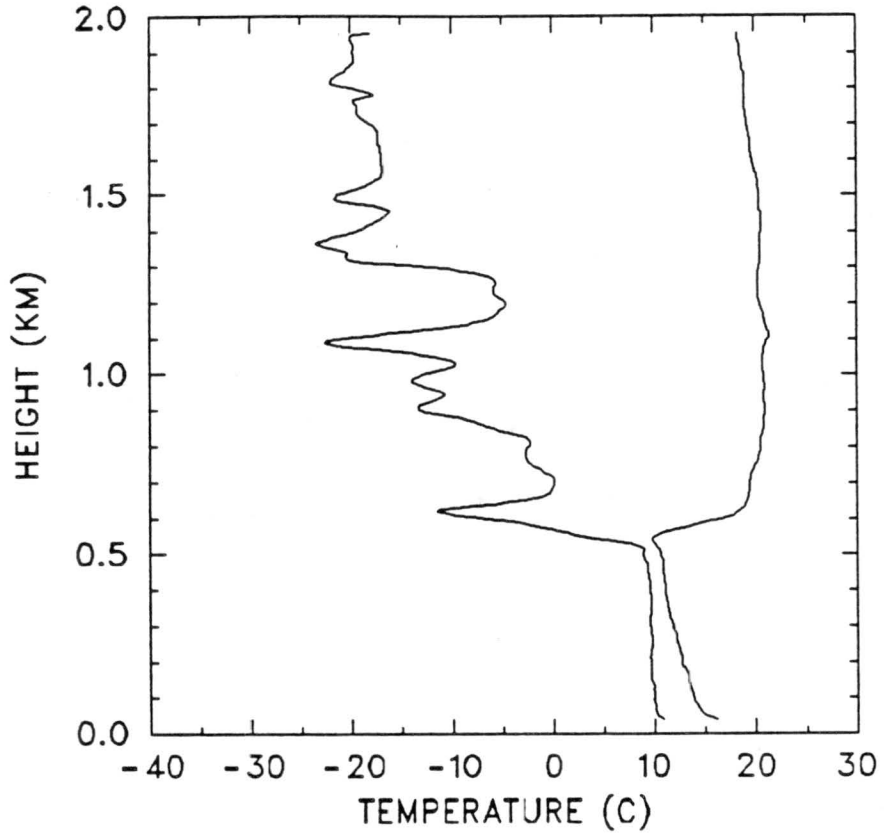
2311 GMT 01 JULY 1987



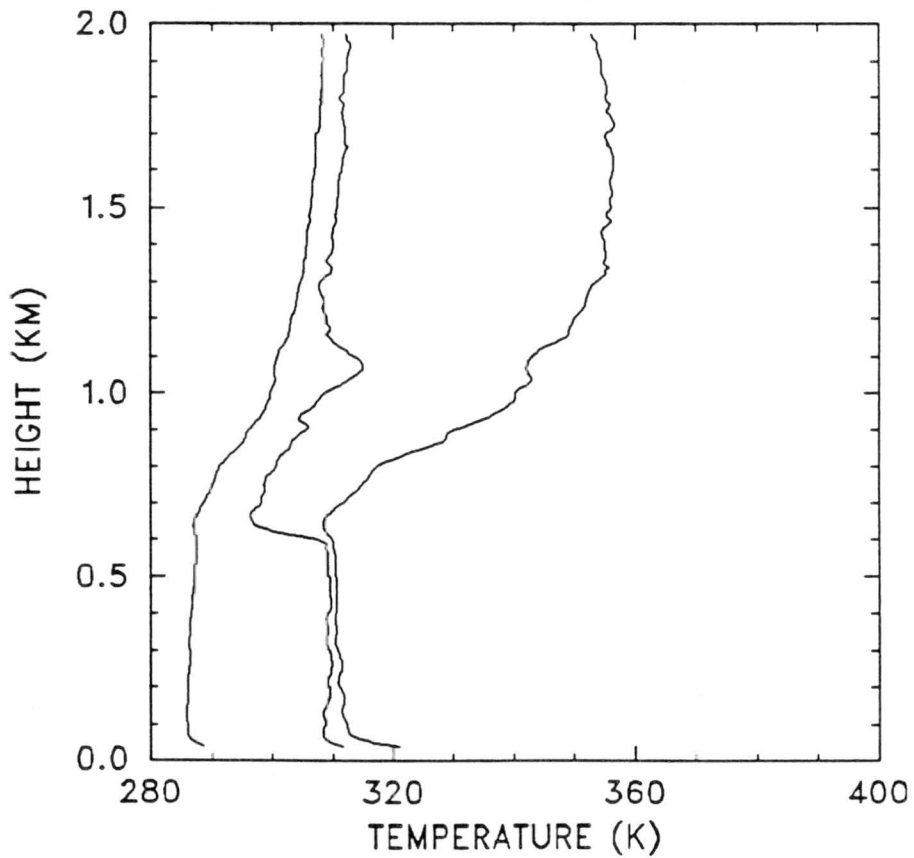
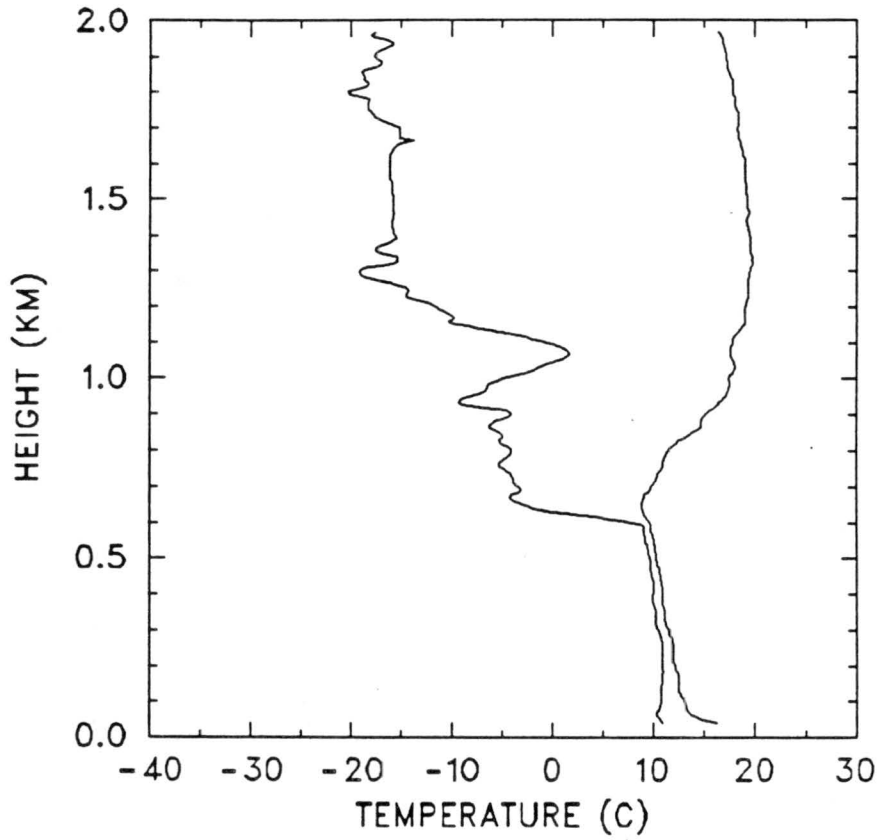
1750 GMT 02 JULY 1987



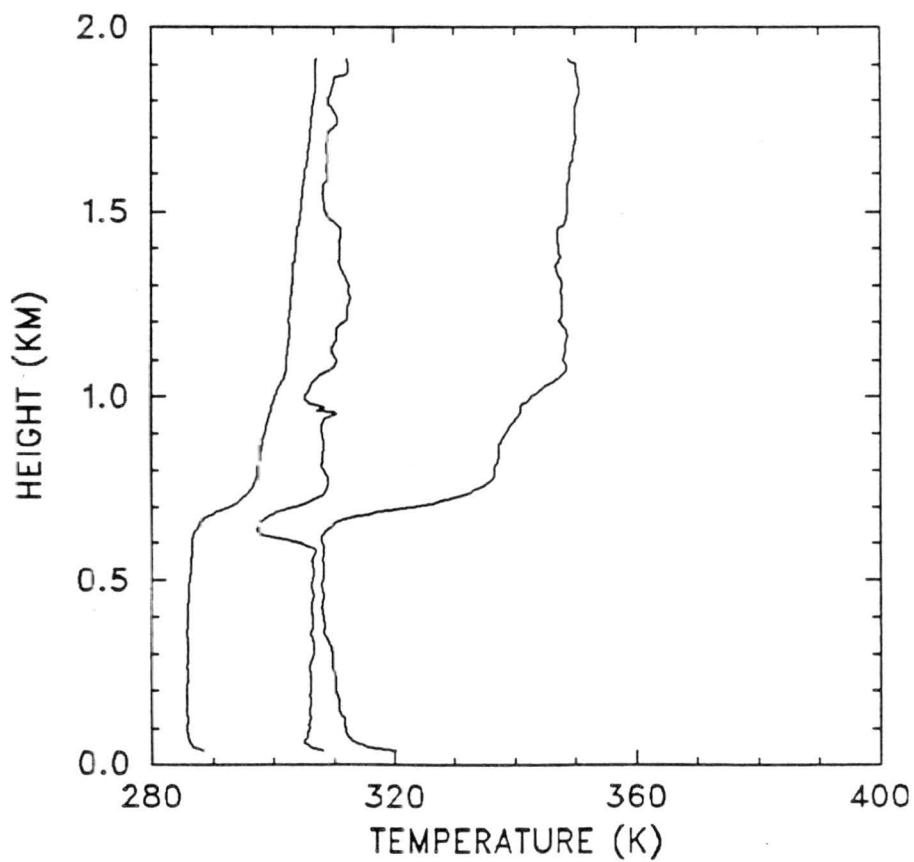
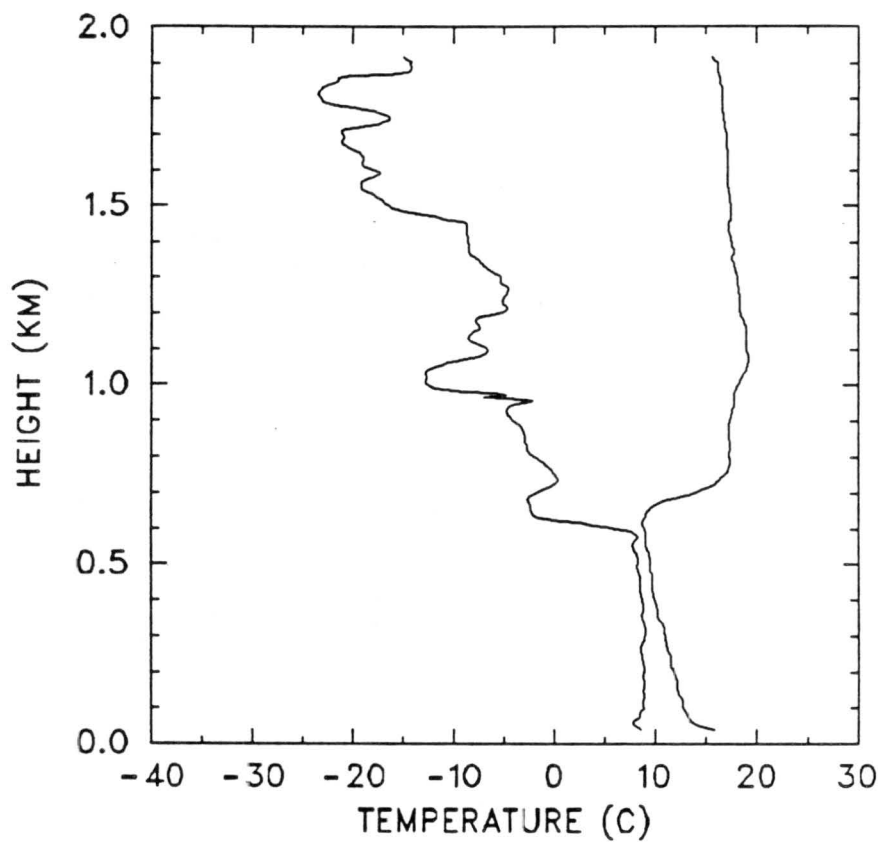
2253 GMT 02 JULY 1987



1208 GMT 03 JULY 1987

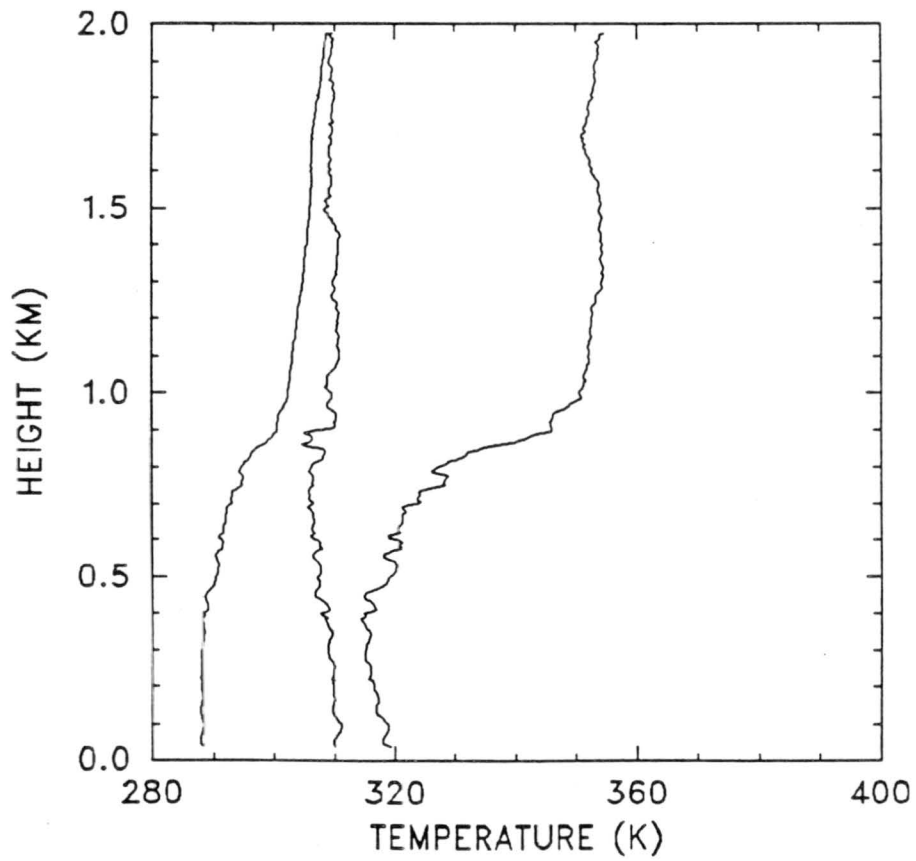
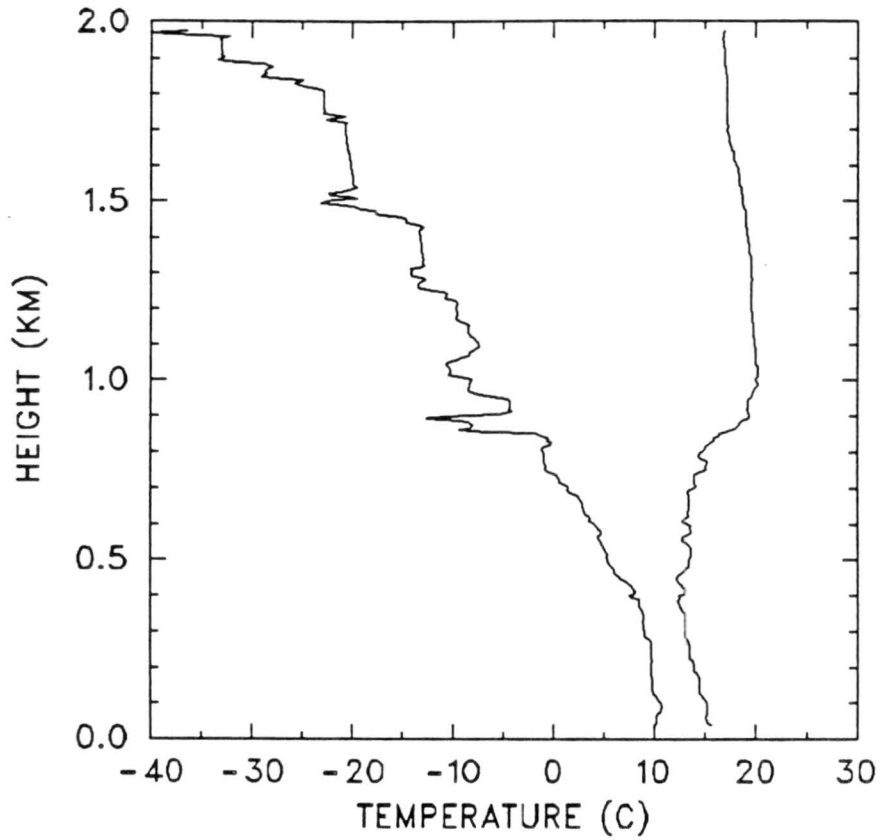


1808 GMT 03 JULY 1987

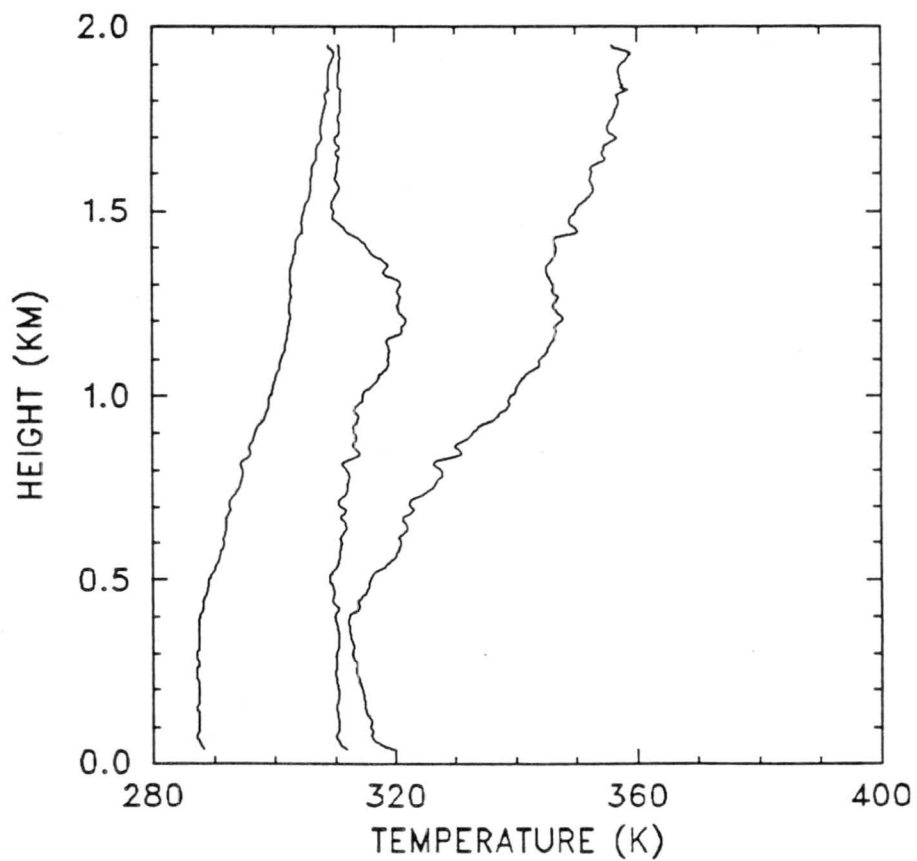
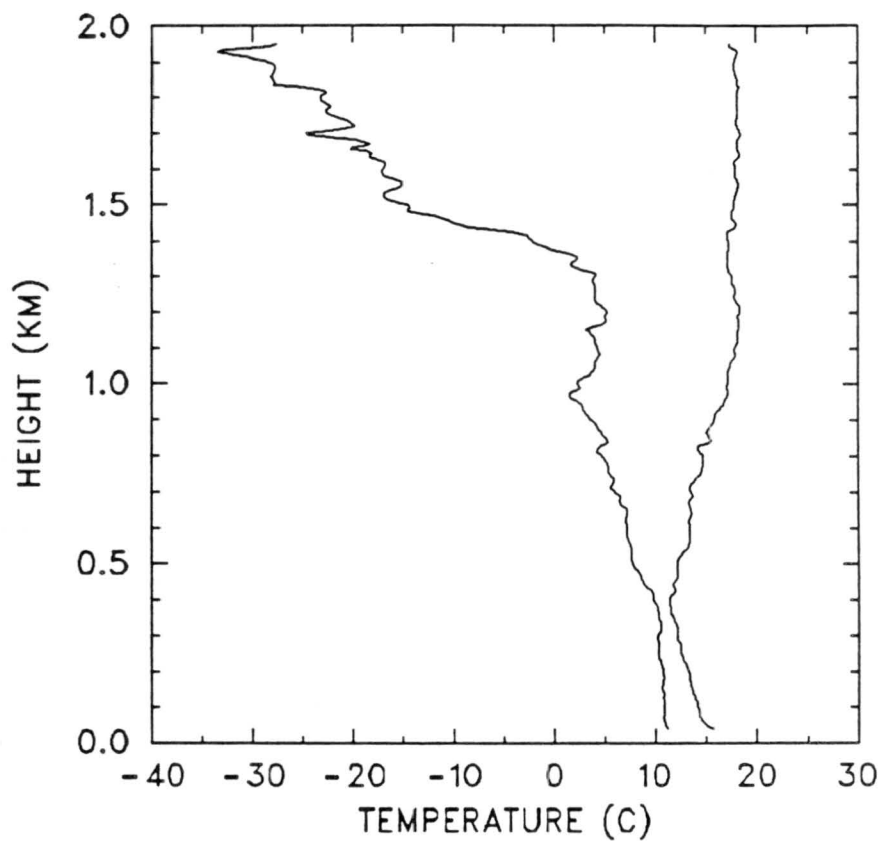




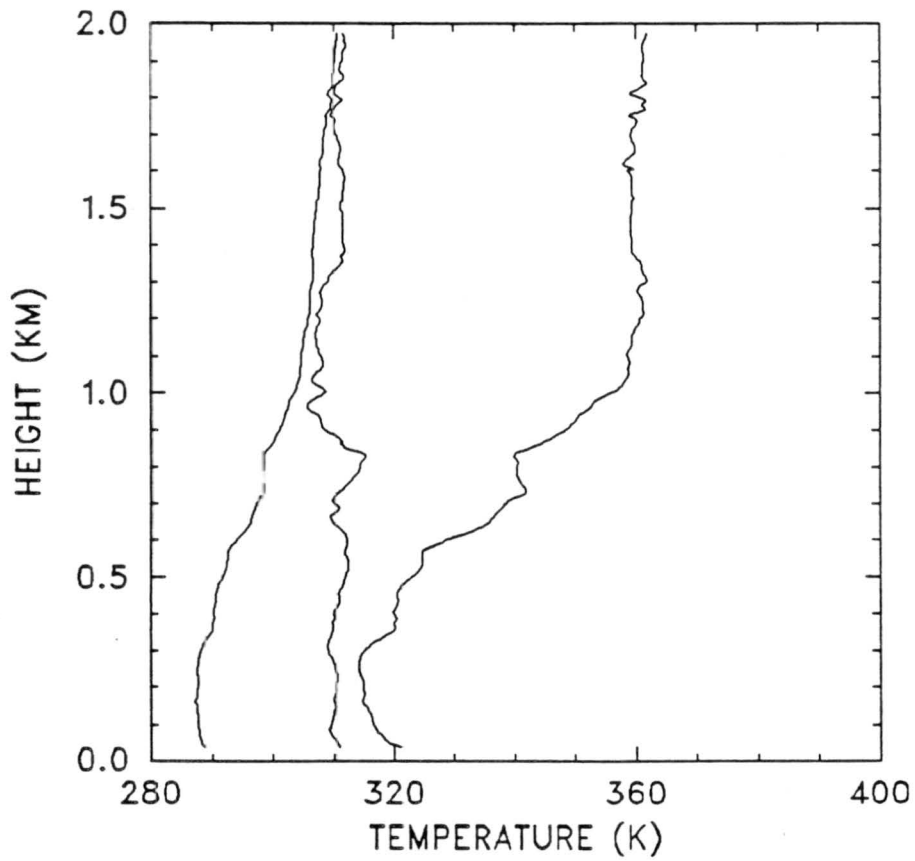
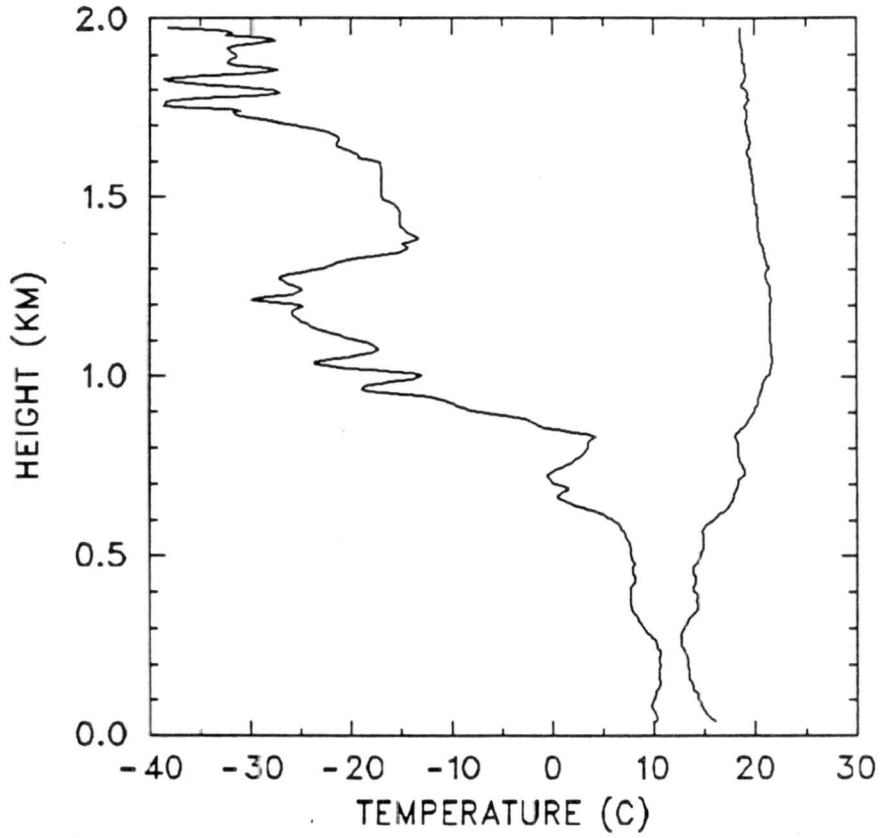
0036 GMT 04 JULY 1987



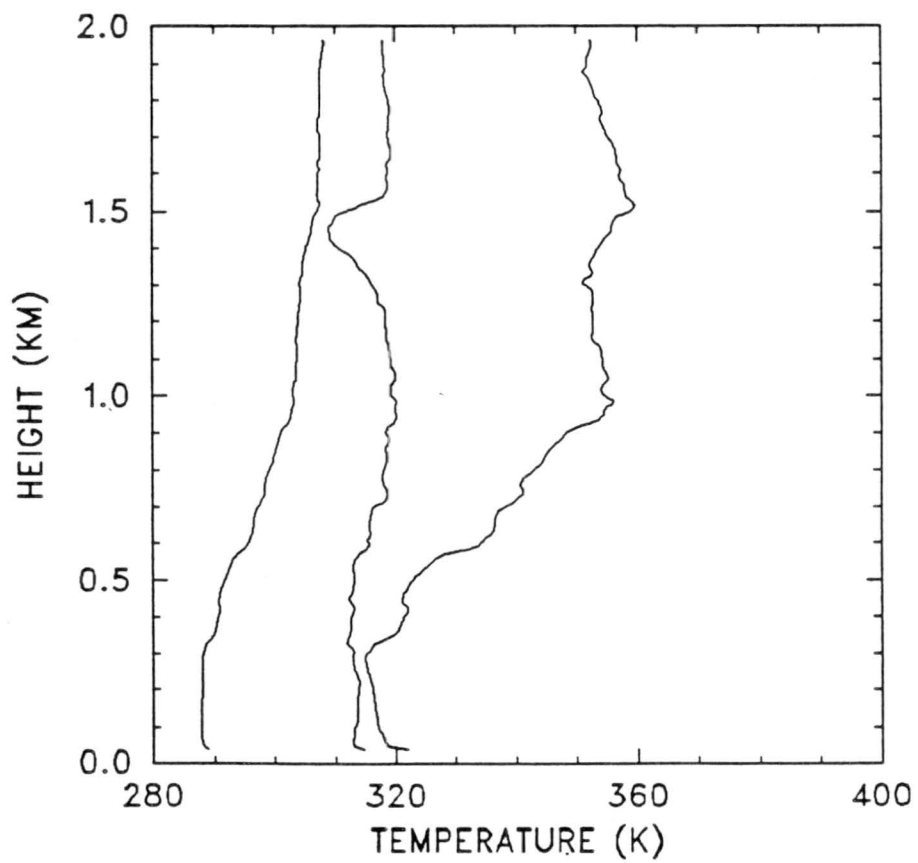
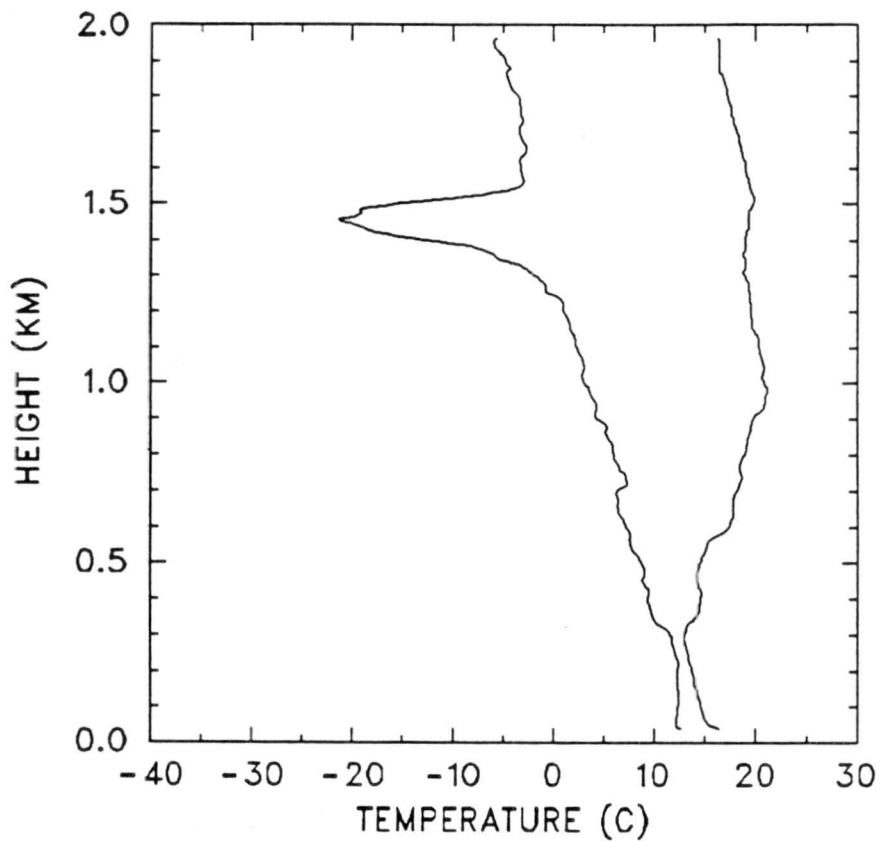
1215 GMT 04 JULY 1987



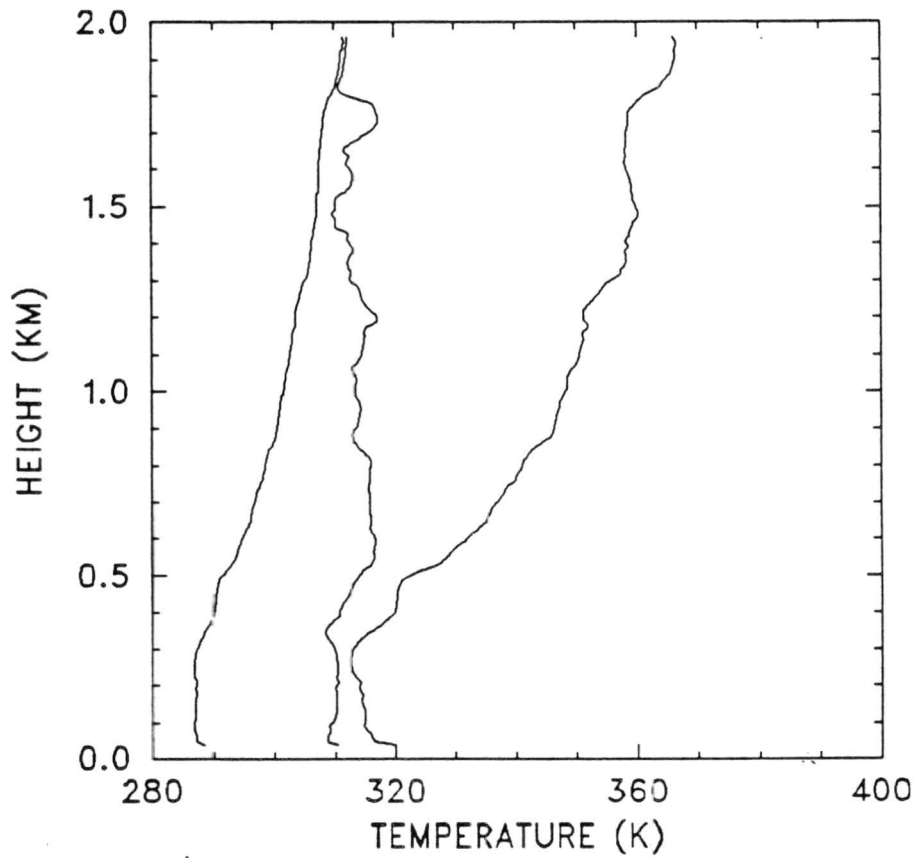
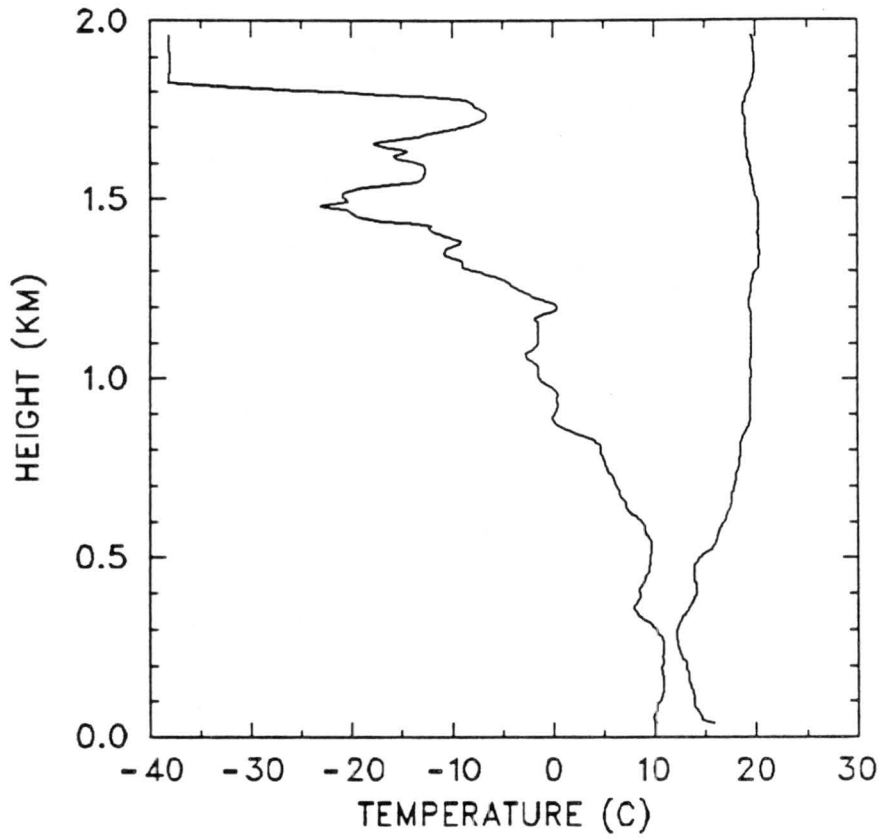
0034 GMT 05 JULY 1987



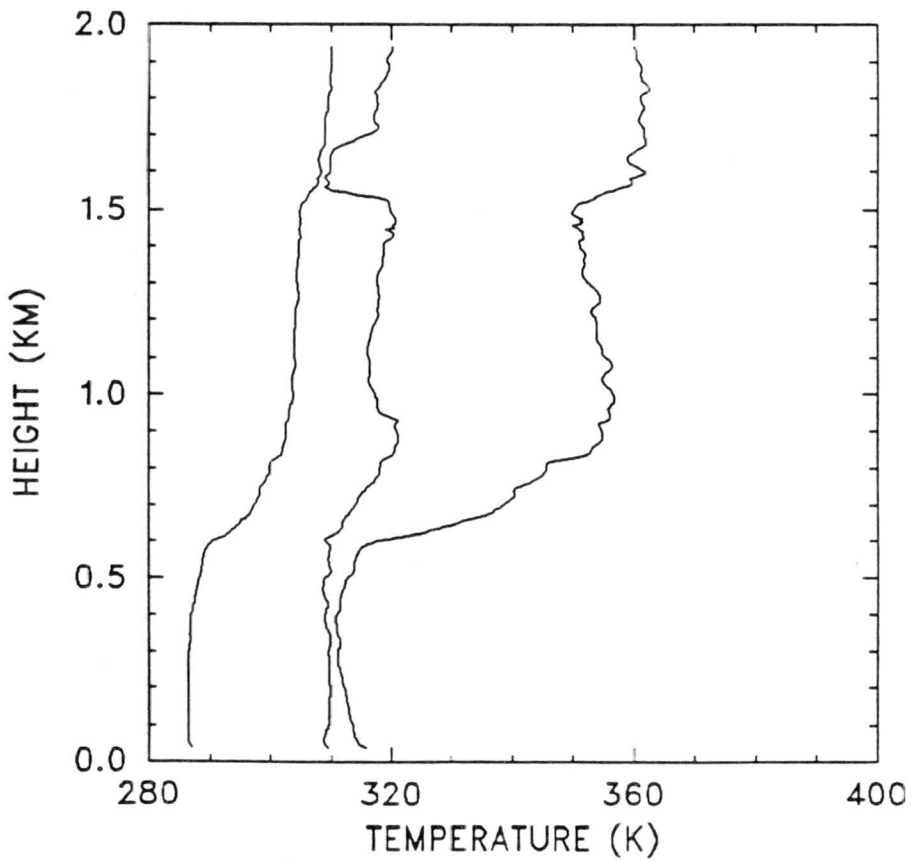
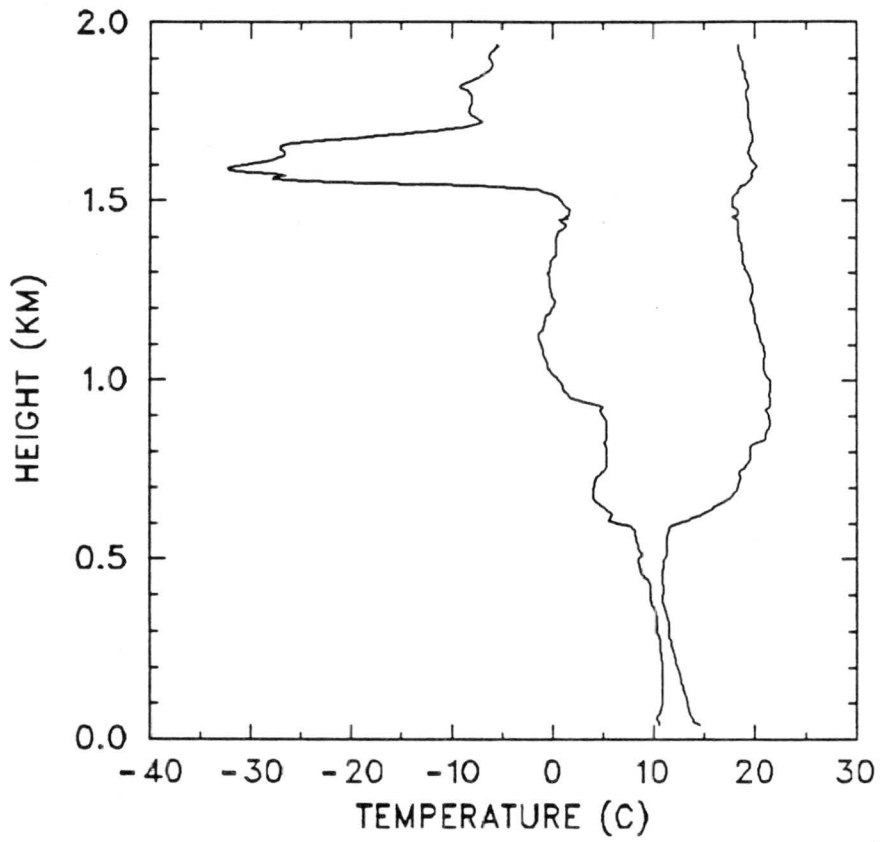
1158 GMT 05 JULY 1987



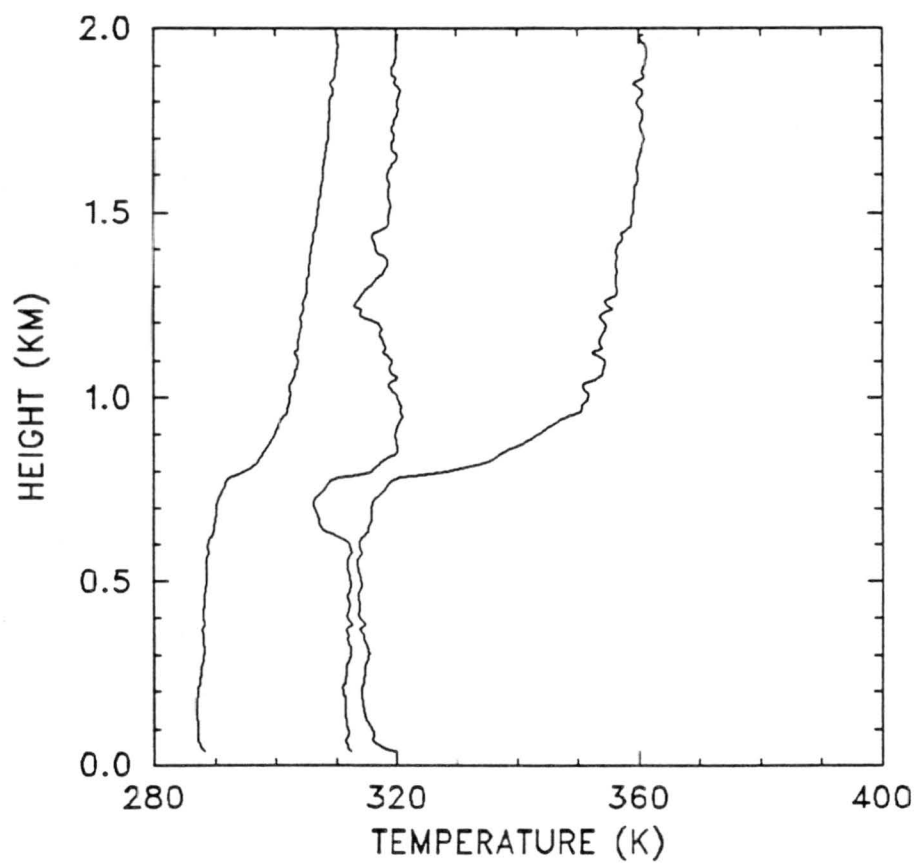
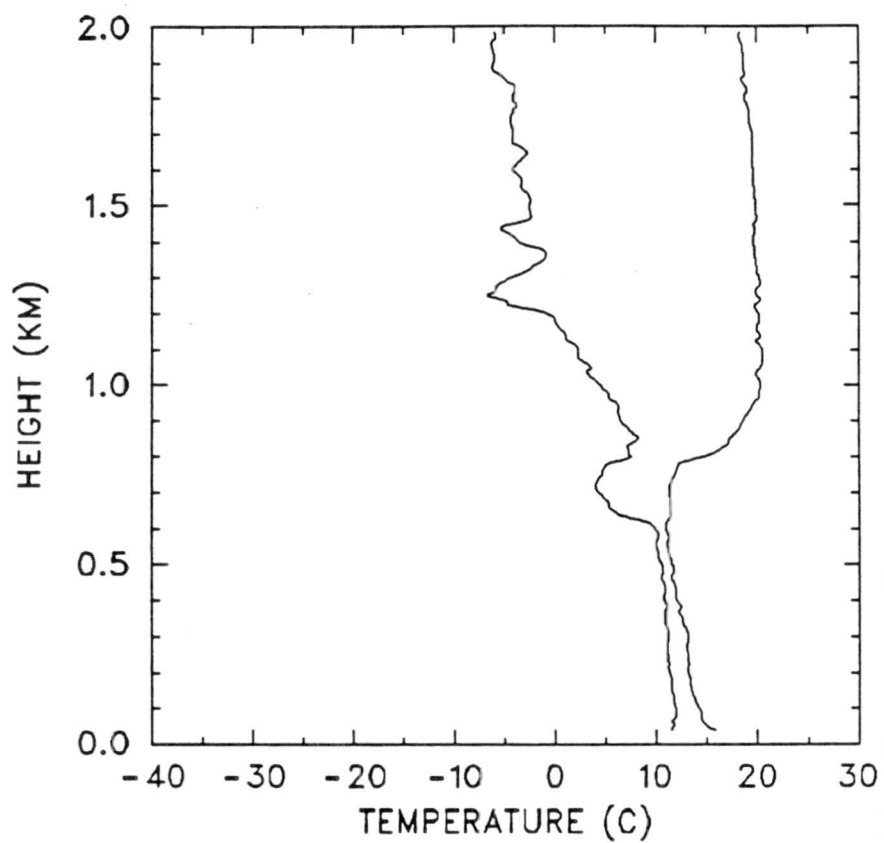
0145 GMT 06 JULY 1987



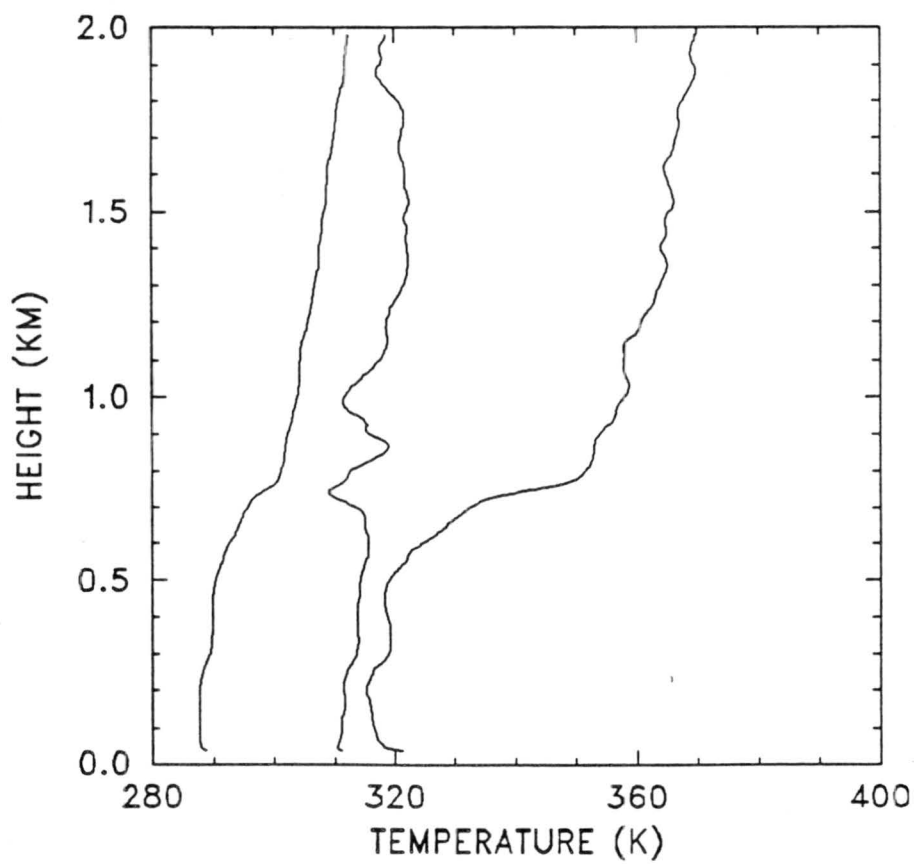
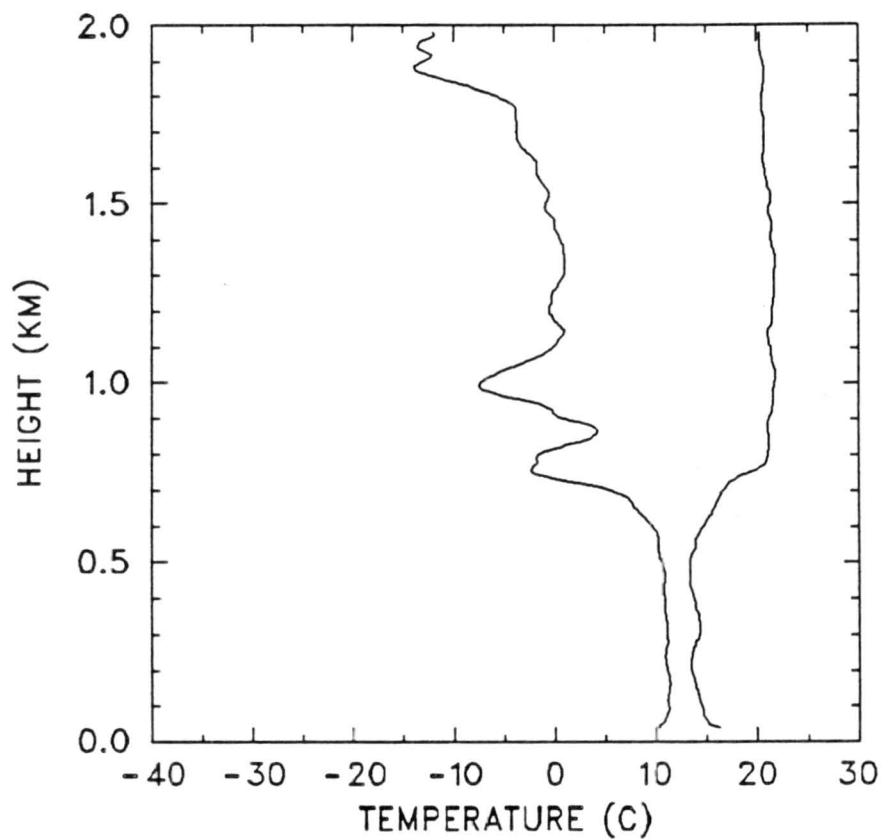
1214 GMT 06 JULY 1987



1607 GMT 06 JULY 1987

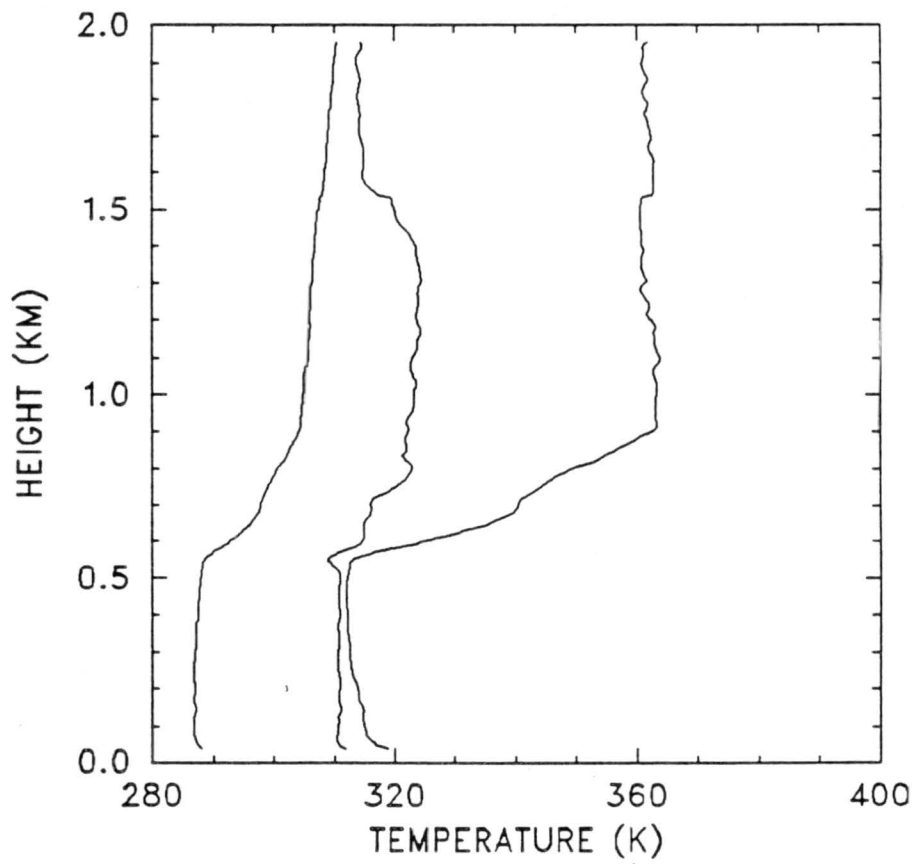
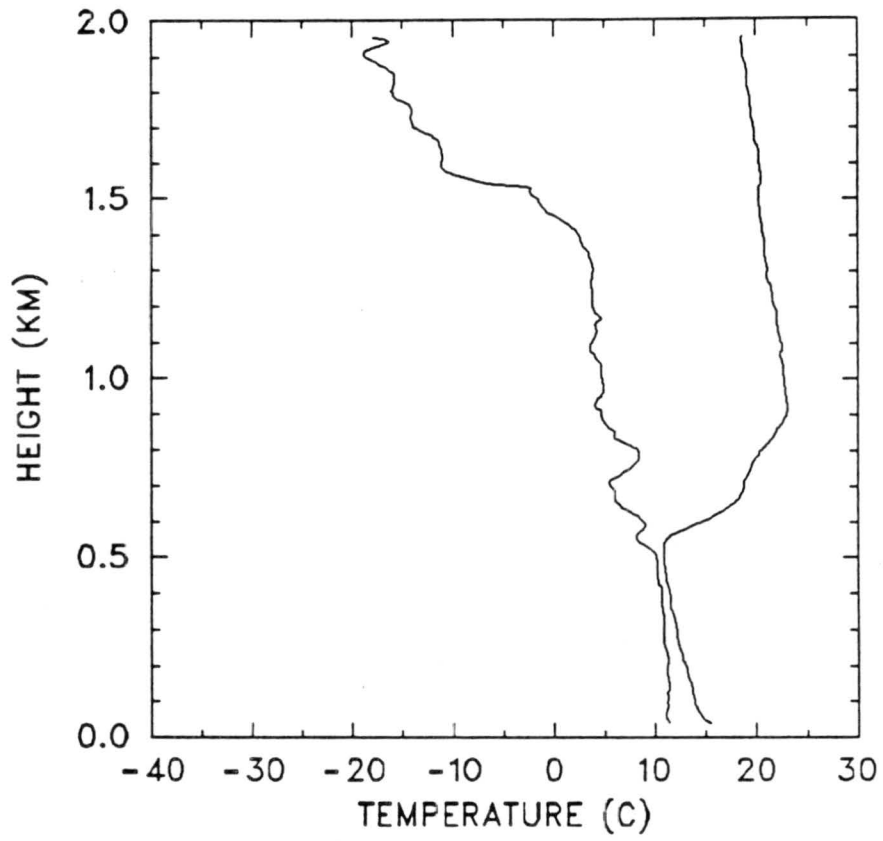


2350 GMT 06 JULY 1987

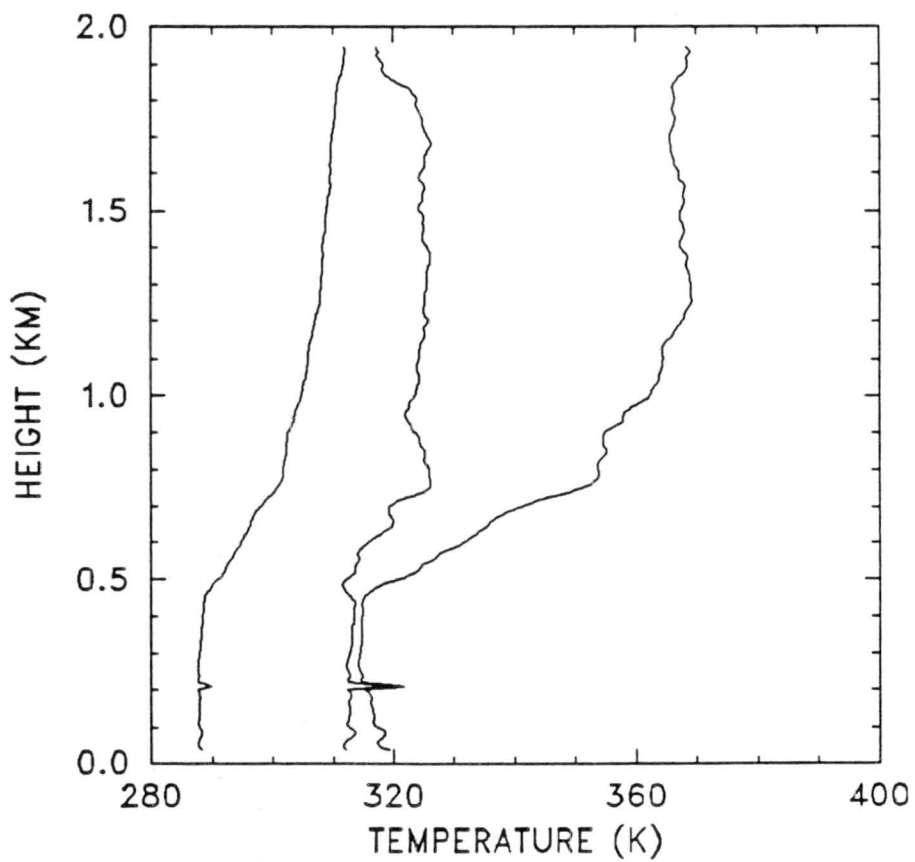
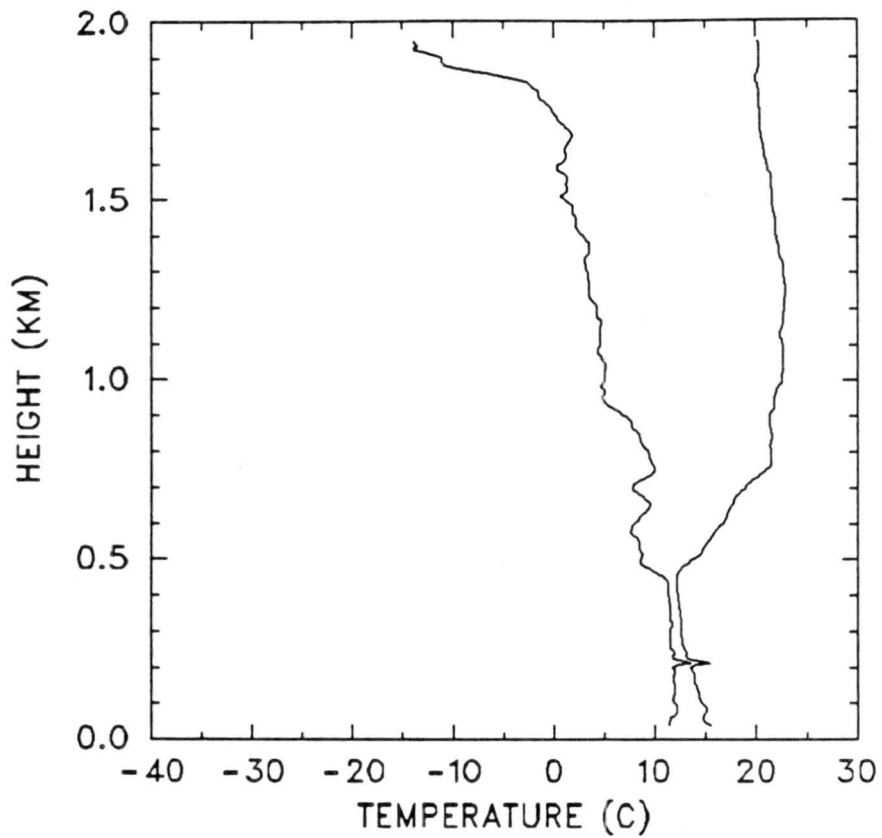




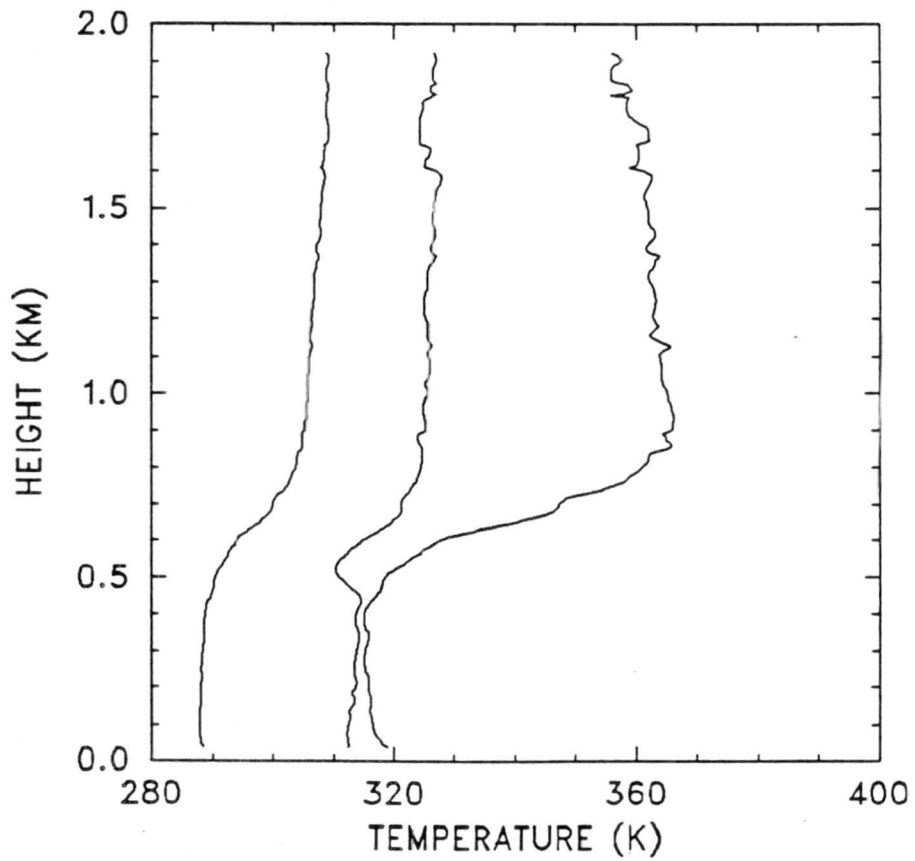
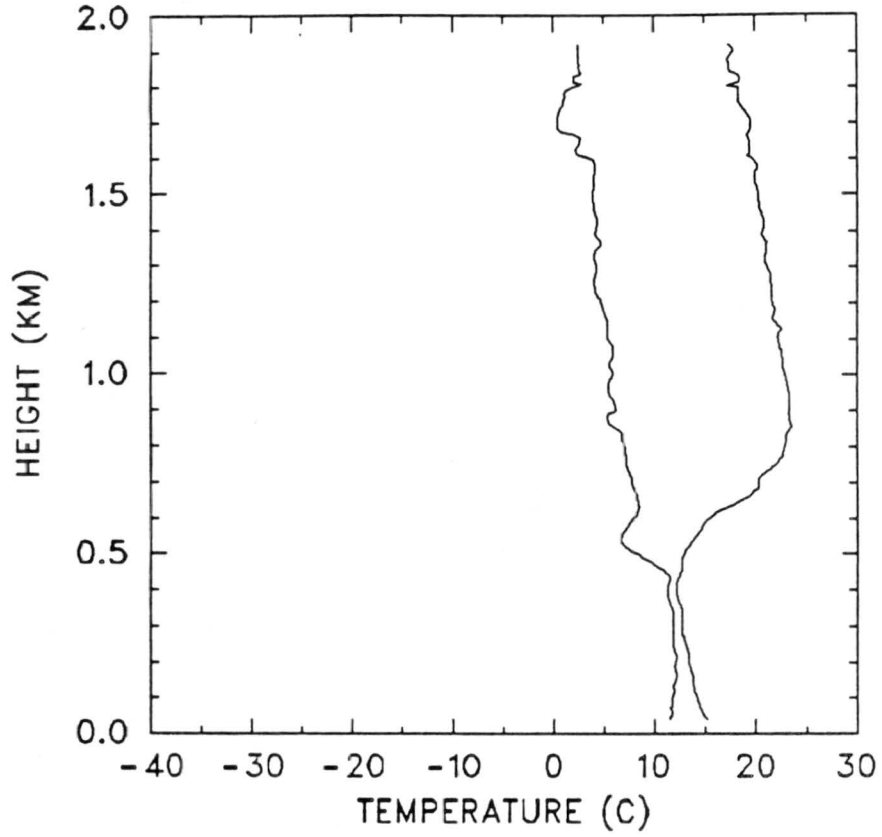
1159 GMT 07 JULY 1987



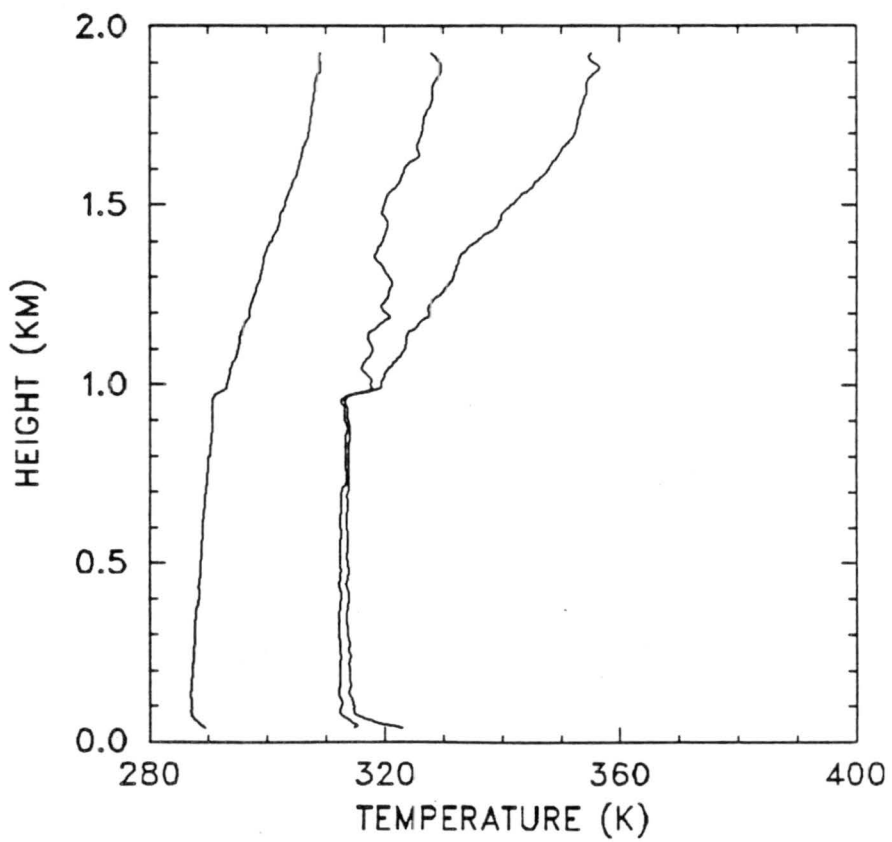
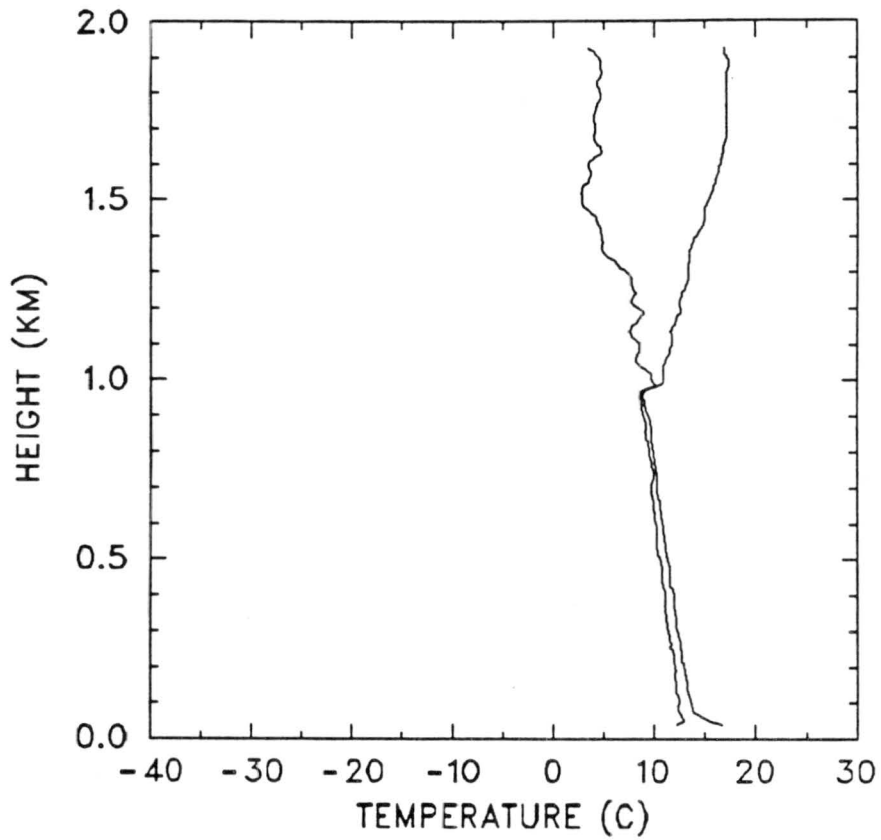
0011 GMT 08 JULY 1987



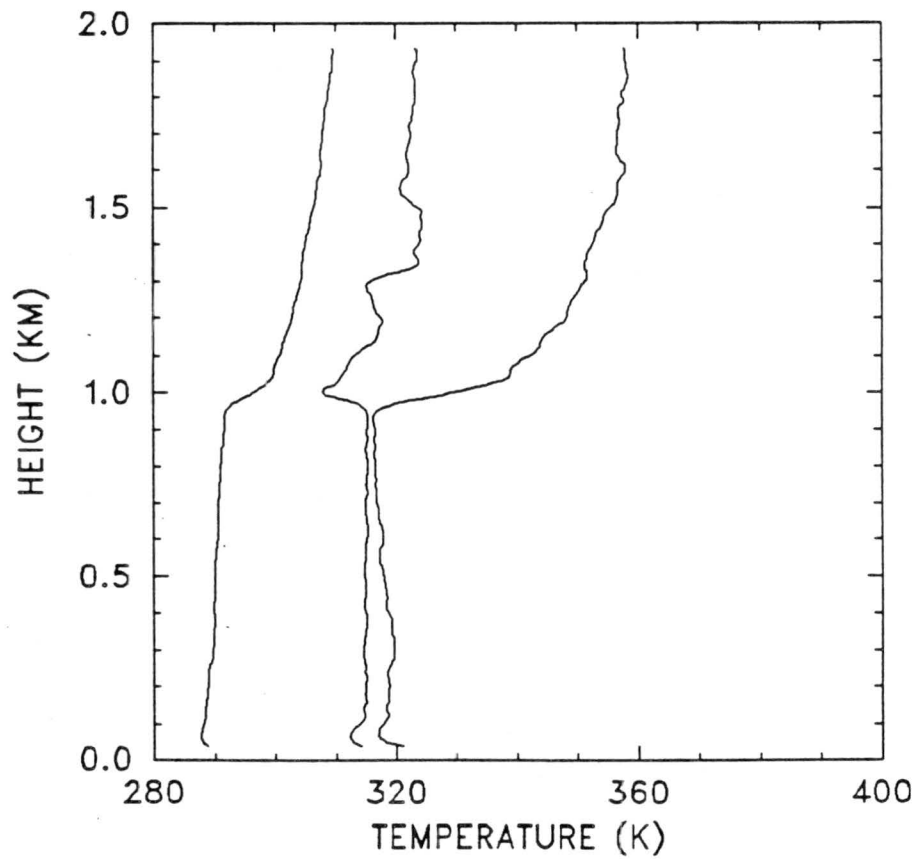
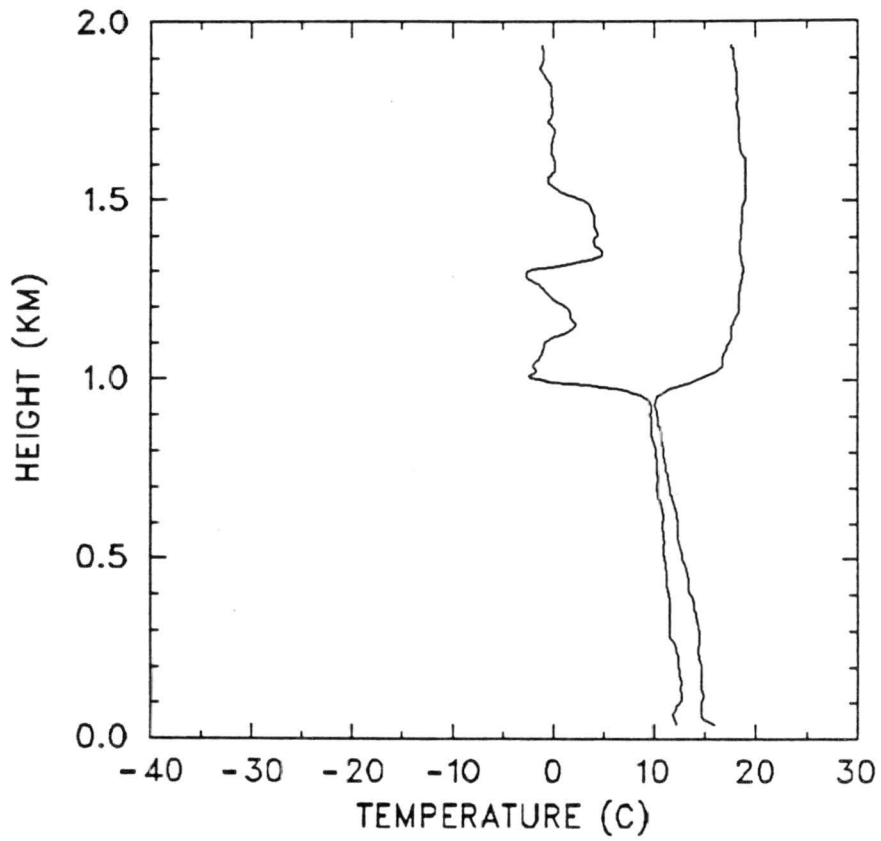
1211 GMT 08 JULY 1987



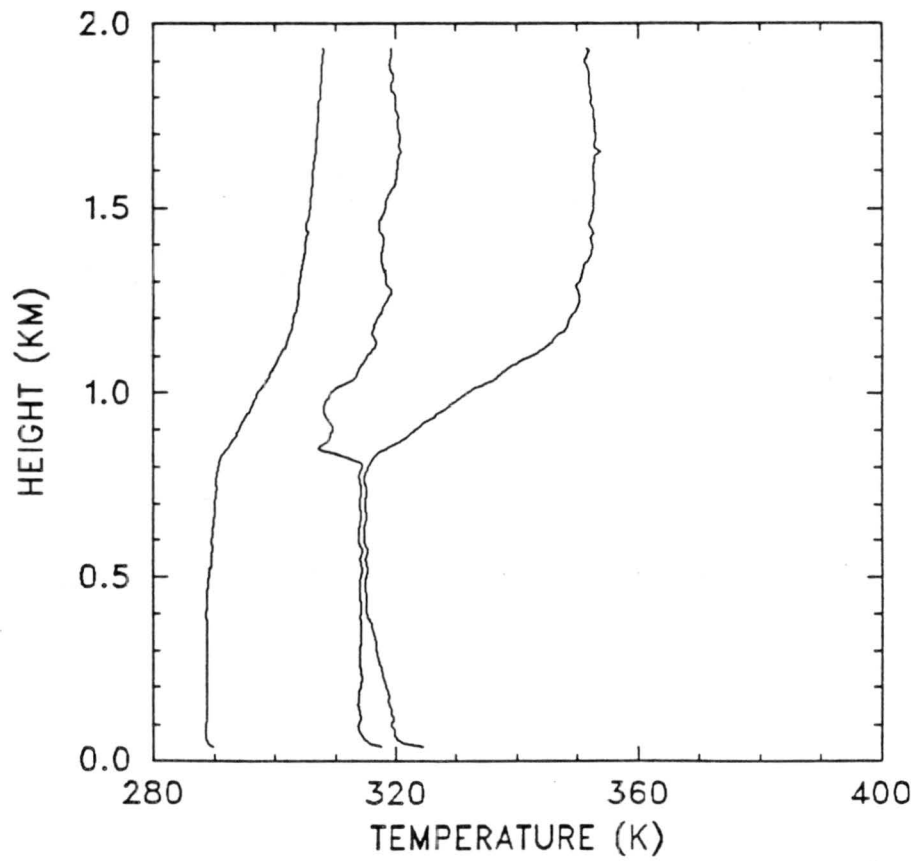
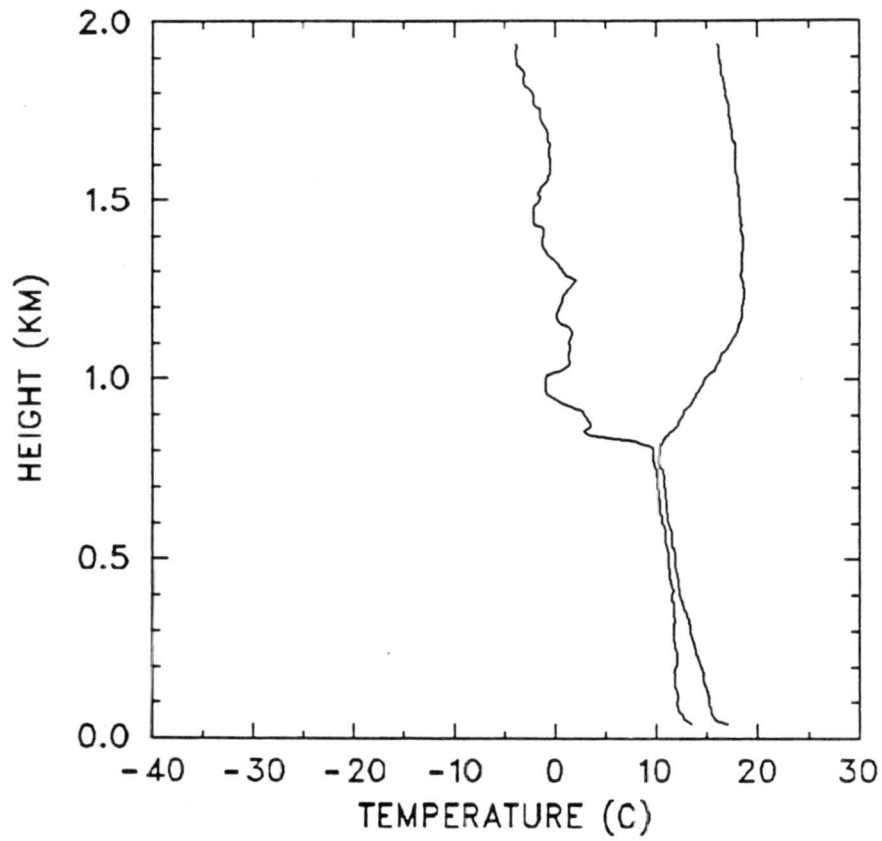
1154 GMT 09 JULY 1987



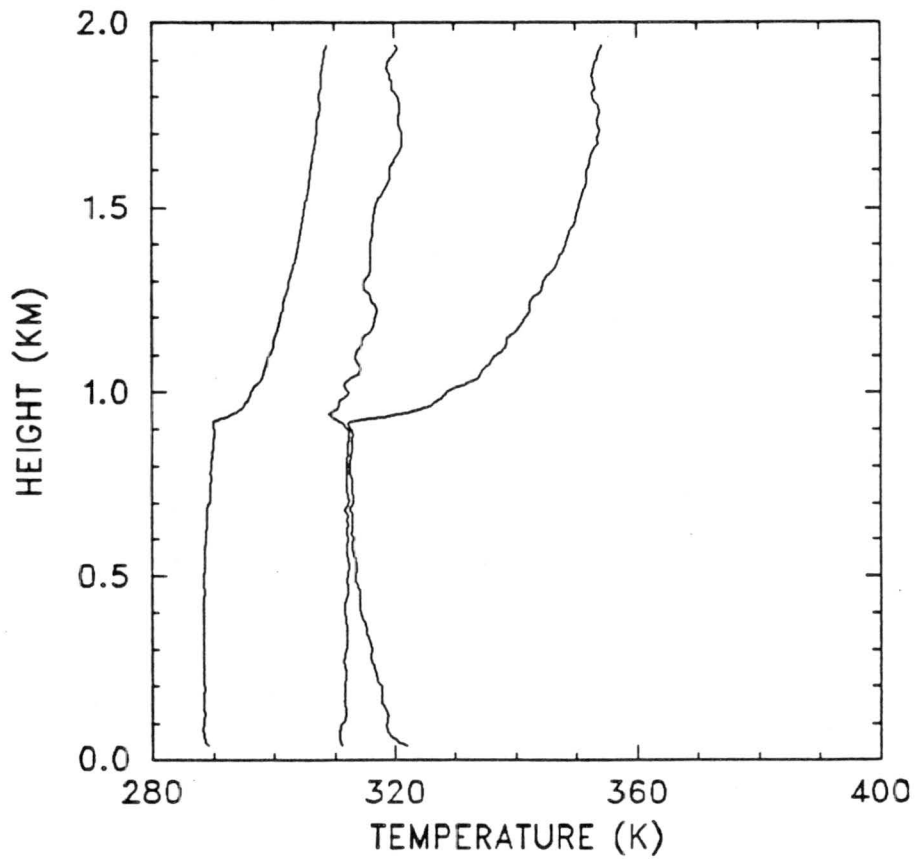
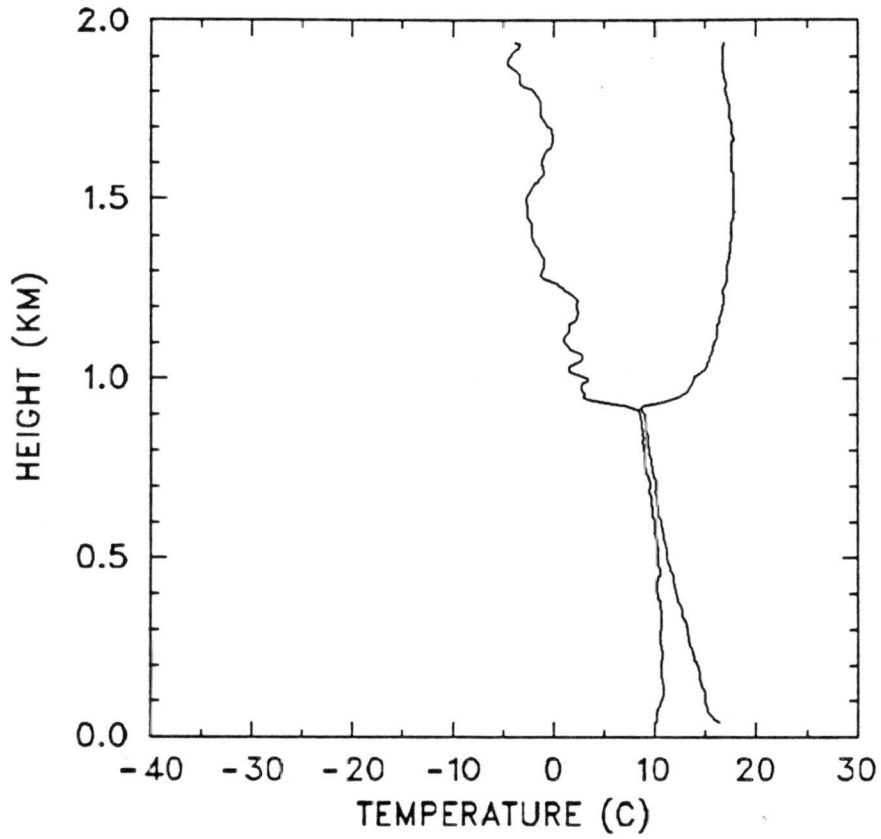
1814 GMT 09 JULY 1987



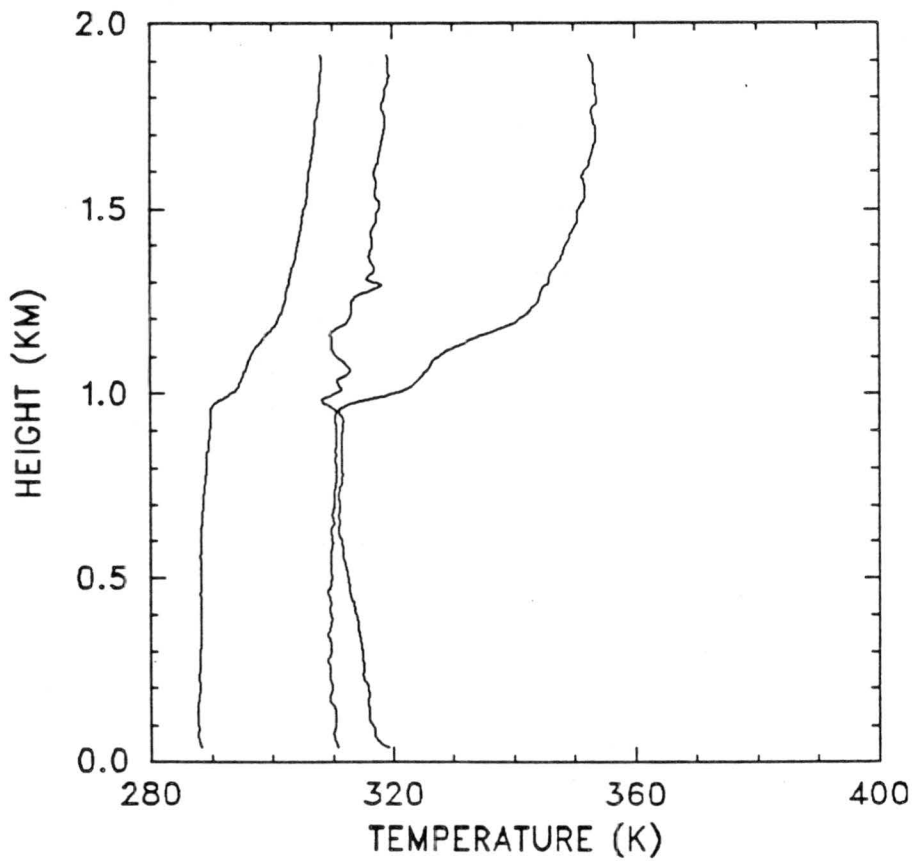
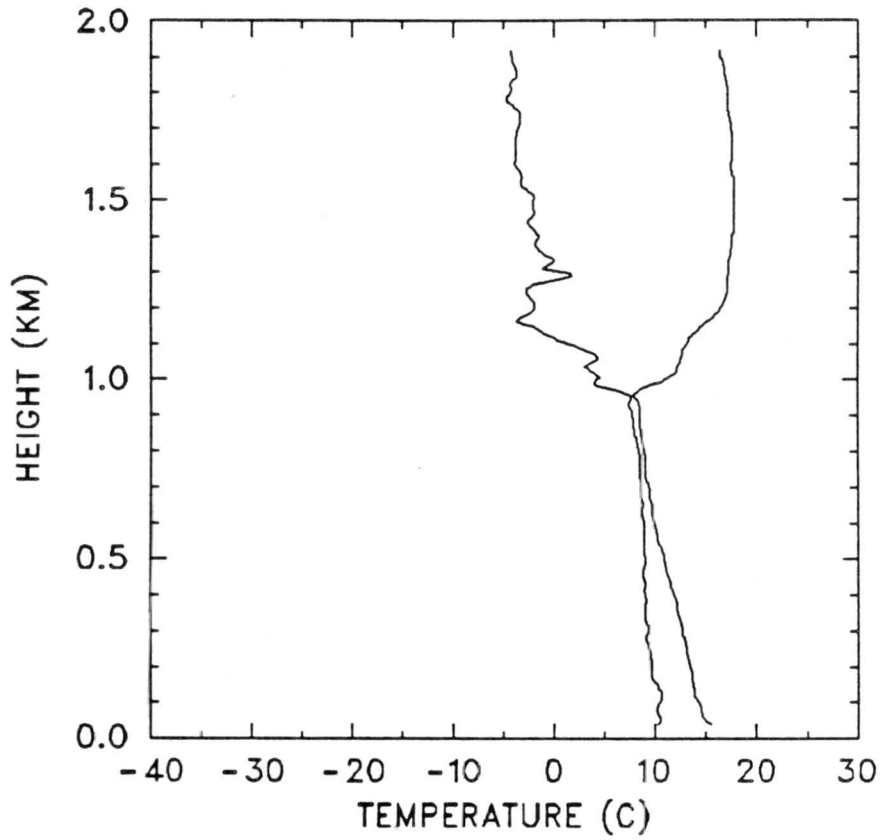
0115 GMT 10 JULY 1987



1222 GMT 10 JULY 1987

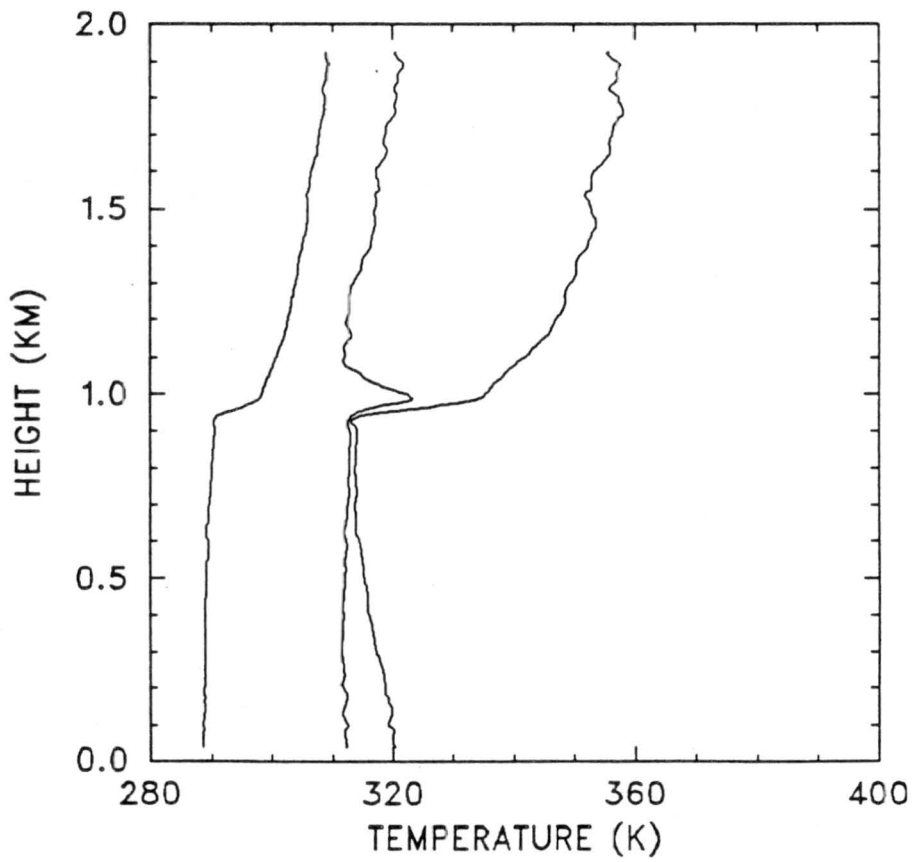
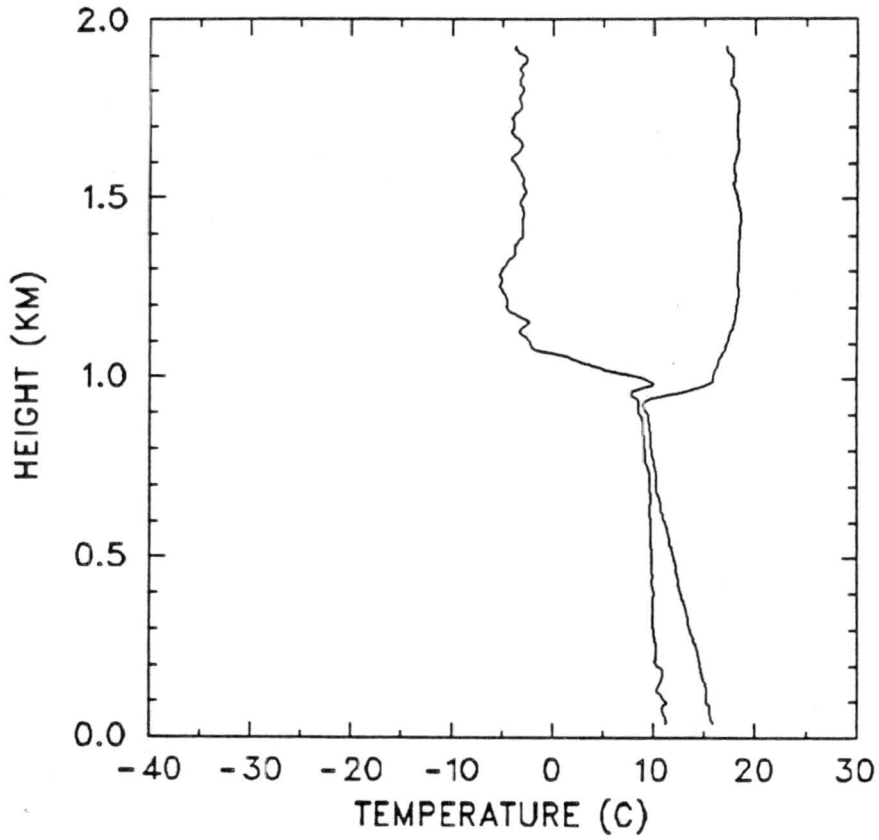


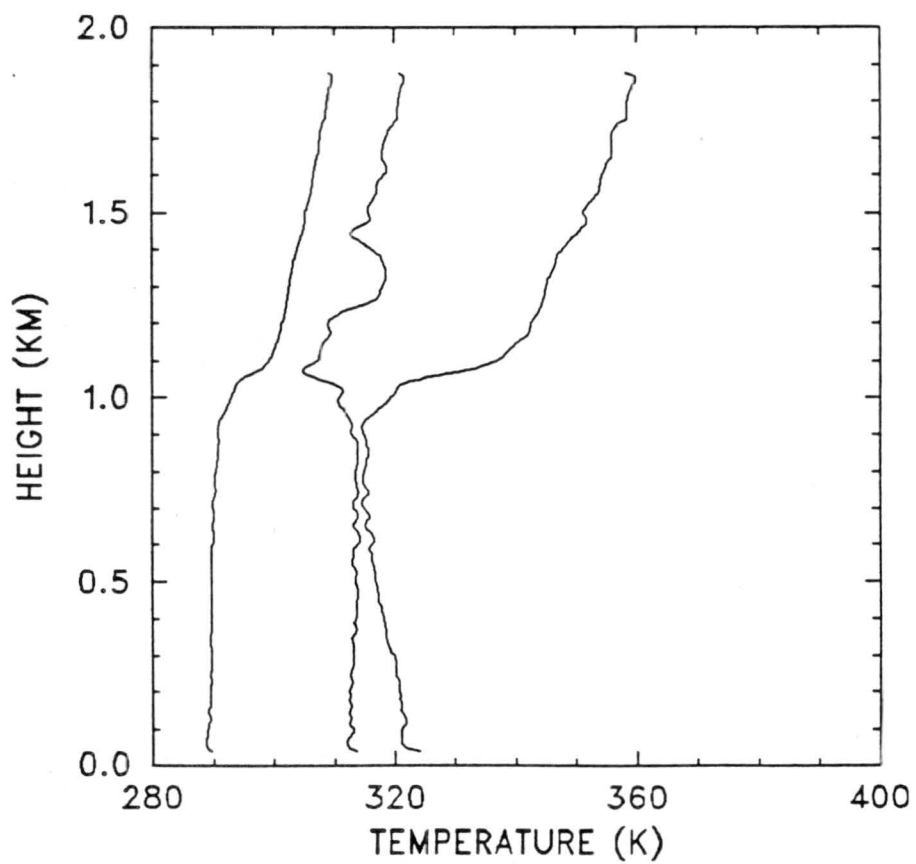
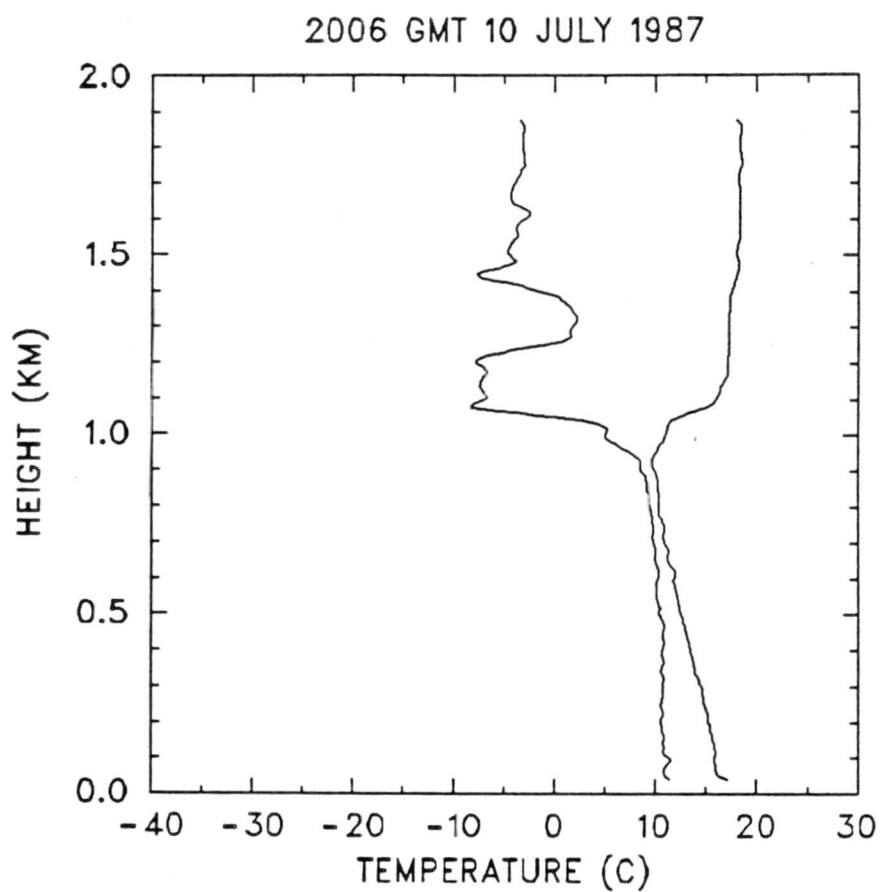
1550 GMT 10 JULY 1987



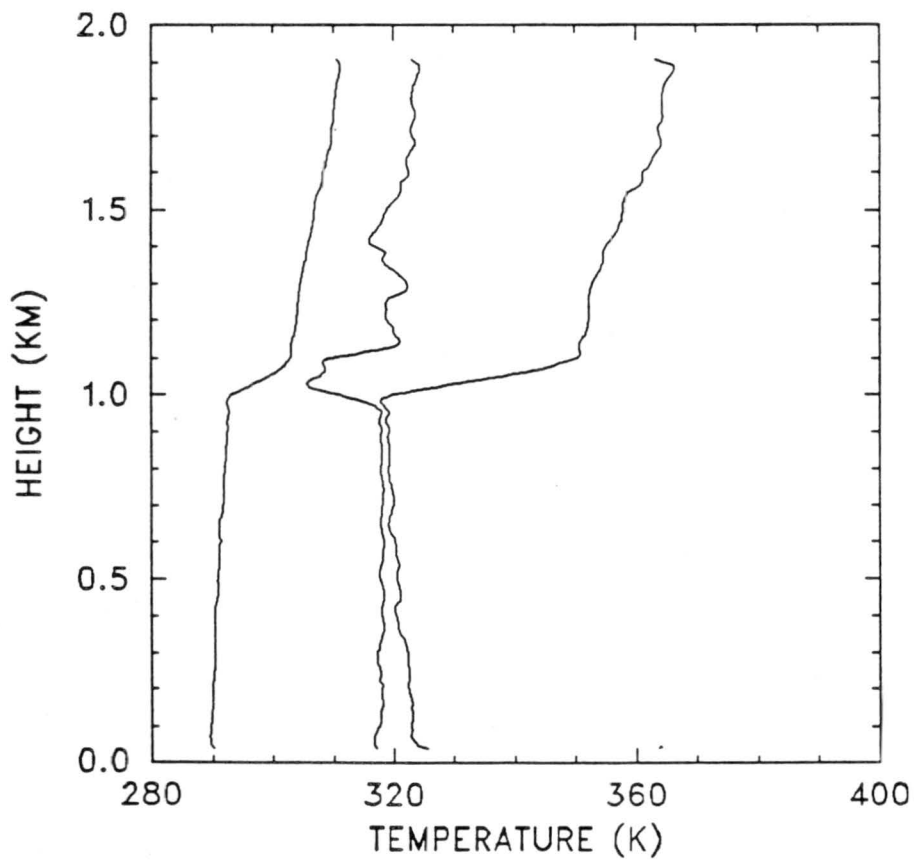
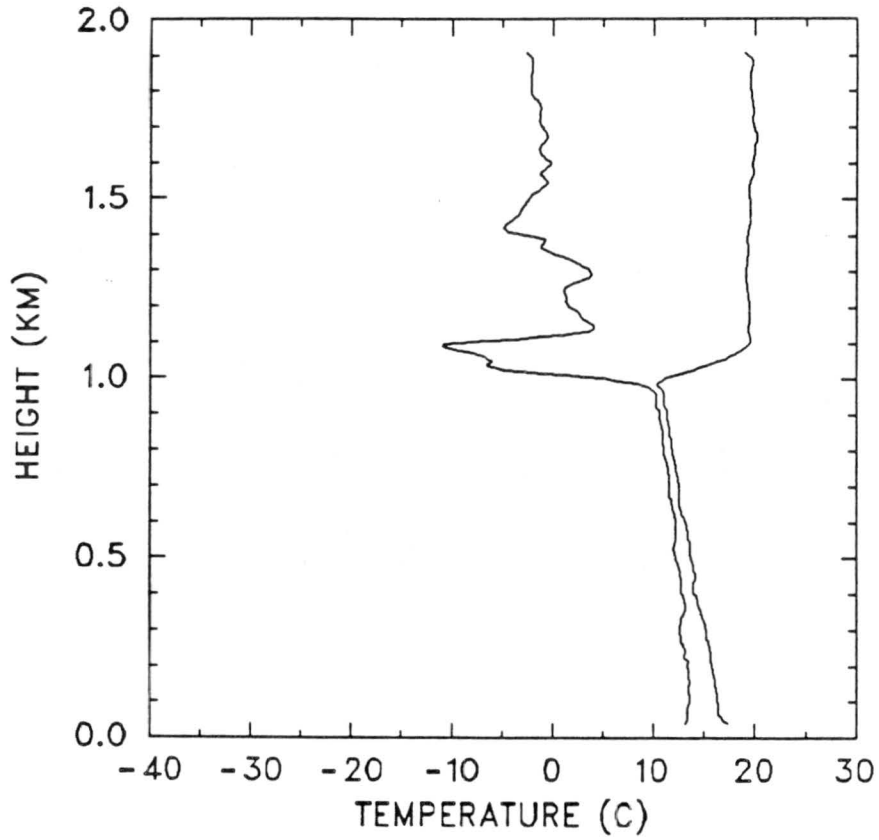


1800 GMT 10 JULY 1987

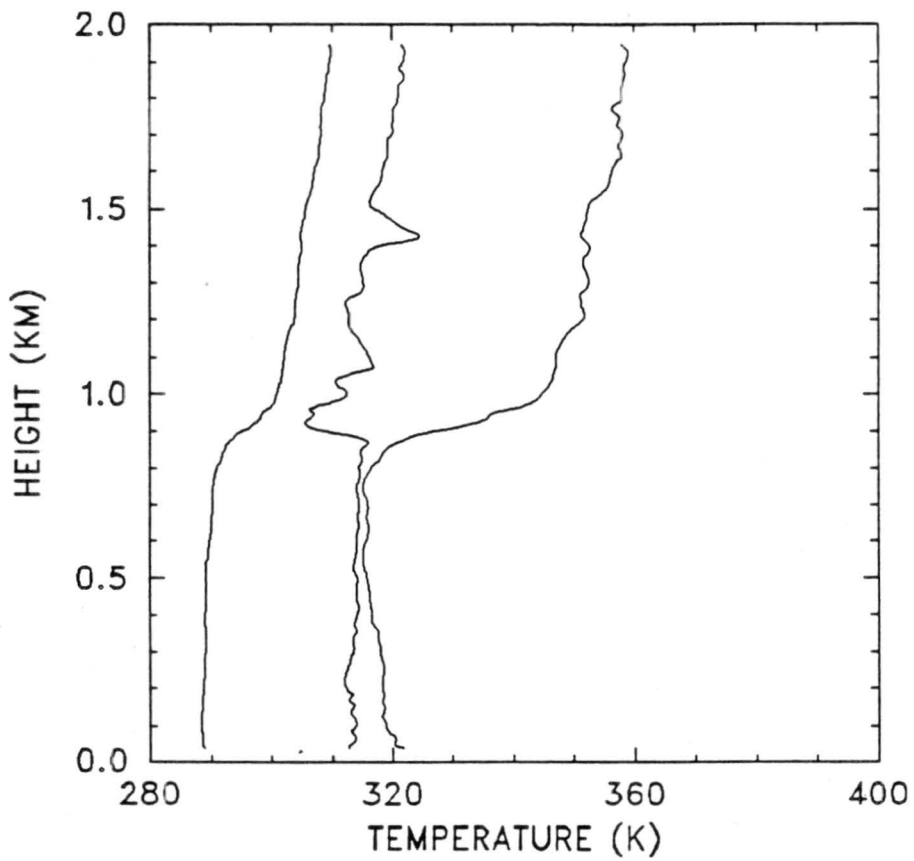
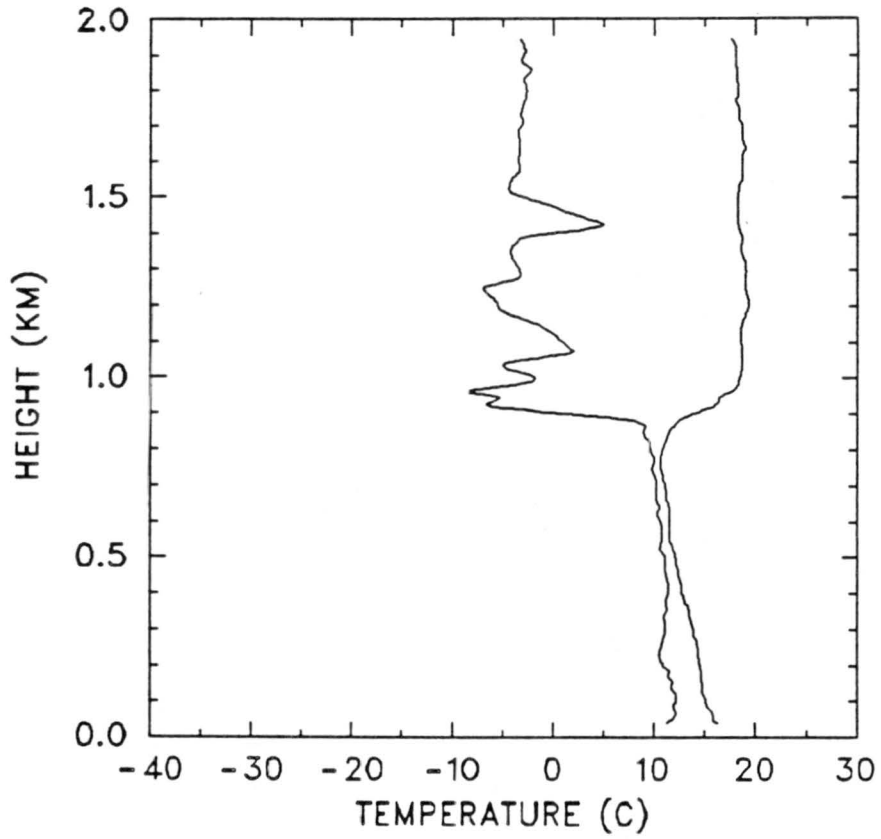




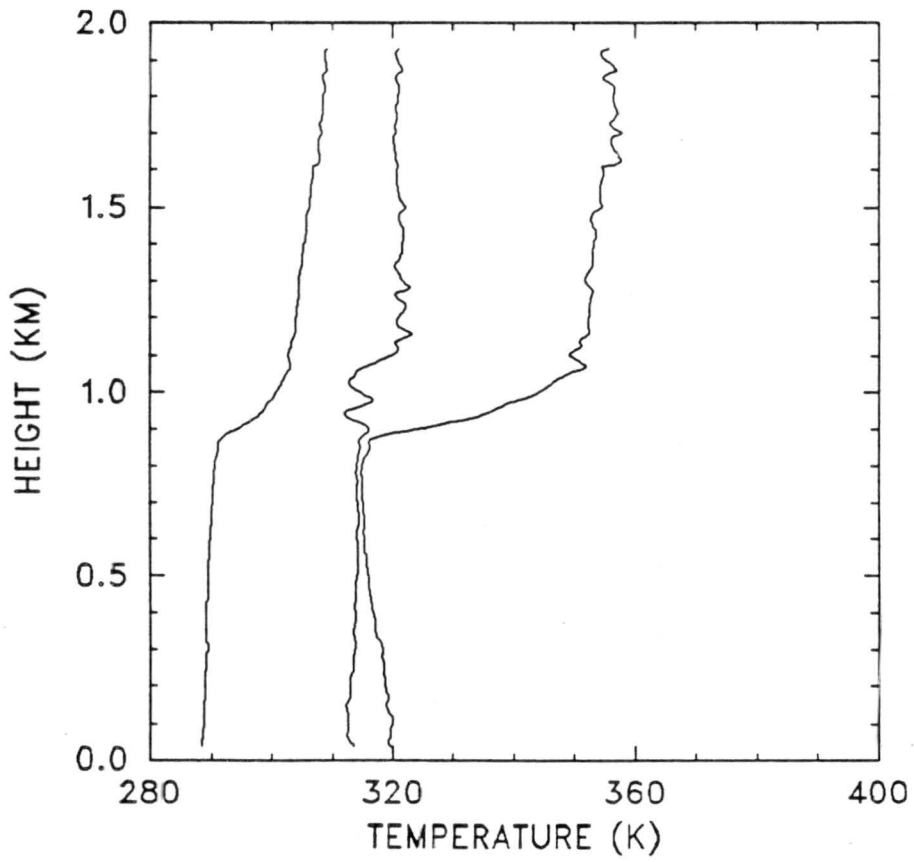
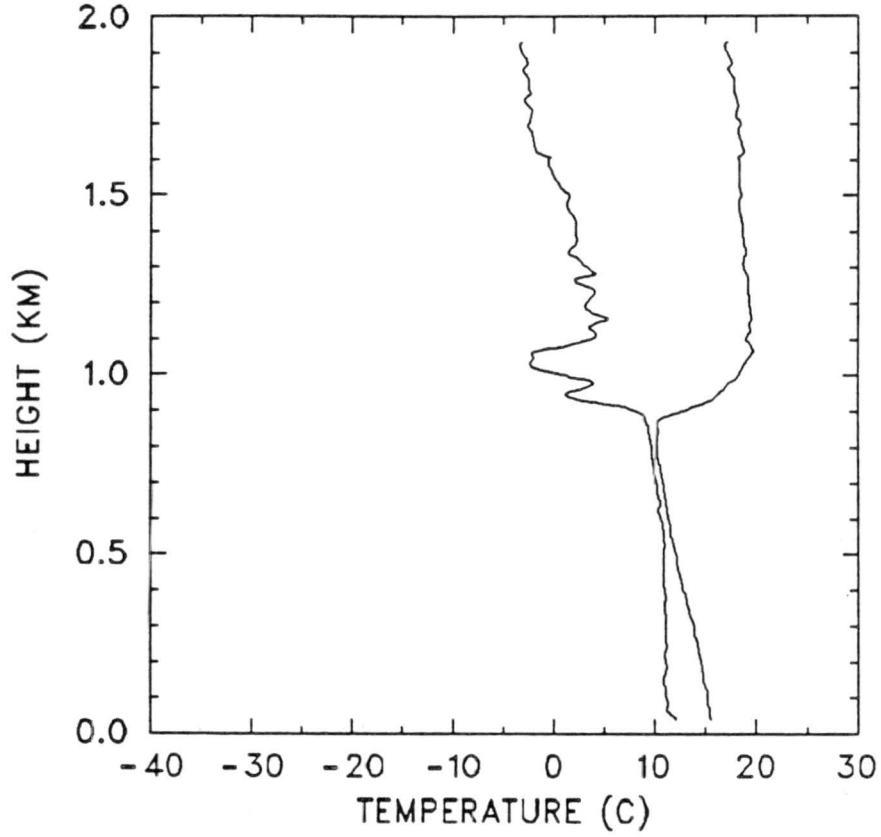
2159 GMT 10 JULY 1987



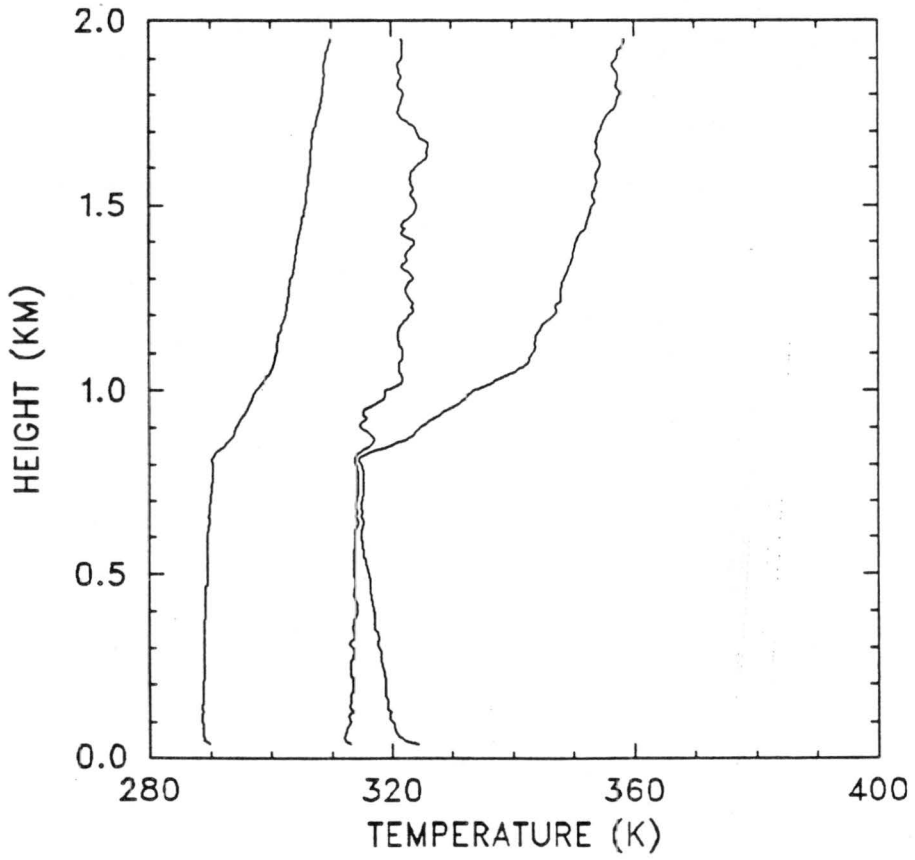
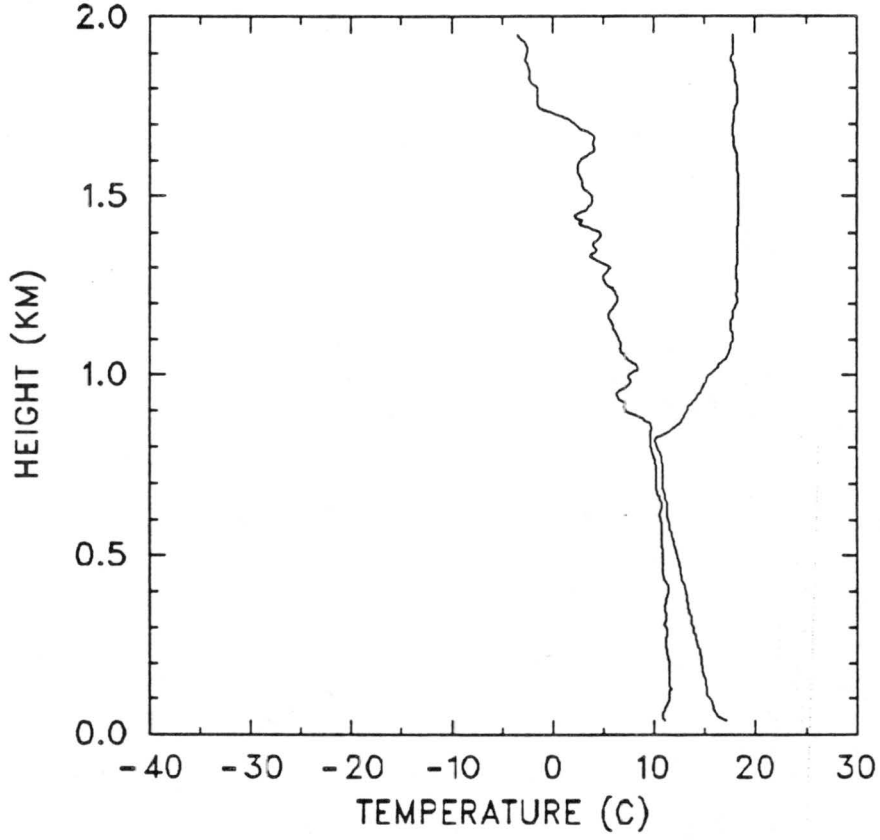
0005 GMT 11 JULY 1987



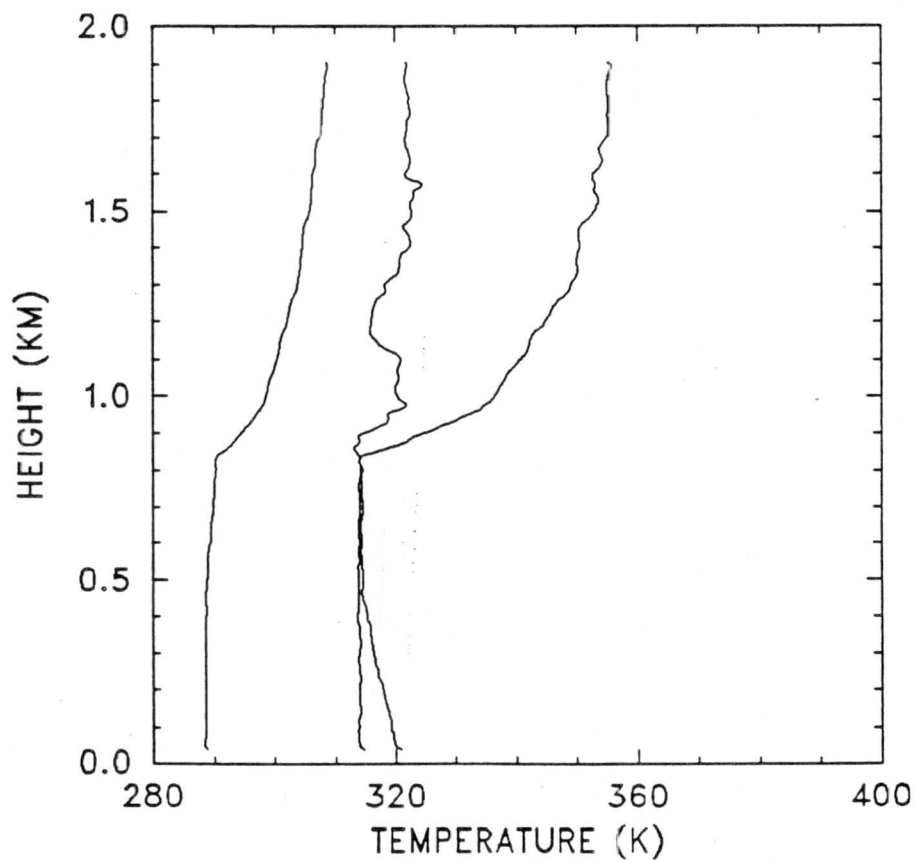
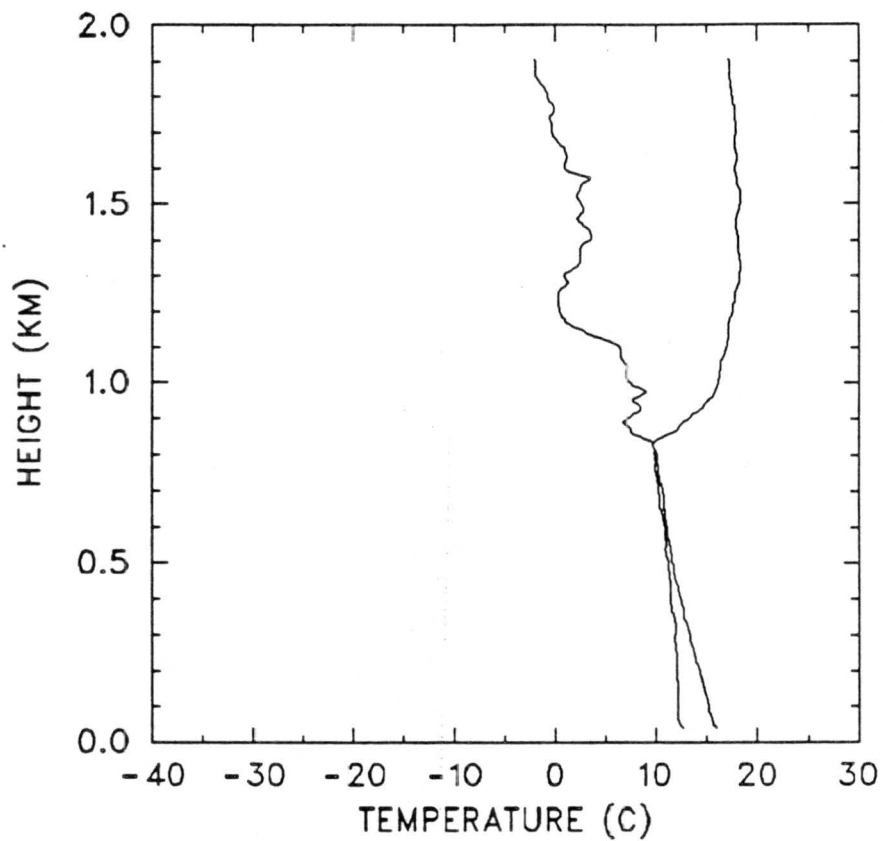
0200 GMT 11 JULY 1987



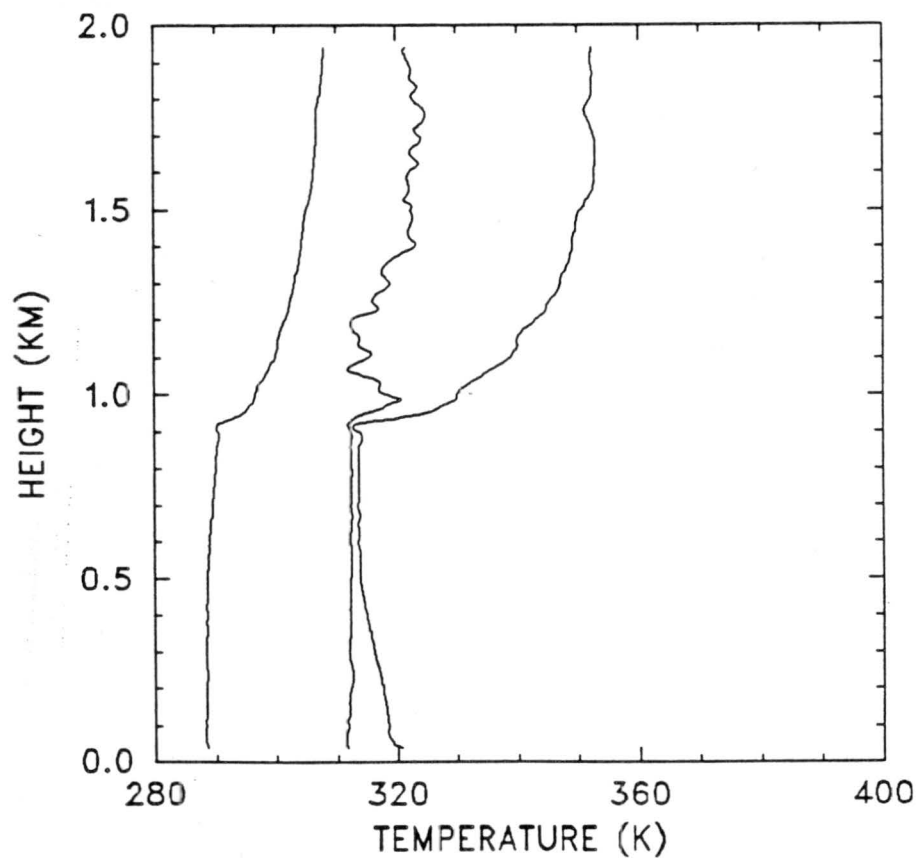
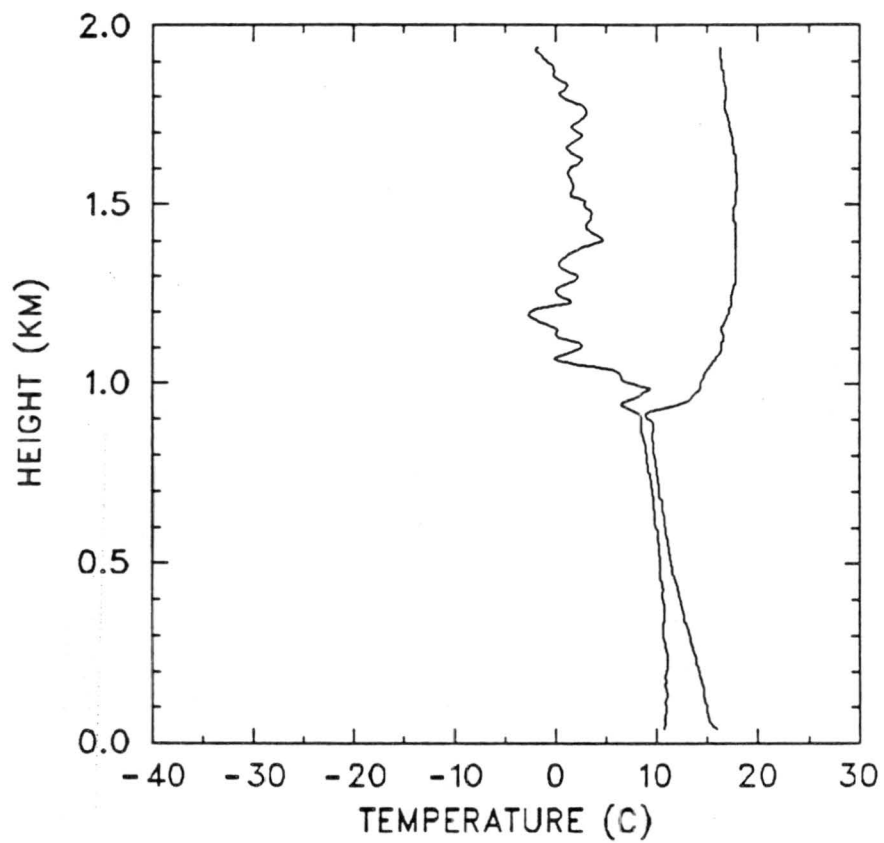
0353 GMT 11 JULY 1987



0616 GMT 11 JULY 1987

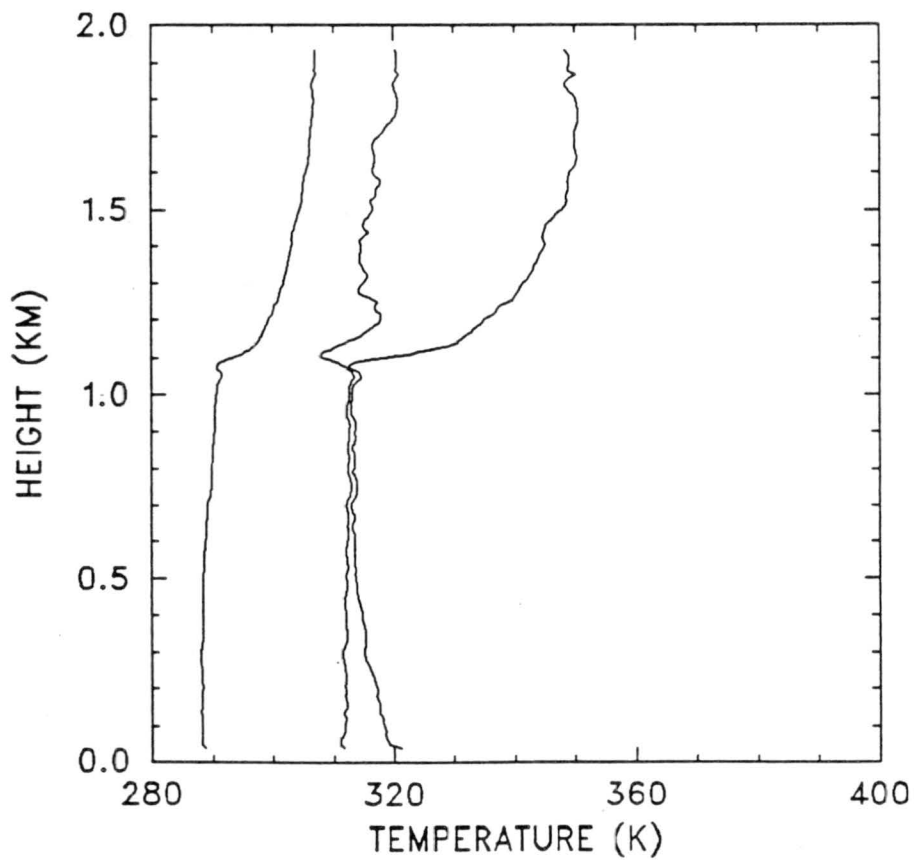
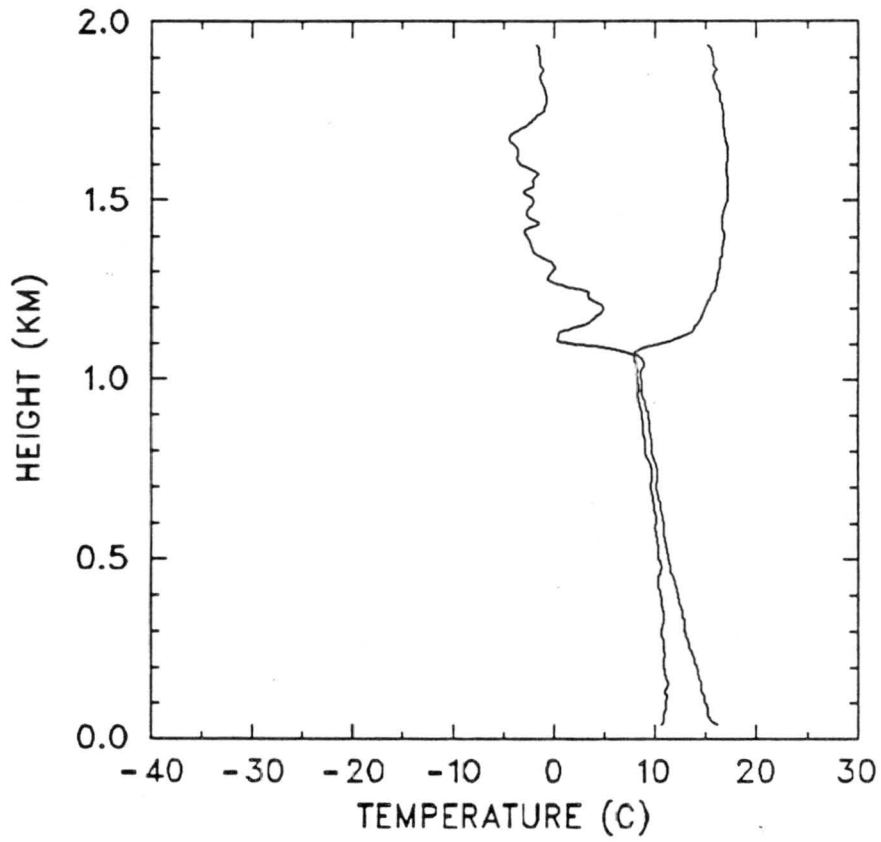


0951 GMT 11 JULY 1987

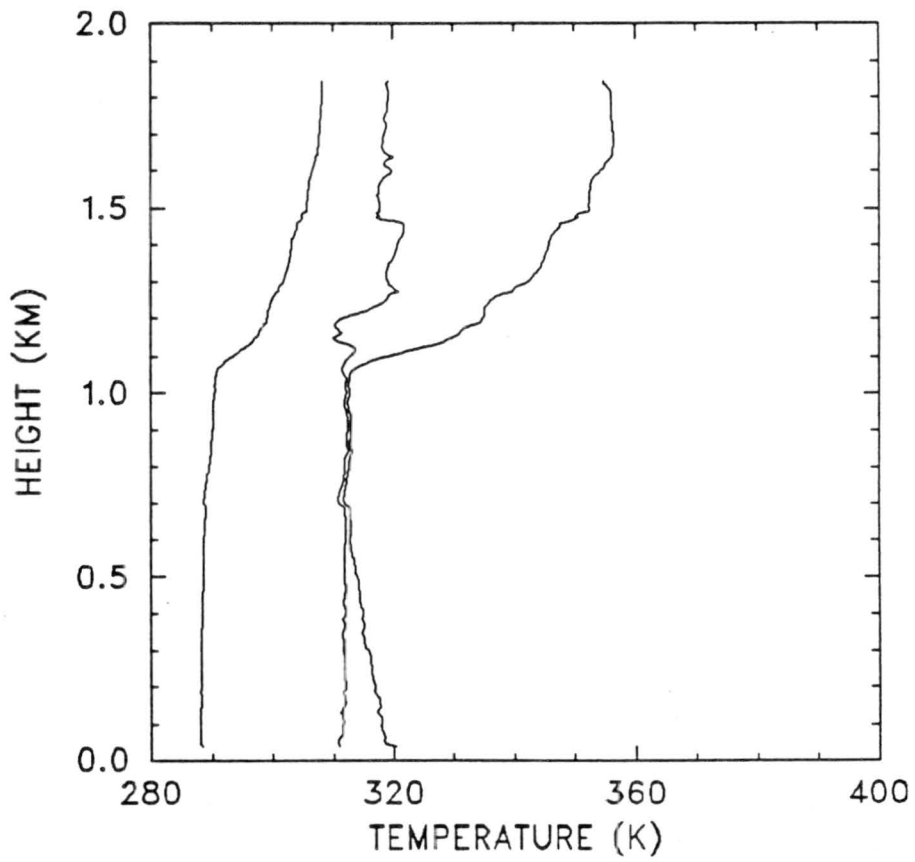
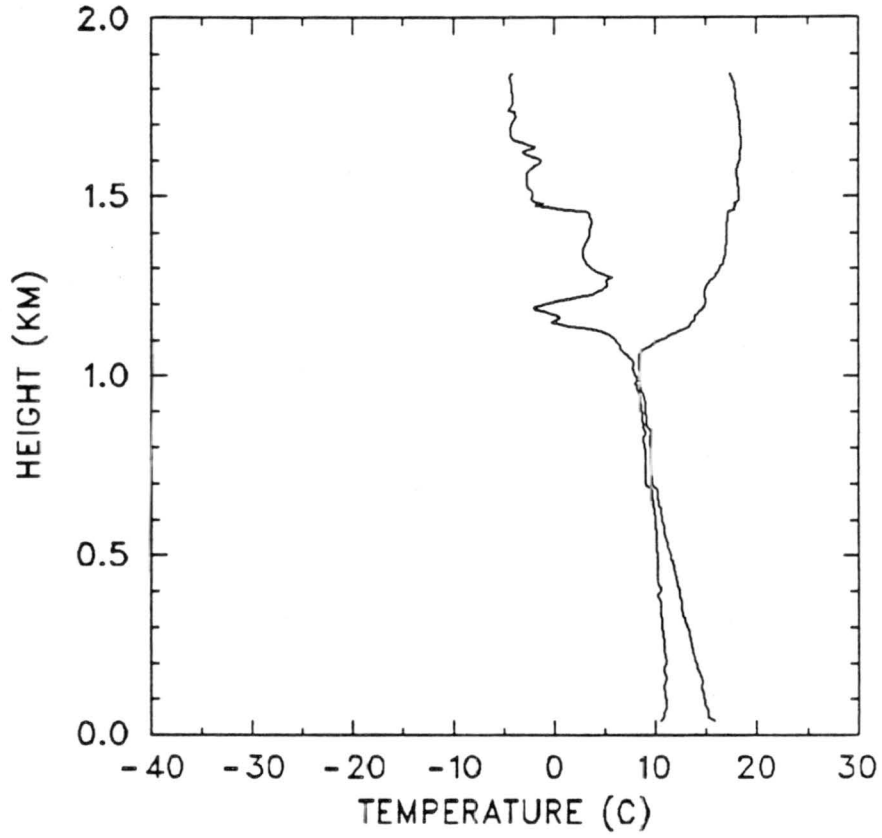




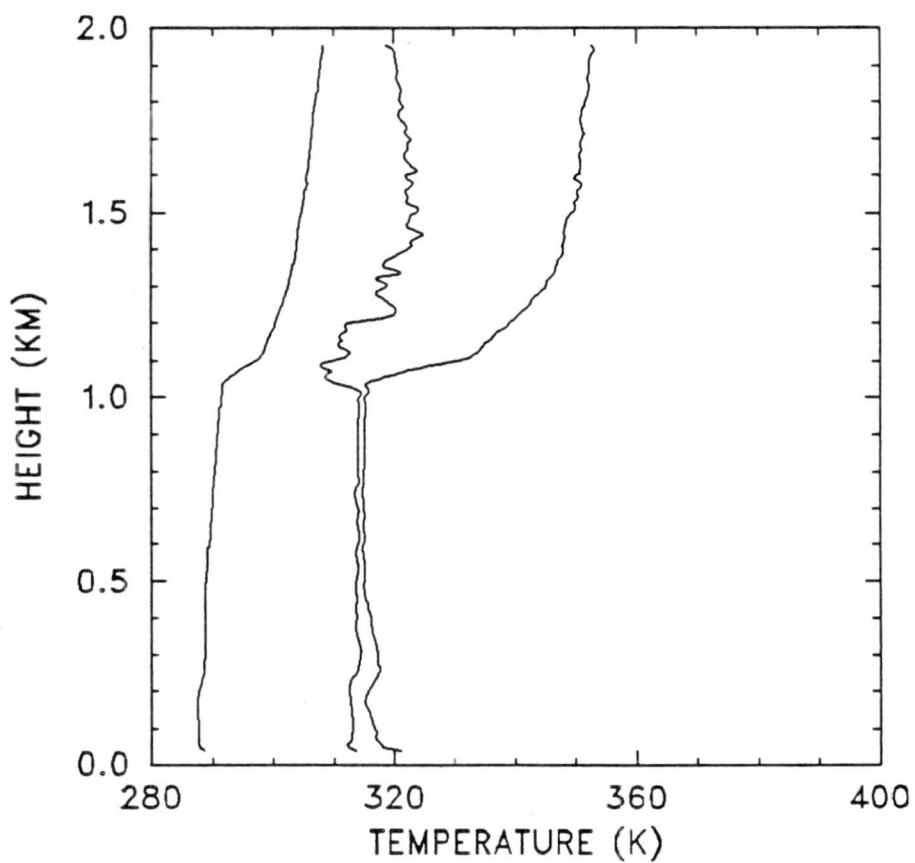
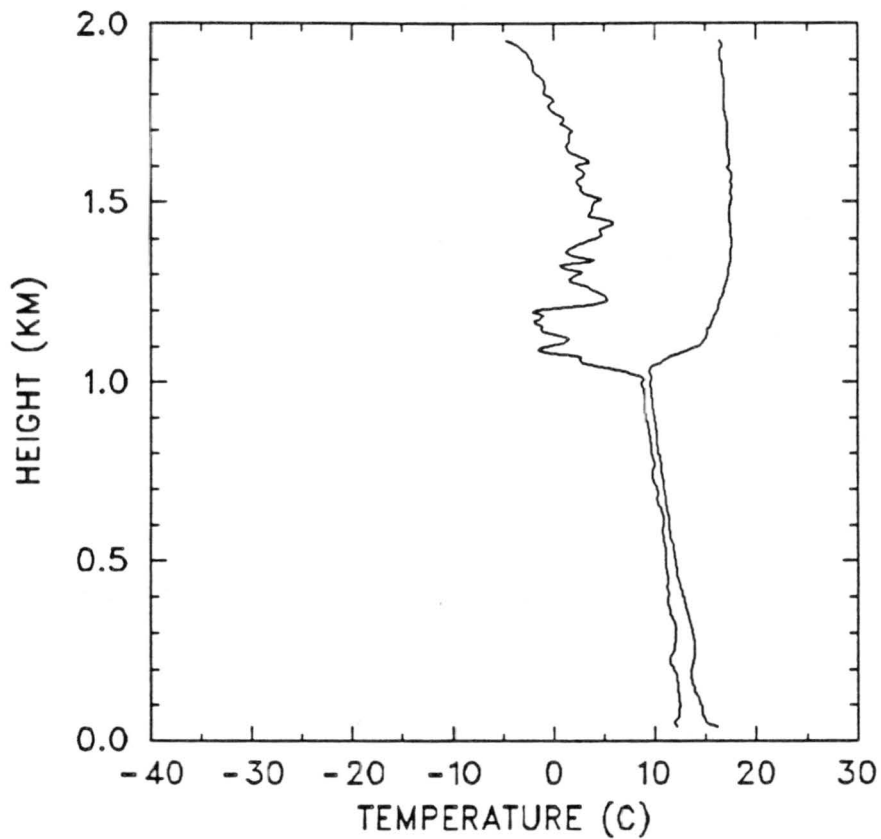
1212 GMT 11 JULY 1987



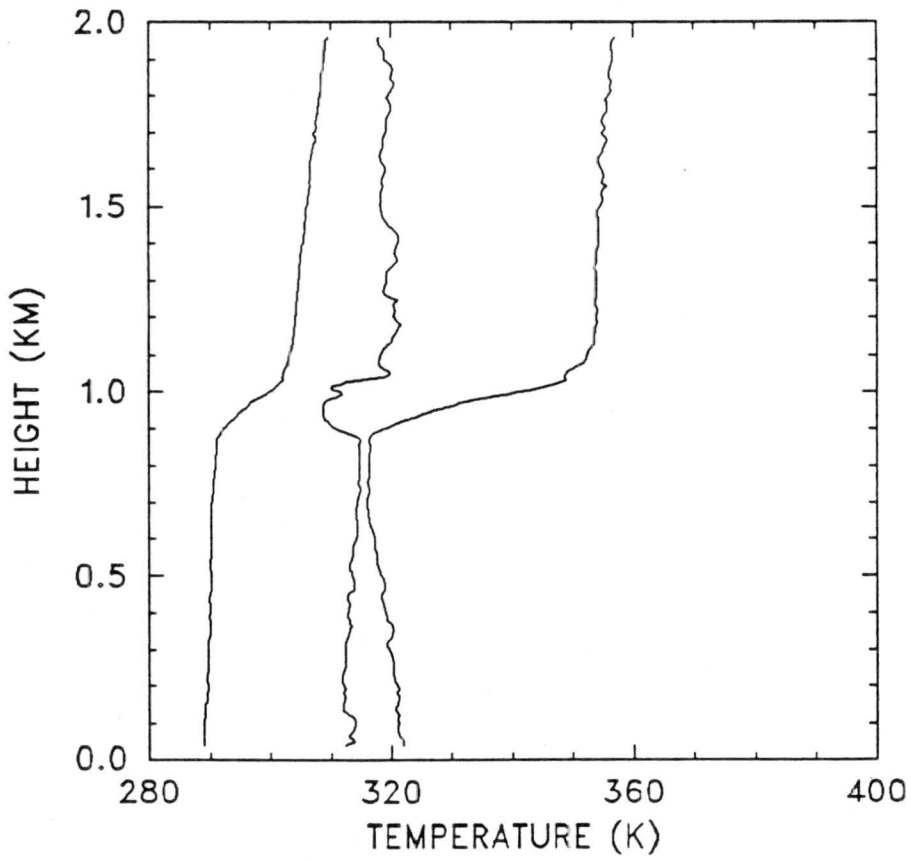
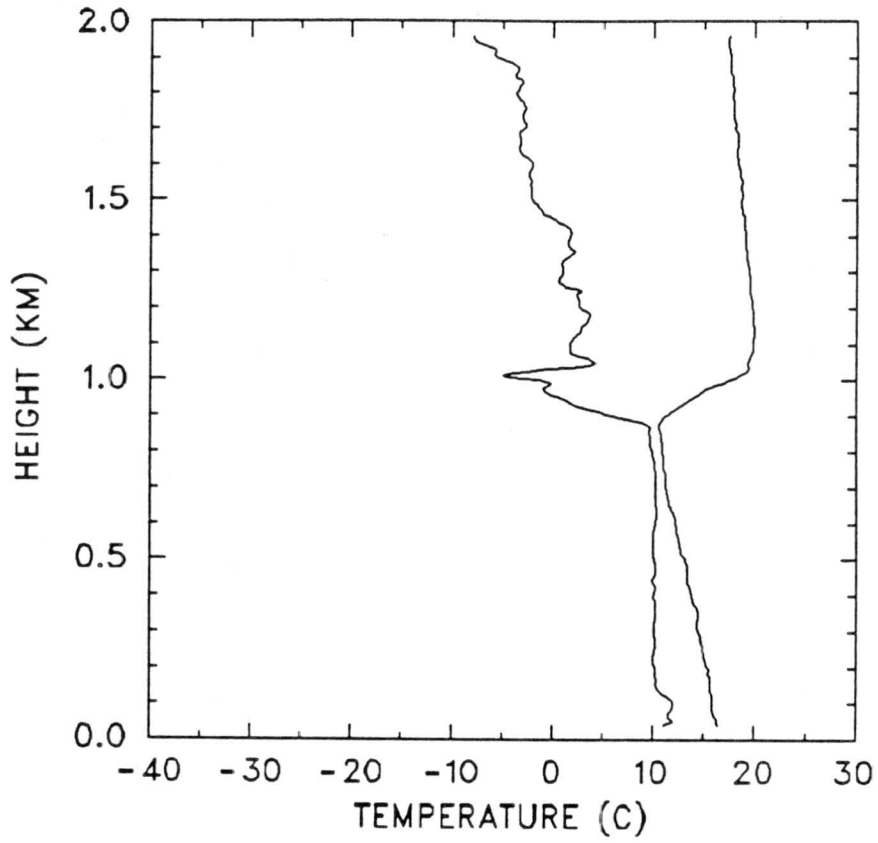
1410 GMT 11 JULY 1987



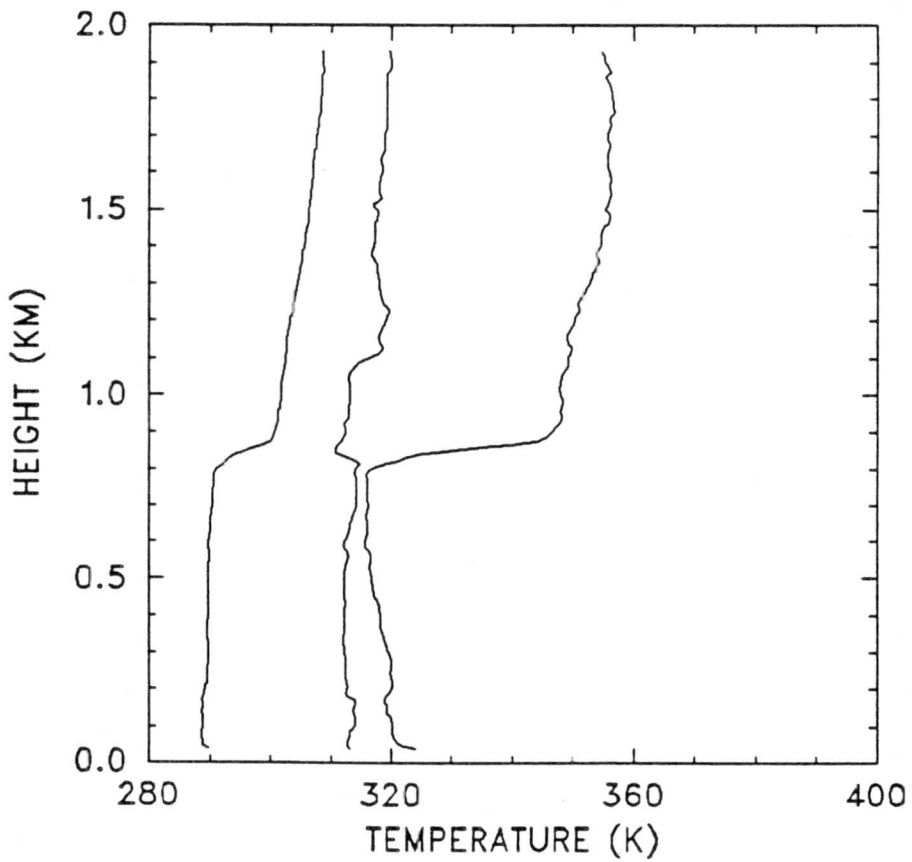
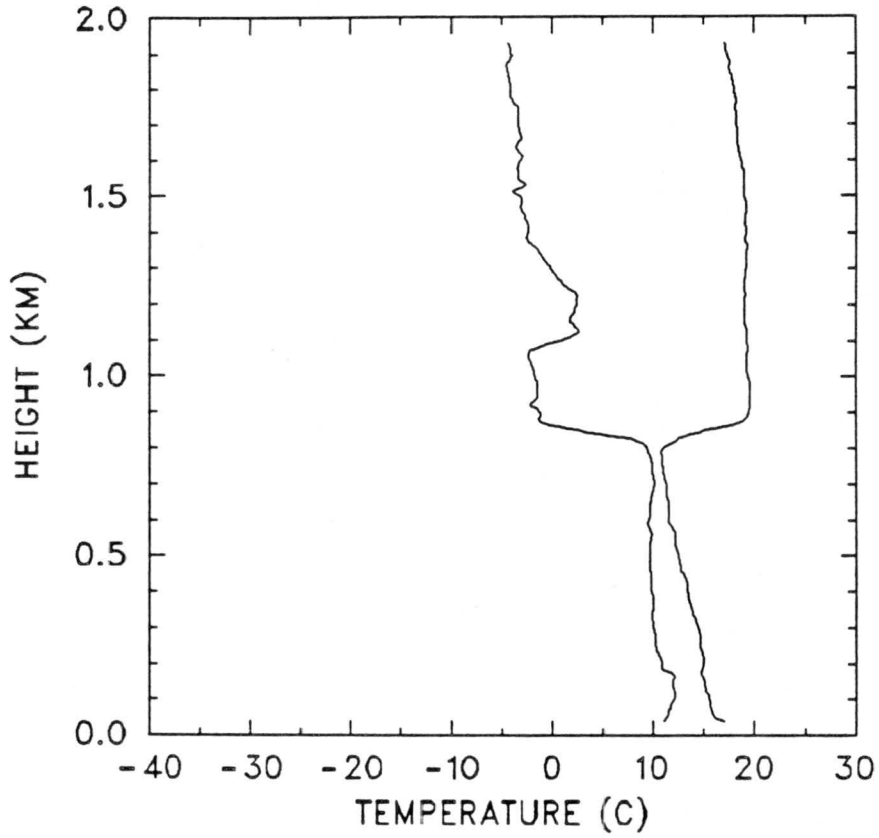
1808 GMT 11 JULY 1987



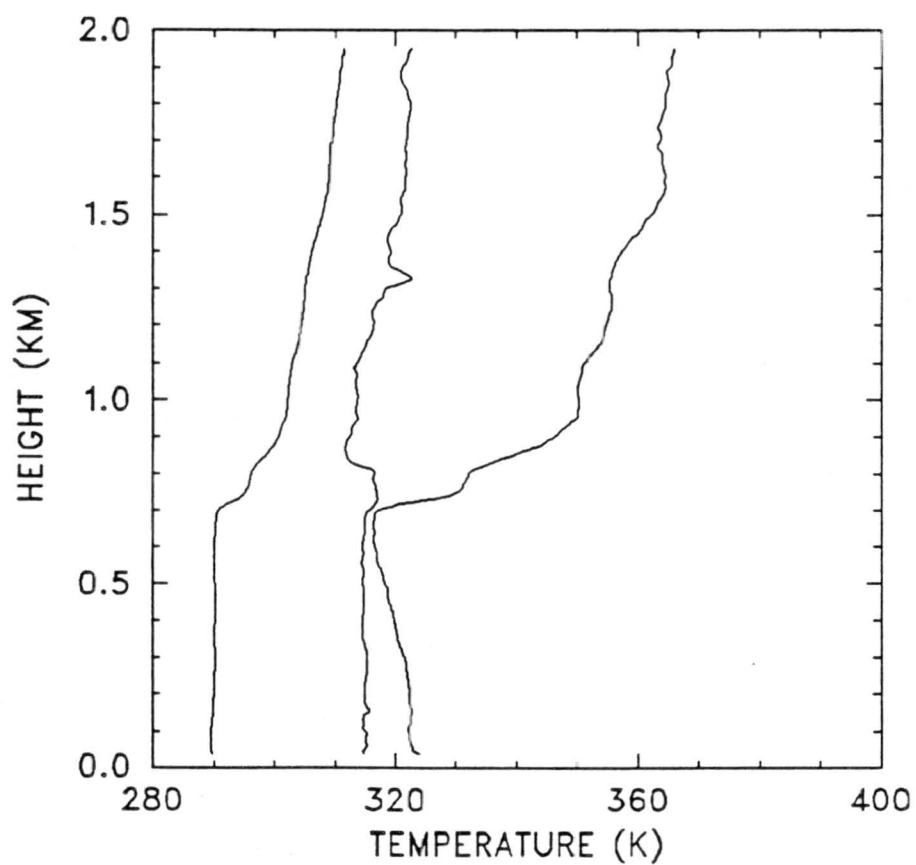
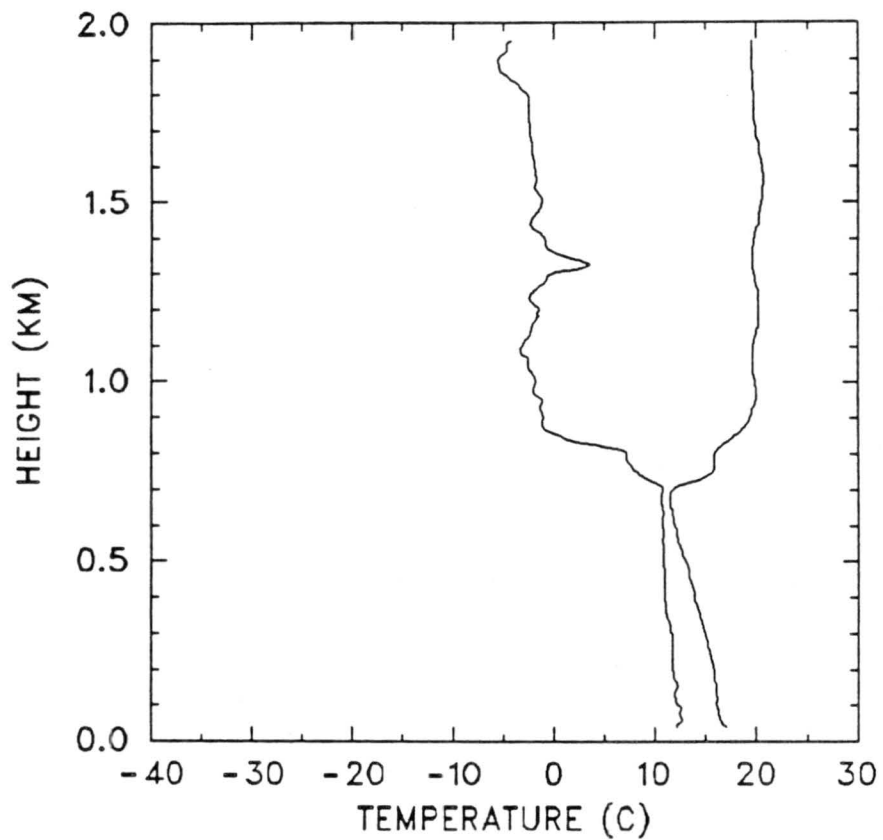
2208 GMT 11 JULY 1987



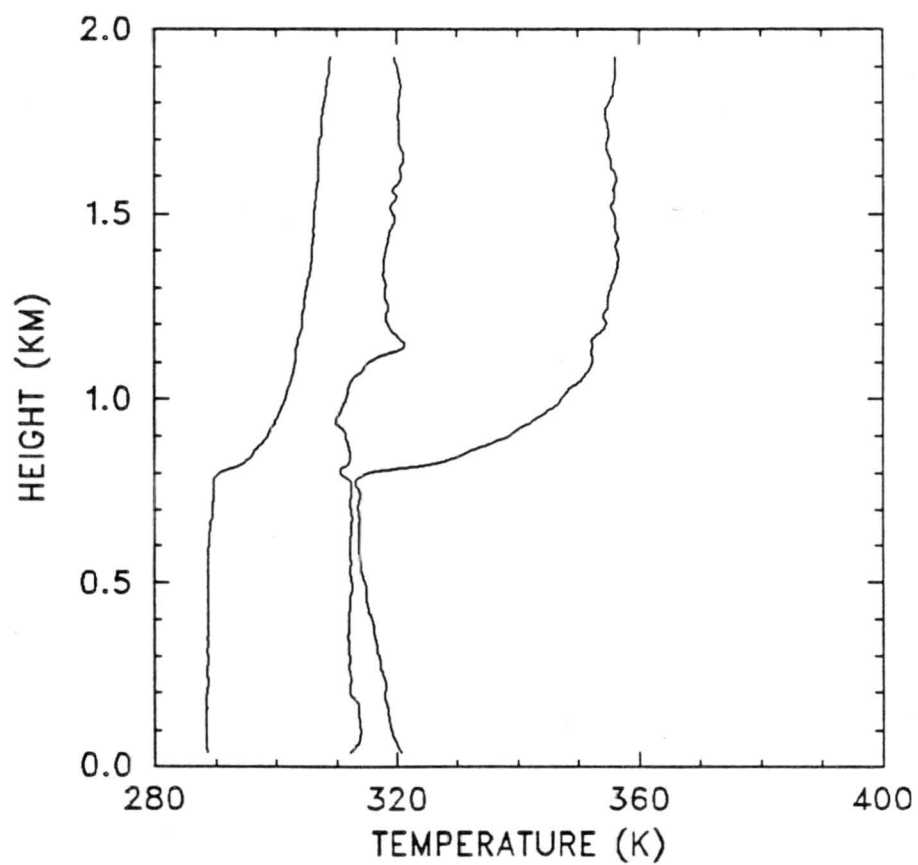
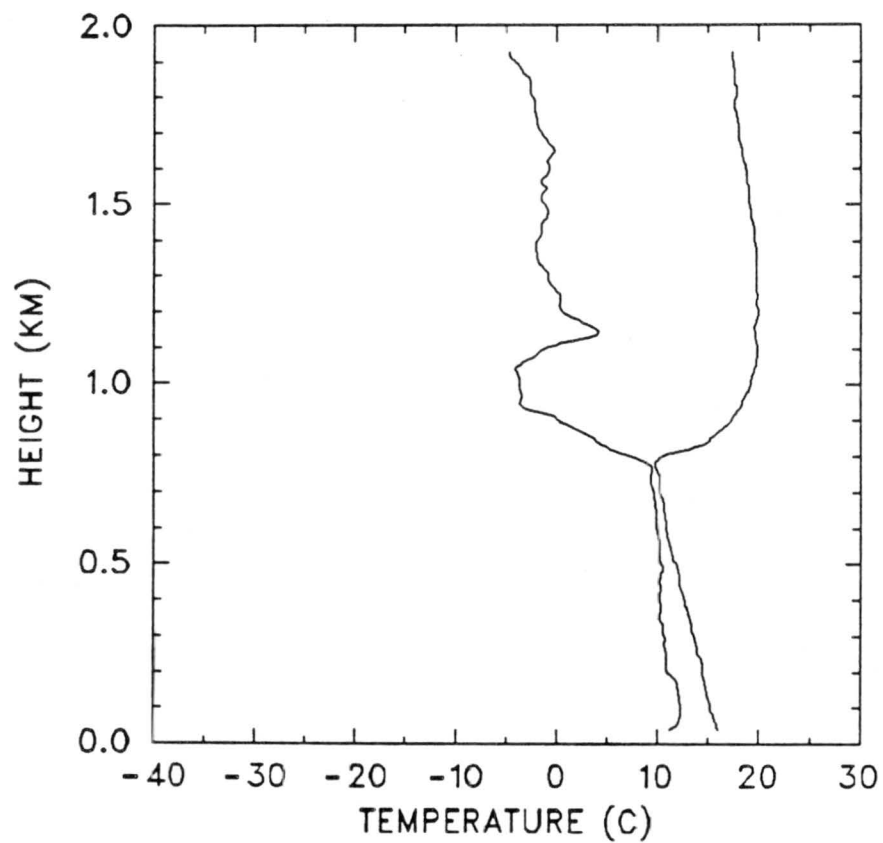
2359 GMT 11 JULY 1987



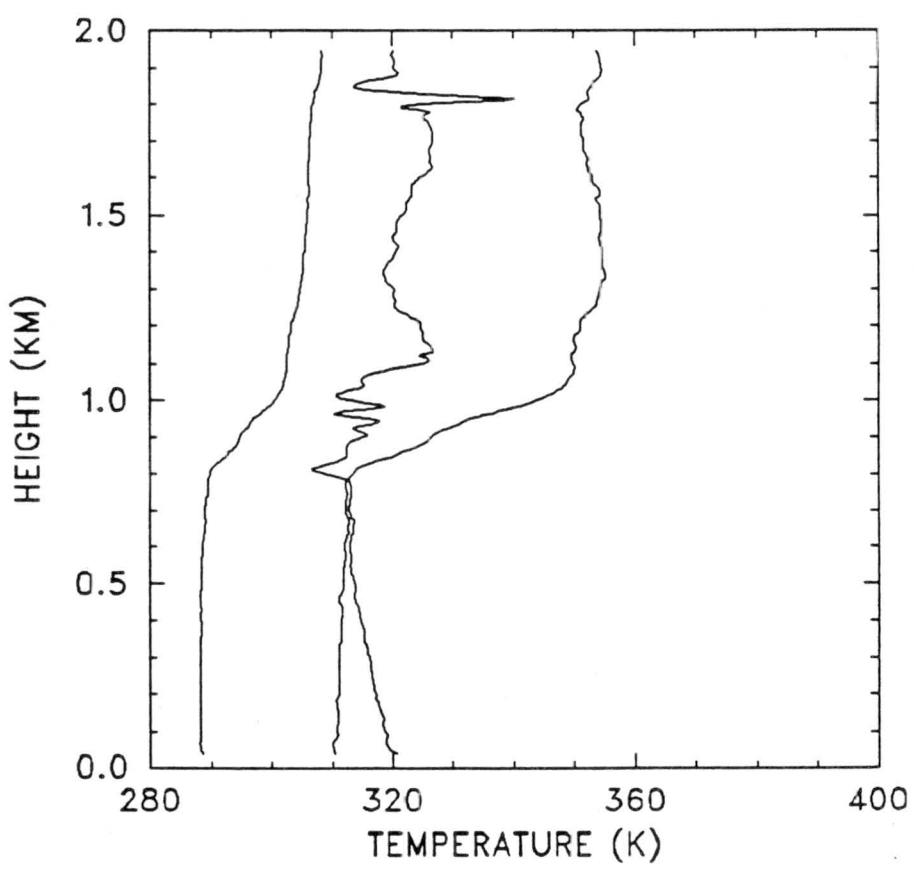
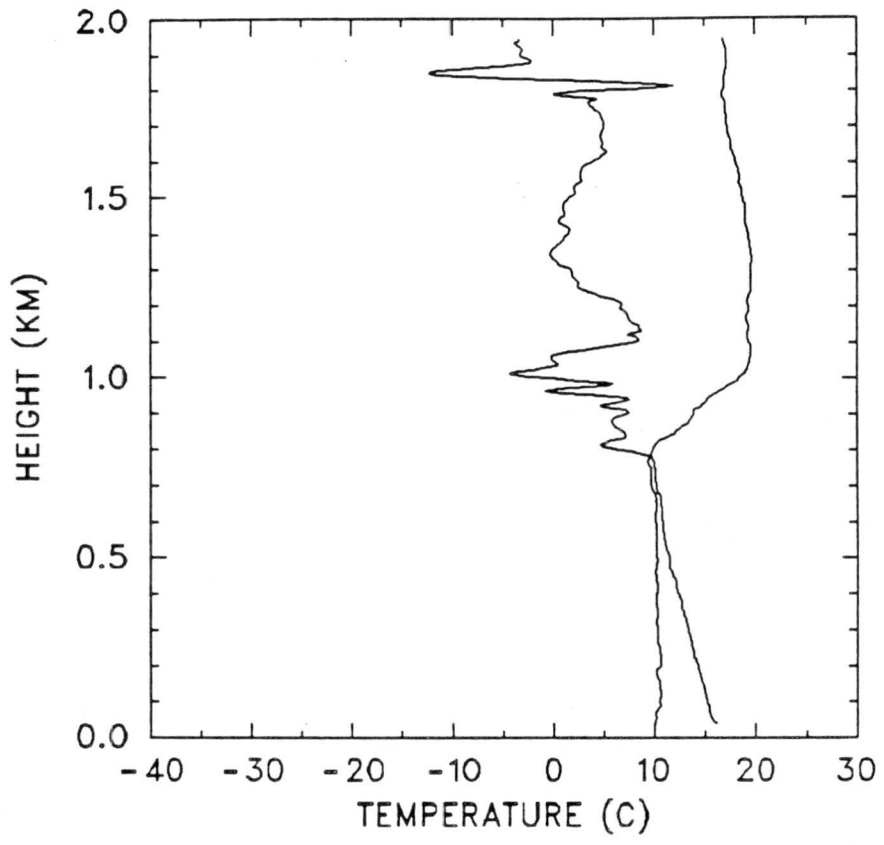
0154 GMT 12 JULY 1987



0610 GMT 12 JULY 1987

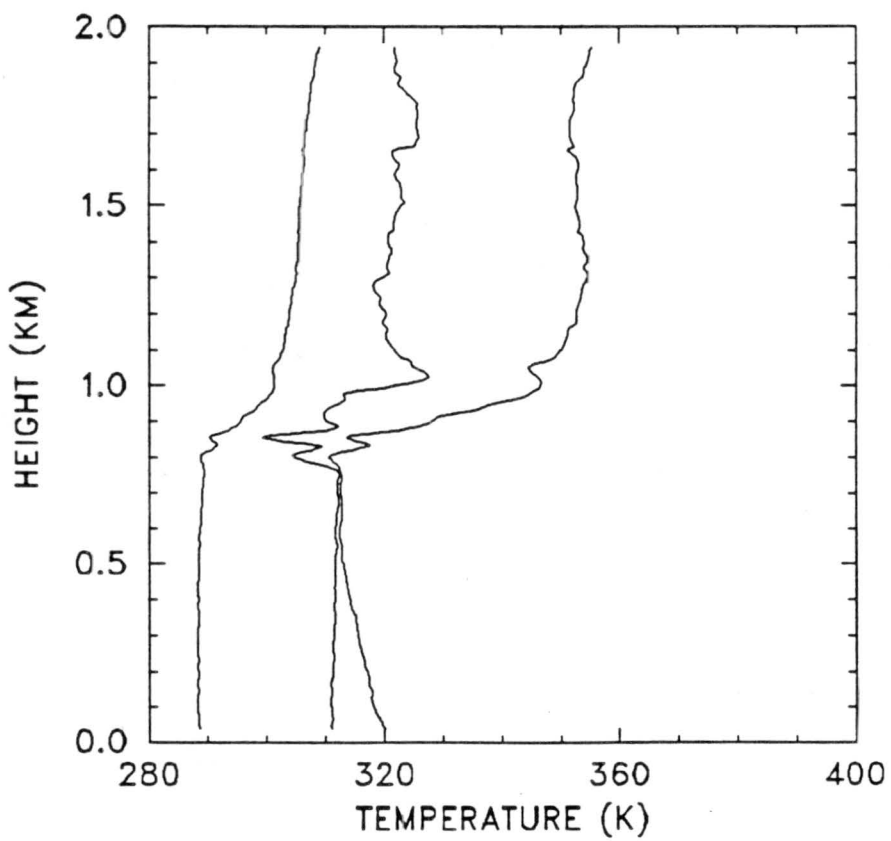
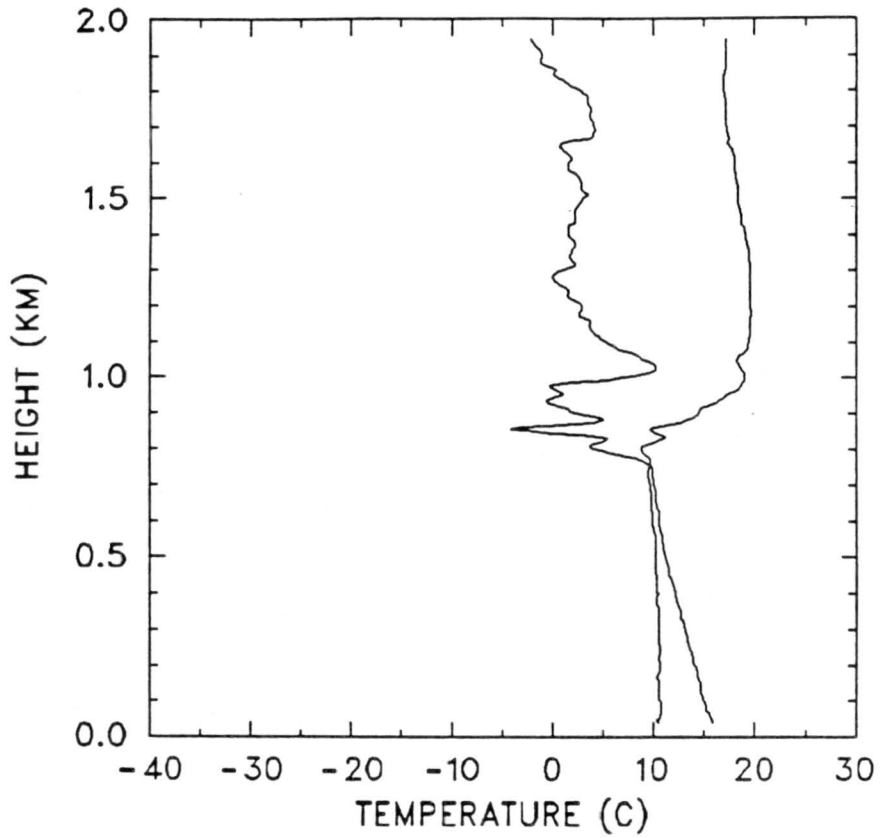


1005 GMT 12 JULY 1987

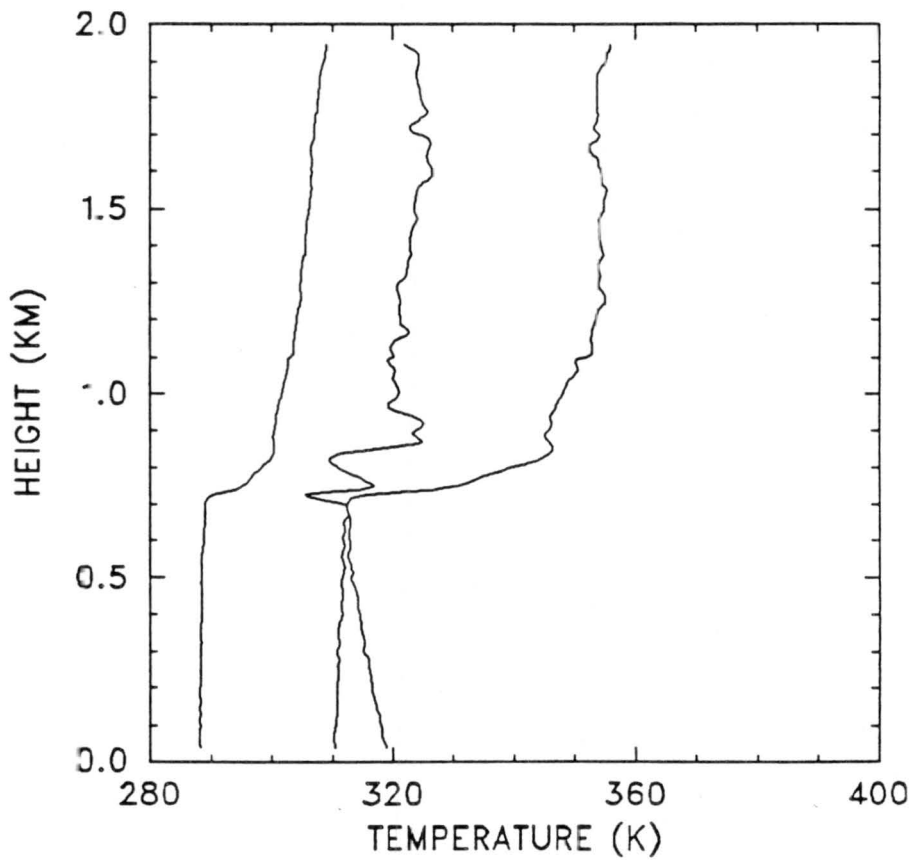
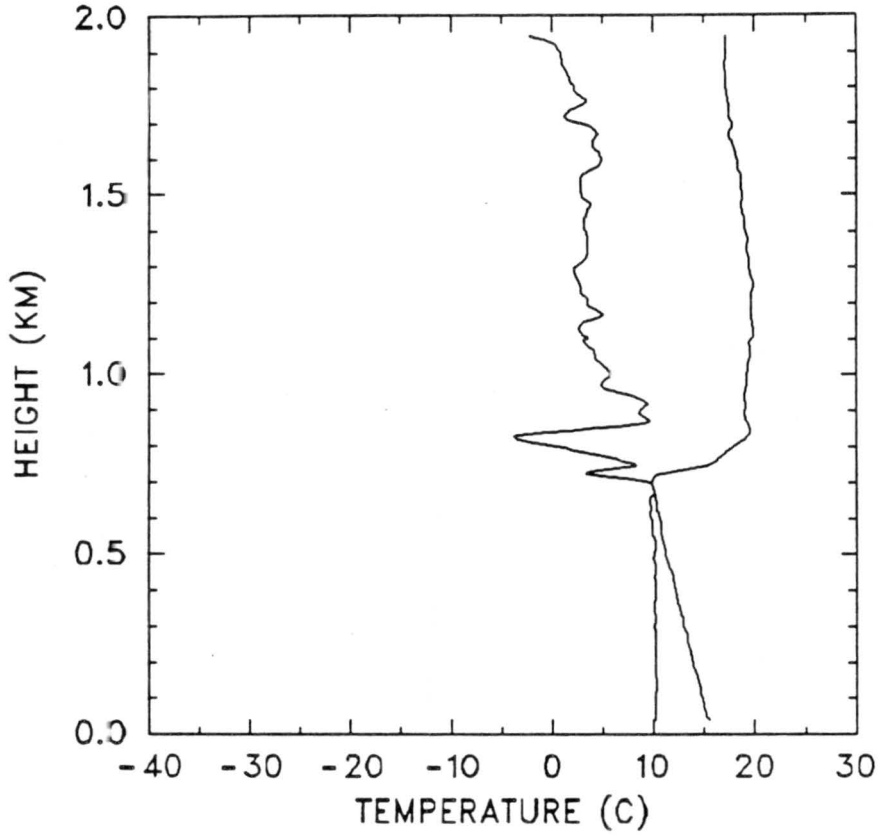




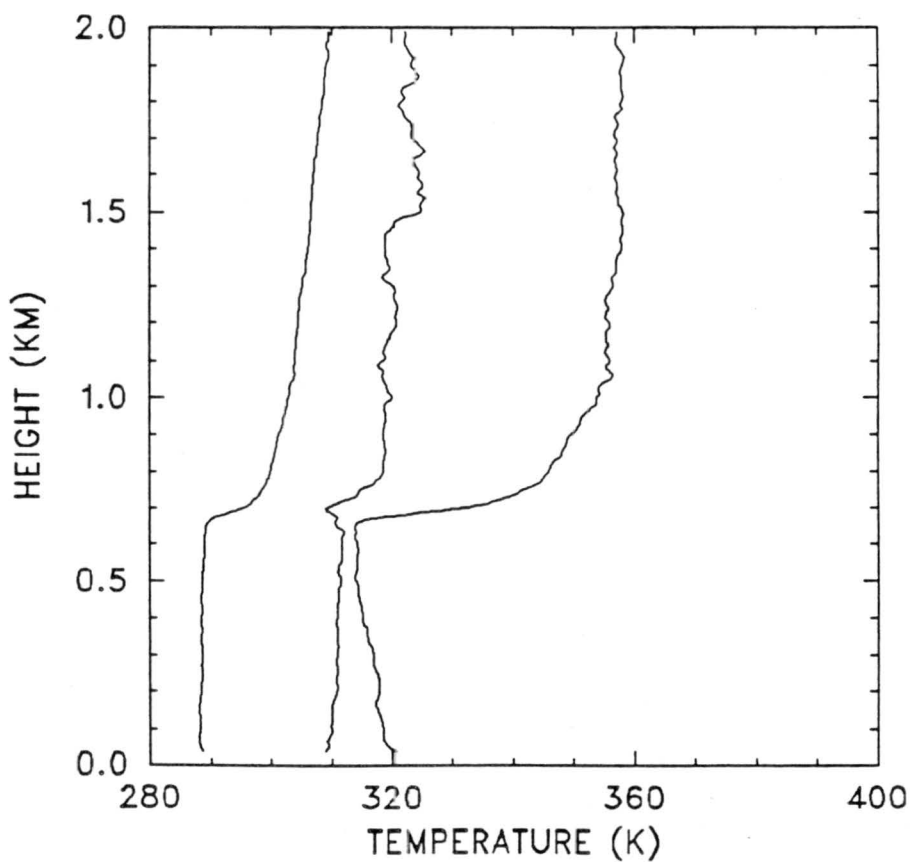
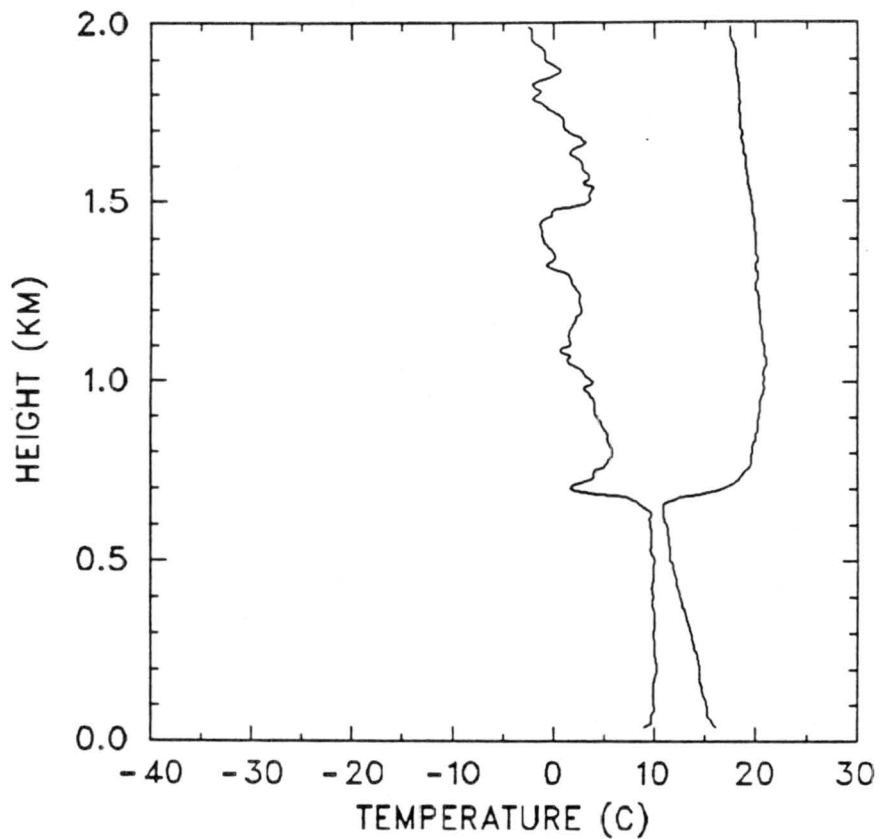
1234 GMT 12 JULY 1987



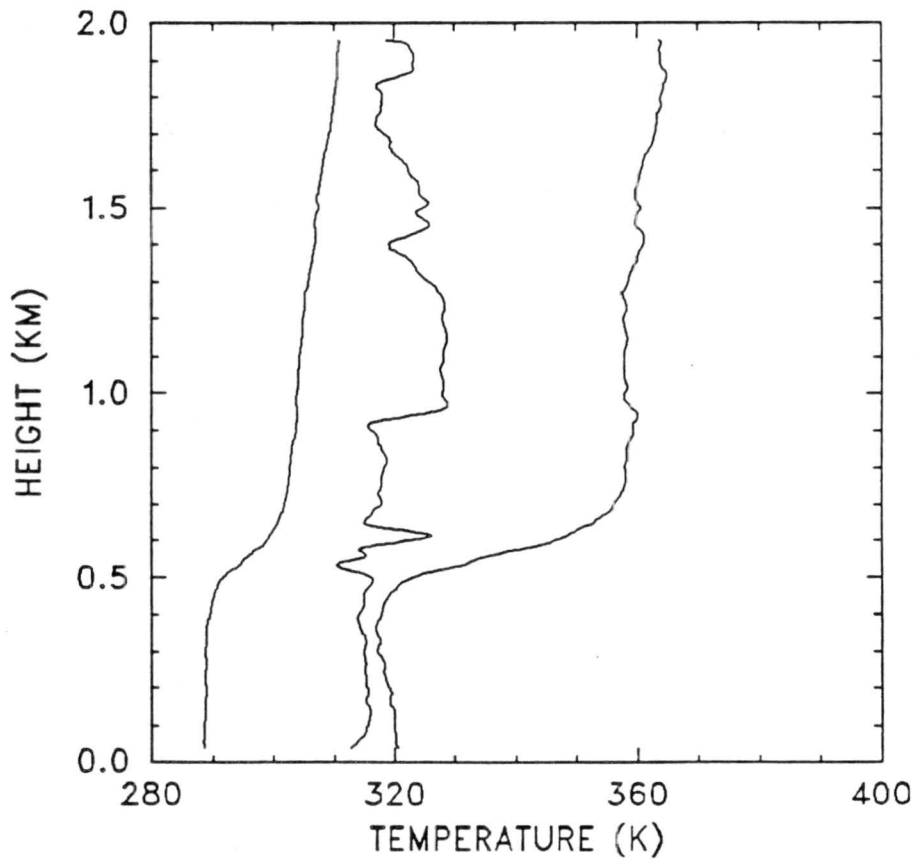
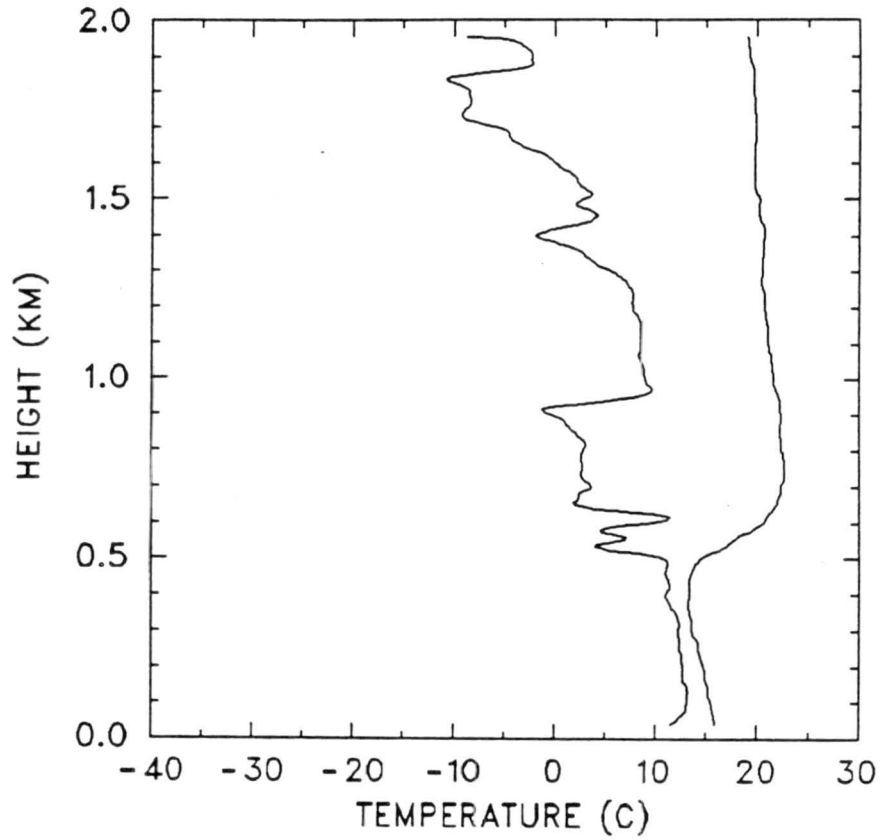
1510 GMT 12 JULY 1987



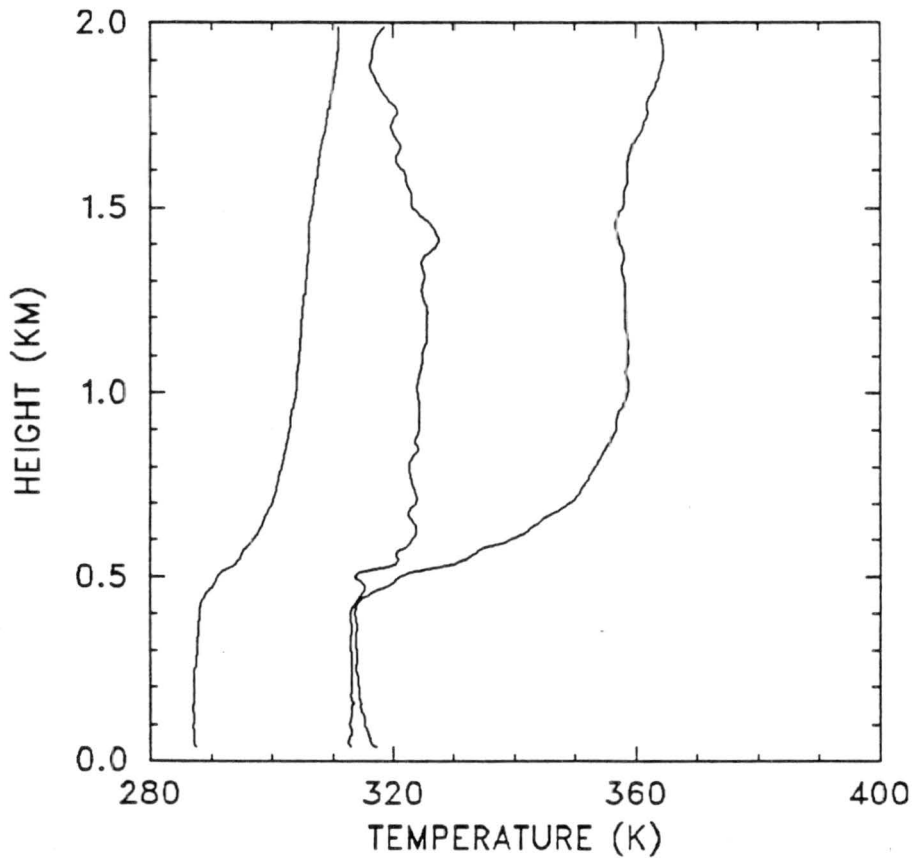
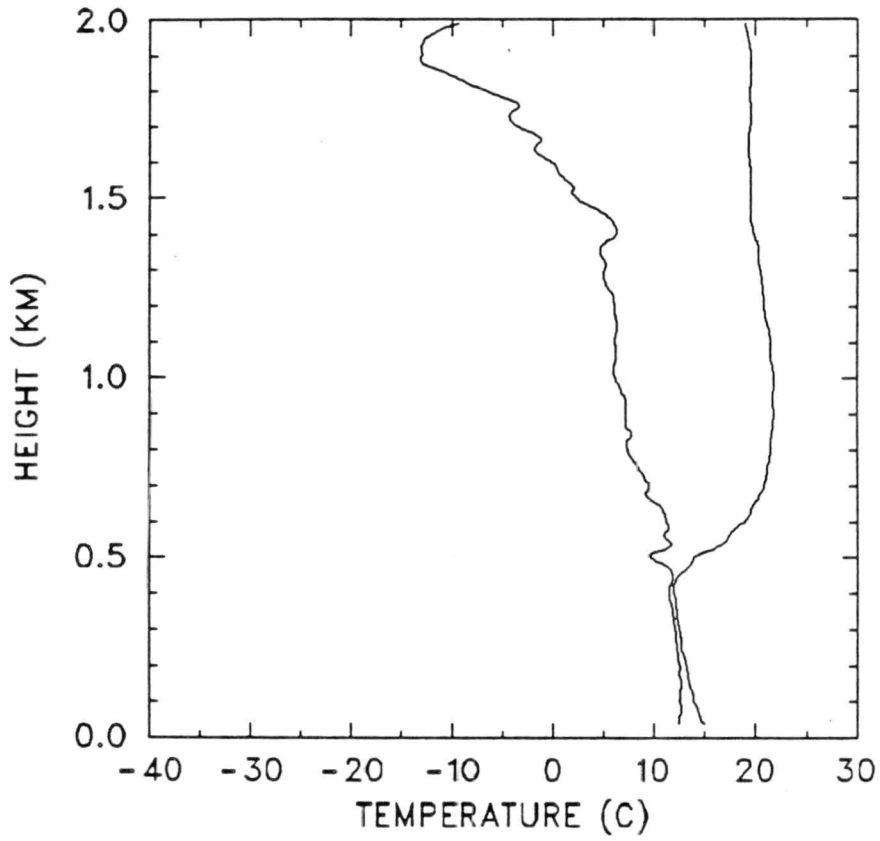
1755 GMT 12 JULY 1987



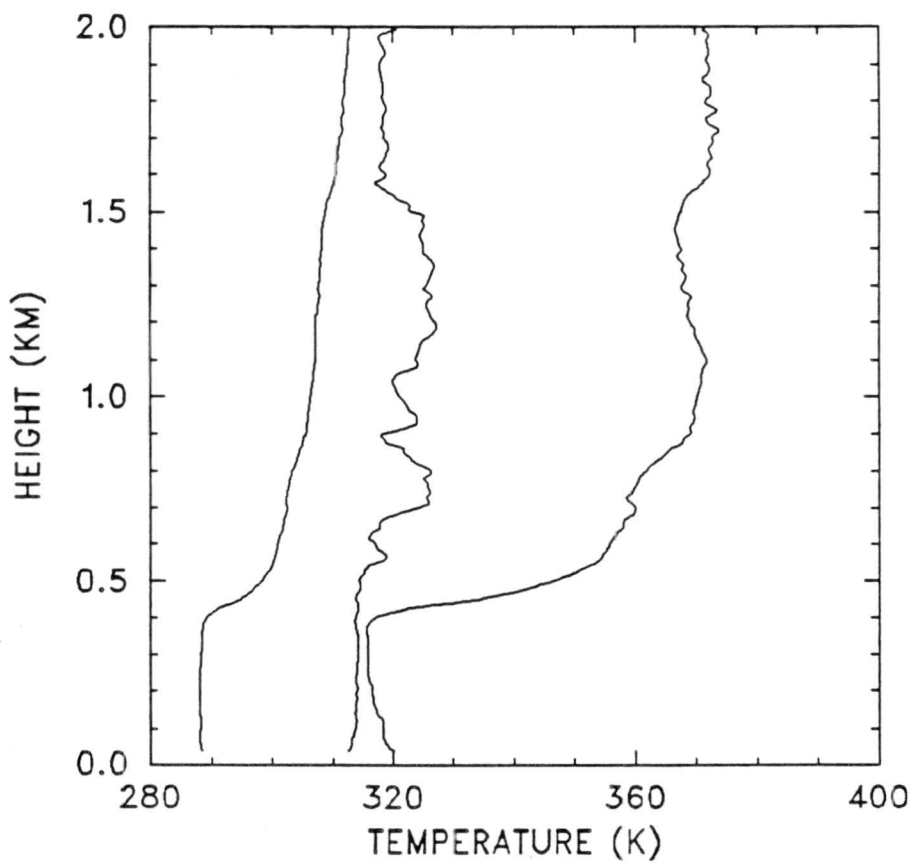
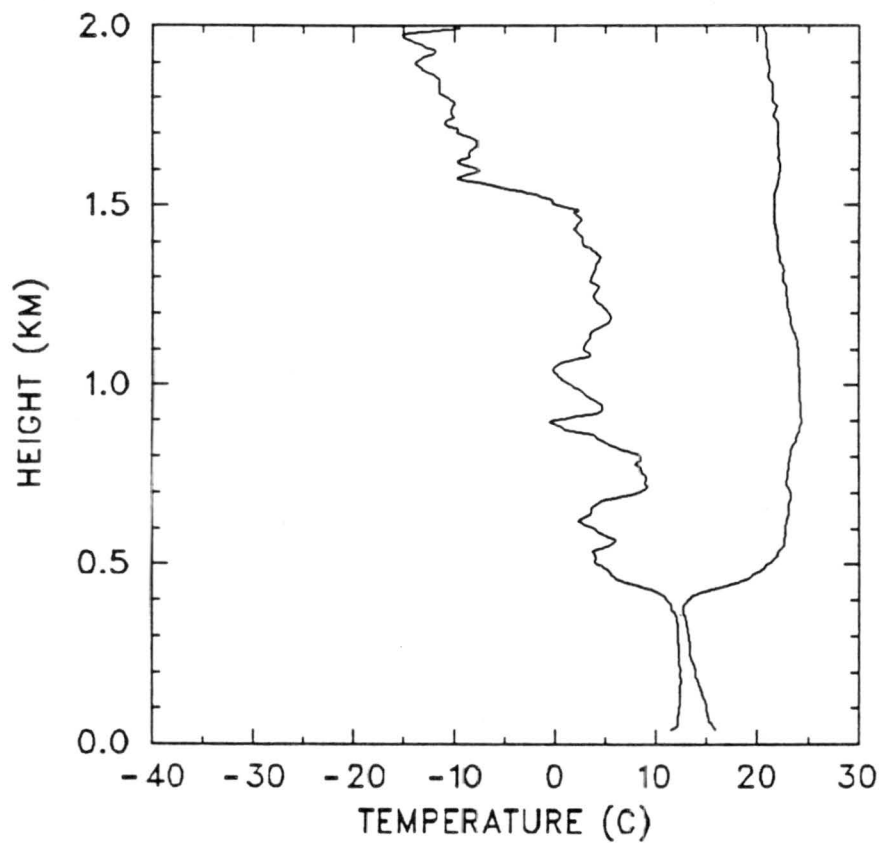
0005 GMT 13 JULY 1987



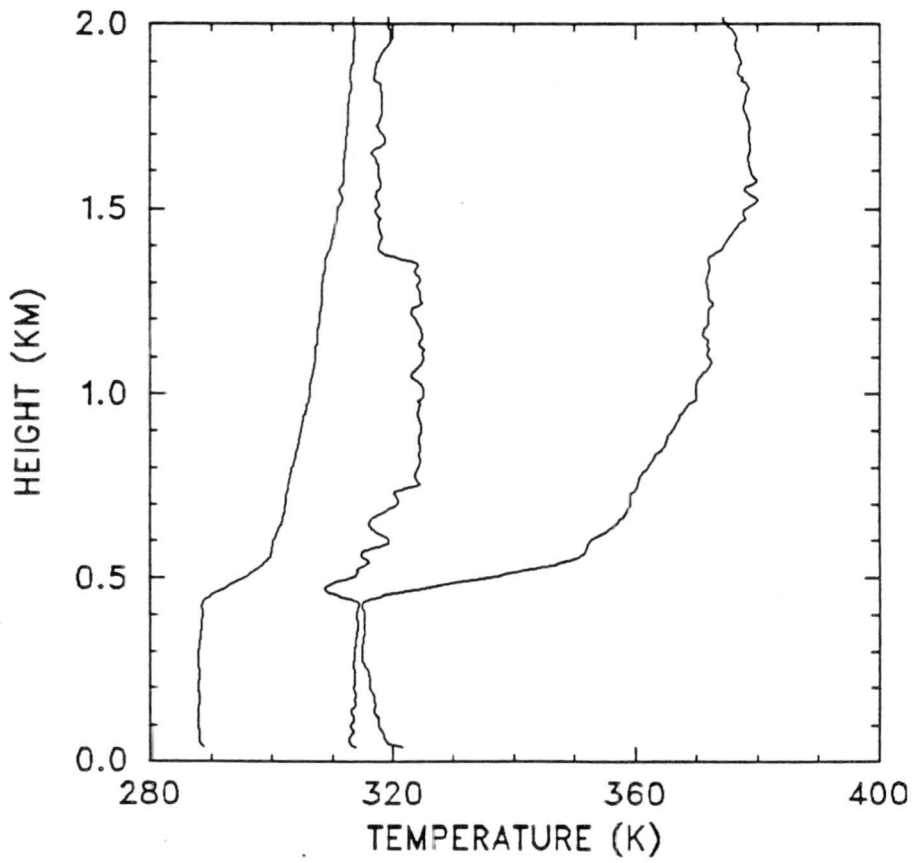
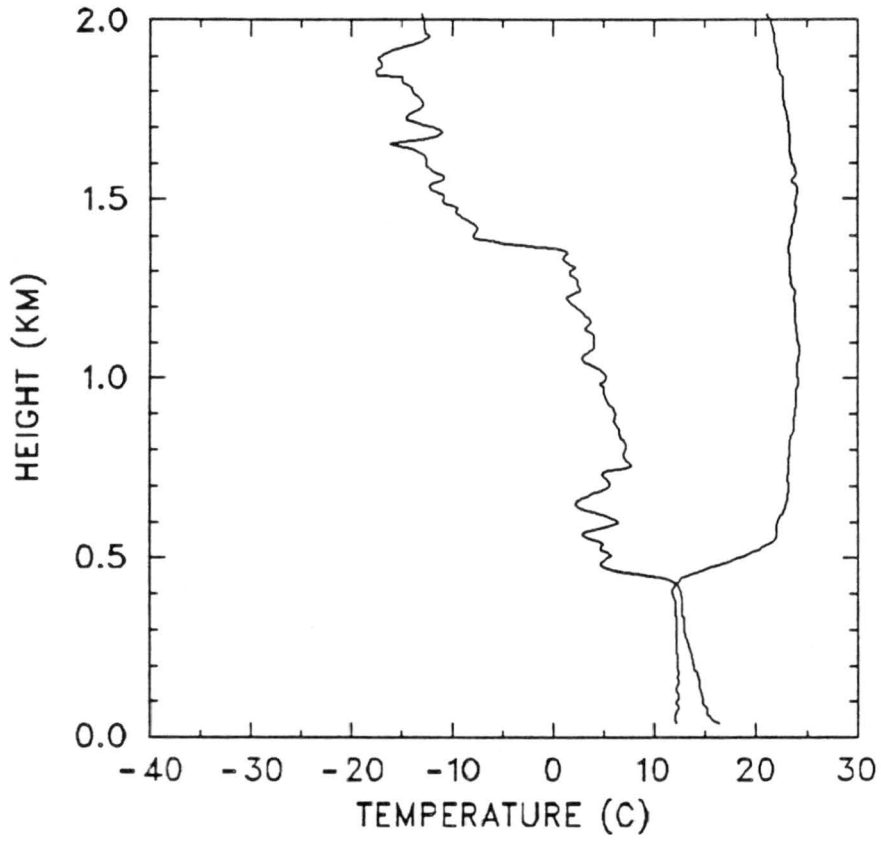
1154 GMT 13 JULY 1987



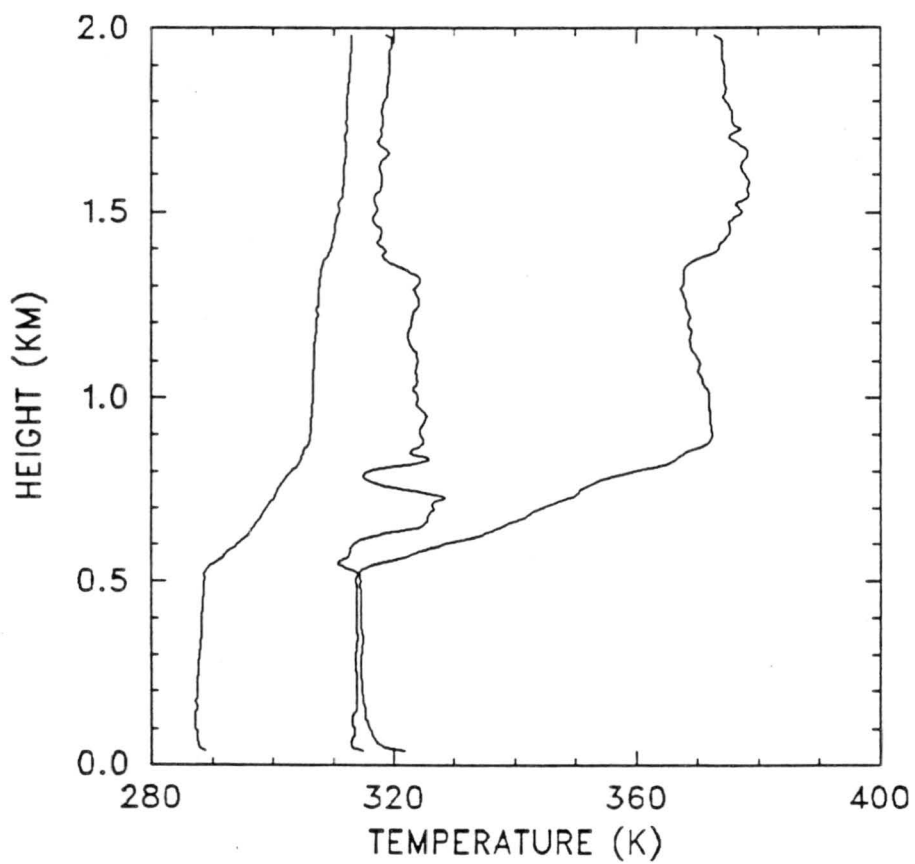
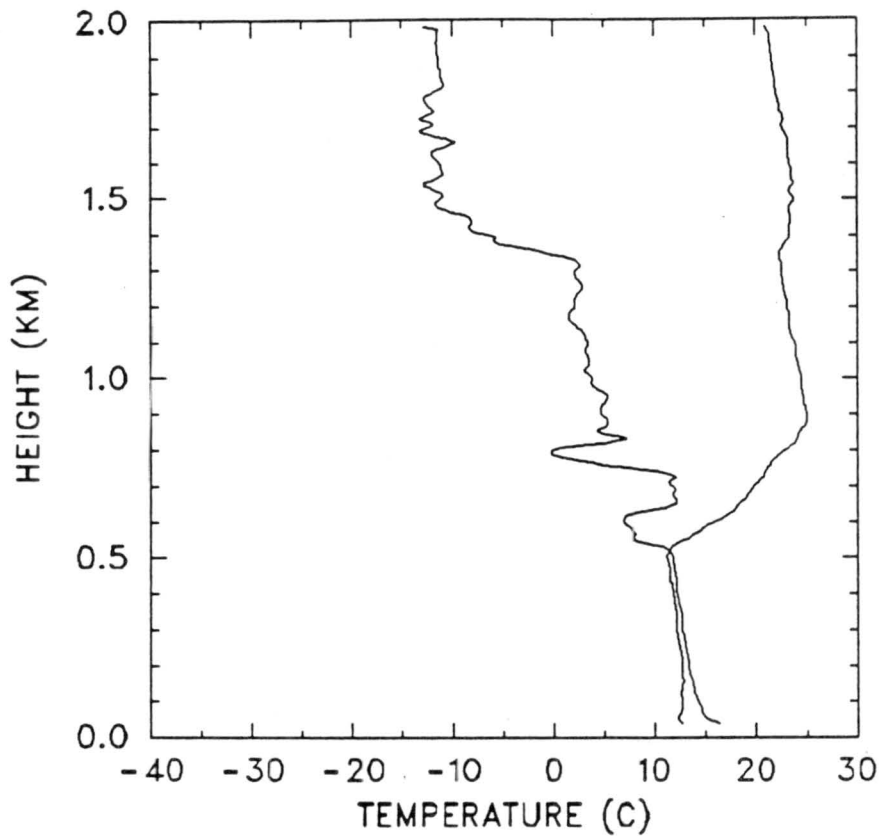
2120 GMT 13 JULY 1987



0014 GMT 14 JULY 1987

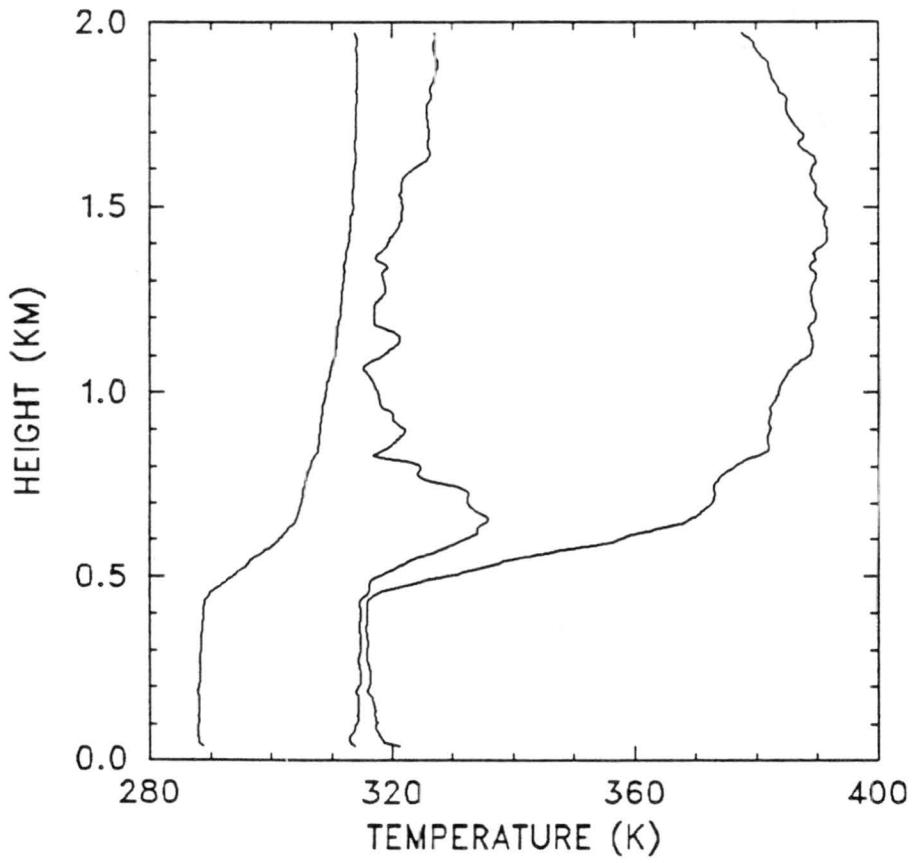
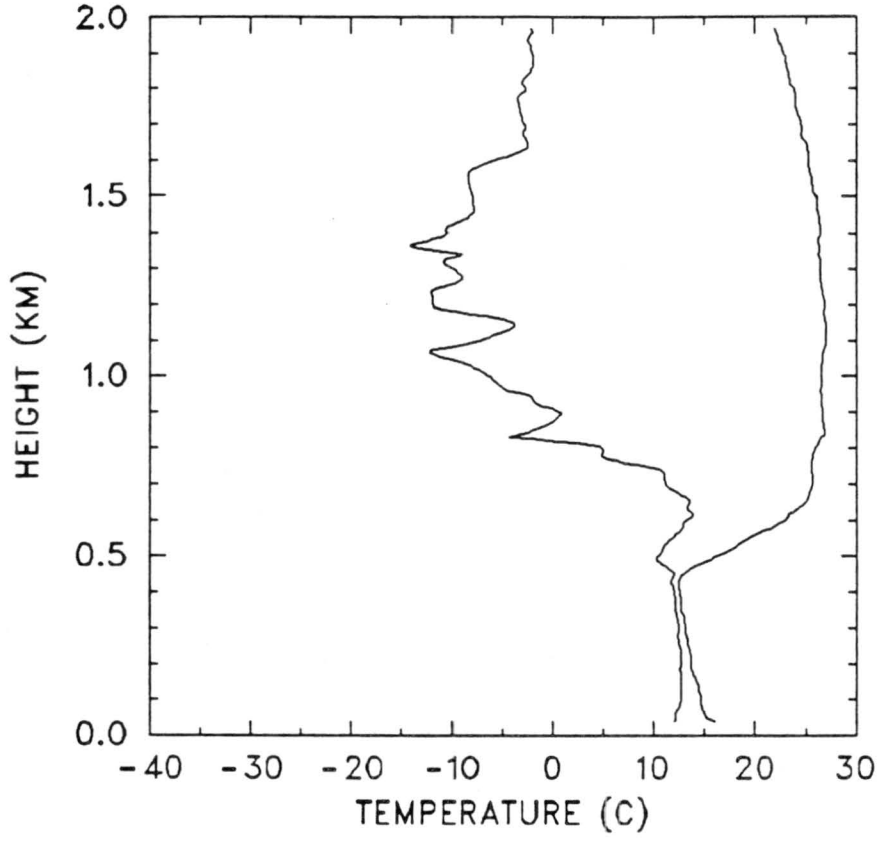


1158 GMT 14 JULY 1987

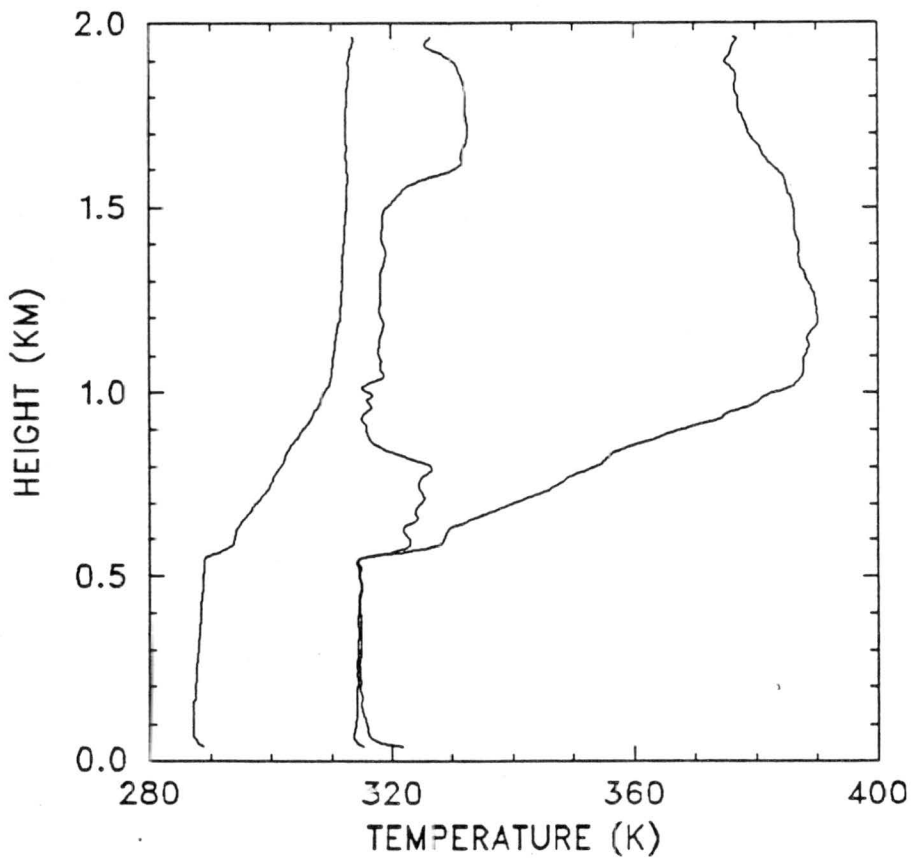
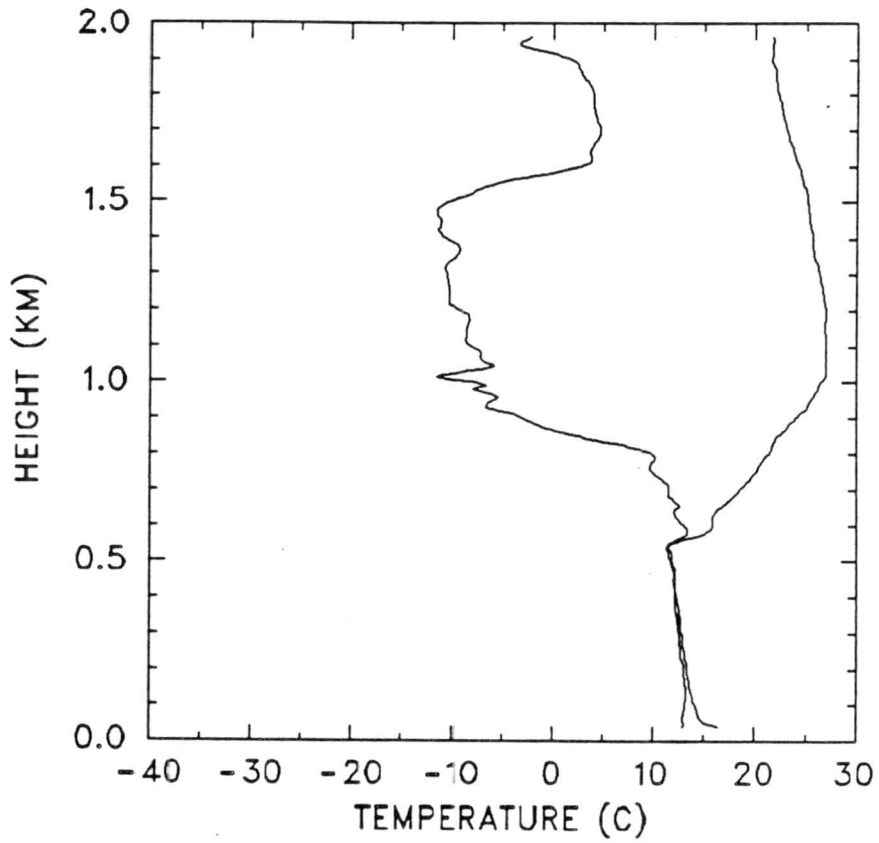




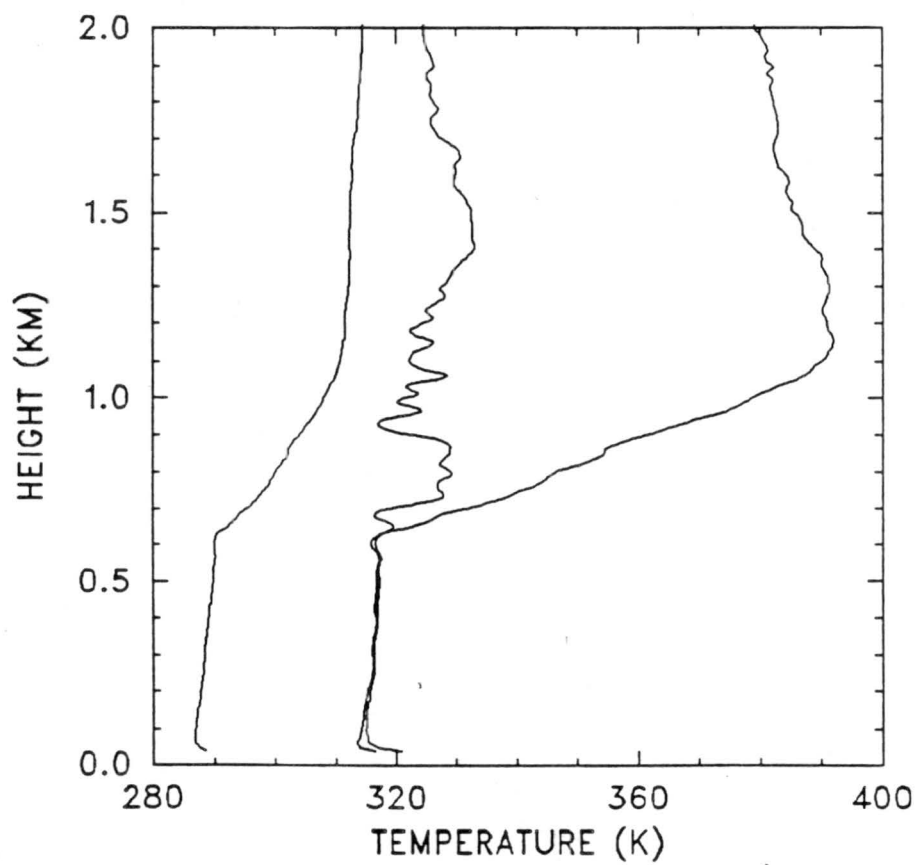
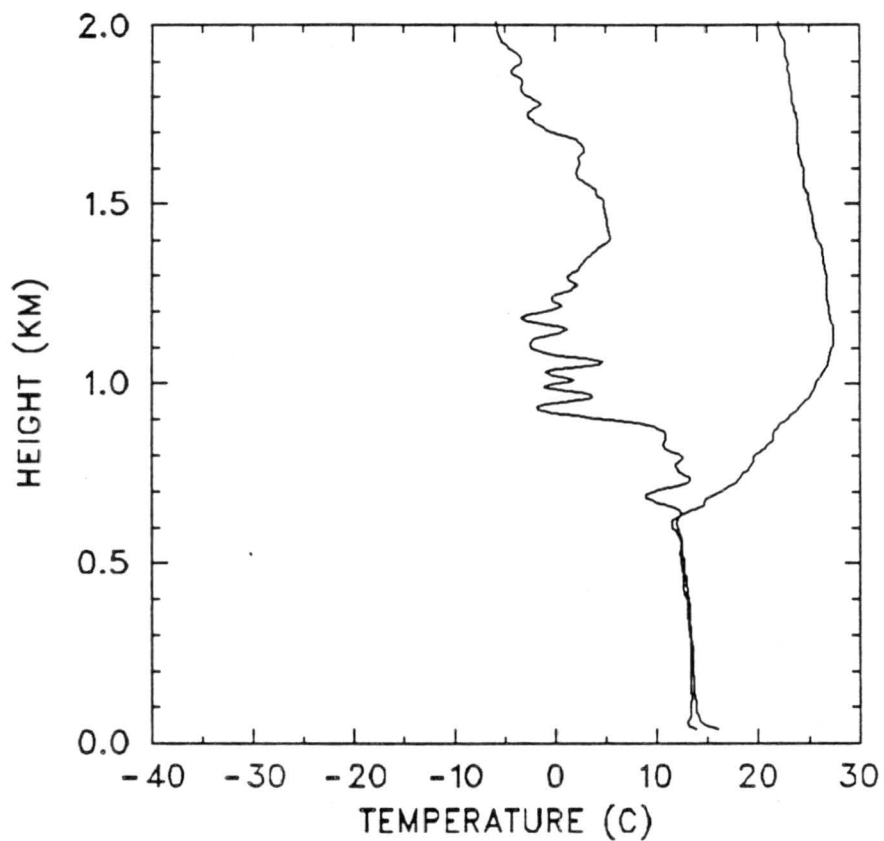
0015 GMT 15 JULY 1987



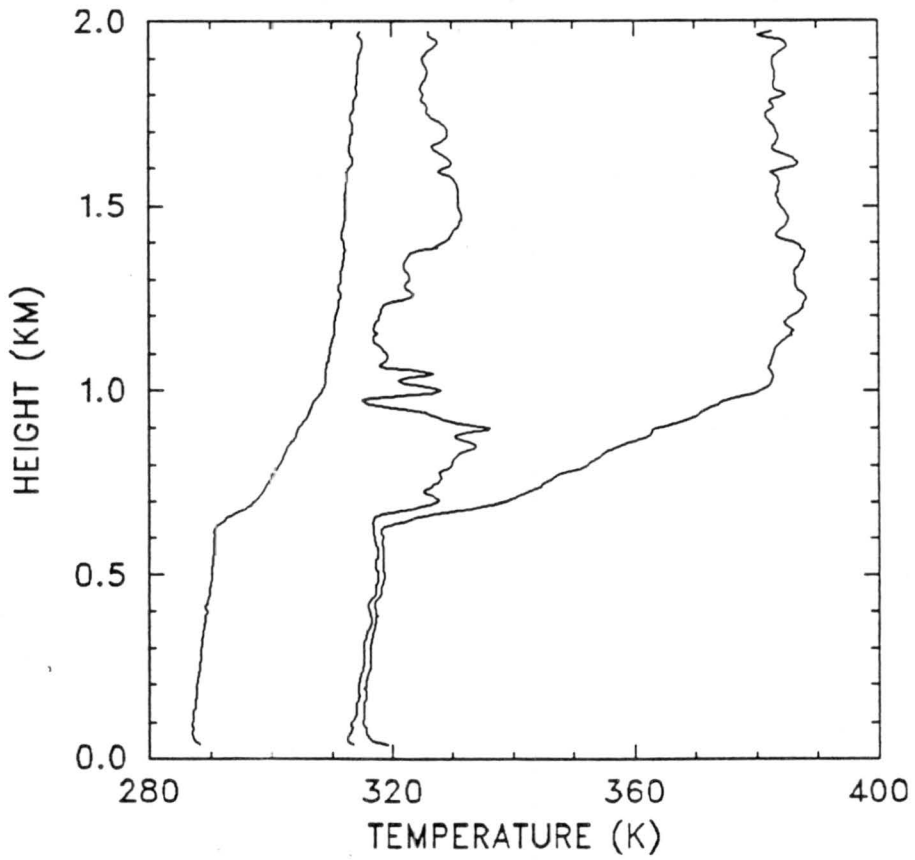
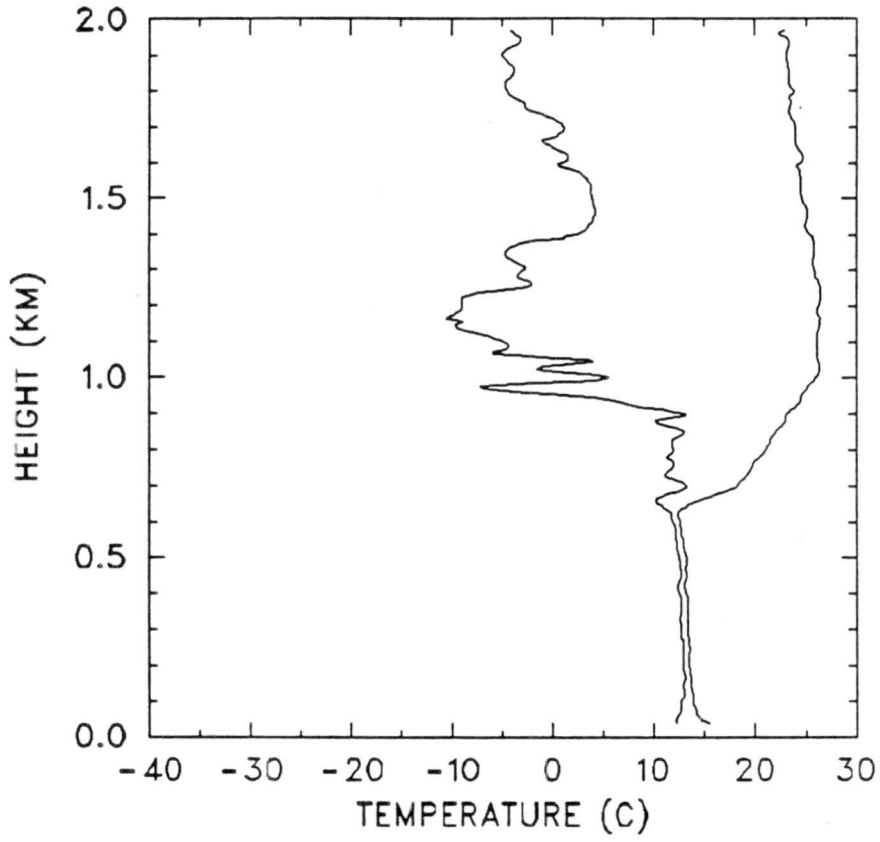
1200 GMT 15 JULY 1987



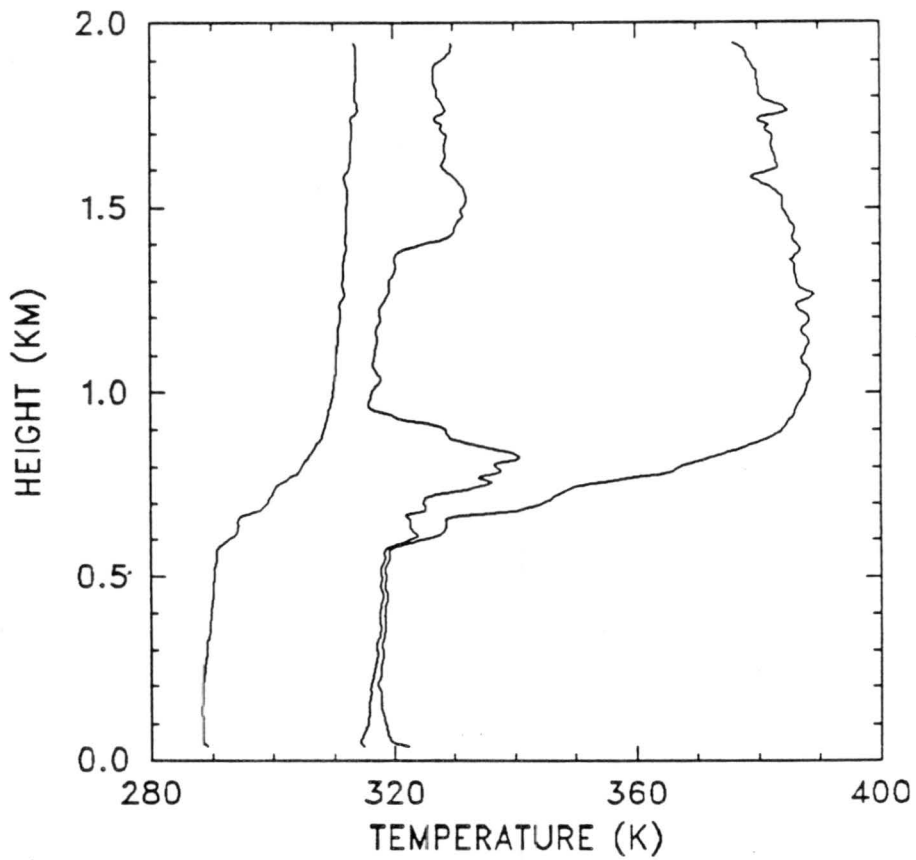
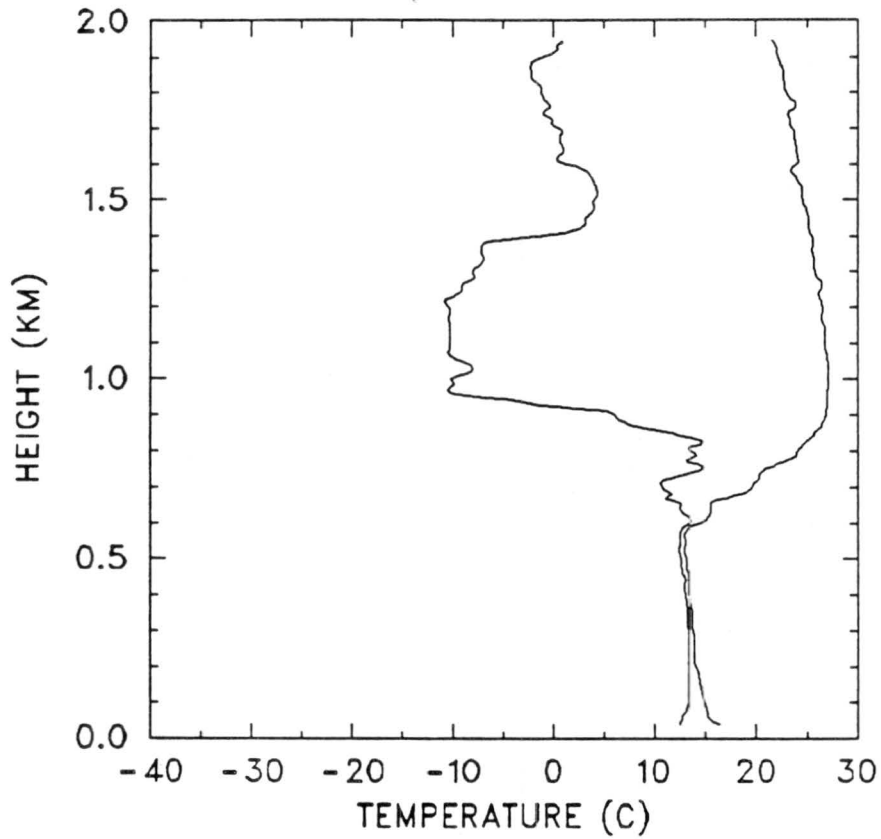
1703 GMT 15 JULY 1987



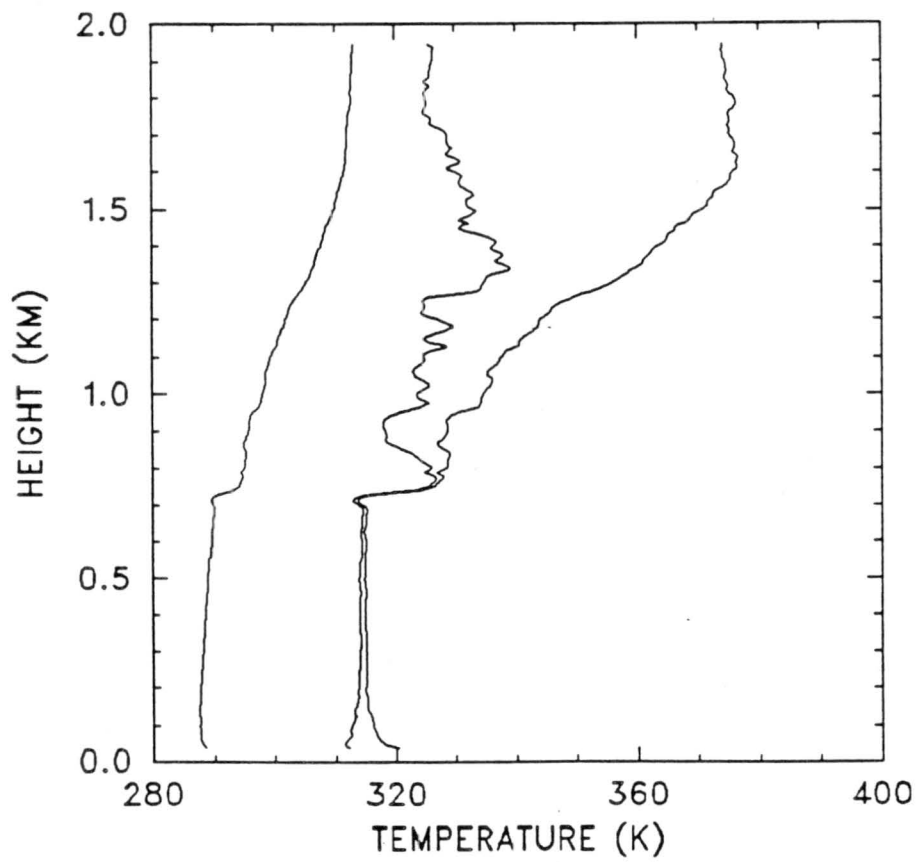
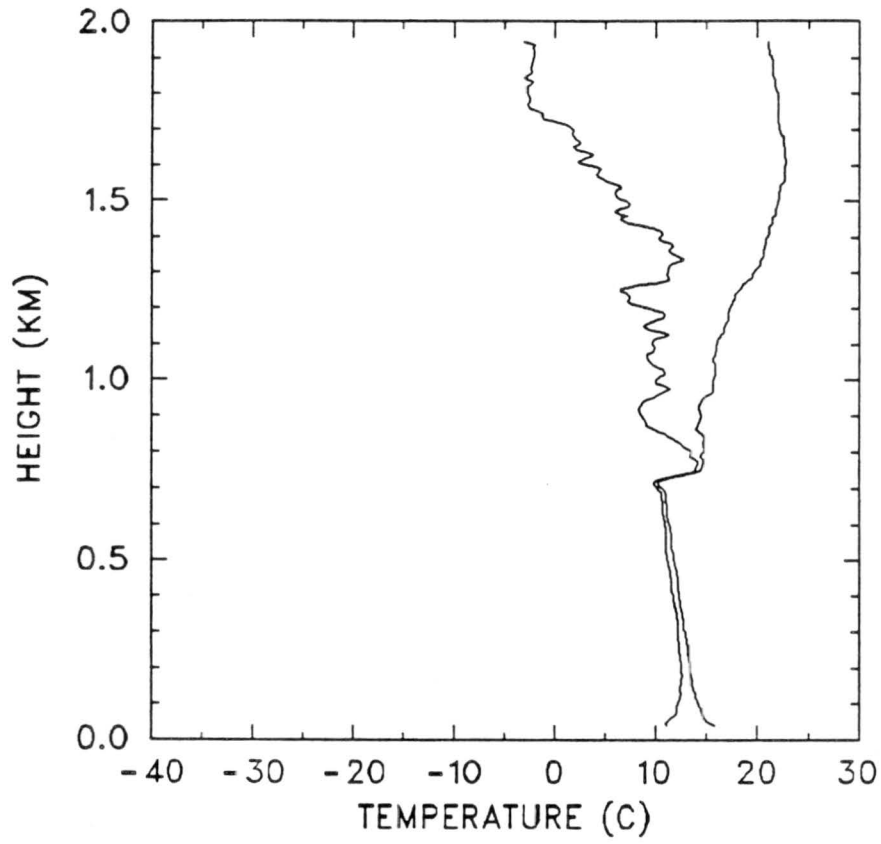
1935 GMT 15 JULY 1987



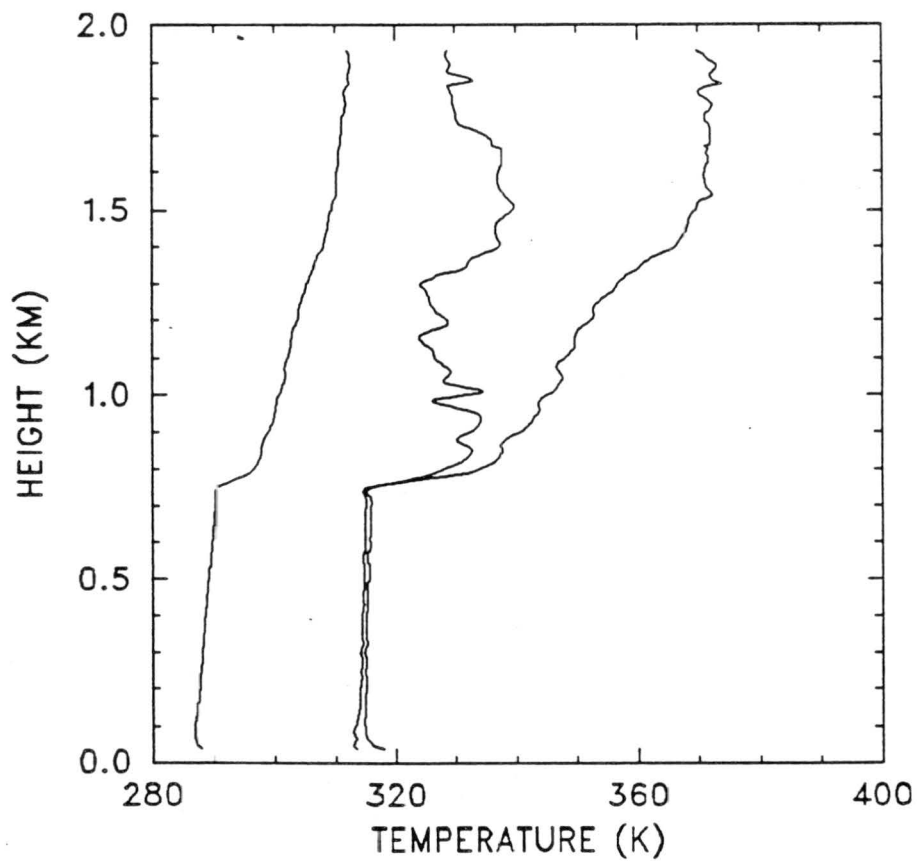
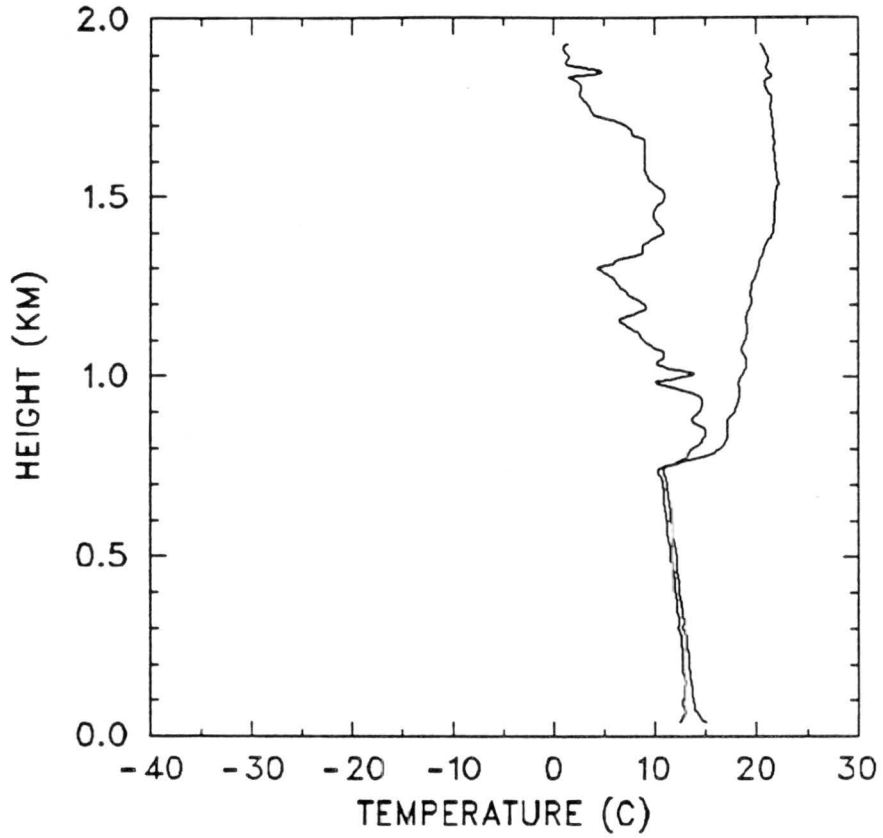
0011 GMT 16 JULY 1987



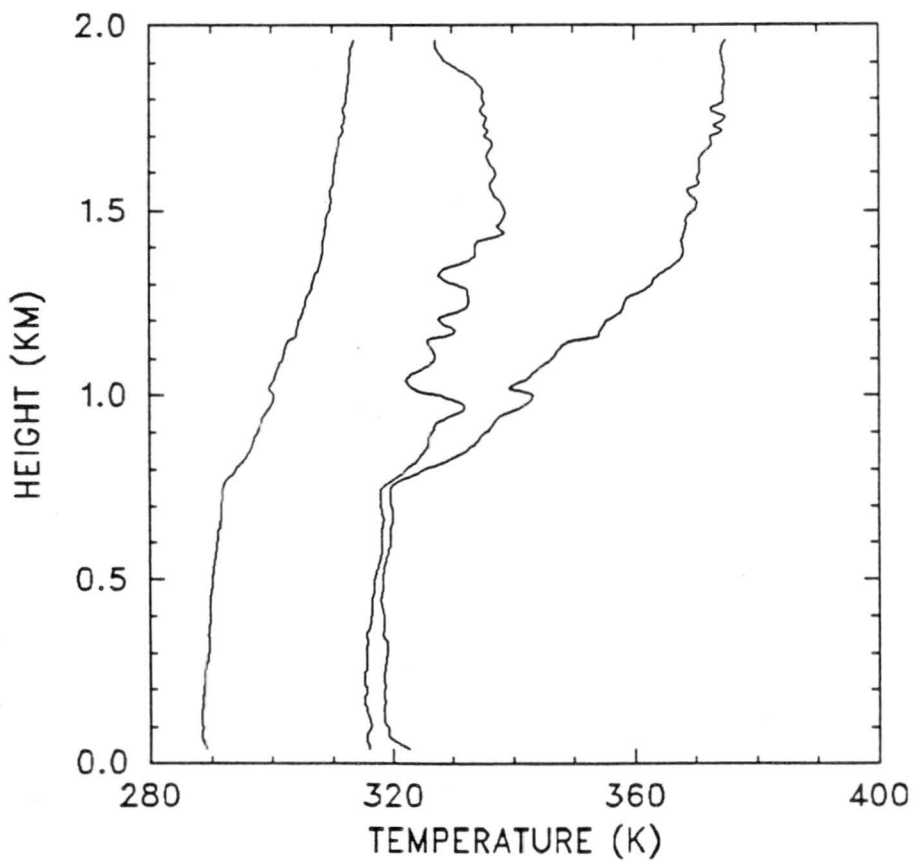
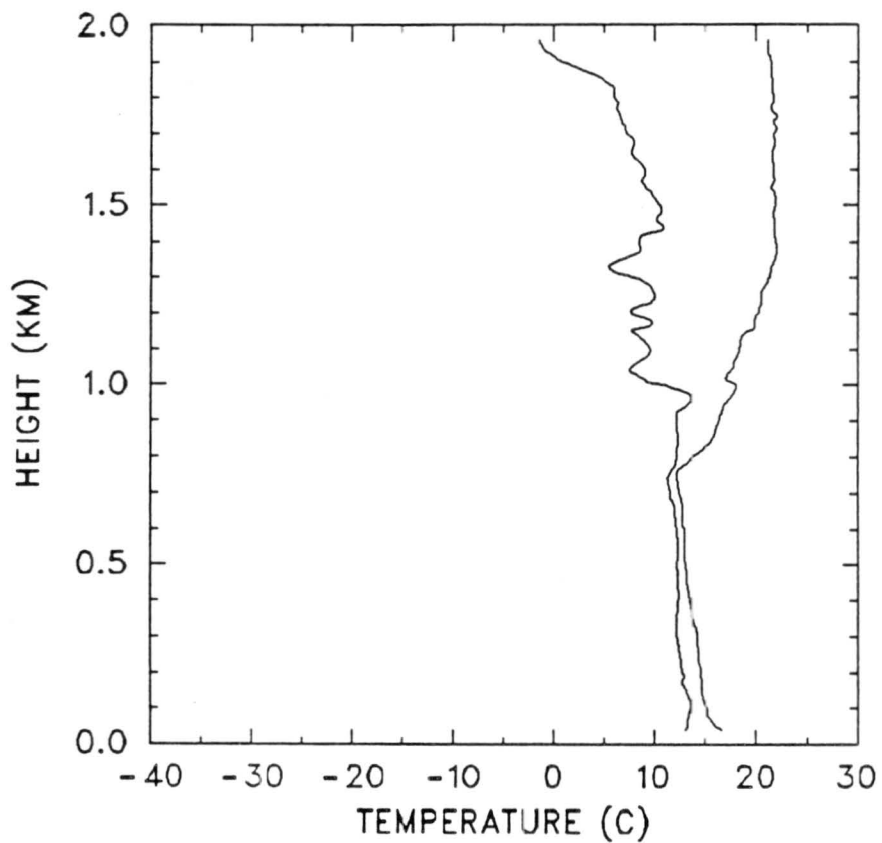
1139 GMT 16 JULY 1987



1600 GMT 16 JULY 1987

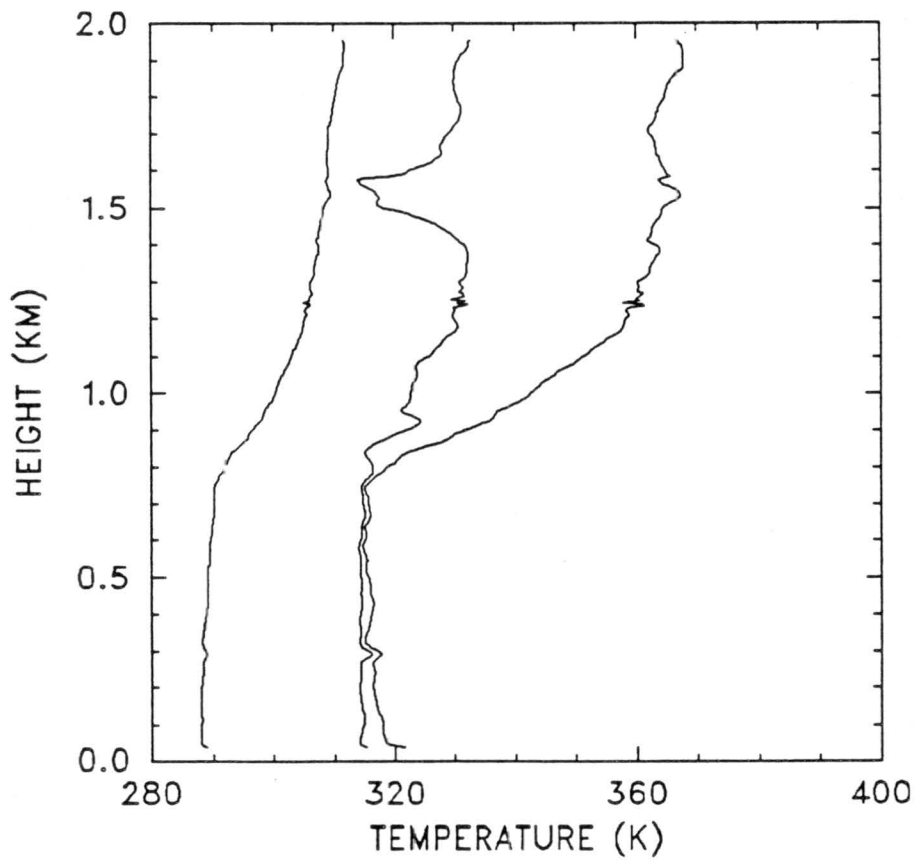
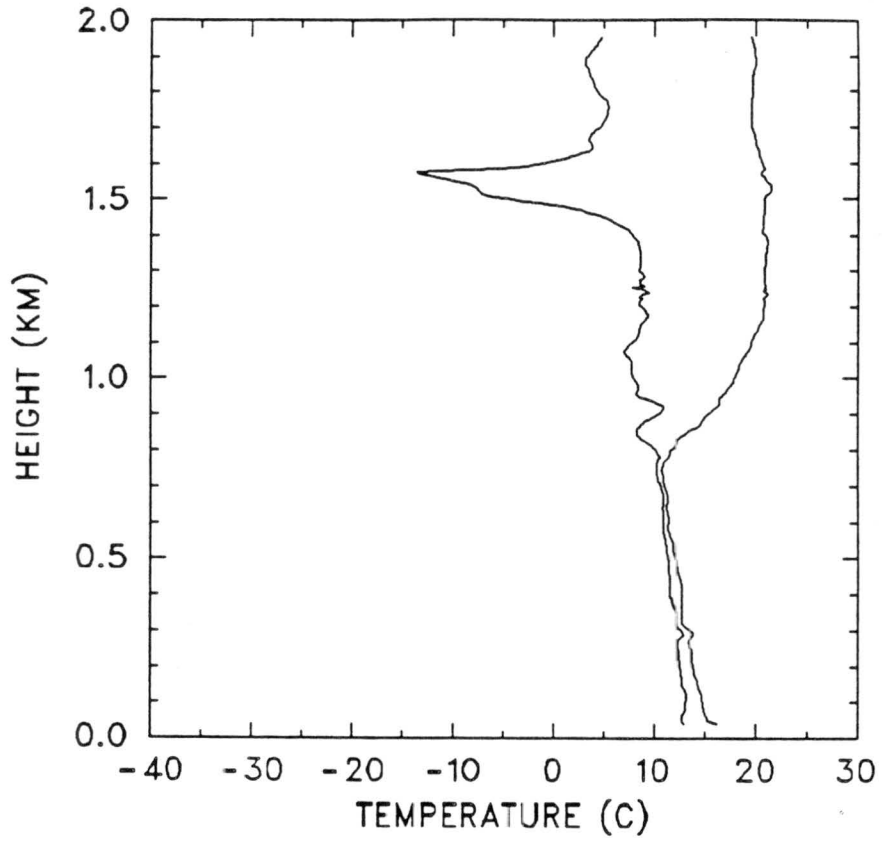


2004 GMT 16 JULY 1987

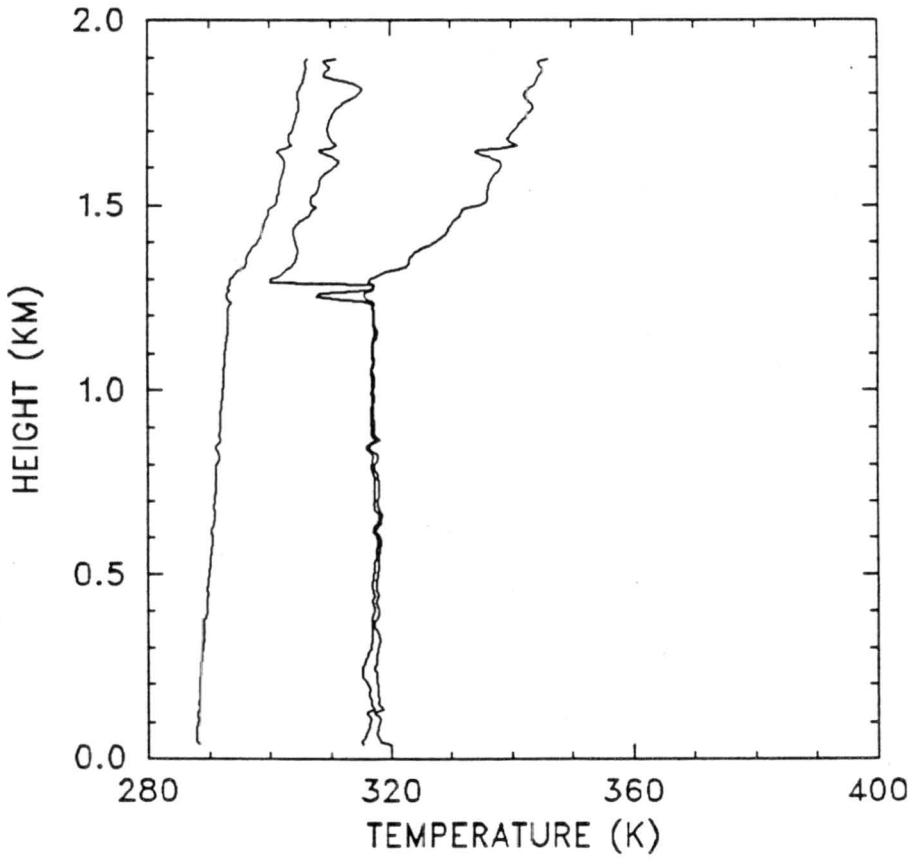
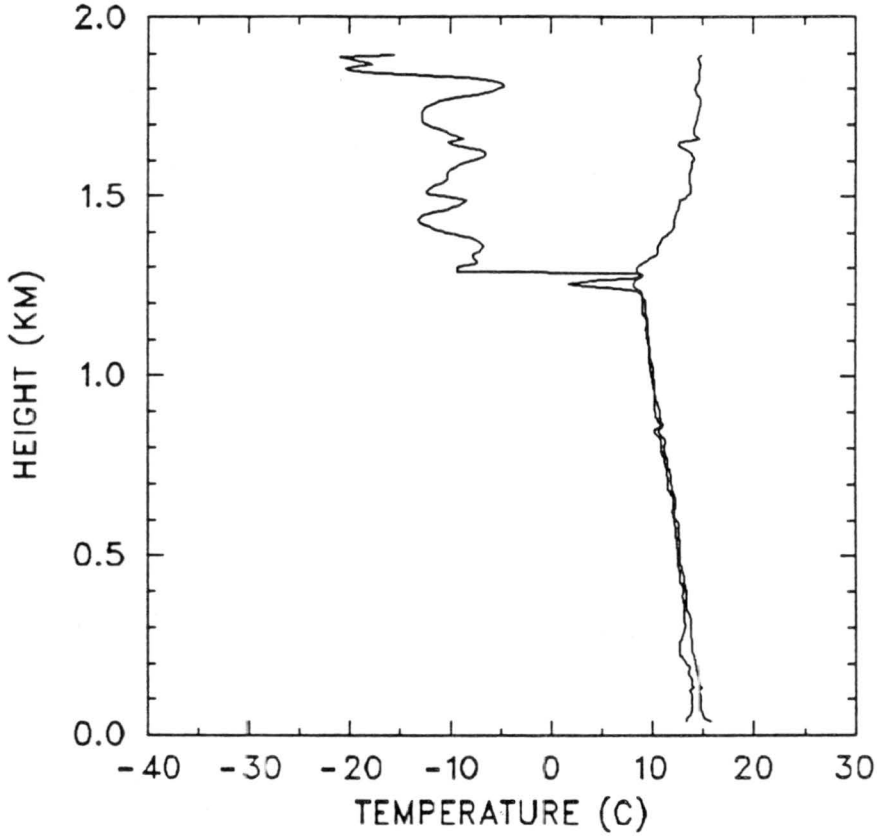




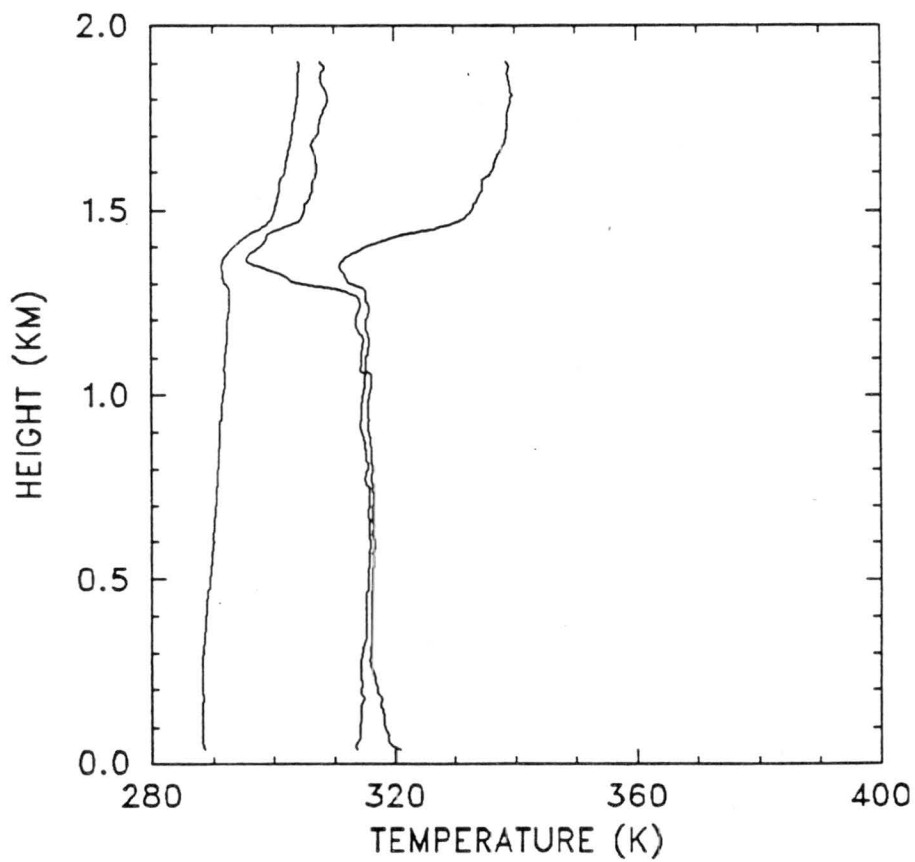
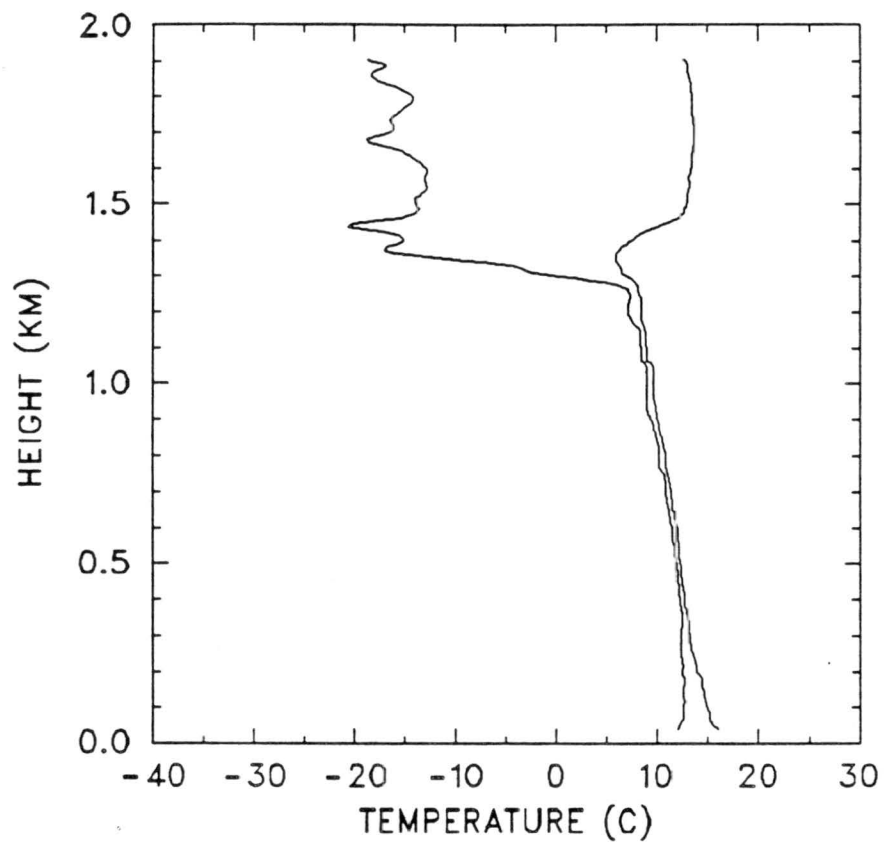
2342 GMT 16 JULY 1987

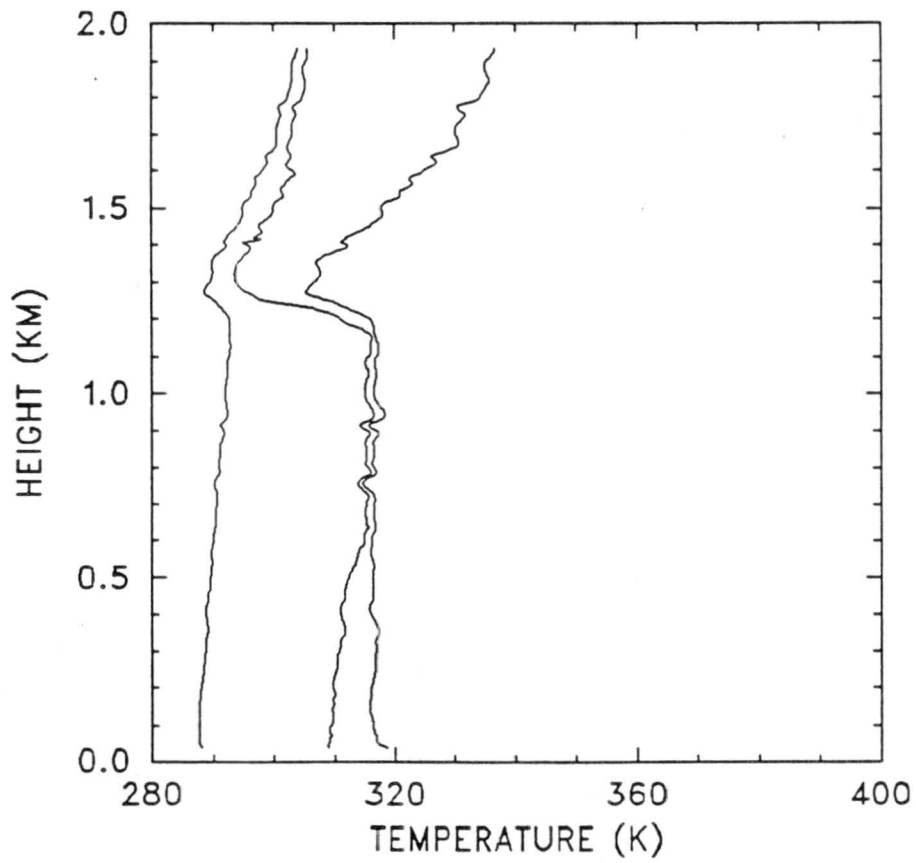
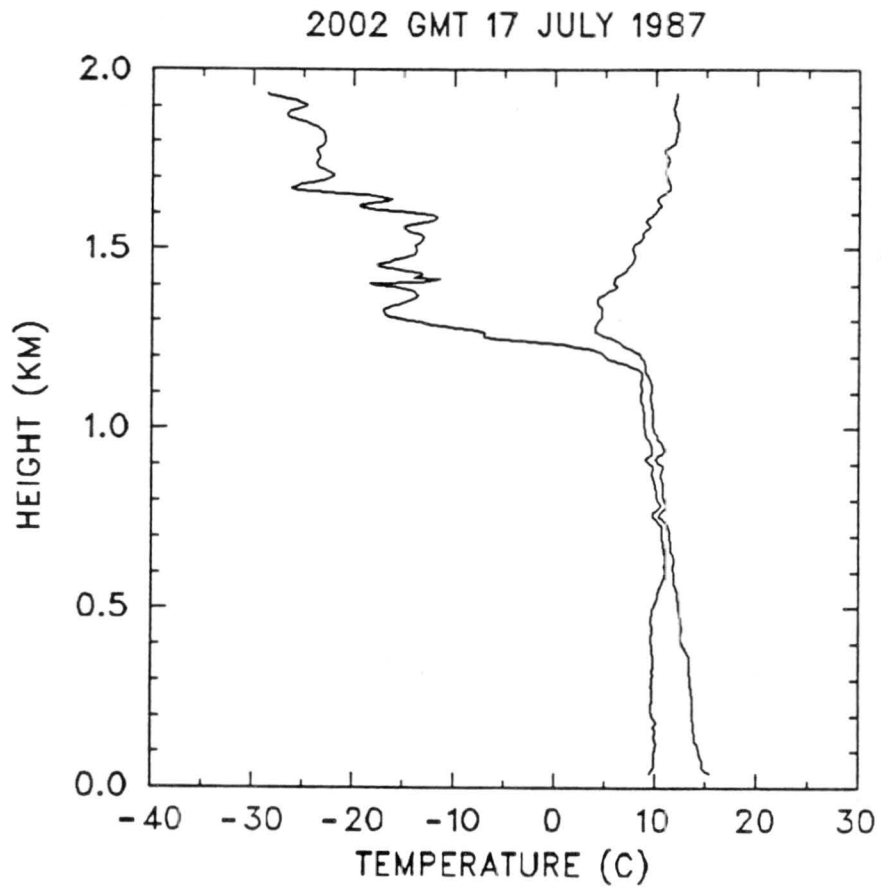


1206 GMT 17 JULY 1987

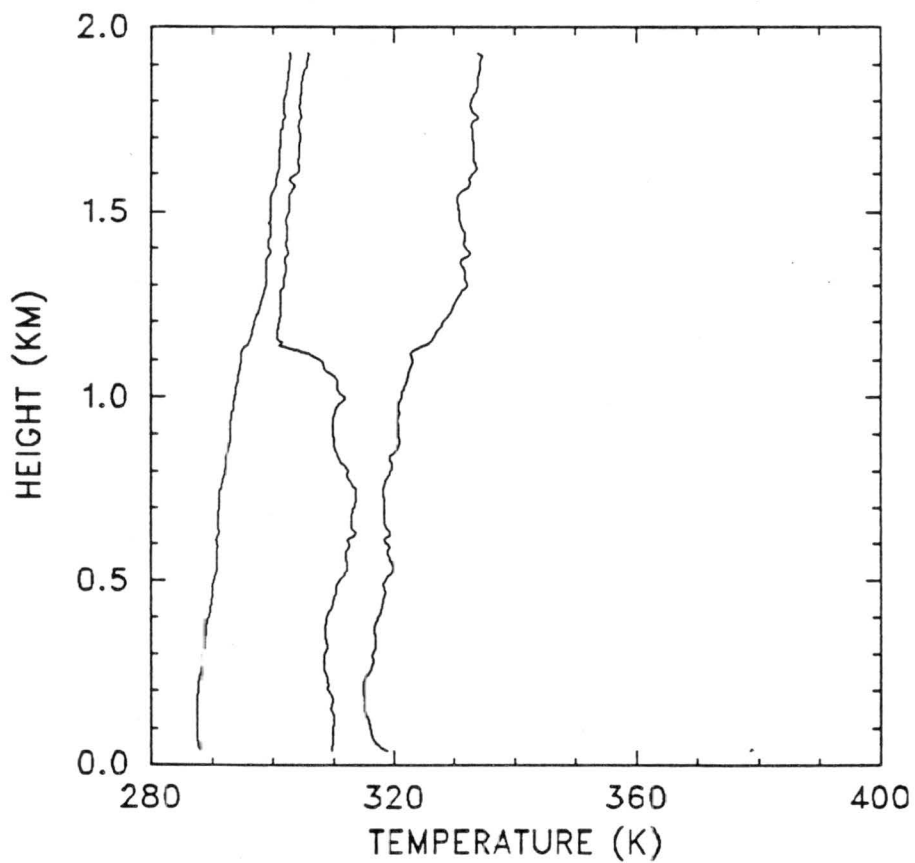
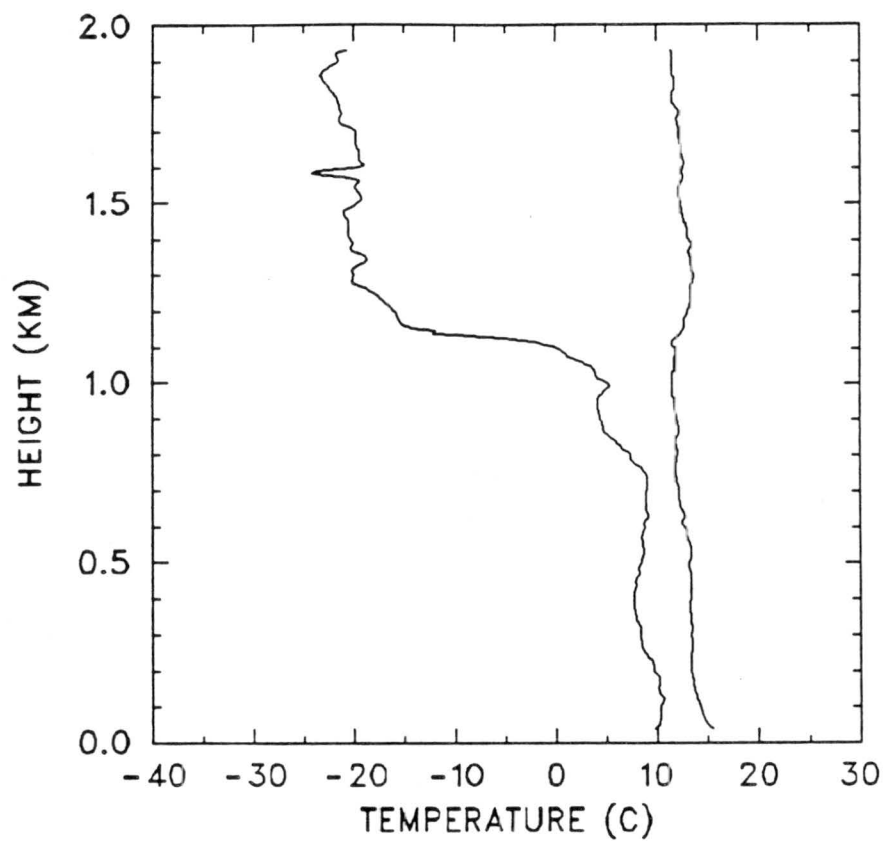


1558 GMT 17 JULY 1987

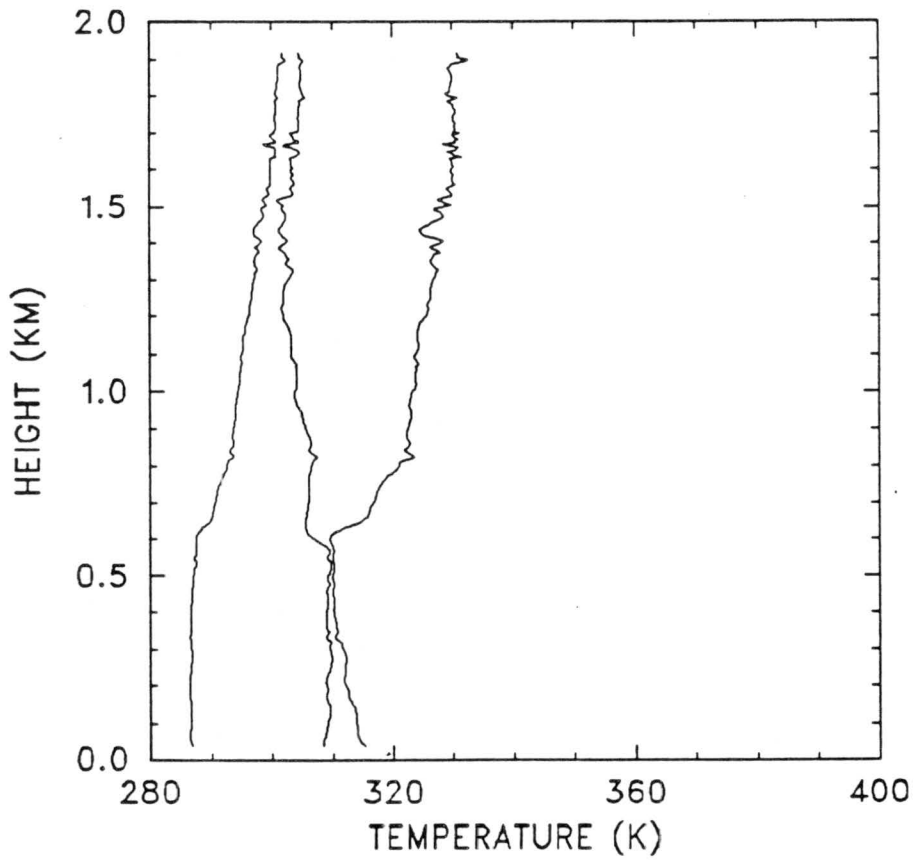
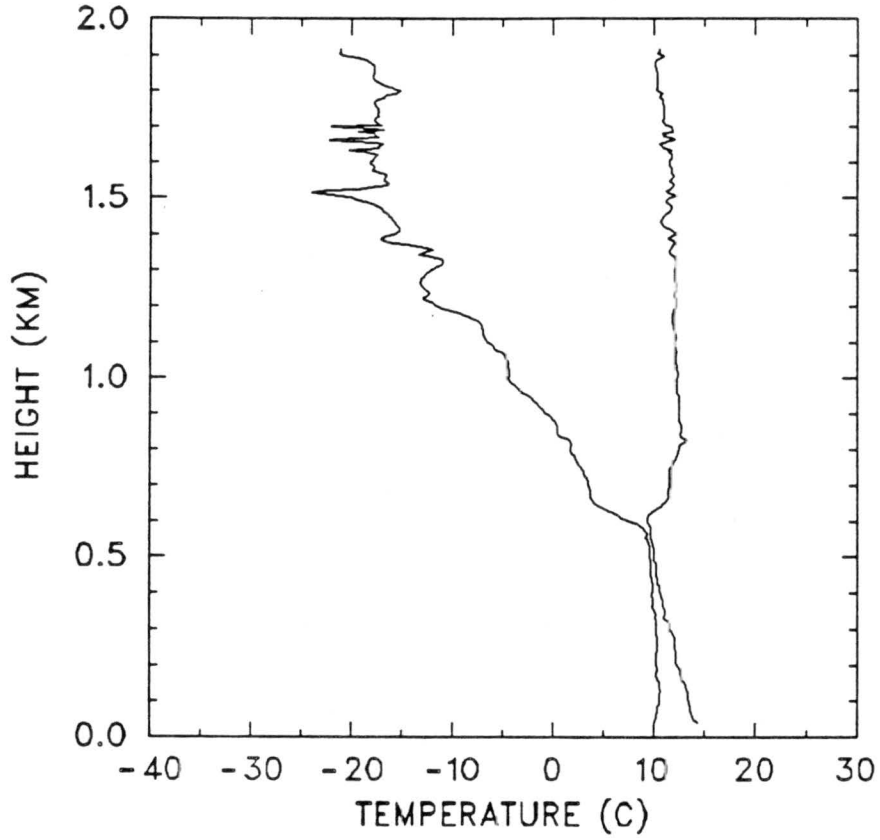




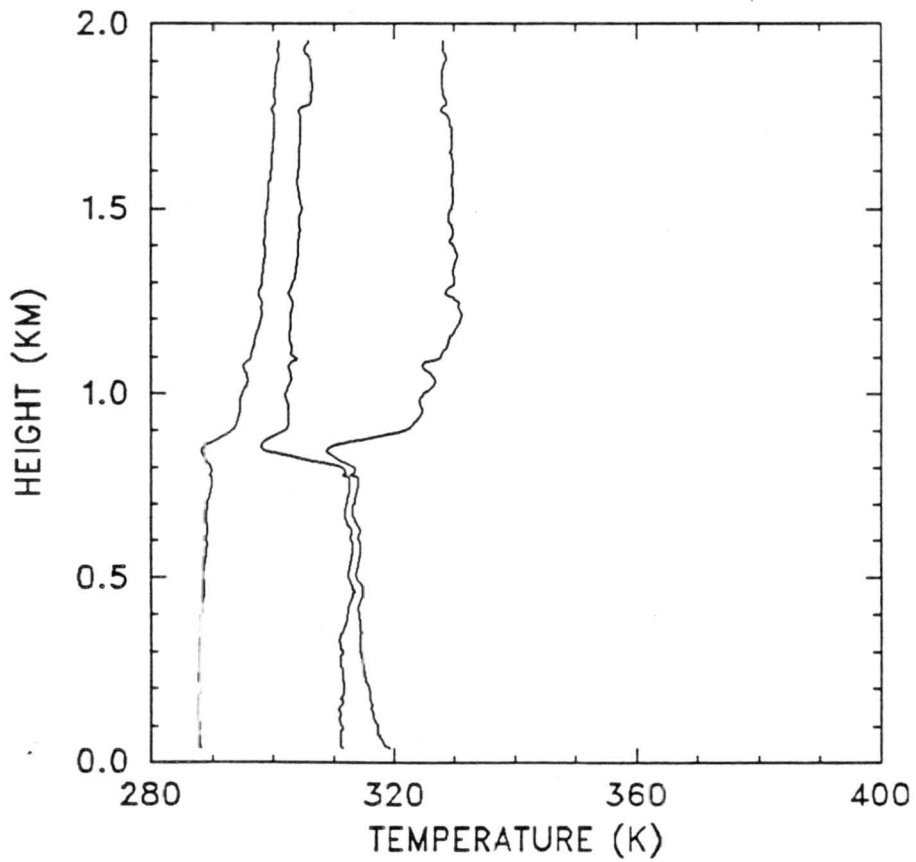
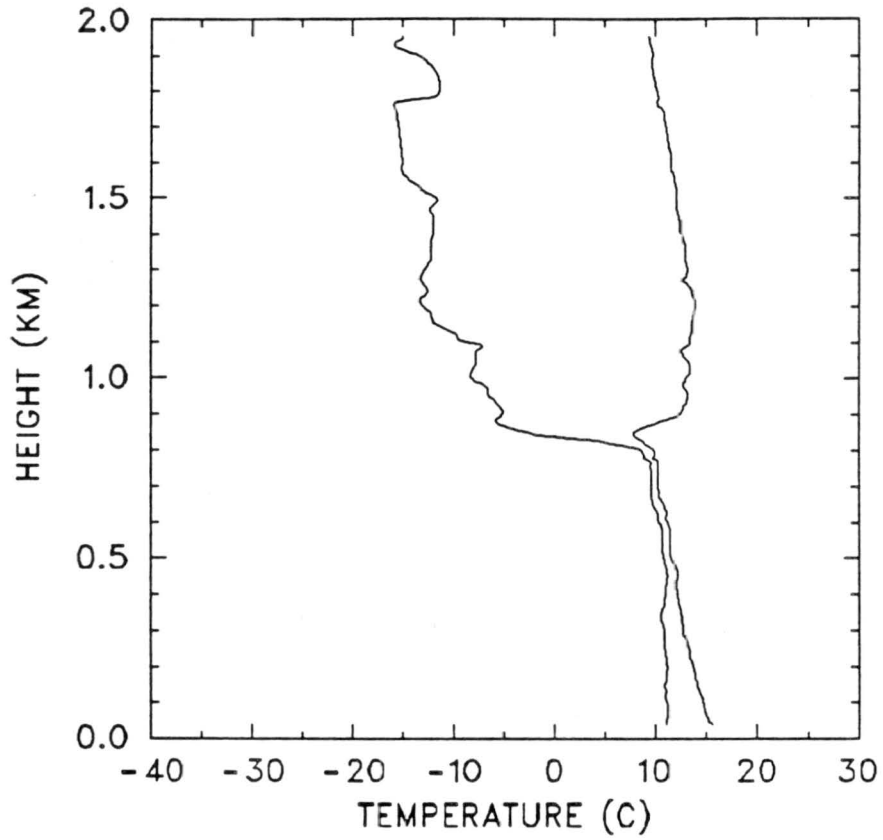
0020 GMT 18 JULY 1987



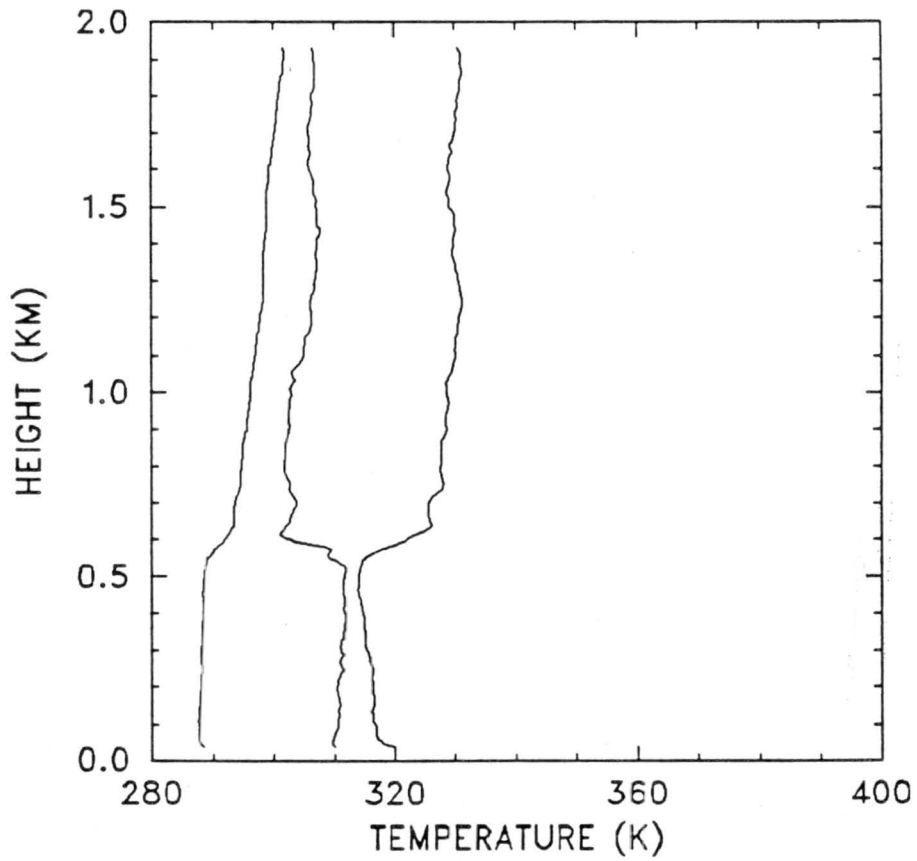
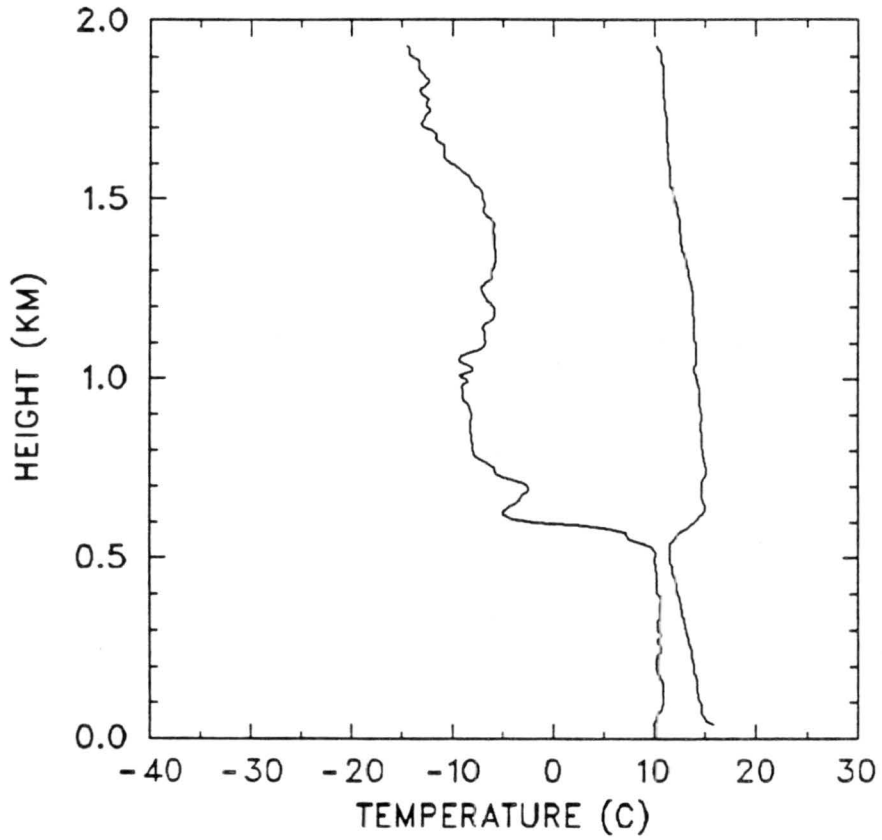
1206 GMT 18 JULY 1987



1557 GMT 18 JULY 1987

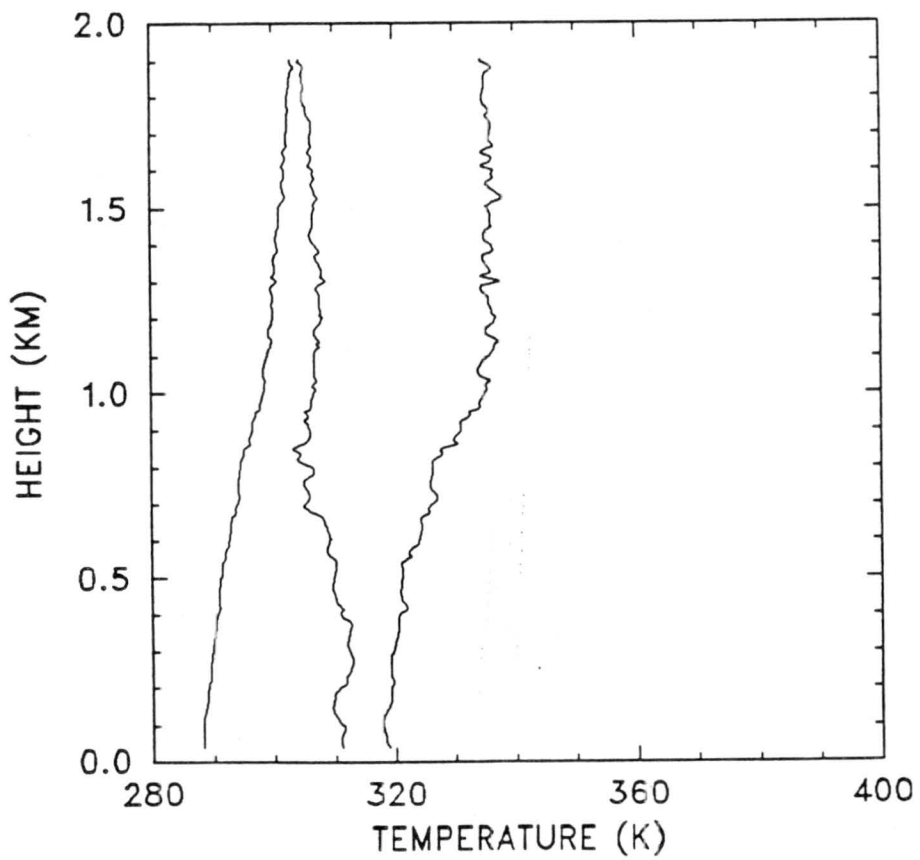
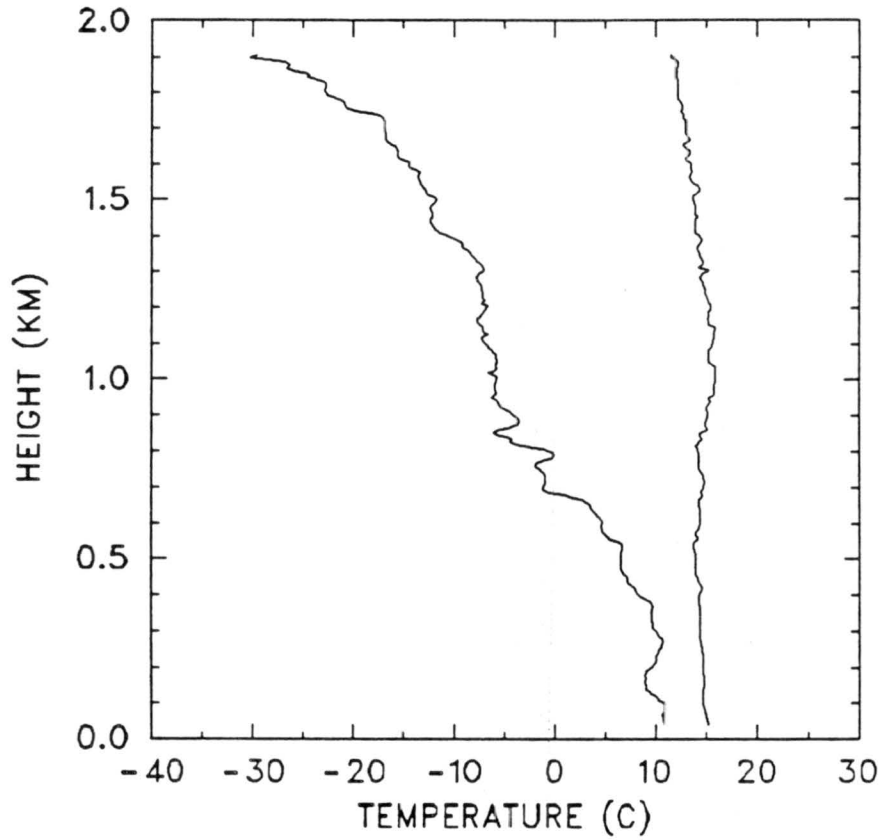


1951 GMT 18 JULY 1987

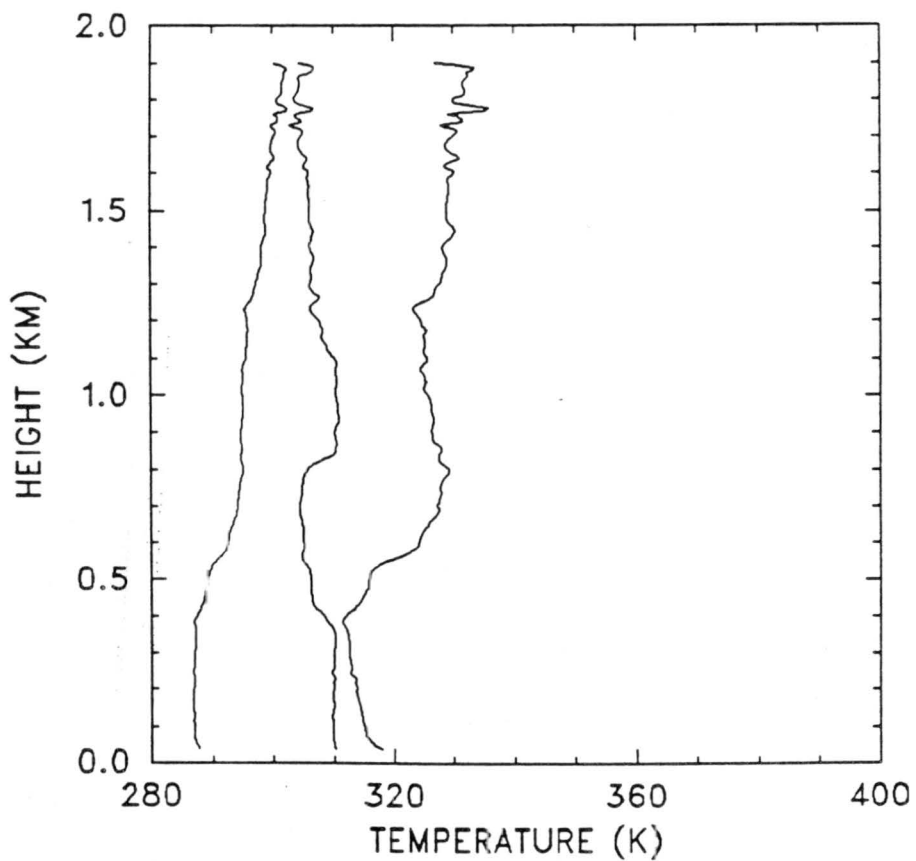
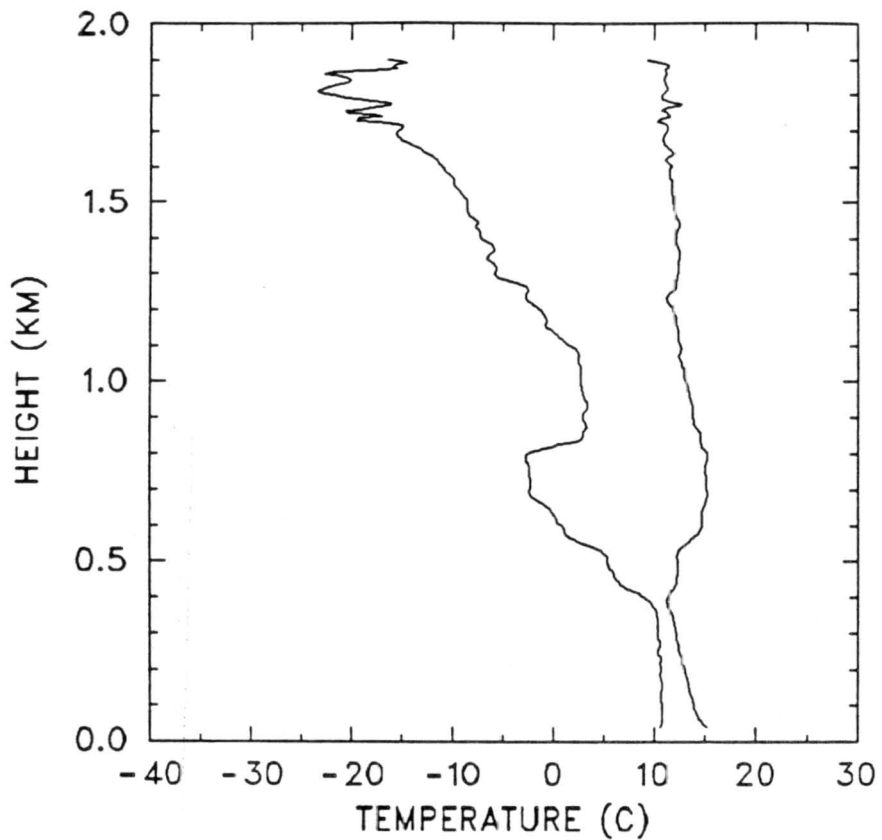




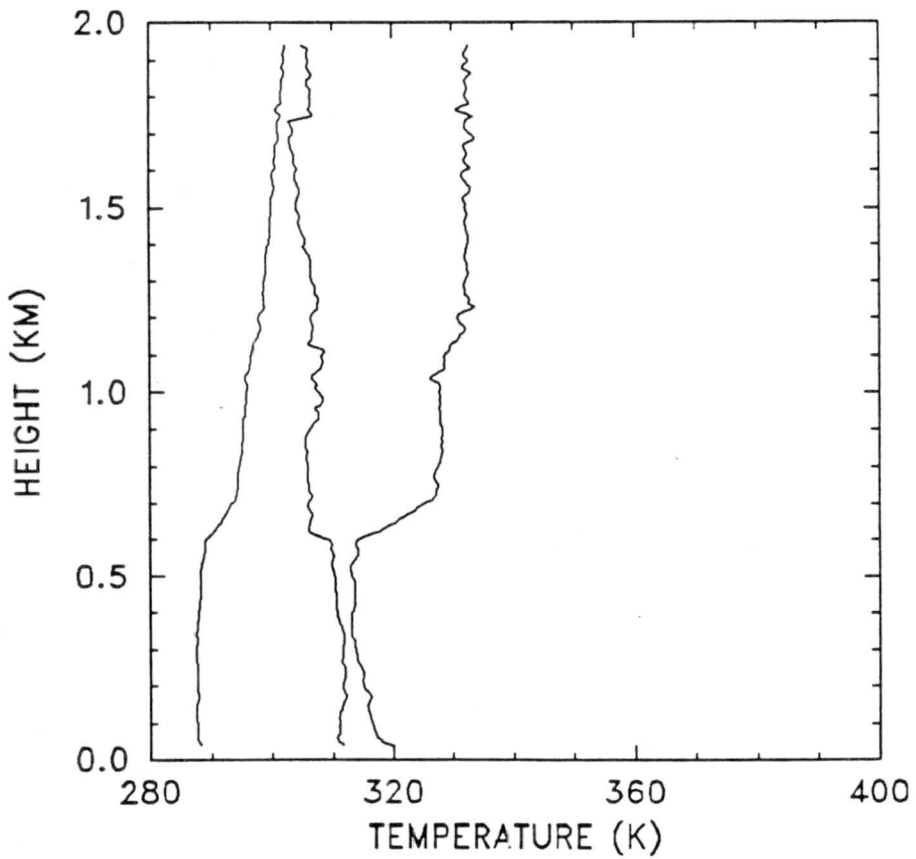
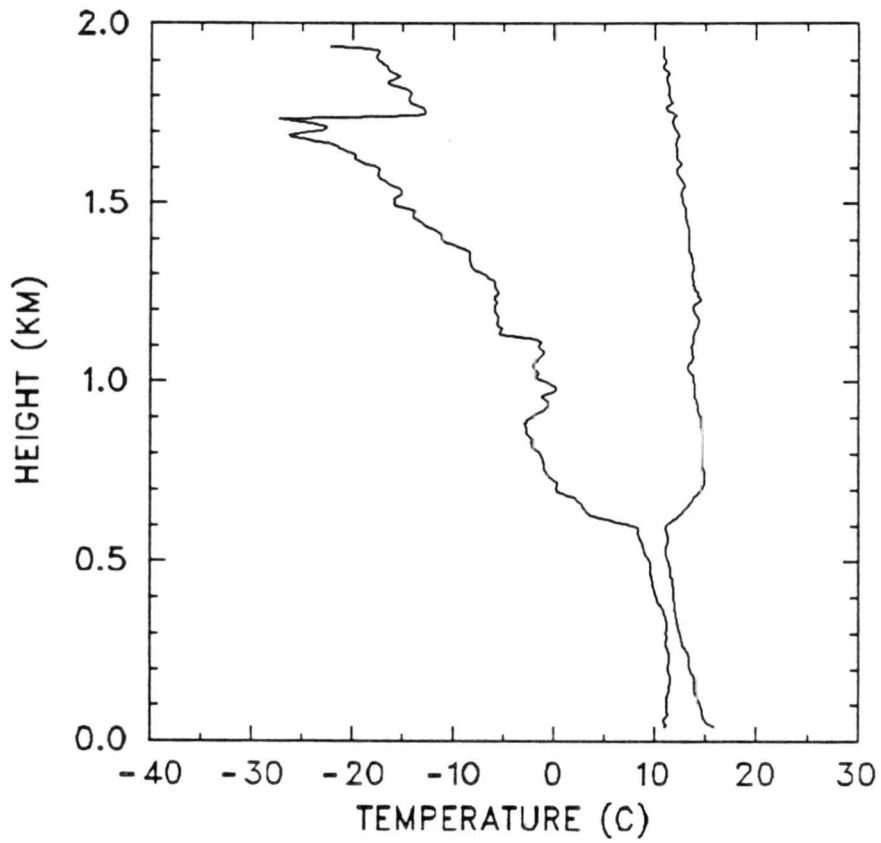
0019 GMT 19 JULY 1987



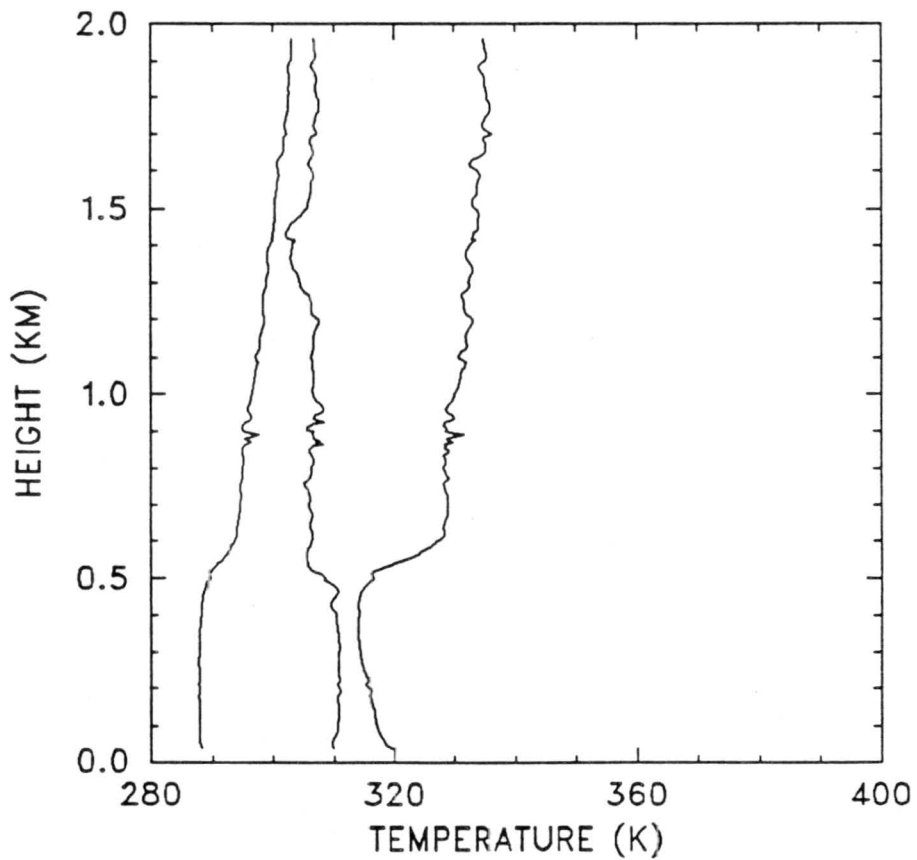
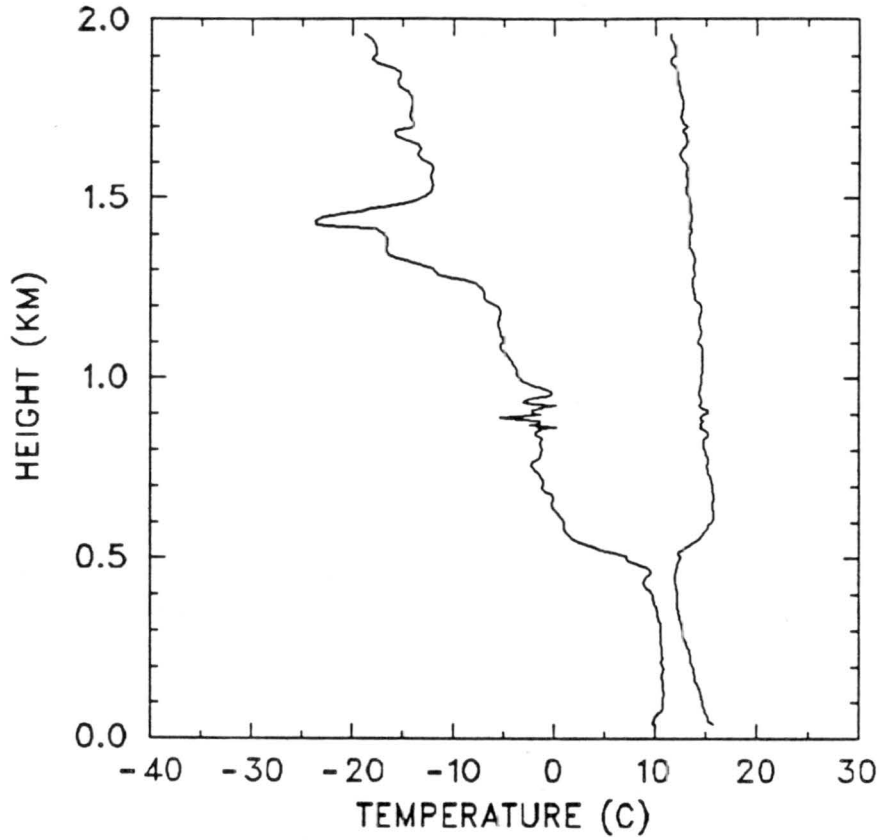
1201 GMT 19 JULY 1987

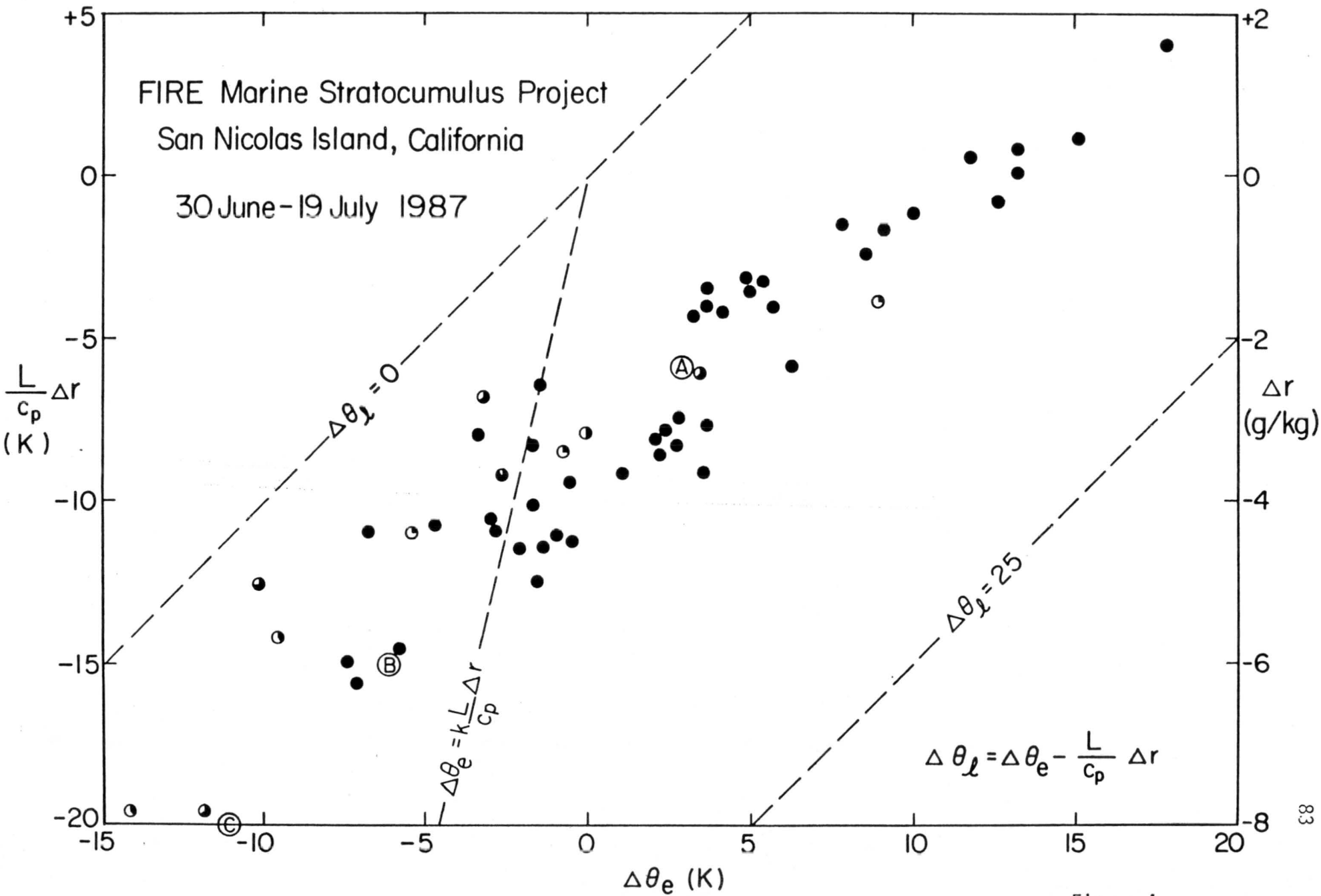


1608 GMT 19 JULY 1987



2015 GMT 19 JULY 1987





**APPENDIX A**

THE CROSS-CHAIN LORAN ATMOSPHERIC SOUNDING SYSTEM (CLASS)

Dean Lauritsen, Zohreh Malekmadani  
Claude Morel and Robert McBeth

National Center for Atmospheric Research \*  
Boulder, CO 80307

1. INTRODUCTION

The Cross-chain Loran Atmospheric Sounding System (CLASS) has been developed to meet the needs of the meteorological community for a research-quality rawinsonde. The National Weather Service has recently upgraded its WBRT-57 rawinsonde with solid-state components, automatic data entry, and improved software. This Automatic Radiotheodolite (ART) still has difficulties in precise measurement of boundary-layer winds and it requires long smoothing intervals at low elevation angles. Radar tracking systems are used in many countries for windsoundings, but equipment costs are high and

maximum range is limited. The Omega navigation system is used extensively for windfinding, but the inherent noise on the VLF navigation signals requires averaging winds for a three or four minute interval.

Loran-C is a navigation aid used primarily along the coasts of North America, Europe, and Asia for ship navigation. A rawinsonde system was developed 20 years ago (Beukers, 1967) using Loran-C to measure winds. The technique was not accepted for general use since coverage does not extend over the central states.

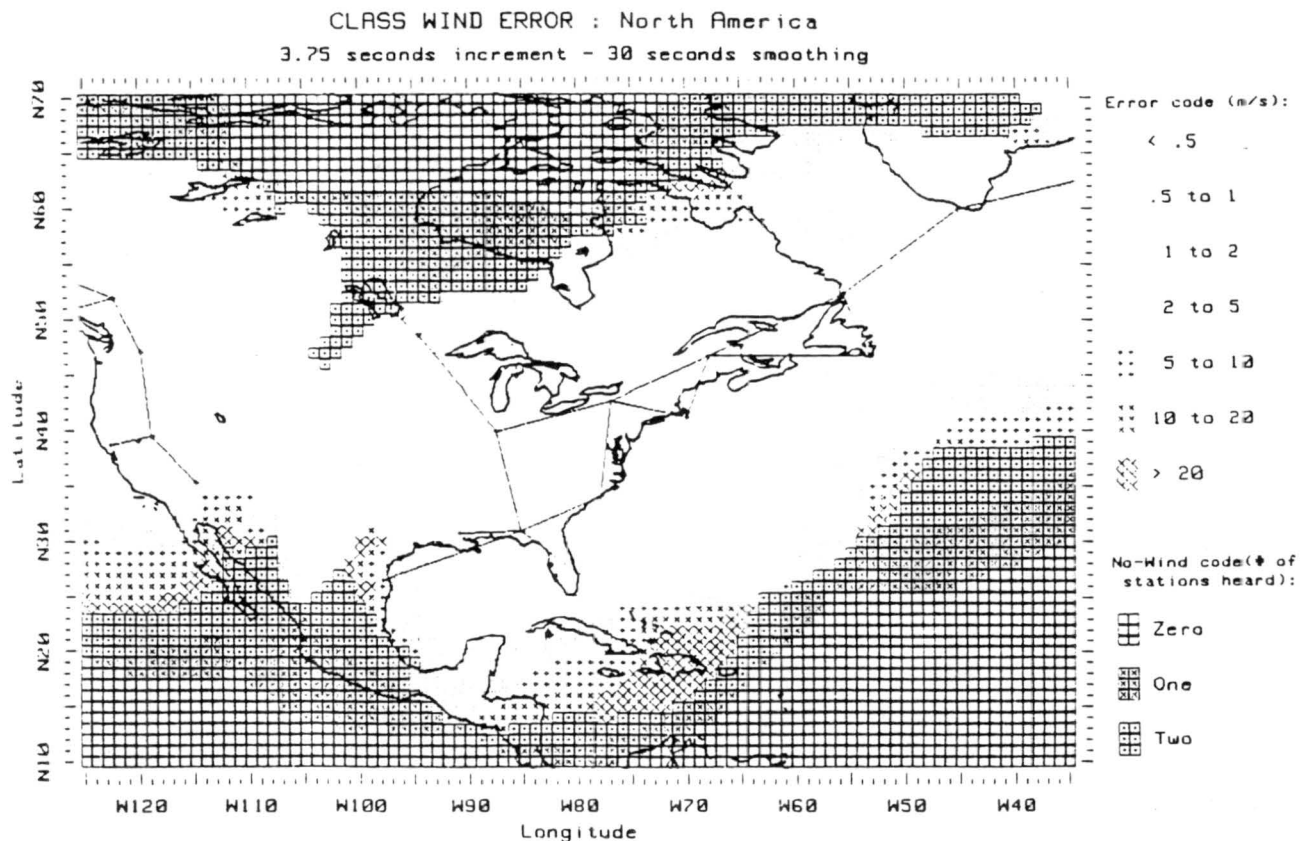


Fig. 1

\* The National Center for Atmospheric Research is sponsored by the National Science Foundation.

## 2. CROSS-CHAIN COVERAGE

The ANI-7000 Loran-C Navigator was developed for aircraft use, which permits coverage across the U.S. by combining data from all Loran chains from which at least two stations can be detected. For wind computation, we can consider that the time-of-arrival (TOA) data is coherent for short-time intervals between any stations regardless of chain. The chart in Fig. 1 indicates the predicted accuracy of wind data over North America, using a least-squares solution in which all detectable stations are used and weighted according to signal-strength (Passi, 1973). Note that coverage is acceptable over all of the U.S. excepting an area in the Southwest and a swath through the central Dakotas.

## 3. SYSTEM DESCRIPTION

CLASS is a completely self-contained, portable upper-air sounding system housed in a 3.6-m x 2.4-m x 2.1-m towable trailer. The trailer contains a balloon inflation and launch apparatus, an electronics rack for receiving the sonde radio frequency (RF) signals, and a scientific desktop computer for data acquisition, processing, and system control. A tower holding the antennas, preamplifier, and a surface weather station is located a short distance from the trailer. An uninterruptible power supply and gasoline-powered generator permit continuous operation should commercial a.c. power fail.

A 200-gram balloon is inflated within a cloth bag attached to a 1.5-m diameter ring in the ceiling of the trailer. At launch time, a motor-driven hatch cover on the trailer roof is moved to expose the balloon. The bottom of the balloon bag has an opening that permits attachment of the sonde line let-down device to the neck of the balloon since the sonde Loran-C antenna is wound on the let-down device. The Loran-C signal is temporarily fed to the sonde by a trailer mounted antenna while flight preparations are being made. At launch, the trailer-mounted antenna disconnects from the sonde and the sonde antenna unwinds from the let-down device.

The 400-MHz RF signal from the RS-80L radiosonde is received by antenna on the tower assembly and fed coaxially to a sensitive, wide bandwidth (500 kHz) FM receiver manufactured by Communitronics, Ltd. The receiver is tunable across the 400-MHz meteorological band width with indicators of frequency and signal strength and a speaker for audio output. Signal outputs are provided for the 7-10 kHz thermodynamic frequencies and the 100 kHz Loran-C frequencies.

The thermodynamic frequencies are processed by the Vaisala PP-11 PTU processor into units of pressure, temperature and humidity. These values are displayed on the PP-11 front panel and sent to an RS-232 serial data port for

computer access. The PP-11 has a paper tape reader for inputting radiosonde sensor coefficients and a keypad for entering sonde baselining data.

The Loran-C frequencies are processed by elements of an aircraft Loran-C navigator, specially modified for use by CLASS. The navigator is an ANI-7000 manufactured by Advanced Navigation, Inc. The ANI-7000 automatically identifies, acquires, and tracks up to eight Loran stations simultaneously. The eight stations can be from any mix of Loran chains, hence the "cross-chain" capability. The CLASS computer obtains the Loran data via an RS-232 port.

The electronics rack also contains circuitry for selecting either the omni-directional or high-gain RF antennas, computer-controlled antenna pointing, and an RS-232 serial port multiplexer for communicating with the hardware components.

Mounted on a 3-m tower assembly are the two 400-MHz RF antennas, an antenna rotor, an antenna switch, a 400-MHz preamp, and a crossarm holding the components of the surface weather station. A unique feature of the surface weather station is that a well-calibrated RS-80L radiosonde is used to measure pressure, temperature and humidity. The pressure and humidity elements are aspirated during measurement and maintained at an elevated temperature when not in use to prevent condensation on the sensitive Humicap element.

The hardware control, data acquisition, data processing, and communications activities are handled by a Hewlett Packard series 200/300 computer. The software was written with HP's advanced BASIC language. Data is stored on a 3 1/2 inch flexible disc for later use. Data communications are provided by a Hayes 1200 baud Smartmodem. A block diagram is presented below.

## 4. SOFTWARE DESCRIPTION

The CLASS software system consists of a main menu with five major segments driven by soft-key functions. These are hardware control, real-time data computation, flight data analysis, miscellaneous functions, and communication. Real-time CLASS data consist of 10-sec smoothed wind data, PTU data and their corresponding quality data. PTU data are smoothed over 20 sec using a least-squares solution. Wind data are computed from time-of-arrival of three or more Loran-C station signals. These data are smoothed over 30 sec using a least-squares solution.

Any number of derived quantities can be made available. Standard outputs include altitude and dew point with the user specifying



## CLASS - SYSTEM HARDWARE BLOCK DIAGRAM

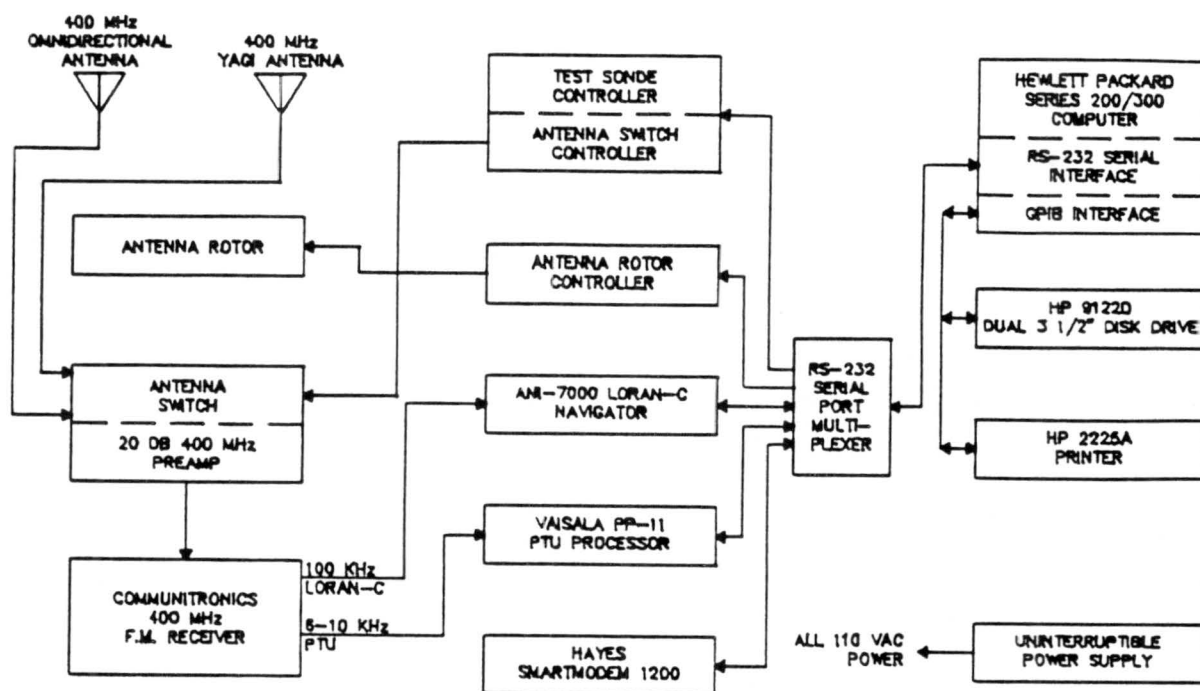


Fig. 2

other derived parameters. Print-outs are available through soft-key access of 10-sec data, pressure-level data for any desired pressure increment, and raw data. Quality flags are assigned to the pressure, temperature, humidity, and wind data indicating the probable error in the measurement. Plots are available both during and post-flight of all parameters. Post-flight plots are available in a number of forms for analysis, including a SKEW T, LOG P presentation.

The unique aspect of the CLASS software is its ease of operation. Operations proceed automatically or by soft-key steps. Screen help is available for most procedures. Unskilled operators with no computer or meteorological experience have been trained in a few hours to operate the system successfully.

### 5. FIELD EXPERIENCE

The decision to build the CLASS system was made in October 1984 after a survey of cross-chain Loran performance in September confirmed the theoretical analysis. A prototype system was tested at the White Sands Missile Range (New Mexico) in January 1985 against range radars. Wind differences between radar and CLASS were  $1.1 \text{ m s}^{-1}$  for 60-sec averages in this marginal region.

In February 1985, the CLASS system was moved to Hatteras where ten flights were made at

hourly intervals during an intense storm to provide a realistic test prior to the GALE program. Wind data were uniformly excellent with track to 220 km in winds up to  $85 \text{ m s}^{-1}$ . PTU data exhibited a few glitches, apparently due to too low a modulation index.

After this successful test, nine CLASS systems were fabricated for use during the GALE program with funds from NSF (6) and ONR (3). Two of the systems were deployed on ships and seven on land. During the GALE program, over 1200 soundings were made from mid-January to mid-March 1986. All soundings were made by a single operator, each of whom had 2 1/2 days of instruction and no prior operator experience. Noteworthy were the 200 soundings made from the R.V. Hatteras with no balloon failures under the severest weather conditions--a tribute to the bag-launch technique. The fix to eliminate glitches in the PTU data introduced a problem in the Loran modulation in the RS-80L radiosonde. The distorted Loran signal at times was interpreted as a sky-wave by the sophisticated ANI-7000 navigator. As a result, some wind data were contaminated on a large number of flights. Since the Loran data were stored on all flights, we were able to edit and correct these errors for the entire GALE data set. A modification to the radiosonde and to the navigator to provide a better match has been accomplished. The problem has not occurred on recent flight series.

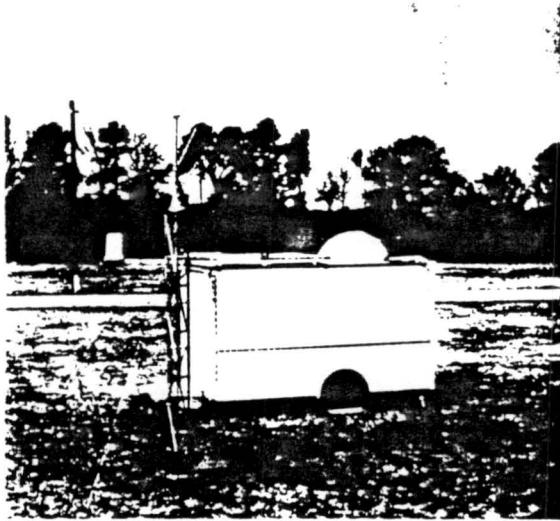


Fig. 3

A typical CLASS installation.  
GALE program, Sumter, S.C., 1986.

#### 6. SUMMARY

The CLASS system has been designed as a research-quality sounding system. It provides accurate wind and thermodynamic data in any form the user wishes. It can be operated on land or sea in the most severe weather conditions. It is readily operated by a single, unskilled person, including even the scientist. Nine systems are now available for use in field experiments.

#### 7. REFERENCES

- Beukers, J.M., 1967: Windfinding using the Loran-C and Omega long range navigational systems. Suppl., IEEE Trans. Aerosp. Electron. Syst., November.
- Passi, R.M., 1973: Errors in wind measurements derived from Omega signals. NCAR Tech Note, TN/STR-38, National Center for Atmospheric Research, Boulder, Colo., 35 pp.

**APPENDIX B**

The RS 80 Radiosondes have been used for routine upper - air observations on several stations since early 1981.

Operational results indicate that the sonde is very reliable and easy to use, allowing savings in the operating budget.

The accuracy of measurement is exceptionally good. Variability of standard pressure level altitudes are approximately half of those observed for any of the previous radiosonde types.

These results are described in detail in Vaisala Information Releases available on request.

## CONSTRUCTION

Features of the mechanical construction are small size and light weight. Attention has been paid to durability in transportation and storage. The solid state sensors are insensitive to mechanical stress, dirt and humidity. Each sonde is packed in a hermetic metal foil bag to protect it against moisture. The package also contains the battery which in turn is also sealed in a hermetic metal foil bag.

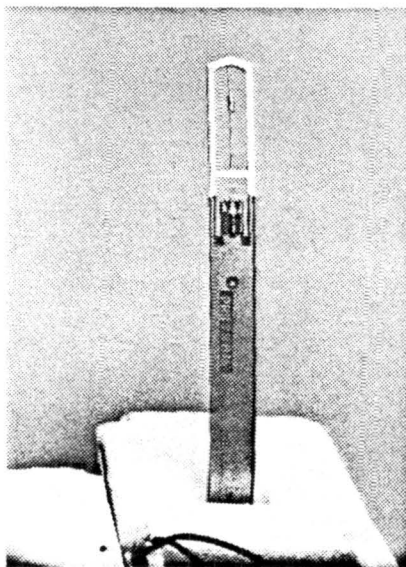


(Left) Radiosonde with flap open showing battery compartment.  
(Below) Sonde packed in hermetic metal foil bag.



Frangibility is ensured by a plastic foam case construction making the sonde a considerable improvement in air safety. As the unwinder and string are separate from the sonde during the flight, the radiosonde weight is only 150 - 190 g depending on the model. The size of a sonde is 55 x 147 x 90 mm (excluding antenna). Total weight of a sonde ready for launch, including sonde, battery, string unwinder and string, is 200 - 240 g depending on model.

For good exposure to free air the temperature and humidity sensors are mounted close to the tip of a support made of flexible circuit material. The support is insulated and coated with thin electrically grounded aluminium film.



Temperature and humidity sensors mounted on support.

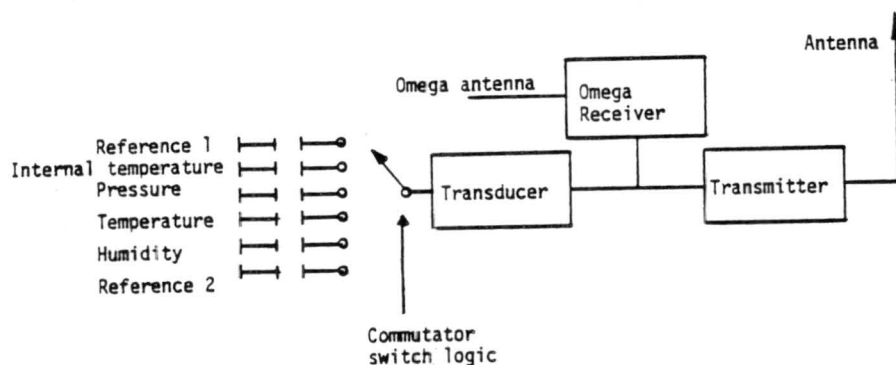
The unique BAROCAP® pressure sensor is mounted as a component on the transducer electronics board. This new type of transducer is fully self-contained and needs no external installation frame. It provides a continuous and unambiguous pressure reading over the full range of operation.

The BAROCAP® is friction-free as there are no mobile contacts. Very high precision welding technology allows assembly to a completely solid state unit, with no adjustments required. The completely welded structure is very rugged and tolerates transportation shocks better than any previous radiosonde pressure sensors. Temperature dependence is very low, approx. 4 mb over 100°C range. An internal temperature sensor is used for accurate compensation.

The solid state temperature and humidity sensors are mounted near the tip of a flexible boom. Thin film metal coating is used to ensure constant radiation characteristics of the sensors. Radiation corrections are small and automatically carried out in the MicroCORA ground instrumentation.

## PRINCIPLE

The PTU (pressure, temperature, humidity) measuring system of the RS 80 radiosonde is based on a time multiplexing principle. Each of the capacitive sensors controls the frequency of the AF oscillator through an electronic commutator switch. The switch is formed by solid state logic gates. The oscillator frequency is fed through a modulator to the radio transmitter. The transducer circuit is patented world-wide. A water-activated battery provides power for the radiosonde.



The frequency generated by the transducer is the measure of the meteorological parameters. Relationship between the frequency and corresponding parameter value is established in the calibration process. The calibration data is obtained separately for every radiosonde and delivered in the form of a 8 channel paper tape as well as a printout table. Fourth degree equation coefficients for each sensor with checksum for entry verification are provided.

The set of solid state sensors consists of an aneroid capsule (BAROCAP®) with capacitive transducers in the inside vacuum, a ceramic temperature sensor (THERMOCAP®) and a thin film humidity sensor (HUMICAP®) which is an improved version of the one produced earlier.

All the sensors are capacitive with compatible dynamic ranges which essentially simplifies the transducer electronics.

In the radiosonde only one reference capacitor is needed to eliminate the influence of drift of the transducer electronics. The basic capacitance of the transducer oscillator circuit is used as the second reference.

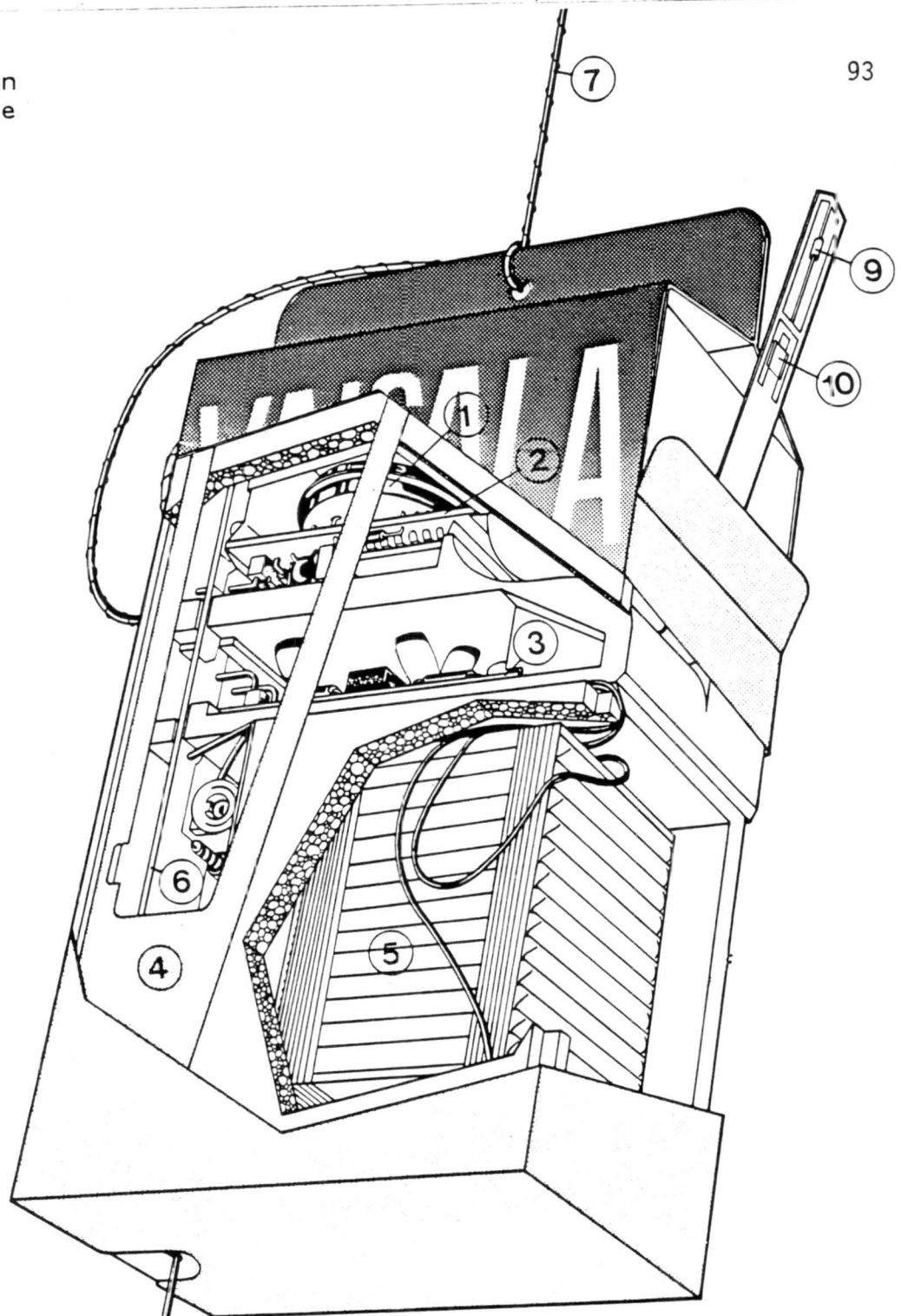
Other viewpoints when selecting the sensing principle were the existence of the capacitive humidity sensor, a simple stable and frictionless barometer construction and small risk of self-heating problems in temperature and humidity measurements.

The transducer circuit developed for the RS 80 radiosondes is capable of measuring with a resolution of 1 fF ( $10^{-3}$  pf). The electronic circuit is insensitive to changes of stray capacitances between sensor terminals and electrical ground. This is of basic importance for the feasibility of the sensor design.

There is an additional temperature sensor to measure the temperature of the pressure sensor for elimination of it's temperature dependence.

Radiosonde calibration data as printout table and perforated tape

203300813	
203300813	
PY0	15729
P0	-6020
P1	19111
P2	-14878
P3	10784
P4	-2474
CS	-26331
DY0	15729
D0	211
D1	-838
D2	1601
D3	-1337
D4	415
CS	6150
SY0	15729
S0	-1882
S1	1094
S2	3950
S3	0
S4	0
CS	-21951
TY0	15729
T0	-1681
T1	1839
T2	362
T3	-156
T4	0
CS	-7423
UY0	655
U0	-17
U1	1089
U2	-2314
U3	0
U4	0
CS	5178



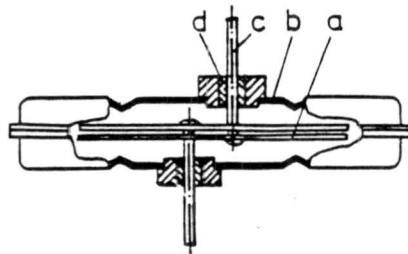
RS 80-15 N radiosonde

- 1. Pressure sensor BAROCAP®
- 2. Transducer electronics
- 3. Omega receiver
- 4. UHF antenna counterpoise
- 5. Battery
- 6. Transmitter
- 7. String and Omega antenna
- 8. UHF antenna radiator
- 9. Temperature sensor THERMOCAP®
- 10. Humidity sensor HUMICAP®

Type:	Capacitive Aneroid
Measuring range:	1060 mb to 3 mb
Resolution:	0.1 mb
Accuracy* (standard deviation)	±0.5 mb

\*) repeated calibration method

The pressure sensor is a small aneroid capsule with capacitive transducer plates inside. The diameter of the capsule is 30 mm and the weight of the complete assembly only 5 g.



Pressure sensor (BAROCAP®)

- a) transducer plate
- b) capsule membrane
- c) supporting rod
- d) glass-to-metal seal

Transducer plates (a) are supported by membranes (b) made of special steel alloy. The supporting rods (c) of the plates are fixed to the membranes with hermetic glass-to-metal seals (d). The inverted construction is used to obtain maximum sensitivity at low pressure. The sensor is assembled with precision welding techniques. The transducer electronics senses the capacitance between the plates only, with no influence of stray capacitances between the transducer plates and the membranes, which are grounded.

Some advantages of the construction are:

- There are no joints in the construction which could "slip" when the sensor is exposed to mechanical stresses. Neither does the construction contain any springs, arms, contacts or assembly frame common in old designs.
- Transducer plates are protected against moisture and dust.
- The absence of an assembly frame and small sensor size has made it possible to achieve a very small temperature dependence. With changing temperature the temperature differences stabilize fast.

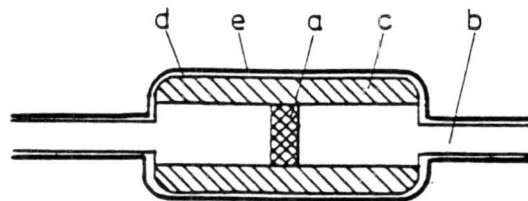


Sensor type:	Capacitive bead
Measuring range:	+60°C to -90°C
Resolution:	0.1°C
Accuracy *	
(Standard deviation):	±0.2°C
Lag (6 m/s flow at 1000 mb):	2.3 s
Solar radiation cor- rection at 60°C solar elevation:	< 1°C at 10 mb

\*) repeated calibration method

The temperature sensor is based on dielectric ceramic materials, the temperature dependence of which can be accurately controlled with selection of materials and processing parameters.

Metal electrodes are formed on both sides of a tiny ceramic chip (0.5 × 0.5 mm, thickness 0.2 mm). The capacitance between the electrodes is a function of temperature. To ensure complete moisture protection the sensor is hermetically sealed in a small glass capsule (2.5 × ø 1.5 mm) with two connecting leads (ø 0.4 mm). To avoid uncontrolled stray capacitances which could be caused, for instance, by water droplets on the glass capsule, an electrically grounded thin film aluminium coating is deposited on the sensor capsule and leads. This coating also has excellent radiation properties for minimizing the radiation error (max 2°C at 10 mb and 45 deg solar elevation) of the observation. An insulation layer on the leads prevents short circuits.



Temperature sensor (THERMOCAP®)

- a) chip with electrodes, b) connecting leads,
- c) glass capsule,
- d) insulating layer
- e) metal coating

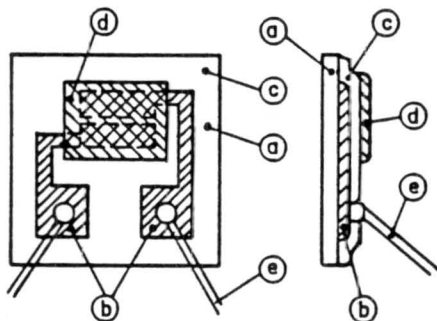
Sensor type:	Thin film capacitor
Measuring range:	0 % RH to 100 % RH
Resolution:	1 % RH
Lag (6 m/s flow at 1000 mb, +20°C):	1 s
Accuracy * (Standard deviation):	±2 % RH

\*) repeated calibration method

The humidity sensor is a thin film capacitor with a polymer dielectric. The polymer is about 1 micron thick. The sensor capacitance is dependent on the water absorption in the sensor's dielectrical material.

The sensor is fabricated using thin film technology similar to that generally used in microelectronics. The sensor is small (4 x 4 x 0.2 mm), hence its thermal mass is also small and the sensor very closely and quickly follows the ambient air temperature. This is obviously necessary for obtaining true relative humidity values in the atmosphere.

Other attractive features of the sensor are fast response, good linearity, low hysteresis and small temperature coefficient. The sensor operates reliably in low temperatures to at least the -60°C level.

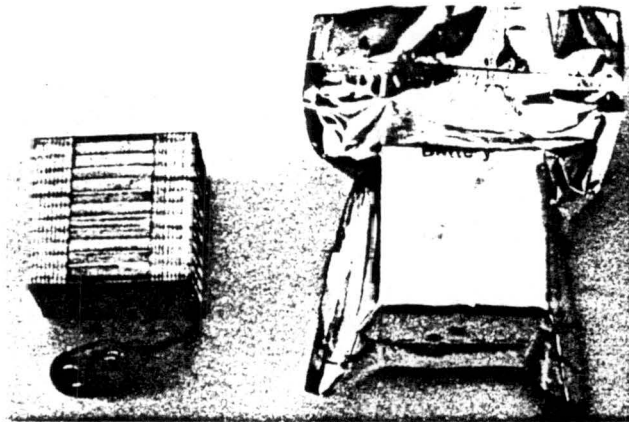


Humidity sensor (HUMICAP)

- (a) glass substrate
- (b) lower electrode
- (c) polymer film
- (d) upper electrode
- (e) leads

The radiosonde battery is very light and small. Its main features are:

- efficient cost/performance ratio
- simple, reliable and lightweight construction
- long storage life
- good dynamic performance in cold
- easy to operate
- a high standard of quality can be assured through in-house production.



RSB 20 battery together with hermetic metal foil bag which protects it in transportation and storage.

The battery is of a magnesium-cuprous chloride type. A sheet of special magnesium alloy is used as anodic material and a compressed mixture of cuprous chloride, sulphur and graphite is used as cathodic material (depolarizer). The cathode material (pellets) is in contact with a copper sheet painted with conductive paint for protection against corrosion.

The anode and cathode are separated with water absorbing non-woven material. It is immersed in the electrolyte (tap water) during activation. The desirable nominal voltage is determined by the number of cells which are stacked and strapped with fiber glass tape. The batteries are sealed hermetically under vacuum in a bag of metal and plastic film laminate. This kind of package protects the battery from humidity which is, as well as known, harmful to cuprous chloride batteries during long storage.

Nominal voltage of the battery is  $19 \text{ V} \pm 2 \text{ V}$  and nominal current when loaded at  $220 \Omega$  is 85 mA. Fulfillment of the battery specifications are measured in a laboratory simulator for the ICAO standard atmosphere.

Dimension of the battery are 29 x 48 x 48 mm. The latter dimension is the thickness of the cell stack which may vary depending on the raw materials available. Weight of a dry battery is approx. 65 g and activated 90 g.

## UNWINDER

The RS 80 Radiosonde includes as a standard accessory an unwinder with 30 meters of string. In the Navaid sondes the Omega antenna forms part of the string.

The unwinder (also known as the spool-off device) is attached directly to the neck of the balloon. At launch the operator is able to hold the balloon with one hand and the sonde with the other. This way one-man launch can be made in even high wind conditions.

The unwinder string length improves the accuracy of temperature measurement as it ensures that the radiosonde is always outside the balloon thermal wake regardless of launch conditions.

The unwinder includes a device for closing the balloon neck. Most balloon types are adequately closed with this device so that no string tie is necessary (available early 1983).

## PREPARATION AND LAUNCH

The RS 80 radiosondes need only a minimum of preparation for launch. Thanks to the small size and light weight the sonde is easy to handle by one man.

The sensors are precalibrated at the factory. Only a preliminary ground check that the sonde operates is required before launch.

For launch you take out the sonde from the bag, activate the battery and place it in its compartment and perform the ground check.

You then fasten the radiosonde to the balloon with the unwinder and the sonde is ready for launch.

## APPENDIX C

The CLASS sounding data set can be obtained from the FIRE Central Archive by addressing your inquiries to:

National Space Science Data Center  
Goddard Space Flight Center  
Greenbelt, Maryland 20771

The CLASS sounding data is also available on NCAR's Mass Storage System (MSS). Shown below is a sample NCAR job which will access the Mass Storage file E301155.DAT (i.e, the sounding data for June 30, 1155 GMT) and dispose it to the your IBM reader at NCAR.

```
JOB,JN=jjjjjj,T=10,*MS,CL=FG1.  
ACCOUNT,AC=uuuupppppppp.  
ACQUIRE,DN=E301155,MF=MS, ^  
TEXT='USER=CIESIELS,FLNM=' 'FIRE/SOUND/E301155.DAT.01'''.  
DISPOSE,DN=E301155,MF=IO,DC=ST,TEXT='FLNM=E301155,FLTY=DAT'.  
\ EOF
```

where

jjjjjj is an arbitrary job name  
uuuu is your user number  
pppppppp is your project number

Listed on the following pages are the files available at NCAR along with their corresponding date and time.

file name on MSS	Date	Start Time (GMT)
/CIESIELS/FIRE/SOUND/E301155.DAT.01	June 30	1155
/CIESIELS/FIRE/SOUND/E302351.DAT.01	June 30	2351
/CIESIELS/FIRE/SOUND/Y011216.DAT.01	July 01	1216
/CIESIELS/FIRE/SOUND/Y012009.DAT.01	July 01	2009
/CIESIELS/FIRE/SOUND/Y021750.DAT.01	July 02	1750
/CIESIELS/FIRE/SOUND/Y022253.DAT.01	July 02	2253
/CIESIELS/FIRE/SOUND/Y031208.DAT.01	July 03	1208
/CIESIELS/FIRE/SOUND/Y031808.DAT.01	July 03	1808
/CIESIELS/FIRE/SOUND/Y040036.DAT.01	July 04	0036
/CIESIELS/FIRE/SOUND/Y041215.DAT.01	July 04	1215
/CIESIELS/FIRE/SOUND/Y050034.DAT.01	July 05	0034
/CIESIELS/FIRE/SOUND/Y051158.DAT.01	July 05	1158
/CIESIELS/FIRE/SOUND/Y060145.DAT.01	July 06	0145
/CIESIELS/FIRE/SOUND/Y061214.DAT.01	July 06	1214
/CIESIELS/FIRE/SOUND/Y061607.DAT.01	July 06	1607
/CIESIELS/FIRE/SOUND/Y062350.DAT.01	July 06	2350
/CIESIELS/FIRE/SOUND/Y071159.DAT.01	July 07	1159
/CIESIELS/FIRE/SOUND/Y080011.DAT.01	July 08	0011
/CIESIELS/FIRE/SOUND/Y081211.DAT.01	July 08	1211
/CIESIELS/FIRE/SOUND/Y091154.DAT.01	July 09	1154
/CIESIELS/FIRE/SOUND/Y091814.DAT.01	July 09	1814
/CIESIELS/FIRE/SOUND/Y100115.DAT.01	July 10	0115
/CIESIELS/FIRE/SOUND/Y101222.DAT.01	July 10	1222
/CIESIELS/FIRE/SOUND/Y101550.DAT.01	July 10	1550
/CIESIELS/FIRE/SOUND/Y101800.DAT.01	July 10	1800
/CIESIELS/FIRE/SOUND/Y102006.DAT.01	July 10	2006
/CIESIELS/FIRE/SOUND/Y102159.DAT.01	July 10	2159
/CIESIELS/FIRE/SOUND/Y110005.DAT.01	July 11	0005
/CIESIELS/FIRE/SOUND/Y110200.DAT.01	July 11	0200
/CIESIELS/FIRE/SOUND/Y110353.DAT.01	July 11	0353
/CIESIELS/FIRE/SOUND/Y110616.DAT.01	July 11	0616
/CIESIELS/FIRE/SOUND/Y110951.DAT.01	July 11	0951
/CIESIELS/FIRE/SOUND/Y111212.DAT.01	July 11	1212
/CIESIELS/FIRE/SOUND/Y111410.DAT.01	July 11	1410

file name on MSS	Date	Start Time (GMT)
/CIESIELS/FIRE/SOUND/Y111808.DAT.01	July 11	1808
/CIESIELS/FIRE/SOUND/Y112208.DAT.01	July 11	2208
/CIESIELS/FIRE/SOUND/Y112359.DAT.01	July 11	2359
/CIESIELS/FIRE/SOUND/Y120154.DAT.01	July 12	0154
/CIESIELS/FIRE/SOUND/Y120610.DAT.01	July 12	0610
/CIESIELS/FIRE/SOUND/Y121005.DAT.01	July 12	1005
/CIESIELS/FIRE/SOUND/Y121234.DAT.01	July 12	1234
/CIESIELS/FIRE/SOUND/Y121510.DAT.01	July 12	1510
/CIESIELS/FIRE/SOUND/Y121755.DAT.01	July 12	1755
/CIESIELS/FIRE/SOUND/Y130005.DAT.01	July 13	0005
/CIESIELS/FIRE/SOUND/Y131154.DAT.01	July 13	1154
/CIESIELS/FIRE/SOUND/Y132120.DAT.01	July 13	2120
/CIESIELS/FIRE/SOUND/Y140014.DAT.01	July 14	0014
/CIESIELS/FIRE/SOUND/Y141158.DAT.01	July 14	1158
/CIESIELS/FIRE/SOUND/Y150015.DAT.01	July 15	0015
/CIESIELS/FIRE/SOUND/Y151200.DAT.01	July 15	1200
/CIESIELS/FIRE/SOUND/Y151703.DAT.01	July 15	1703
/CIESIELS/FIRE/SOUND/Y151935.DAT.01	July 15	1935
/CIESIELS/FIRE/SOUND/Y160011.DAT.01	July 16	0011
/CIESIELS/FIRE/SOUND/Y161139.DAT.01	July 16	1139
/CIESIELS/FIRE/SOUND/Y161600.DAT.01	July 16	1600
/CIESIELS/FIRE/SOUND/Y162004.DAT.01	July 16	2004
/CIESIELS/FIRE/SOUND/Y162342.DAT.01	July 16	2342
/CIESIELS/FIRE/SOUND/Y171206.DAT.01	July 17	1558
/CIESIELS/FIRE/SOUND/Y171558.DAT.01	July 17	1154
/CIESIELS/FIRE/SOUND/Y172002.DAT.01	July 17	2002
/CIESIELS/FIRE/SOUND/Y180020.DAT.01	July 18	0020
/CIESIELS/FIRE/SOUND/Y181206.DAT.01	July 18	1206
/CIESIELS/FIRE/SOUND/Y181557.DAT.01	July 18	1557
/CIESIELS/FIRE/SOUND/Y181951.DAT.01	July 18	1951
/CIESIELS/FIRE/SOUND/Y190019.DAT.01	July 19	0019
/CIESIELS/FIRE/SOUND/Y191201.DAT.01	July 19	1201
/CIESIELS/FIRE/SOUND/Y191608.DAT.01	July 19	1608
/CIESIELS/FIRE/SOUND/Y192015.DAT.01	July 19	2015